

Diesel Fuel Component Contribution to Engine Emissions and Performance

Final Report

Jimell Erwin
Thomas W. Ryan, III
David S. Moulton
*Southwest Research Institute
San Antonio, Texas*

NREL technical monitor:
C. Colucci



National Renewable Energy Laboratory
1617 Cole Boulevard
Golden, Colorado 80401-3393

A national laboratory of the U.S. Department of Energy
Operated by Midwest Research Institute
for the U.S. Department of Energy
Under Contract No. DE-AC36-83CH10093

Prepared under Subcontract Number YZ-2-11215-1

November 1994

MASTER
DISTRIBUTION OF THIS DOCUMENT IS UNLIMITED

This publication was reproduced from the best available camera-ready copy submitted by the subcontractor and received no editorial review at NREL.

NOTICE

This report was prepared as an account of work sponsored by an agency of the United States government. Neither the United States government nor any agency thereof, nor any of their employees, makes any warranty, express or implied, or assumes any legal liability or responsibility for the accuracy, completeness, or usefulness of any information, apparatus, product, or process disclosed, or represents that its use would not infringe privately owned rights. Reference herein to any specific commercial product, process, or service by trade name, trademark, manufacturer, or otherwise does not necessarily constitute or imply its endorsement, recommendation, or favoring by the United States government or any agency thereof. The views and opinions of authors expressed herein do not necessarily state or reflect those of the United States government or any agency thereof.

Available to DOE and DOE contractors from:
Office of Scientific and Technical Information (OSTI)
P.O. Box 62
Oak Ridge, TN 37831
Prices available by calling (615) 576-8401

Available to the public from:
National Technical Information Service (NTIS)
U.S. Department of Commerce
5285 Port Royal Road
Springfield, VA 22161
(703) 487-4650



Printed on paper containing at least 50% wastepaper and 10% postconsumer waste

DISCLAIMER

Portions of this document may be illegible in electronic image products. Images are produced from the best available original document.

Table of Contents

SECTION	PAGE
INTRODUCTION	1
Background Literature	2
OBJECTIVE	2
APPROACH	3
Materials and Processing	4
Petroleum Stocks and Products	4
Fischer-Tropsch Liquids	4
Processing	6
Distillation	8
Laboratory Evaluation	8
Combustion Experiments	11
Ignition Quality	11
Engine Tests	11
Test Engine	12
Instrumentation	12
Test Procedures	14
RESULTS AND DISCUSSIONS	16
Analyses	16
Aromatics	16
Cetane Index	22
CVCA Results	24
Engine Ignition Quality	32
Performance and Emissions	39
Task 3 Clean-Fuel Study	47
Determining Blend Composition for Low-Emission Fuels	47
Clean-Fuel Experimental Results and Discussions	49
Fischer-Tropsch Fuels	49
Low Emissions Fuels	55
Clean-Fuel Discussion	60
SUMMARY AND CONCLUSIONS	61
Acknowledgments	64
References	65
Appendix A. Detailed analytical results.	A-1
Appendix B. VCR Engine modification	B-1
Appendix C. Task 3 "Clean Fuel" results	C-1

List of Figures

FIGURE	PAGE
1	Sequence of operations for making the test fuels 3
2	Schematic diagram for the diesel-fuel assay 7
3	Constant volume combustion apparatus 12
4	Variable compression ratio profile schematic 13
5	Cetane number calibration curve 15
6	Aromatic carbon vs. the 50% point temperatures for LCGOs 16
7	Aromatics vs. boiling point for LCOs 20
8	Aromatics vs. boiling point for LCGOs 20
9	Aromatics vs. boiling point for SRDs 20
10	LCO aromatics distribution 21
11	Cetane index by ASTM D 976 & D 4737 vs. LCO D 86 50% temperature 23
12	Cetane index vs. the 50-percent point for LCGOs 24
13	CVCA cetane number calibration curves 24
14	CVCA cetane number of LCOs at 582°C 29
15	CVCA cetane number of LCGO at three test temperatures 29
16	CVCA cetane number of SRD at three test temperatures 30
17	CVCA cetane number of LCGOs at 582°C 30
18	CVCA cetane number of SRDs at 582°C 31
19	CVCA cetane number vs. aromatics for the three feedstocks 31
20	CVCA cetane number vs. cetane index for the light-cycle oils 33
21	CVCA cetane number vs. cetane index for the straight-run diesel fuels 33
22	VCR cetane number vs. CVCA cetane number 34
23	Cetane number (VCR) vs. the average boiling point for the light-cycle oil 35
24	Cetane number (VCR) vs. the average boiling point for the light-coker gas oil 35
25	Cetane number (VCR) vs. the average boiling point for the straight-run diesel fuels and Fischer-Tropsch fuels 36
26	Effect of hydrogenation by boiling range 37
27	Cetane numbers of blends of F-T distillate with diesel components 38
28	Hydrocarbon emissions vs. viscosity for the Mode 1 test condition 40
29	Power variations in Mode 1 vs. apparent combustion efficiency 41
30	NO _x emissions vs. NMR aromatic content for Mode 1 41
31	NO _x vs. cetane number (VCR) for Mode 1 42
32	HC emissions vs. fuel fractions for the F-T fuels at Mode 2 46
33	Bosch smoke number vs. fuel fractions for the F-T fuels at Mode 2 46
34	VCR cetane ratings of the Fischer-Tropsch materials 51
35	Nitric oxide emission data for the Mode 2 test condition 51
36	Bosch smoke numbers for the Mode 2 test condition 52
37	Hydrocarbon emissions for the Mode 1 test condition 52
38	Hydrocarbon emissions for the Mode 2 test condition 53
39	Emissions parameters for all test materials at the Mode 2 test conditions 53
40	Aromatic content of the low-emission fuels 56
41	VCR cetane numbers of the low-emission fuels 56
42	NO _x emissions for the low-emissions fuel at Mode 2 57
43	Hydrocarbon emissions for the low-emissions fuels at Mode 2 57
44	CO emissions for the low-emissions fuel at Mode 2 58

List of Figures (Continued)

FIGURE		PAGE
45	Bosch smoke for the low-emissions fuels at Mode 2	58
46	Emissions parameter, calculated and measured, at Mode 2	59
47	Emissions parameter, calculated and measured, at Mode 1	59
48	Emissions parameters for all test materials at the Mode 1 test conditions	60

List of Tables

TABLE		PAGE
1	Feedstock Properties	5
2	Processing Parameters	6
3	Corresponding Boiling Ranges of Fractions	9
4	Engine Specifications	14
5	Test Condition for Ignition Quality Rating	14
6	Test Condition for Performance and Emissions	15
7	Partial Results for Distillation Fractions	17
8	Ignition Delay Times, CVCA Cetane Numbers, and Arrhenius Coefficients	26
9	Low-Emissions Fuels Description	48
10	Computed and Measured Properties of the Low-Emissions Fuels	49
11	Task 3 Correlation Inputs	54

Executive Summary

Emissions and performance have become the dominant factors governing the acceptability of diesel fuel. The properties of the diesel-blending components and the role of alternative fuels for exhaust emissions are the subjects of this report. Correlations were made for exhaust emission components and engine performance from a very carefully prepared set of test fuels designed to reveal the relationships arising from blendstock composition and origin.

Because full-boiling diesel fuels show wide quality variations and the history of most commercial fuel is difficult to determine, a detailed study was made of three petroleum blendstocks and two alternative components in the diesel boiling range. The blendstocks were hydrogenated at two severities to make reduced sulfur (0.05 mass%) and low aromatic-content (10 vol%) products for each one. The original stocks and components and their processed products were then each distilled into six to eight narrow boiling fractions at 40°F intervals. This effort produced a set of 80 test fuel samples for the program.

Each sample was then subjected to physical and chemical analyses in the laboratory followed by combustion testing in a constant volume combustion apparatus (CVCA) and a variable compression ratio (VCR) engine. Ignition quality was measured in several ways, and exhaust emissions composition were obtained for all samples that could be run in the combustion tests (several fractions were too viscous to test). The matrix of results thus obtained was examined statistically for coverage of the variable space and for autocorrelation. This large data set was used to construct correlations for cetane number and the key emissions components.

The properties of the test fractions and the correlations were inputs to the last phase of the work — a "Clean Fuel Study". A set of fuel specifications was devised to represent a future low-emission diesel fuel. Using linear programming to calculate proportions of each component to use, several blending concepts were examined. These included:

- minimum overall emissions with and without alternative components,
- a series of varied aromatic compositions at 55 cetane number,
- a series of blends with 15 vol% aromatics having variable cetane number.

A set of 10 minimum-emissions recipes was developed, test fuels were blended, and combustion tests were made just as had been performed on the 80 fractions. The predictions compared very well with measured results and were the basis for 13 conclusions. The rest of the executive summary outlines some of the details of the project.

RATIONALE

The broad objective was to relate diesel fuel exhaust emissions to chemical composition and physical properties. The approach usually used for such a study has been to blend or analyze full boiling-range test fuels for engine studies. In the current work, the broadest region of concentrations of the various hydrocarbon types encountered in diesel fuel was preserved by working with the diesel fuel components directly, rather than specification fuels. To separate the effects of boiling range (or molecular weight), distillation was used as a probe of the test fuels, and by this means, a broad range of physical properties was also obtained.

This emphasis on stretching the boundaries of physical and chemical variables assured good coverage of the variable space for the mathematical correlation of measured performance and emissions. This course was settled upon because a study of pure compounds in the diesel range represents an impossible amount of work, and the ability to describe the multiple interactions is not developed. The more practical approach

of making narrow boiling-range cuts and using hydrocarbon type analyses gave good coverage of the variables and still allowed attribution of results to the hydrocarbon stream used for the source.

The correlations were used to design low-emission, proof-of-concept test fuels in the last phase of the work. This too required careful reasoning in the choice of general diesel specifications. While exploring the lowest emissions available from the current set of 10 diesel blendstocks, the blends were kept within specifications recognizable by contemporary engines. Also, by making several low-emission test fuels, the effect of cetane number was allowed to float and represents the options facing engine designers and regulators today.

FEEDSTOCKS

In today's refineries, diesel fuel is blended from a variety of streams in the 350° - 650°F (177° - 343°C) boiling range, but it is the materials made from boiling-range conversion processes that are most often implicated in poor performance and emissions. These problem materials include products of coking and cracking. Accordingly, feedstocks for the *Diesel Assay* were:

- light cycle oil (LCO), product of catalytic cracking
- light coker gas oil (LCGO), made by thermal cracking

Cracked materials typically come from gas oil or residuum conversion and thus represent the higher-boiling, more aromatic materials in the refinery. A typical, high quality diesel component was selected to balance the blends:

- straight-run diesel (SRD), a paraffinic basestock

An alternative fuel stock available in pilot-plant quantities and attractive to consider for future use in diesel fuel is the diesel fraction of indirect coal liquefaction such as Fischer-Tropsch (F-T) liquid.

In this study, two different F-T diesels were included:

- diesel distillate (F-T1), from Arge wax cracking
- straight-run diesel (F-T2), from the Air Products DOE pilot plant

These materials are almost all paraffins and represent a high cetane-number candidate for diesel blending.

PROCESSING

Hydrogenation was used at two severities: (1) to lower sulfur to ~0.05 mass%, and (2) to lower aromatic concentration to 10 vol%. These levels were chosen in view of current and projected pollution-control regulations, which prescribe limits on sulfur and aromatics. For all work, commercial nickel molybdenum catalyst was used with reactor temperatures in the 630° - 710°F range and pressure 600 - 2300 PSIG. The SRD was low in sulfur, so only a low aromatic, straight-run diesel was produced (LASRD). For the LCO and LCGO, both low sulfur (LSCLO and ISLCGO) and low aromatic (LALCO and LALCGO) products were produced. The F-T liquids required no processing. All the processing work was done in the U.S. Department of Energy (DOE) Alternative Fuels Utilization Program, Alternative Fuel Center at Southwest Research Institute, which was established under the DOE Alternative Fuels Utilization Program (AFUP).

This work yielded 10 materials for further study. The first step was to distill each of the 10 liquids into six to eight fractions of approximately 40°F (22°C) boiling range. The distillations were conducted with

a procedure similar to the ASTM D 2892 vacuum distillation. This gave a set of 80 samples, each approximately two liters in volume, for laboratory and combustion testing.

LABORATORY ANALYSES

The suite of laboratory analyses was applied to the 80 fractions made by vacuum distillation. These tests were selected to emphasize the properties believed to be most responsible for performance and emissions, aromatic structure and boiling range. The tests included:

- Distillation
 - D 86
 - D 2887
- Hydrocarbon Type
 - D 1319, FIA
 - D 2425, GC-MS
 - NMR
 - UV Aromatics
- Density
- Elemental
 - carbon, D 3178
 - hydrogen
 - sulfur, D 2622
- Aniline Point
- Smoke Point
- Pour Point & Cloud Point
- Viscosity
 - 40°C
 - 100°C
- Refractive Index

The multiple measures for aromatics represented by the four hydrocarbon type methods were chosen because of variation in values determined among aromatics content measurement methods. While some duplication resulted, different purposes were served including a more definitive determination in the case of the NMR analysis and more widespread availability exemplified by ASTM D 1319 Fluorescent Indicator Analysis (FIA).

COMBUSTION TESTING

CVCA

The 80 fuels in the main fuel matrix were tested at three different temperatures and pressures in a constant volume combustion apparatus. The results of these experiments, in the form of autoignition delay times, were used to develop Arrhenius expressions of the delay time as functions of temperature. These results indicated that the ignition delay times were strong functions of the boiling point distribution and the temperatures. The activation energies were also observed to be related to the boiling point distribution. Cetane numbers, determined from the delay times, also were strongly related to the boiling point of the fuel fractions and the feedstocks used to produce the fractions.

VCR Engine Tests

The 80 fuels were also tested at six different speed-load conditions in a direct-injection, variable-compression-ratio (VCR) test engine. The engine was designed specifically for fuels evaluation, and incorporated a bore-to-stroke ratio, swirl ratio, injection system characteristics, and combustion chamber geometry similar to current technology, two-valve engines. The engine was used to rate the ignition quality of the materials and to document the performance and emissions characteristics at five different speed-load test conditions.

STATISTICAL ANALYSIS

The results of the ignition quality measurements, in terms of a VCR cetane rating, compared very well with similar results obtained in the CVCA. The performance and emissions data were used to develop regression equations for the emissions and selected performance parameters in terms of the fuel composition and properties. Eighty-one different fuels and engine combustion variables were included in the statistical analysis. Preliminary analysis indicated the importance of (1) aromatic type and quantity, (2) cetane number, (3) boiling point, and (4) relationships to other hydrocarbon constituents. These relationships all appeared to be linear in the range of interest in this study.

CLEAN FUEL STUDY

The fact that the fuel properties were linearly related to the emissions justified the use of linear programming to design 10 low-emissions fuels using the same blendstocks and components that were used to develop the data base. These new fuels were tested following the same procedures that had been used in measuring the properties of the 80 test fuel samples. The results indicated that using standard linear programming techniques, where the emissions were treated as properties of the components used in the blending, that low emissions fuels can be formulated using the emissions as blending parameters of the fuel.

Introduction

Contemporary diesel fuel is a blend of several refinery streams chosen to meet specifications. The need to increase yield of transportation fuel from crude oil has resulted in converting increased proportions of residual oil to lighter products. This conversion is accomplished by thermal, catalytic, and hydrocracking of high molecular weight materials rich in aromatic compounds. The current efforts to reformulate California diesel fuel for reduced emissions from existing engines is an example of another driving force affecting refining practice: regulations designed to reduce exhaust emissions. Although derived from petroleum crude oil, reformulated diesel fuel is an alternative to current specification-grade diesel fuel, and this alternative presents opportunities and questions to be resolved by fuel and engine research.

Various concerned parties have argued that regulations for fuel reformulation have not been based on an adequate data base. Despite numerous studies (Ryan et al., 1981; and Ryan, and Erwin 1994), much ambiguity remains about the relationship of exhaust parameters to fuel composition, particularly for diesel fuel. In an effort to gather pertinent data, the automobile industry and the oil refiners have joined forces in the Air Quality Improvement Research Program (AUTO/OIL) to address this question for gasoline (Burns, et al., [1992]). The objective of that work is to define the relationship between gasoline composition and the magnitude and composition of the exhaust emissions. The results of the AUTO/OIL program will also be used, along with other data bases, to define the EPA "complex model" for reformulated gasolines. Valuable insights have been gained for compression ignition engines in the Coordinating Research Council's VE-1 program, but no program similar to AUTO/OIL has been started for diesel fuel reformulation. A more detailed understanding of the fuel/performance relationship is a readily apparent need.

The increasingly stringent restrictions on emissions from diesel fuel-powered vehicles pose a challenge for both existing petroleum fuels and proposed fuels from alternative sources. The U.S. Environmental Protection Agency (EPA) regulation limit particulates to 0.25 grams per braking horse power-hour (g/bhp-hr) in 1991 for trucks and 0.1 g/bhp-hr for city buses in 1993; in 1994, the limit will drop to 0.1 g/bhp-hr for all vehicles (Slodowske et al., [1992]). Canada is expected to adopt the same limits eventually, and Mexico will have similar standards for urban vehicles.

EPA has not prescribed the method for meeting the emissions requirements for diesel engines. Engine manufacturers have developed significantly cleaner engines without meeting the proposed standard in all cases. EPA issued regulations that limit sulfur content of diesel fuel to 0.05 weight percent (wt%) and impose a minimum 40 cetane index to cap aromatics content at present levels (Federal Register, 1989). The California Air Resources Board has also announced regulations that control diesel fuel sulfur content to less than 0.05 wt% and the aromatics content to less than 10 vol%.

Available data indicate that the control of sulfur, aromatics, and cetane number will add significantly to the cost of producing diesel fuel. Moreover, the cost will probably increase further because the legislative forces driving the quality of gasoline generally have adverse effects on the quality of diesel fuel feed and blending stocks. These factors, and the ultimately limited supply of petroleum, place continued importance on the role of alternative fuels in transportation.

This report presents the findings, of our study "Diesel Fuel Assay of Performance and Emissions". With the broad objective of relating diesel exhaust emissions and diesel performance to chemical composition and physical properties, this study also addressed the more specific concerns of the effect of hydrocarbon type. Southwest Research Institute (SwRI) chose the starting materials to provide insight about source and

upgrading method as they affect ignition quality and emissions from different samples meeting the same limits on sulfur and aromatics, but with different processing histories.

Background Literature

Sulfur and aromatics concentrations increase with boiling point. For example, lower concentrations of aromatics and sulfur typically occur in D-1 fuel, whose boiling range of 300°– 550°F (149° – 288°C) is lower than that of D-2 fuel with a 350°– 650°F (177°– 343°C) range. What has not been shown is which of the highest boiling components are most responsible for particulate emissions or which components of refinery streams would benefit the most from processing to reduce emissions precursors (Grant et al., 1991). The approach used for determining the effects of fuel composition on engine behavior has been to blend or measure full boiling range fuels for engine tests (Tosaka et al., 1989). For instance, studies at the University of Wisconsin (Foster et al., 1987) and the Pennsylvania State University (Buzza et al., 1987) found little effect on performance and emissions attributable to fuel composition.

In contrast, Weidmann (1988) found that fuel properties have a small, measurable effect on emissions using a VW 1.67-liter, 4-cylinder engine. Hydrocarbon emissions were found to be a function of fuel cetane number, with volatility exerting a stronger influence for low cetane-number fuels. Particulate formation was a strong function of fuel density and distillation range.

Southwest Research Institute studied engine emissions for the U.S. Bureau of Mines to investigate the effect of diesel fuel composition to benefit engines used in underground mines (Ryan, 1986). Test fuels included reference diesel, JP-7 (a narrow-cut jet fuel with extremely low aromatic and sulfur contents and naturally high cetane number), alcohol/diesel mixtures, water/diesel emulsions, and methane with pilot injection. The results of these experiments indicated that the jet fuel was lower in emissions than diesel, but that the water emulsions were more effective in reducing both nitrogen oxides (NO_x) and particulates. Aromatics and sulfur were also shown to affect particulate emissions. Fortnagel et al., (1983) found NO_x, hydrocarbon (HC), carbon monoxide (CO), and particulate emissions to be subject to aromatic content in a Mercedes Benz prechamber-type engine. Gairing (1985) found large effects on exhaust emissions and fuel consumption attributable to fuel properties.

The work of Ullman et al., (1989,1990), in support of the CRC VE-1 Program, demonstrated that dominant fuel parameters affecting diesel engine performance and emissions are sulfur content, cetane number and aromatics content. Recently reported work by Miyamoto et al., (1992), McCarthy et al., (1992), Nikanjam (1993), and Cowley et al., (1993) all confirmed these findings, with the general consensus that sulfur content has a significant effect on the particulate emissions, and the cetane number may be the dominant factor in controlling both the particulate and the NO_x emissions.

The diversity of these results is typical of the literature and emphasizes the strong influence that the engine type has on emissions from a given fuel. These studies were also performed with full-boiling fuels and made no attempt to segregate fuel properties by boiling range. Cookson et al., (1988) attempted to determine the effect of hydrocarbon-type composition on the diesel index (Method IP21) and cetane index (ASTM D 976) in 54 fuels, again using full-boiling materials.

Objective

The overall objective of this work was to determine the relationships between the fuel feedstocks and fuel processing, properties, and composition, and the resulting combustion and emissions characteristics in a diesel engine. One tool for this determination was the selection of blendstocks, rather than full-boiling

diesel fuels; therefore, a subordinate goal was to choose materials with greatest significance for performance and emissions — the cracked stocks and aromatics.

Approach

Achieving the primary objective required meeting several intermediate objectives. These intermediate objectives included producing a consistent set of performance, emission, and composition measurements on a matrix of diesel fuel components distinguished by source and processing history. To do this, we had to obtain careful physical and chemical characterizations.

The next step was the use of boiling range as a probe for the measured properties, and this goal was achieved by producing narrow distillation cuts of the test fuels much like fractions are produced in a crude oil assay. This led to the nickname for the project, the Diesel Fuel Assay.

The results obtained were evaluated for their ability to describe the influence of the measured properties on the ignition quality and exhaust composition of the test samples. These results were then mathematically fit to the property descriptions to derive predictive equations. Finally, a matrix of test fuels was prepared. In summary, the steps were:

- Feedstock selection and characterization
- Processing feedstock to controlled sulfur and aromatics compositions
- Fractionation and detailed analysis of products and fractions
- Updating combustion tests to reflect near-term technology
- Performance and emission tests of stocks, products, and fractions
- Study and correlation of analyses and combustion tests
- Demonstration and verification by low-emission fuel blends

Figure 1 shows the sequence of operations for making test fuels. Petroleum and coal-derived components were selected to represent the most difficult portions of the blending pool to conform to performance and emission goals of modern diesel engines. The petroleum components were reduced in sulfur and aromatic content by pilot-plant hydrogenation before distillation into selected boiling point ranges. The approach attempted to improve on the resolution of previous studies using full-boiling test fuels by examining the five starting materials in narrow fractions of the diesel fuel boiling range.

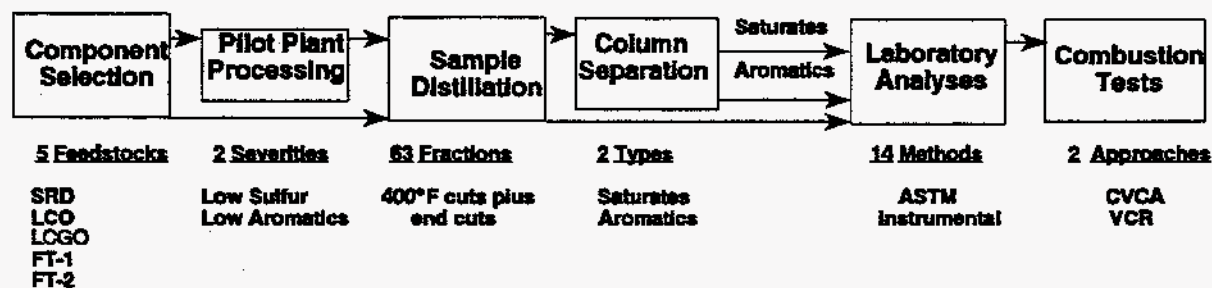


Figure 1. Sequence of operations for making the test fuels

We analyzed the resulting fractions of feedstocks and products for chemical composition and physical properties that would be most revealing for ignition quality and particulate generation. All samples were then tested for engine performance and emissions. Correlations of the emission behavior were used to guide the blending of proof-of-concept test fuels. This "Clean Fuel Study" was intended to deliver low-emission fuels while observing all other necessary (ASTM D 975-type specifications) properties. The low-emission fuels were tested in a similar manner as were the original samples. The details for each of the steps are presented in the following sections.

Materials and Processing

In modern refinery practice, diesel fuel has become a blended product composed containing a variety of streams in the 350°F – 650°F boiling range. The need to increase the yield of transportation fuel from crude oil has resulted in converting increased proportions of gas oil (>440°F or >227°C) and residual oil (resid) to lighter products. This is accomplished by thermal, catalytic, and hydrocracking of higher carbon number compounds rich in aromatics. Of the refinery streams blended into diesel fuel, the higher boiling and more aromatic ones are implicated in particulate and hydrocarbon emissions.

Products from resid conversion and gas oil cracking contribute a variety of aromatic and high molecular weight compounds to the diesel fuel blending component pool. In this study, we chose the test components to emphasize the streams which present the greatest challenge to performance and emissions.

Petroleum Stocks and Products

Efforts were made to obtain typical streams of the desired composition from willing refiners. Accordingly, we choose feedstocks for this study to include products from resid conversion and gas oil cracking. The test components ultimately chosen were:

- full-boiling straight-run diesel (SRD)
- light cycle oil from catalytic cracking (LCO)
- light coker gas oil (LCGO)

These materials, their products of pilot-plant processing (having controlled sulfur and aromatics concentration), and two Fischer-Tropsch samples were examined in laboratory and engine tests. The properties of the feedstocks appear in Table 1.

Fischer-Tropsch (F-T) Liquids

Two F-T liquids were considered in the current work to compare with the petroleum stocks. Indirect coal liquids pose opportunities for diesel fuel both as a Btu source for motive force and as a high-cetane, low-emission component for exhaust emissions control. F-T liquids are synthetic products made from coal or other sources by gasification followed by reaction over a polymerization catalyst bed. The products of this process are almost entirely normal paraffins. The DOE Office of Coal Conversion provided the first material. The production and properties of this F-T distillate are fully described by Bludis et al., 1991. An imported Arge wax was subjected to hydrocracking to produce liquid in the distillate boiling range. We have designated this material FT1.

The second F-T sample was made by Air Products under DOE Contract (Bhatt et al., 1993). The materials were supplied as hydrocarbon liquid and light wax. These samples were combined in a ratio of 1.6:1 according to their proportion in production. This material, being lower in boiling range than the

Table 1. Feedstock Properties

Test	ASTM Method	Straight-Run Diesel	Light Cycle Oil	Light Coker Gas Oil	Fischer-Tropsch1	Fischer-Tropsch2
Density Specific Gravity °API g/mL	D 1298	0.8458 35.8 0.8453	0.9490 17.6 0.9485	0.8676 31.6 0.8671	0.7770 50.6 0.7767	0.8081 43.6 0.8077
Distillation, °C/°F	D 86					
IBP*		353	367	385	368	363
5%		428	457	420	396	391
10		466	476	435	407	406
30		523	509	462	449	461
50		551	536	492	502	509
70		581	573	528	550	547
90		635	634	574	592	588
95		657	656	590	606	606
EP*		672	689	608	620	627
Carbon, wt%	D 3178	86.82	88.84	85.18	84.92	82.62
Hydrogen, wt%		13.31	9.84	12.58	15.12	13.76
Sulfur, wt%	D 2622	0.052	0.69	1.41	0.003	0.031
Hydrocarbon Type, vol%	D 1319					
Saturates		74.7	20.9	41.7	97.8	ND
Olefins		1.0	3.6	5.9	1.1	
Aromatics		23.6	75.5	52.4	1.1	
Viscosity @ 40°C @ 100°C	D 445	3.52 1.34	3.16 1.20	2.56 1.10	2.42 1.05	
Refractive Index @ 20°C	D 1218	1.4718	1.5537	1.4797	1.4342	1.4414
Cetane Index	D 976 D 4737	52.6 54.6	26.1 23.89	39.3 38.9	75.4 81.4	62.2 64.6
UV Aromatics Analysis Wt% Aromatic Carbon	Total Mono Di Tri	11.4 4.3 5.8 1.3	43.7 6.3 28.3 9.1	15.7 8.4 5.9 1.4	0.2 0.0 0.0	1.6 0.1 0.0
Cloud point, °C/°F	D2500	1/34	-10/14	Too dark	-20/-4	-5/23
Pour point, °C/°F	D 97	-1/30	-12/10	-30/-22	-20/-4	-7/19
Aniline point, °C/°F	D 611	73.0/163	9.8/50	47.6/118	92.8/199	43.2/110
Smoke point, mm	D 1322	17.2	6.2	13.3	35+	40.0

* IBP - Initial boiling point; EP - End point; ND - Not Determined

Arge wax, contained light process oils and oxygenates. From this mixture, a 350°– 650°F straight-run diesel sample was distilled, designated FT2.

Both F-T liquids were fractionated into controlled boiling-range samples. Batches of about 40 liters were distilled in a stainless steel distillation column under vacuum, and these samples were reserved for laboratory and engine testing.

Processing

The three petroleum feedstocks were processed to reduce sulfur and aromatics, then distilled into analytical samples. The processing and distillation sequence was shown in Figure 2. The LCO and LCGO were hydrogenated at two severities to reduce sulfur to 0.05 mol% and aromatic concentration to 10 vol% (per ASTM D 1319). These levels were chosen in contemplation of the limits being applied to diesel fuel in California and nationally. The straight-run diesel was naturally low in sulfur and was hydrotreated at one severity to reduce aromatics to 10 vol%. The F-T stocks required no hydrogenation.

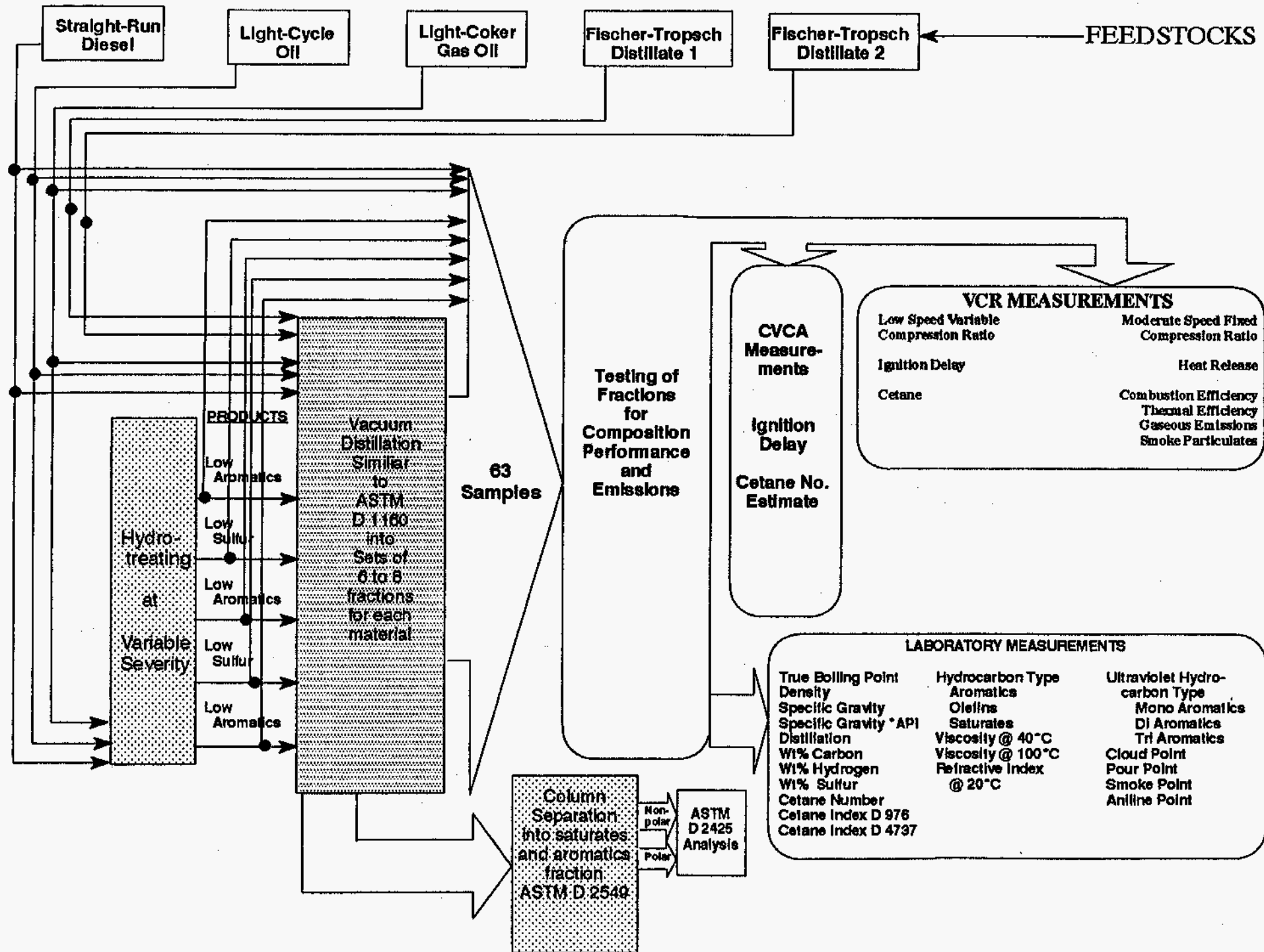
The hydrotreating was performed in the pilot plant of the U.S. DOE Alternative Fuel Center at Southwest Research Institute.¹ The reactor was a fixed bed (7.5 ft × 2 in. diameter), containing 1.56 gallons of Criterion Trilobe HDN 60 nickel-molybdenum catalyst. The feedstocks were combined with hydrogen gas preheated, and fed to the top of the reactor bed. After the reactor, two stages of pressure letdown and product separation removed unreacted hydrogen and byproduct gases. The hydrogen was cleaned and recycled, and the product was stripped to remove light ends and dissolved gases.

The process parameters for the hydrogenations are summarized in Table 2. The principal measure of processing severity is the liquid hourly space velocity (LHSV), an inverse expression of residence time in the reactor equal to the feed flowrate divided by the reactor volume expressed in consistent units.

Table 2. Processing Parameters

	Avg Temp, °F/°C	Total Press, psig	Feed Rate, gal/hr	Total H ₂ , SCFH	LHSV, hr ⁻¹
STRAIGHT-RUN DIESEL					
High severity — low aromatics	630/332	1500	1.6	60	1.03
LIGHT-CYCLE OIL					
Low severity — low sulfur	710/377	650	1.9	110	1.05
High severity — low aromatics	686/363	2300	0.74	130	0.41
LIGHT COKER GAS OIL					
Low severity — low sulfur	650/343	600	2.2	140	1.22
High severity — low aromatics	676/358	2200	0.98	117	0.56

¹DOE Subcontract XS-2-12130-1



Distillation

Efforts to separate fuels such as these into the individual compounds have been partially successful in the laboratory. However, the number of compounds is extremely large, and therefore, it is, not possible to study the combustion of each individual compound and all the possible interactions among the various compounds. A more practical approach — and the one used in this project — is to separate the fuels into a reasonable number of fractions that can be studied in detail.

Each of the five feedstocks and the five hydrotreated products were distilled under vacuum into congruent (corresponding cut point) boiling-range fractions. The following boiling point ranges were selected for the cuts:

Fraction 1	Fraction 2	Fraction 3	Fraction 4	Fraction 5	Fraction 6	Fraction 7
Initial Boiling Point - 440°F	440° - 480°F	480° - 520°F	520° - 560°F	560° - 600°F	600° - 640°F	640° - End Point
<227°C	227°- 249°C	249°- 271°C	271°- 293°C	293°- 315°C	315°- 338°C	>338°C

Approximately 40 liters of each material were charged to a stainless steel kettle and column, which was operated along the lines of a ASTM D 1160 distillation. The actual ranges of the sample fractions differed from these ideal cuts, and boiling range comparisons should be made among the cuts of closest temperature range rather than fraction number. The number of fractions distilled from each feedstock and product vary in number depending on the boiling range of the starting material. The most even alignment of fractions is presented in Table 3. With the original five materials, the processed products, and all their fractions, 80 samples comprised the test fuel matrix for the Diesel Assay.

LABORATORY EVALUATION

The five basestocks, five hydrotreated products, and their distillation fractions were characterized by physical and chemical tests and by combustion experiments as shown in Figure 2. The results appear in Appendix A as Tables A-1 through A-10 and were the subject of an American Chemical Society paper (Erwin, 1992). The laboratory measurements listed in the tables were applied to each of the 80 fractions made by vacuum distillation. The list includes two measures of aromatic content: D 1319 and the ultraviolet (UV) method (Kohl et al., 1991). Similar information can be inferred from the nuclear magnetic resonance (NMR) measurements. The fluorescent indicator analysis (ASTM D 1319) is widely used and is included in emissions regulations. This analysis is regularly applied to diesel fuel samples, although the method is designed for deparaffinized gasoline and relies on measurements of column length taken up by saturates, aromatics, and olefins, made visible by fluorescent dye, hence the name FIA (fluorescent indicator analysis). The vol% aromatics determined this way can be affected by cycloparaffins or polar materials. The low aromatic content and high cycloparaffin content of FT1, as well as the oxygenates in FT2, made the results of D 1319 unworkable for these samples.

The UV method compares sample absorbance at selected wavelengths with reference spectra of solutions of aromatics composed of representative compounds in the diesel boiling range. Because the absorbance is proportional to the aromatic rings, wt% aromatic carbon is reported without regard to substituents. Both methods are indirect, so instrumental analysis by gas chromatography/mass spectrometer (GC/MS) and NMR were indicated.

The hydrocarbon-type determinations by ASTM D 2425 are presented in Appendix A, Tables A-11 through A-15. This method requires a separation of each sample into polar and nonpolar fractions, which

Table 3. Corresponding Boiling Ranges of Fractions

Feed	#1	#2	#3	#4	#5	#6	#7	#8
°E Selected Temp. Ranges	<400 <204	400-440 204-227	440-480 227-249	480-520 249-271	520-560 271-293	560-600 293-316	600-640 316-338	640+ 338+
IBP-EP and 5%-95% shown (°F)								
STRAIGHT-RUN DIESEL								
FL-1627	FL-1793	FL-1794	FL-1795	FL-1796	FL-1797	FL-1798	FL-1799	FL-1800
°F 353-672	282-475	452-515	476-529	502-556	536-576	570-610	610-643	657-698
°C 178-356	139-246	233-268	247-276	261-291	280-302	299-321	321-339	347-370
°F 428-657	324-462	464-506	484-521	509-550	542-568	576-602	616-638	663-691
°C 220-347	162-219	240-263	251-272	265-288	283-298	302-317	324-337	351-366
Vol%	11.5	9.0	8.0	16.5	16.5	14.0	11.0	13.5
LOW-AROMATIC STRAIGHT-RUN DIESEL								
FL-1873	FL-1876	FL-1877	FL-1878	FL-1879	FL-1880	FL-1881	FL-1882	FL-1883
°F 262-664	201-351	361-455	427-488	474-526	520-562	559-597	605-641	659-715
°C 128-351	94-177	183-235	219-253	246-274	271-294	293-314	318-338	348-379
°F 380-644	212-334	381-447	438-480	480-515	528-557	567-591	613-635	670-705
°C 193-340	100-168	194-231	226-249	249-268	276-292	297-311	323-335	354-374
Vol%	5.0	10.0	9.5	15.0	16.5	17.5	13.5	13.0
LIGHT-CYCLE OIL								
FL-1538	FL-1555	FL-1556	FL-1557	FL-1558	FL-1559	FL-1560	FL-1561	-
°F 367-689	382-460	442-492	477-518	508-544	542-575	578-614	616-734	-
°C 186-365	194-238	228-256	247-270	264-284	283-302	303-323	324-390	-
°F 457-656	384-449	444-479	481-503	514-534	546-566	582-601	636-709	-
°C 236-347	196-232	229-248	249-262	268-279	286-297	306-316	336-376	-
Vol%	8.9	9.2	19.9	15.0	14.3	11.7	21.0	-
LOW-SULFUR LIGHT-CYCLE OIL								
FL-1615	FL-1850	FL-1851	FL-1852	FL-1853	FL-1854	FL-1855	FL-1856	-
°F 392-682	317-510	422-544	458-548	495-572	533-595	593-630	641-738	-
°C 200-361	158-266	217-284	237-281	257-300	278-312	312-332	324-390	-
°F 436-642	356-481	440-516	469-533	502-559	541-585	593-622	645-727	-
°C 224-339	180-249	227-269	243-278	261-293	283-307	312-328	341-386	-
Vol%	12.3	15.7	20.5	16.5	14.1	10.0	10.9	-
LOW-AROMATIC LIGHT CYCLE OIL								
Lo-Arom LCO	(#0)*	(#1)*	(#2)*	(#3)*	(#4)*	(#5)*	(#6)*	-
FL-1562	FL-1566	FL-1567	FL-1568	FL-1569	FL-1570	FL-1571	FL-1572	-
°F 390-657	340-419	402-453	439-488	472-514	511-544	543-574	599-715	-
°C 199-347	171-215	206-234	226-253	244-268	266-284	284-301	315-379	-
°F 354-694	354-411	411-439	444-474	476-501	513-534	546-565	603-694	-
°C 179-368	179-210	211-226	229-246	247-261	267-279	286-296	317-368	-
Vol%	11.3	13.9	17.8	18.3	15.1	10.0	13.6	-

**Table 3. Corresponding Boiling Ranges of Fractions
(Continued)**

Feed	#1	#2	#3	#4	#5	#6	#7	#8
LIGHT-COKER GAS OIL								
FL-1440	FL-1546	FL-1547	FL-1548	FL-1549	FL-1550	FL-1551	-	-
°F 385-608	379-461	440-491	480-526	521-565	559-595	599-645	-	-
°C 196-320	193-238	227-255	249-274	272-296	293-313	315-341	-	-
°F 420-590	391-436	445-478	485-512	529-551	564-583	601-635	-	-
°C 216-310	199-224	229-248	252-267	276-288	296-306	316-335	-	-
Vol%	25.0	17.0	17.0	16.0	13.0	18.0	-	-
LOW-SULFUR LIGHT-CYCLE GAS OIL								
FL-1442	FL-1862	FL-1863	FL-1864	FL-1865	FL-1866	FL-1867	-	-
°F 380-599	337-457	379-453	421-492	462-526	500-550	558-607	-	-
°C 193-315	169-236	193-234	216-256	239-274	260-288	292-319	-	-
°F 416-572	354-441	395-467	430-481	472-512	510-543	565-624	-	-
°C 213-300	179-227	202-242	221-249	244-267	266-284	296-329	-	-
Vol%	13.5	15.5	19.5	18.0	15.5	18.0	-	-
LOW-AROMATIC LIGHT-CYCLE GAS OIL								
FL-1443	FL-1597	FL-1598	FL-1599	FL-1600	FL-1601	FL-1602	FL-1603	-
°F 412-612	358-430	394-466	429-485	466-520	498-546	537-574	585-644	-
°C 211-322	181-221	201-241	221-252	241-271	259-286	281-301	307-340	-
°F 429-597	371-421	401-449	442-477	472-509	506-536	547-570	594-632	-
°C 221-314	188-216	205-232	228-247	244-265	263-280	286-299	312-333	-
Vol%	8.5	15.5	18.3	16.1	15.0	12.5	14.0	-
FISCHER-TROPSCH 1								
FL-1840	FL-1898	FL-1899	FL-1900	FL-1901	FL-1902	FL-1903	FL-1904	-
°F 368-620	336-456	386-474	424-488	467-521	511-557	547-589	595-638	-
°C 187-327	169-236	197-246	218-253	242-272	266-292	286-309	313-337	-
°F 396-606	352-438	395-463	436-482	477-511	519-549	555-583	605-633	-
°C 202-319	178-226	202-239	224-250	247-266	271-287	291-306	318-334	-
Vol%	20.0	11.5	11.0	11.5	13.0	15.5	15.7	-
FISCHER-TROPSCH 2								
FL-2095	FL-2115	FL-2116	FL-2117	FL-2118	FL-2119	FL-2120	FL-2121	-
°F 363-627	216-392	316-428	358-537	392-522	442-526	482-565	529-603	-
°C 184-331	102-200	158-220	181-281	200-272	228-274	250-296	276-317	-
°F 391-606	266-372	326-408	377-459	418-482	462-516	506-558	549-591	-
°C 199-319	130-189	163-209	192-237	214-250	239-269	263-292	287-311	-
Vol%	16.3	10.1	12.0	10.5	18.2	17.3	15.7	-

* LA-LCO fractions were numbered differently as shown.

is a laborious process. To remain within budget, groups of samples were mixed to represent the middle portion of the boiling range in some cases, as noted on the tables. We believed that little information would be lost by combining similar samples in this way. This presumption was verified by measuring the whole set of samples for the low-aromatic straight-run diesel. In these tables, the usual D 2425 report for saturates and aromatics was simplified into a unified listing of hydrocarbon types for each sample.

This characterization of the test fuel and fuel fractions was aimed at identifying the components in fuel that contribute to differences in engine performance in terms of both power and emissions. A comprehensive analysis of the diesel fuel would entail identifying each compound present in the fuel (if such level of detail were possible). This approach would create more data than could be reasonably handled and is extremely time-consuming and expensive, requiring two-dimensional GC analysis and laborious interpretation of the resulting data.

The next set of results concern the nuclear magnetic resonance spectroscopic examination of the samples. The work was performed at the University of Utah Chemistry Department. Table A-16 lists the regions of chemical shift into which the responses for the samples were divided. The instrumental procedures for the integration of these samples included:

1. Long acquisition time (AT) is used to guarantee the necessary digital resolution.
2. Wide spectral width (SW = 20000 \rightarrow 40 ppm) is used to guarantee that all protons are equally excited.
3. Long d1 delay used to let protons fully recover between pulses.

The procedure for making the quantitative integration of the NMR spectra was as follows: Each spectrum was first phased manually to have as flat a baseline as possible. Next, the spectrum was individually referenced to the observed TMS line. The spectrum was then accurately divided into five chemical-shift regions (Table A-16). This division of shifts has been used for correlation of fuel properties in the past (Bailey et al., 1986). The baseline was again corrected with the TMS line also covered by a segment of the integration line; integration was taken after the segment has been removed.

The results for all samples are reported in Table A-17. Variability (uncertainty) with each value is reported in the table because the reproducibility of manual phasing could not be guaranteed. By repeated integration on selected spectra the variability was estimated as around $\pm 1.0\%$. For example, 30.5 should be read as $30.5 \pm 1.0\%$.

COMBUSTION EXPERIMENTS

SwRI has developed two different apparatus and procedures specifically for determining the effects of fuel composition on performance and emissions. Several different pure compounds, fuel blends, and fuel components have already been evaluated in these devices in previous DOE-sponsored projects at SwRI (Ryan, 1987).

Ignition Quality

Ignition quality was determined in a constant volume combustion apparatus (CVCA). A small quantity of sample is injected into a volume of hot air to simulate the conditions in a compression ignition engine cylinder for estimation of cetane number. The CVCA, described in detail by Ryan (1985) and Ryan et al. (1987, 1988) is shown schematically in Figure 3. The equipment consists of the constant volume combustion bomb, a single-shot fuel injection system, and a data acquisition system to monitor the various temperatures and pressures as the fuel is injected into the bomb, ignites, and burns. The pressure in the bomb is measured and used to determine the ignition delay and the combustion rates. The ignition delay

times, measured at various initial temperatures, have been used to develop Arrhenius expressions for the delay time as functions of temperature. In addition, the ignition delay time has been used to determine the cetane number using a procedure described below.

The CVCA has been used to determine the cetane number of unknown fuels by comparing the ignition delay time of the unknown fuels to a calibration of cetane number versus the ignition delay time. The calibration is developed using several different blends of the primary reference fuels — hexadecane and heptamethylnonane. Researchers have observed in previous studies that the calibrations shift periodically. They have found, however, that the calibrations can be checked and adjusted using the results of measurements of the 100 cetane number (CN) reference fuels. In the work reported here, the calibrations were checked daily, and the calibrations did not shift appreciably over the duration of the measurements. The CVCA measurements were studied by Ryan et al, (1992), who measured the ignition and basic combustion characteristics at three different initial temperatures in the CVCA.

Engine Tests

The results obtained to measure combustion quality and emissions were from a single-cylinder research engine designed at SwRI for studying fuel effects on combustion. The engine, described in detail by Ryan (1987), was modified for this work to be representative of current-technology, two-valve per cylinder engines. The engine was used to perform two types of experiments. Each fuel was rated for ignition quality in one procedure and tested for emissions and performance in another procedure involving five speed-load test conditions (termed Modes 1 through 5). Details of the engine design and configuration are presented in this section, as are the test conditions and test procedures.

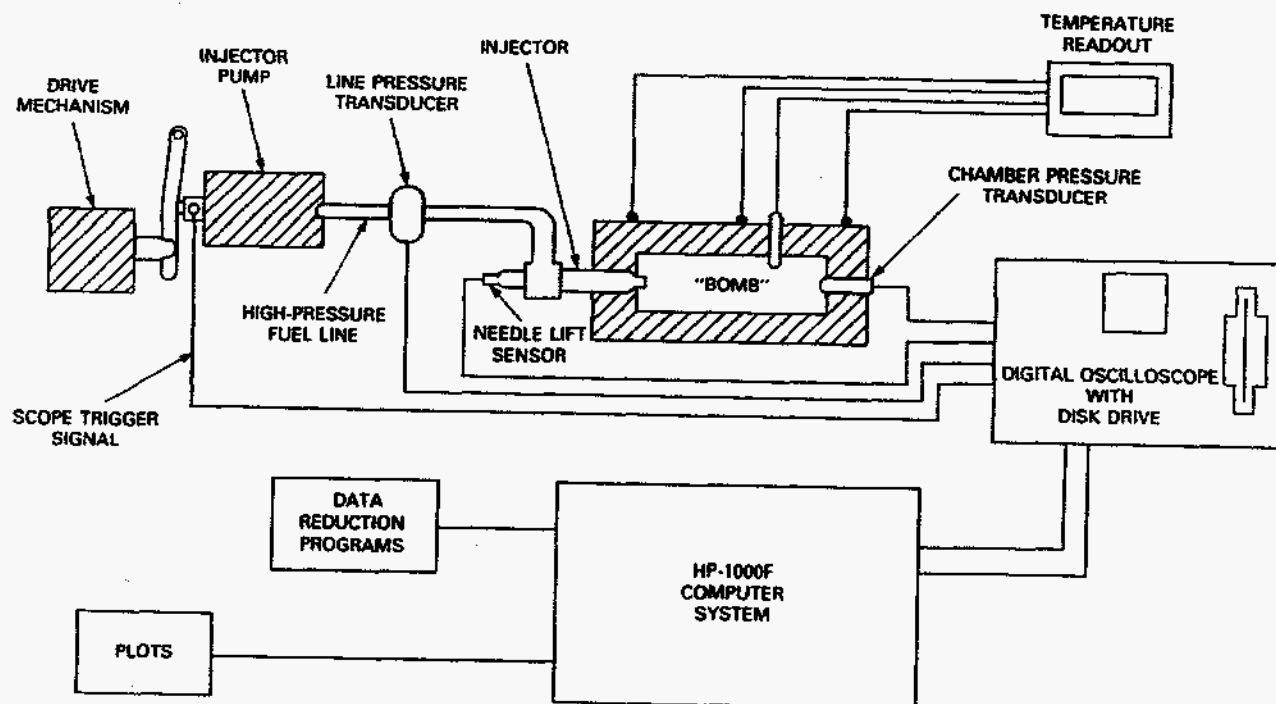


Figure 3. Constant volume combustion apparatus

Test Engine

The test engine is a single-cylinder research engine designed at SwRI for fuel-combustion research. The general configuration is a two-valve, direct-injection, variable compression ratio (VCR) engine. The design is based on a CLR-type crankcase and a head and cylinder liner assembly designed and built at SwRI. Variable compression ratio is achieved by moving the head and cylinder liner assembly relative to the centerline of the crankshaft. A variation from 12:1 to 20:1 compression ratio was possible in the configuration used for these experiments.

The engine was modified to be geometrically similar to current, two-valve engines. The modifications, as compared to the previously reported configuration (Ryan et al., 1988), included a new connecting rod length and stroke length to achieve the desired bore-to-stroke ratio, and a modified intake port and valve to achieve a swirl ratio of 2.7. The analysis used to arrive at this head design is presented in Appendix B. The head and cylinder liner assembly are shown schematically in Figure 4, and details of the engine configuration are presented in Table 4.

Instrumentation

The amounts of test fuel available for testing were generally limited; therefore, efforts were made to minimize the quantity of fuel required for flushing and filling the fuel system. Fuel flow was measured volumetrically using a calibrated burette that was connected to both the fill and return ports of the injection pump. The intake air was supplied using a large compressor. The air temperature, pressure, and humidity were all controlled, and air flow rate was measured and controlled using a metering control valve.

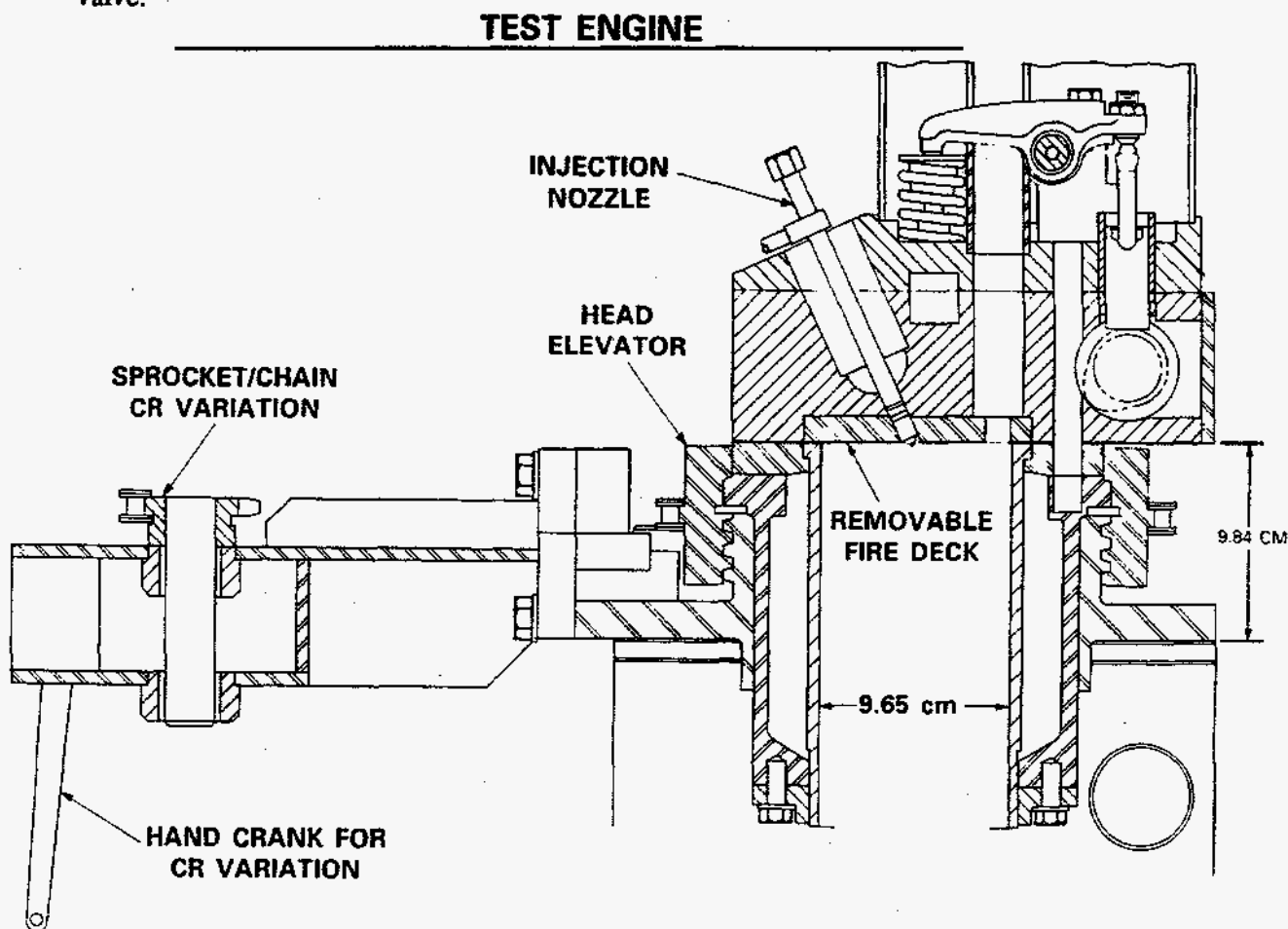


Figure 4. volume combustion ratio profile schematic

Table 4. Engine Specifications

Bore × Stroke (mm)	96.5 × 104.9
Rod Length (mm)	166.5
Corrosion	12:1 to 20:1
Displacement (cm ³)	767.2
Deck Height (mm)	7.9 to 0.4
Injection Pump (mm × mm)	11 × 11
Injection Pressure (MPa)	100
Combustion Chamber	Mexican Hat
Re-entrant	
Re-entrant Angle	25°
Bowl Opening (mm)	43.3
Bowl Depth (mm)	19.3
Swirl Ratio	2.7

The engine temperatures and pressures were monitored using a PC-based data acquisition system that logged the data every 30 seconds. A water-cooled piezoelectric pressure transducer was installed in the combustion chamber to measure the cylinder pressure. These data, as well as the corresponding injection pressure and nozzle needle lift data, were logged every 0.5 degree of crankshaft rotation, using a Preston Scientific A/D and Hewlett Packard A900 computer system. We used a First Law Analysis of the cylinder pressure data to compute heat release rates, which were used as an indication of combustion quality.

The exhaust emissions were sampled downstream of a mixing tank located in the exhaust of the engine. The gases were analyzed for CO₂ and CO using nondispersive infrared spectroscopy. Hydrocarbons were measured using a flame ionization detector. Nitrogen oxides (NO_x) were measured using a chemiluminescence instrument, and smoke was determined using a Bosch smoke meter.

Test Procedures

Each of the test fuels was examined in two different types of experiments in the engine. First, each fuel was rated for ignition quality following a procedure very similar to that used in the standard cetane rating procedure (ASTM D 613).

The procedure developed for ignition quality rating was based on operating the engine at a selected "standard condition" for both the test fuels and selected blends of the primary reference fuels for cetane rating (Hexadecane with a CN of 100, and Heptamethylnonane with a CN of 15). Table 5 lists the conditions that were selected for this work. The injection timing was fixed at 12° Before Top Dead Center (BTDC). The engine was operated on each reference fuel blend, and the compression ratio varied until ignition occurred at Top Dead Center (TDC). A calibration curve was then developed in which the cetane number was presented as a function of the compression ratio. The test fuels were then operated at the "standard condition," and the compression ratio was varied to give ignition at TDC. This compression ratio was then used in the calibration curve to determine the cetane number.

Table 5. Test Condition for Ignition Quality Rating

Speed	900 rpm
Air/Fuel Ratio	50:1
Injection Timing	12° BTDC
Intake Temperature	38°C
Intake Pressure	115 kPa
Coolant Temperature	66°C

The calibration curve used in this work is presented in Figure 5, along with the regression equation for the data. The test conditions were selected to give the broadest possible variation of compression ratio for the range of cetane number used in the reference fuel blends.

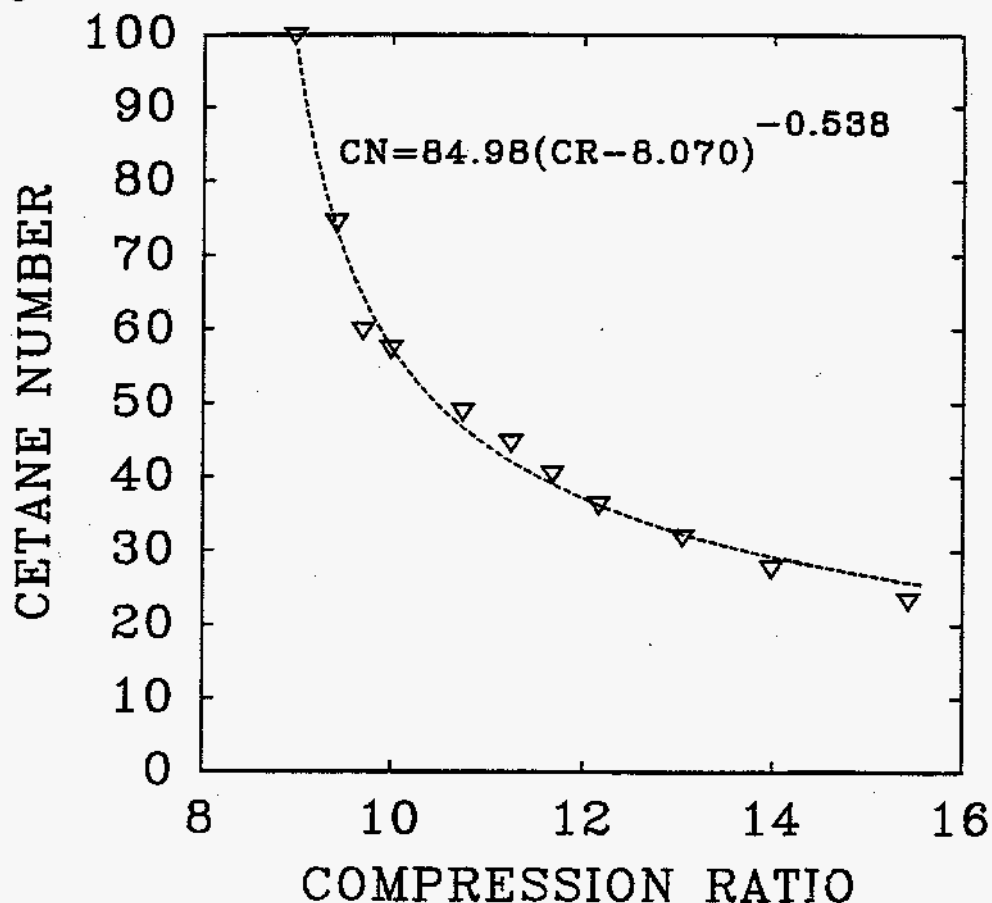


Figure 5. Cetane number calibration curve

Performance and emissions data were obtained at five different test conditions or modes. These data consisted of the normal power and efficiency measurements, as well as engine heat-release analysis and gaseous emissions and smoke. The test conditions included rated torque at fixed timing, rated torque using the best torque timing for each fuel, the rated power condition, and two part-load conditions at the rated power speed. Details of the modes are presented in Table 6.

Table 6. Test Condition for Performance and Emissions.

Mode	Speed (rpm)	Air Fuel Ratio	Injection Timing
1	1200	28:1	3° BTDC
2	1200	28:1	Variable
3	1500	28:1	3° BTDC
4	1500	40:1	3° BTDC
5	1500	50:1	3° BTDC

Results and Discussion

ANALYSES

The laboratory analyses were selected to cover the ASTM D 975 specification properties and to measure gross chemical composition categories, which correlate most strongly with performance and emissions. The set of ASTM tests in Figure 1 were applied to the cuts from fractional distillation. Table 7 presents a partial list of the results, with the complete set in Appendix A.

Aromatics

Figure 6 shows the effect of hydrotreating the LCGO as reflected in the changing aromatic carbon distribution. The curve for the feedstock shows high aromatics across the boiling range with increasing values in the high end of the curve. This result is one reason that some people have suggested a limitation of the 90% distillation temperature as a way of reducing particulate emissions. Mild hydrotreating to reduce sulfur concentration lowered the curve about 20%. High severity hydrotreating made the desired reduction in aromatics, but made the greatest reductions in the upper end of the boiling range representing polycyclic aromatics, which contribute most strongly to particulate emissions. The distribution of aromatics by all of the fuels are presented in Figures 7 to 9. Figure 10 details the distribution of aromatic carbon by UV for LCO by ring type and processing severity

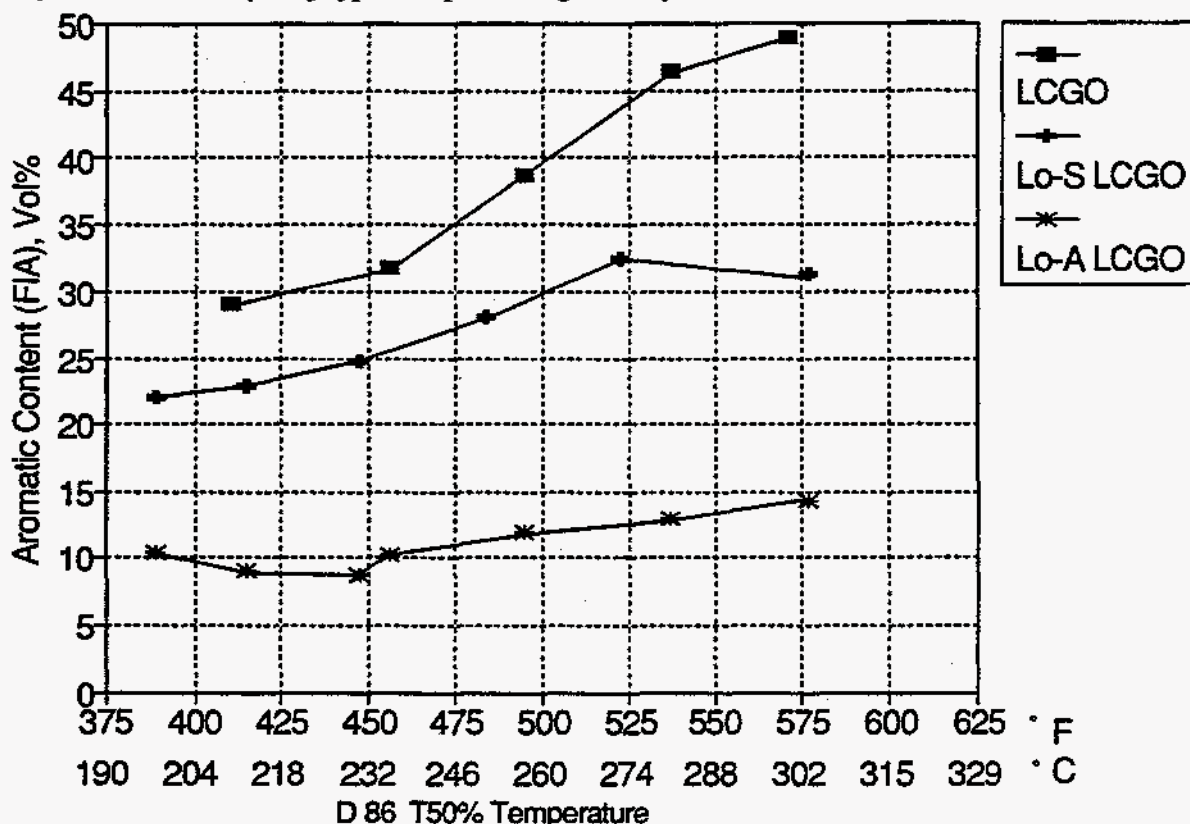


Figure 6. Aromatic carbon versus the 50% point temperature for LCGOs

The trend for high-severity hydrogenation to limit total aromatics showed the greatest decrease in polycyclics. The overall reduction in monocyclic aromatics was slightly greater for higher boiling ranges.

Table 7. Partial Results for Distillation Fractions

Property	Feed	#1	#2	#3	#4	#5	#6	#7	#8
STRAIGHT-RUN DIESEL									
Specific Gravity	0.8458	0.8146	0.8445	0.8483	0.848	0.845	0.847	0.859	0.863
Distribution °F	241/288	170/207	241/249	252/259	268/273	284/288	303/307	325/328	352/356
T10/T50 °C	116/142	426/97	116/121	122/126	131/134	140/142	150/152	163/164	178/180
T90/EP °F	335/356	233/246	261/268	269/276	283/291	296/302	314/321	334/339	364/370
°C	168/180	112/119	127/131	132/136	139/144	147/150	157/161	168/171	184/188
Cetane Index D976/D4737	52.6/54.6	41.4/41.5	44.8/45.1	46.0/47.0	49.0/52.2	52.8/59.3	54.5/64.8	52.7/66.2	52.0/80.7
LOW-AROMATIC STRAIGHT-RUN DIESEL									
Specific Gravity	0.8280	0.7892	0.8251	0.8373	0.8368	0.8304	0.8203	0.8314	0.8373
Distribution °F	228/282	116/137	197/207	227/233	250/257	277/281	297/303	324/327	356/362
T10/50 °C	109/139	47/58	92/97	108/112	121/125	136/138	147/151	162/164	180/183
T90/EP °F	328/351	162/177	226/235	246/253	266/274	289/294	308/314	333/338	371/379
°C	164/177	72/81	108/113	119/123	130/134	143/146	153/157	167/170	188/193
Cetane Index D976/D4737	57.7/60.1	13.0/23.8	37.4/38.1	42.6/42.7	49.3/51.3	56.7/64.1	62.1/78.4	61.7/81.5	60.5/82.2
LIGHT-CYCLE OIL									
Specific Gravity	0.9490	0.8849	0.9147	0.9321	0.9440	0.9541	0.9685	0.9979	NS
Distribution °F	247/280	196/210	231/237	251/254	268/272	287/289	306/309	339/344	NS
T10/T50 °C	119/138	91/99	111/114	122/123	131/133	142/143	152/154	171/173	
T90/EP °F	334/365	228/256	245/256	259/270	277/284	294/302	313/323	358/390	NS
°C	168/185	109/124	118/124	126/132	136/140	146/150	156/162	181/199	
Cetane Index D976/D4737	26.1/23.8	20.2/19.4	22.6/17.8	23.8/17.5	25.5/18.6	26.7/20.1	26.9/20.2	24.9/20.6	NS
LOW-SULFUR LIGHT-CYCLE OIL									
Specific Gravity	0.9200	0.8849	0.9082	0.9153	0.9230	0.9352	0.9484	0.9497	NS
Distribution °F	239/270	188/218	229/242	244/253	262/271	284/292	313/317	343/351	NS
T10/T50 °C	115/132	87/103	109/117	118/123	128/133	140/144	156/158	173/177	NS
T90/EP °F	323/361	243/266	261/284	272/287	287/300	394/313	325/332	372/392	NS
°C	162/183	117/130	127/140	133/142	142/149	201/156	163/167	189/200	NS
Cetane Index D976/D4737	43.5/44.1	36.4/37.4	38.0/38.2	40.7/40.5	42.7/42.7	44.5/45.5	47.2/52.6	NS	NS

NS - No Sample

**Table 7. Partial Results for Distillation Fractions
(Continued)**

Property	Feed	#1	#2	#3	#4	#5	#6	#7	#8
LOW-AROMATIC LIGHT CYCLE OIL									
Specific Gravity	0.8628	0.8479	0.8623	0.8676	0.8708	0.8745	0.8703	0.8448	NS
Distribution °F	215/253	183/196	211/217	230/234	247/252	268/271	286/282	319/327	NS
T10/50 °C	102/123	84/91	99/103	110/112	119/122	131/133	141/139	159/164	NS
T90/EP °F	305/347	208/215	222/234	243/254	259/268	277/284	294/301	354/379	NS
°C	152/175	98/102	106/112	117/123	126/131	136/140	146/149	179/193	NS
Cetane Index D976/D4737	40.1/39.8	24.6/24.5	28.8/26.5	33.3/31.0	37.4/35.3	40.9/40.3	45.0/47.3	56.9/72.3	NS
LIGHT-COKER GAS OIL									
Specific Gravity	0.8676	0.8403	0.8565	0.8740	0.8871	0.8927	0.9094	NS	NS
Distribution °F	224/256	202/210	230/236	252/256	277/281	296/299	317/321	NS	NS
T10/T50 °C	107/124	94/99	110/113	122/124	136/138	147/148	158/161	NS	NS
T90/EP °F	301/320	221/238	245/255	264/274	286/296	304/313	329/341	NS	NS
°C	149/160	105/114	118/123	129/134	141/147	151/156	165/172	NS	NS
Cetane Index D976/D4737	39.3/38.9	33.3/32.6	37.0/35.6	37.9/36.0	39.2/38.3	40.6/41.8	38.8/41.6	NS	NS
LOW-SULFUR LIGHT-CYCLE GAS OIL									
Specific Gravity	0.8463	0.8184	0.8299	0.8403	0.8524	0.8628	0.8697	NS	NS
Distribution °F	219/247	182/198	204/213	222/231	245/251	267/273	297/303	NS	NS
T10/T50 °C	104/119	83/92	96/101	106/111	118/122	131/133	147/151	NS	NS
T90/EP °F	289/315	219/236	228/242	245/256	262/274	282/288	314/329	NS	NS
°C	143/157	104/113	109/117	118/124	128/134	139/142	157/165	NS	NS
Cetane Index D976/D4737	43.5/44.1	36.4/37.4	38.0/38.2	40.7/40.5	42.7/42.7	44.5/45.5	47.2/52.6	NS	NS
NS - No Sample									

**Table 7. Partial Results for Distillation Fractions
(Continued)**

Property	Feed	#1	#2	#3	#4	#5	#6	#7	#8
LOW-AROMATIC LIGHT-CYCLE OIL									
Specific Gravity	0.8393	0.8203	0.8265	0.8324	0.8418	0.8490	0.8498	0.8524	NS
Distribution °F	224/255	190/199	207/214	225/231	246/251	264/269	287/291	315/317	NS
T10/T50 °C	107/124	88/93	97/101	107/111	119/122	129/132	142/144	157/158	NS
T90/EP °F	302/322	212/221	227/241	242/252	262/271	277/286	297/301	328/340	NS
°C	159/161	100/105	108/116	117/122	128/133	136/141	147/149	164/171	NS
Cetane Index D976/D4737	48.0/49.2	36.1/36.6	39.7/39.9	43.6/44.0	46.1/47.2	47.9/50.3	51.7/57.7	53.8/65.9	NS
FISCHER-TROPSCH 1									
Specific Gravity	0.7770	0.7538	0.7633	0.7710	0.7783	0.7853	0.7913	0.7989	NS
Distribution °F	208/261	179/189	203/213	226/234	248/254	272/277	292/297	319/324	NS
T10/T50 °C	98/127	82/87	95/101	108/112	120/123	133/136	144/147	159/162	NS
T90/EP °F	311/327	216/236	233/246	246/253	264/272	285/292	304/309	331/337	NS
°C	155/164	102/113	112/119	119/123	129/133	141/144	151/154	166/169	NS
Cetane Index D976/D4737	75.4/81.4	62.7/67.2	67.9/73.3	71.0/78.9	73.2/84.2	74.9/90.4	75.1/95.4	74.6/102. 2	NS
FISCHER-TROPSCH 2									
Specific Gravity	0.8081	0.7783	0.7936	0.8058	0.8086	0.8104	0.8132	0.8146	NS
Distribution °F	406/509	274/306	334/354	380/403	424/442	468/489	514/537	557/571	NS
T10/T50 °C	208/265	134/152	168/179	193/206	218/228	252/254	268/281	292/299	NS
T90/EP °F	588/627	354/392	395/428	442/537	470/522	508/526	553/565	585/603	NS
°C	309/331	179/200	202/220	228/281	243/272	264/274	289/296	307/317	NS
Cetane Index D976/D4737	62.2/64.6	28.9/35.3	37.3/40.5	44.7/46.2	51.6/53.8	58.6/63.2	63.2/72.3	65.5/80.1	NS

NS - No Sample

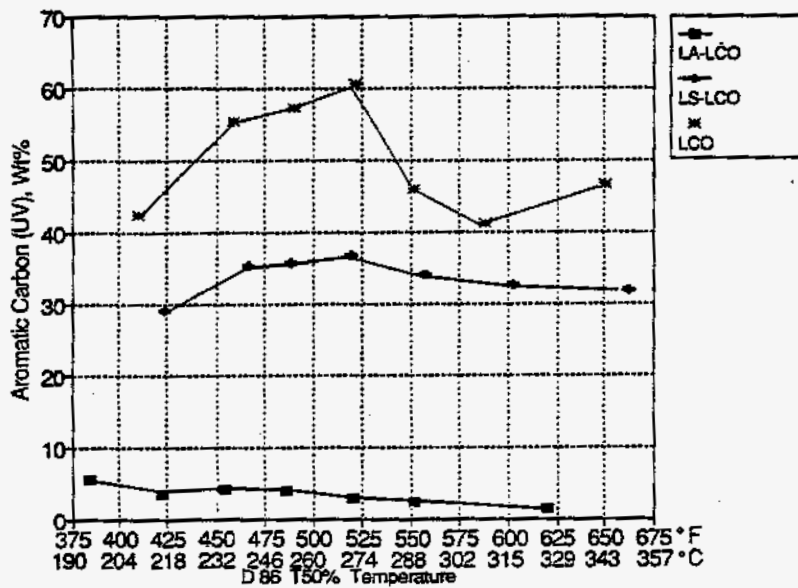


Figure 7. Aromatics vs boiling point for the LCOs

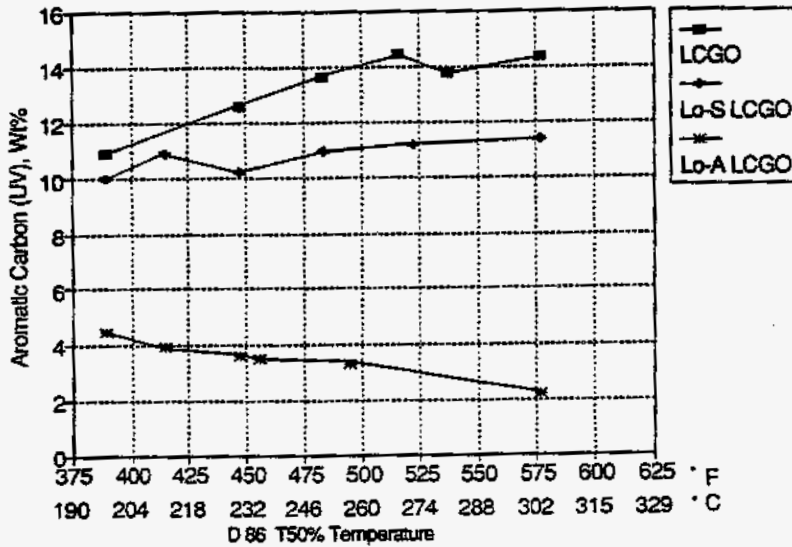


Figure 8. Aromatics vs boiling point for the LCGOs

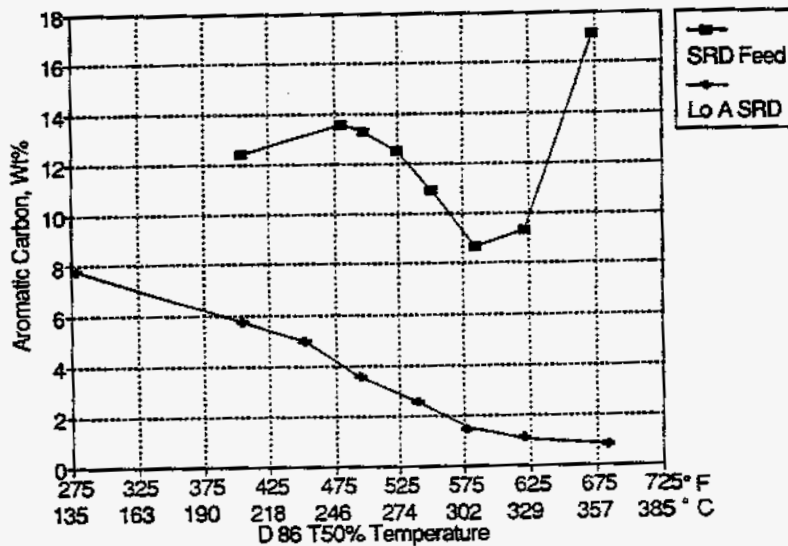


Figure 9. Aromatics vs boiling point for the SRDs

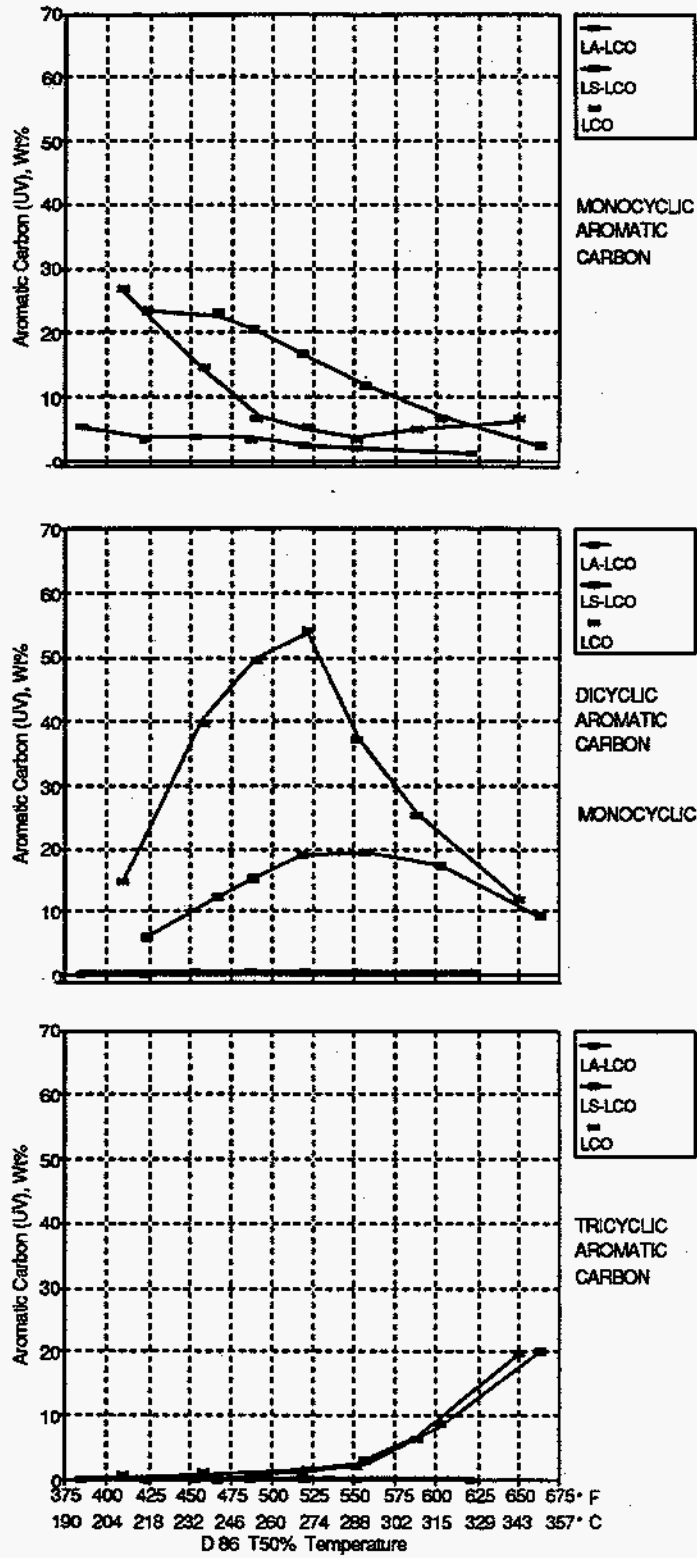


Figure 10. LCO aromatics distribution

The aromatics are uniformly distributed over the boiling range for the light-cycle oils, as seen in Figure 7. Moderate hydrotreatment accomplished significant reduction of the sulfur without a significant effect on the aromatics content. Severe hydrotreating had a significant effect on the aromatics, and hydrotreating was effective in reducing the aromatics over the entire boiling range, as seen in Figure 7.

The results for the light-coker gas oils presented in Figure 8 indicate that the aromatics are concentrated in the heavier fractions, at least for the raw material. Hydrotreating first to the low-sulfur level and then for reduced aromatics was effective in lowering the aromatic content of the heavier fractions.

The aromatic content of the straight-run diesel fuel is uniformly distributed across the boiling range. Unlike the higher aromatic content light-cycle oil, however, hydrotreating was much more effective in reducing the aromatics content of the heavier fractions.

The results for aromatic composition of the LCO are presented in the series of graphs of Figure 10. This series of graphs is representative of the changes made by hydrogenation. The total aromatic carbon was reduced moderately in concentration as the sulfur was reduced by low severity treatment. The distribution of aromatics decreased most in the highest-boiling point fractions, which display the most tricyclic compounds. A similar decrease is noted for dicyclic aromatics, but monocyclics increase across the boiling range. In addition to creating corresponding cycloparaffins from the two- and three-ring aromatics, the hydrogenation opened rings in the multicycles to form alkylbenzenes distributed throughout the lower boiling ranges.

The above results suggest that hydrotreating could be used more effectively to reduce the aromatics content of fuels if selected fractions of certain feedstocks are treated. The results also suggest that the proposed reductions in the end point of diesel fuels for emission control will have a significant effect on the aromatics content of fuels from selected feedstocks, in addition to the benefits obtained from the decrease in volatility.

Cetane Index

The plot of cetane index versus 50% recovered temperatures (T50) by D 86 in Figure 11 was made by two estimating methods — ASTM D 976 and D 4737. Both correlations use density and T50, but in different ways. D 976 uses API gravity and T50 in two terms, while D 4737 uses specific gravity and T50 in four terms. Furthermore, the new four-term correlation used a larger fuel matrix including cracked components and shale oil to develop its correlation. D 4737 gave lower cetane index in the front end of the boiling range and higher estimates in the back end. These calculations may be compared with the CVCA and VCR results below where the fractions at highest boiling ranges increased the most in ignition quality from the whole fuel. This is consistent with the results of Weidmann et al., (1988) for full-boiling test fuels.

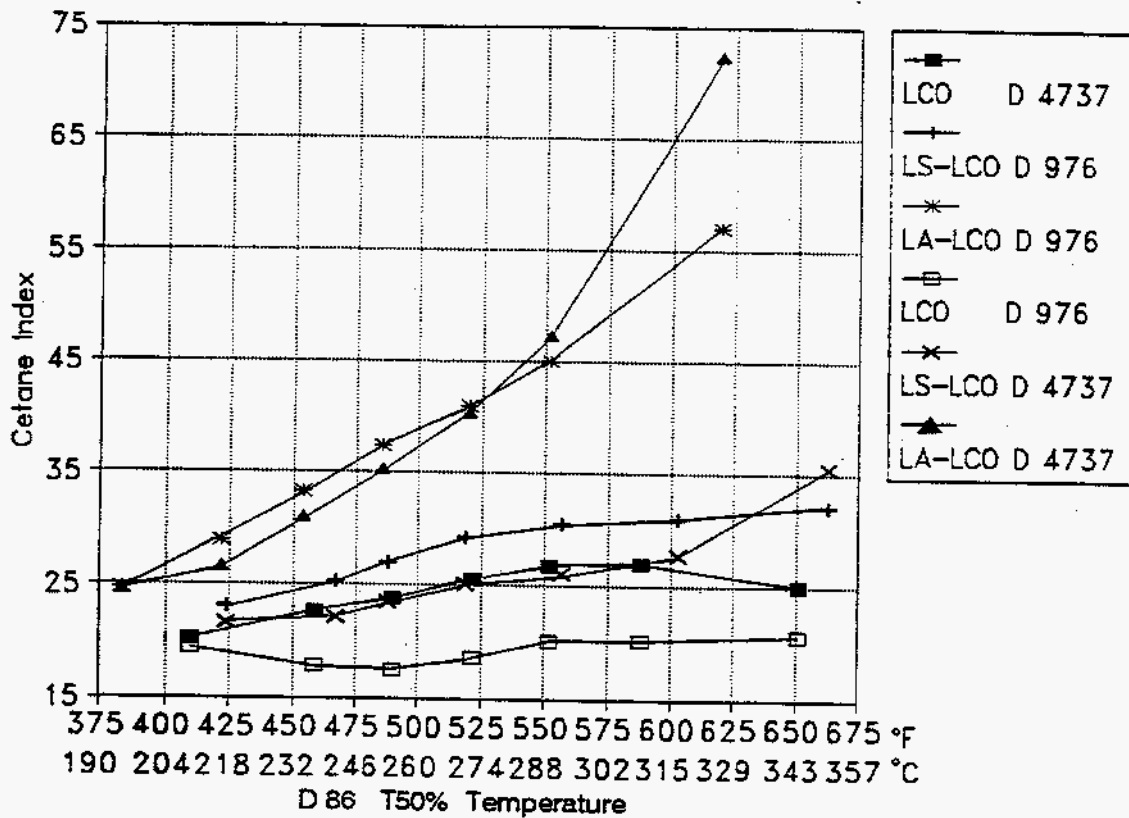


Figure 11. Cetane index by ASTM D 976 and D 4737 versus LCO D 86 50% temperature

The corresponding results for cetane index of the LCGO and its hydrotreated products are presented in Figure 12.

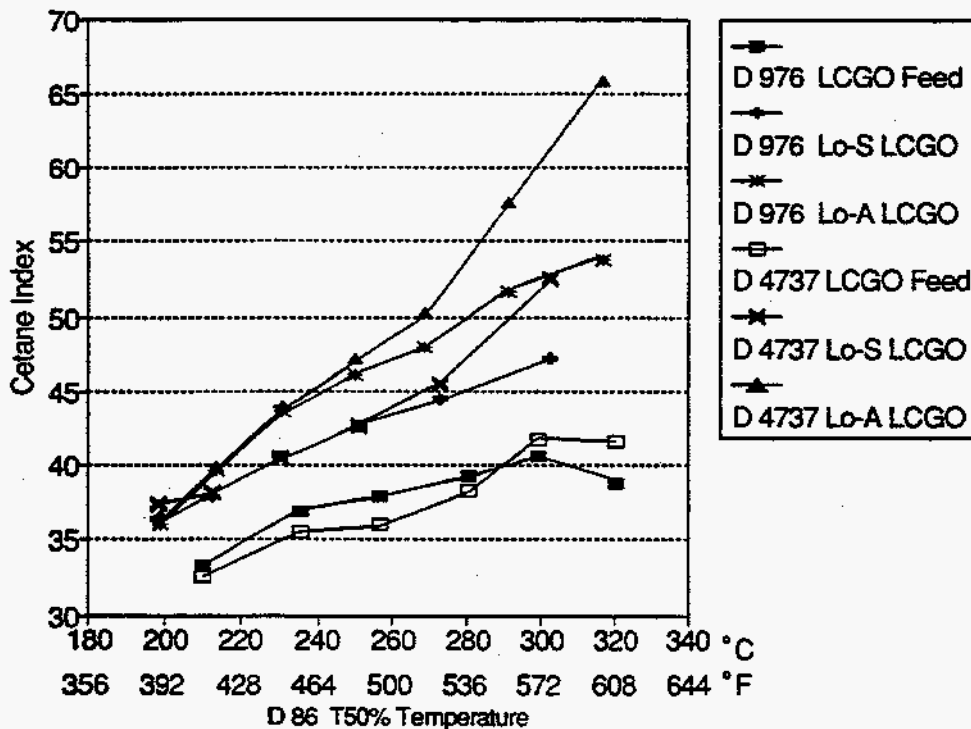


Figure 12. Cetane Index versus the 50-percent point for the LCGOs

CVCA RESULTS

The early goals of the CVCA development work included both the short-term goal of determining cetane number and the broader goal of providing an improved measure of ignition-quality specification. The CVCA was also developed to rate nonspecification fuel. For the latter goal, we measured the ignition delay times on each test material at three initial temperatures (427°, 482°, and 582°C) and constant density.

The data generated at these initial temperatures were used to examine the Arrhenius nature of the ignition data. In addition, we used these data to examine a potential technique for directly rating the cold-start characteristics of fuels for diesel engines. In this cold-start study, calibrations using several different blends of the primary reference fuels were generated at each of the three different initial temperatures. The lower temperatures were selected to correspond to compression temperature during cold start, and the higher temperatures were selected to correspond to the estimated range of compression temperatures in the standard CFR engine during a fuel cetane rating evaluation.

The test fuels were rated using the three test conditions and calibrations. The effects of the three different initial temperatures are demonstrated in Figure 13 for the same blends of the primary reference fuels. The data have been reduced to hyperbolic form in terms of cetane number as functions of the ignition delay times. The results of this comparison indicate that even the *primary reference fuels* for cetane rating display different relationships between the cetane number and the ignition delay, depending upon the test temperature.

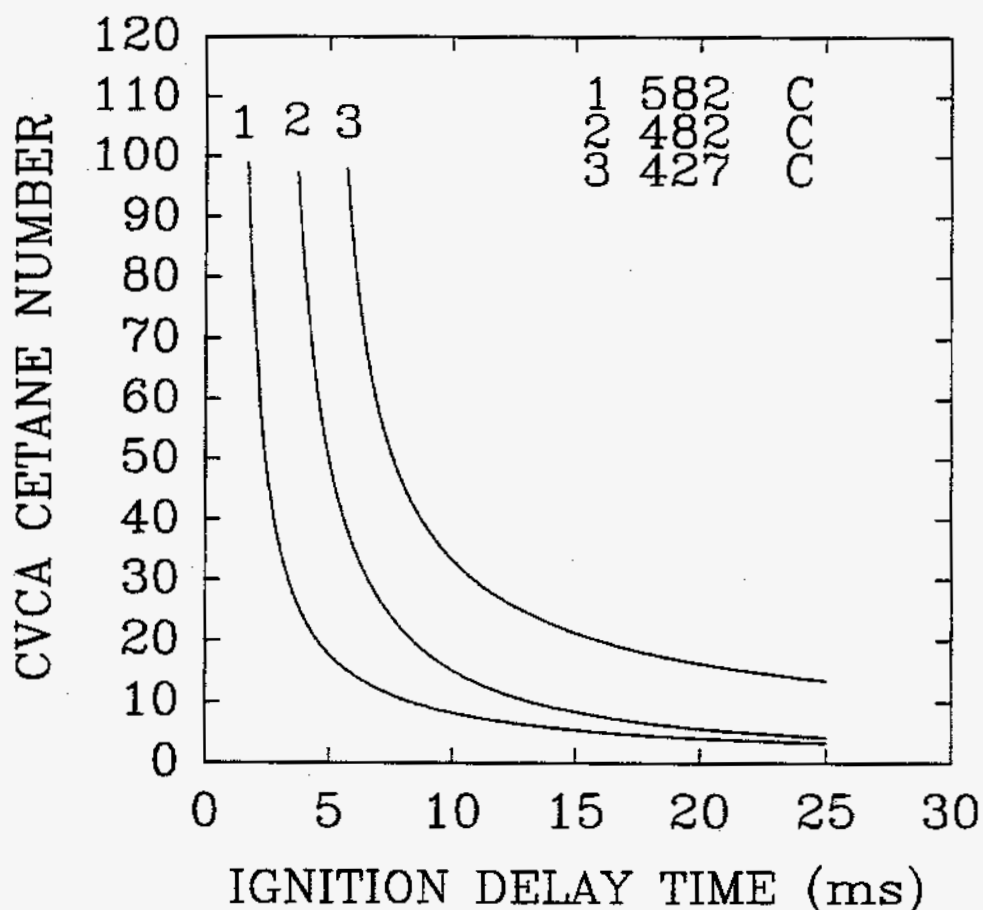


Figure 13. CVCA cetane number calibration curves

The experimental results are presented in Table 8 in the form of the ignition delay times and the corresponding cetane numbers for the three test temperatures. Included in Table 8 are the coefficients for the Arrhenius expressions of the ignition delay time as functions of the temperature. The activation energies that are a part of the A2 coefficients in Table 8 are significantly different for some of the materials, but are very similar for most of the materials. The values are in the range of 5 to 15 kcal, somewhat low, relative to other reported ignition values, but within the range of data obtained earlier with this apparatus Ryan et al., 1988; Siebers, 1985; Spadaccini et al., 1983).

Figure 14 is a bar chart showing the cetane ratings of each fraction for three light cycle oils at 582°C. The indicated cetane numbers of the light-cycle oils are low, but the addition of hydrogen causes the CN to increase somewhat in going to the low-sulfur material, and even more in the more severely processed low-aromatic material. Also, the cetane number is a function of the boiling point of the material. This is shown clearly in Figure 14 by the fact that cetane rating of the lower boiling fractions are all similar and the ratings of the heavier fractions are higher. The results for the other materials are similar, but the relationship between cetane number and the boiling point is not as pronounced for the light-coker gas oils and the straight-run diesel fuels. This can be seen by comparing the results for the LCOs in Figure 14 to the corresponding results for the light-coker gas oils in Figure 15 and the straight-run diesel fuels in Figure 16. As seen in Figures 15 and 16, the test temperature also has an effect on the ratings, with the rating generally increasing as the test temperature is reduced.

The cetane rating of the full-boiling materials is a volume-weighted composite of the individual ratings of the fractions. Consequently, the proposed reduction in the end-point specification of diesel fuels for particulate emission control will apparently have an adverse affect on the overall cetane number of the fuel, and possibly have a corresponding adverse effect on the NO_x emissions.

Addition of hydrogen to the feedstock has the effect of increasing the cetane number, as shown for the LCOs in Figure 14. The cetane rating trends upward in going from the feedstock to the processed materials. The 582°C test condition shows in Figure 14 that the effects of hydrogenation are more dominant in the higher boiling fractions. These trends are also more apparent at the lower test temperatures, as shown in Figures 14 to 16. These results also suggest that the proposed reduction in end point will have an adverse impact on the cetane number for the same level of hydrotreatment as the lower boiling ranges.

The light-coker gas oils all had higher cetane ratings than the corresponding light-cycle oils, as seen by comparing the results in Figure 14 to those in Figure 17. While there is a trend for concentration of the cetane rating in the higher boiling fractions, this trend is not as strong as for the light-cycle oils. In addition, it appears that the effects of hydrogenation are reduced; they are more uniformly distributed over the boiling range; and, they show less of an effect arising from test temperature than for the light-cycle oils.

Figure 18 presents the results for the straight-run diesel fuels at the 582°C test temperature. The cetane rating is distributed over the boiling range and is a function of the test temperature, with a general upward trend as the test temperature is decreased. The addition of hydrogen appears to have little effect on the cetane number of the materials. If there is a trend for hydrogenation severity, it appears to be one of *reduced* cetane number.

The relationships between cetane number and aromatics content are shown in Figure 19 for the three feedstocks used in this work. The cetane number appears linearly related to the aromatics content, at least for the specific samples used in this work. The intercepts of the two blendstocks are similar to each other

**Table 8. Ignition Delay Times, CVCA Cetane Numbers, and Arrhenius Coefficients
For Delay (ms) = A₁ exp (A₂/T)**

Sample Name	ID No.	@ 582°C (ms)	CN @ 582°C	@ 582°C (ms)	CN @ 482°C	@ 426°C (ms)	CN @ 426°C	Ln (A1)	A1	A2
LCO	FL-1538	6.2	15.5	9.0	18.6	14.2	21.6	-0.5	0.6	1315
FRAC. 1	FL-1555	6.3	15.2	12.2	11.9	23.8	11.0	-1.8	0.2	2105
FRAC. 2	FL-1556	6.6	17.0	10.8	14.3	16.2	18.1	-1.2	0.3	1692
FRAC. 3	FL-1557	-	-	-	-	-	-	-	-	-
FRAC. 4	FL-1558	6.9	13.9	11.2	13.5	24.9	10.4	-1.6	0.2	2009
FRAC. 5	FL-1559	6.2	15.6	10.6	14.7	18.1	15.6	-1.1	0.3	1708
FRAC. 6	FL-1560	5.9	16.3	9.5	6.6	14.7	20.6	-0.7	0.5	1452
FRAC. 7	FL-1561	5.0	19.1	8.1	22.2	16.0	18.4	-1.6	0.2	1821
LSLCO	FL-1615	5.4	17.9	8.1	20.5	11.2	30.4	-0.3	1.3	892
FRAC. 1	FL-1850	6.9	14.0	11.0	13.1	18.6	12.3	-0.9	0.4	1575
FRAC. 2	FL-1851	6.2	15.4	10.5	14.3	17.6	16.2	-1.0	0.4	1650
FRAC. 3	FL-1852	6.1	15.7	11.1	13.3	16.1	18.1	-0.9	0.4	1557
FRAC. 4	FL-1853	5.6	17.3	9.5	16.9	15.0	20.1	-1.0	0.4	1584
FRAC. 5	FL-1854	5.1	18.6	7.4	25.2	11.8	28.2	-0.7	0.5	1318
FRAC. 6	FL-1855	5.0	19.9	9.5	16.7	14.2	21.0	-1.3	0.3	1688
FRAC. 7	FL-1856	-	-	6.9	38.1	9.7	37.8	-	-	-
LALCO	FL-1562	2.8	38.4	5.7	37.9	7.6	57.0	-1.7	0.2	1616
FRAC. 0	FL-1566	4.4	22.4	7.0	27.0	10.5	33.5	-0.9	0.4	1402
FRAC. 1	FL-1567	4.0	24.5	4.7	30.5	9.2	41.5	-0.9	0.4	1276
FRAC. 2	FL-1568	3.4	30.1	6.0	36.3	9.0	43.2	-1.5	0.2	1558
FRAC. 3	FL-1569	3.3	31.4	6.3	32.9	9.2	41.7	-1.6	0.2	1654
FRAC. 4	FL-1570	2.8	39.6	5.7	39.9	8.7	45.0	-2.1	0.1	1848
FRAC. 5	FL-1571	2.6	42.1	5.6	41.1	7.9	53.5	-2.0	0.1	1767
FRAC. 6	FL-1572	1.9	77.2	4.2	74.3	6.3	83.4	-2.6	0.1	1926

**Table 8. Ignition Delay Times, CVCA Cetane Numbers, and Arrhenius Coefficients
For Delay (ms) = A₁ exp (A₂/T)
(continued)**

Sample Name	ID No.	@ 582°C (ms)	CN @ 582°C	@ 582°C (ms)	CN @ 482°C	@ 426°C (ms)	CN @ 426°C	Ln (A1)	A1	A2
LCGO	FL-1440	3.5	29.0	6.1	35.1	9.2	41.2	-1.4	0.2	1555
FRAC. 1	FL-1546	3.9	25.6	6.4	32.4	9.0	42.8	-1.0	0.4	1355
FRAC. 2	FL-1547	3.6	27.9	6.0	36.5	9.0	42.6	-1.2	0.3	1469
FRAC. 3	FL-1548	3.4	30.1	6.6	30.6	9.8	37.1	-1.7	0.2	1715
FRAC. 4	FL-1549	3.5	29.1	6.9	28.4	8.7	45.4	-1.3	0.3	1490
FRAC. 5	FL-1550	3.2	32.8	6.3	32.8	8.5	47.2	-1.6	0.2	1598
FRAC. 6	FL-1551	3.2	31.7	6.1	34.9	8.3	48.6	-1.4	0.2	1524
LSLCGO	FL-1442	3.1	33.3	5.9	37.0	9.2	41.5	-1.8	0.2	1726
FRAC. 0	FL-1862	3.6	28.2	6.3	33.6	10.6	33.1	-1.7	0.2	1734
FRAC. 1	FL-1863	3.4	29.5	6.4	32.5	9.4	39.8	-1.5	0.2	1618
FRAC. 2	FL-1864	3.5	29.2	6.1	35.3	8.8	44.1	-1.3	0.3	1502
FRAC. 3	FL-1865	3.4	30.4	6.5	31.3	7.7	56.1	-1.0	0.4	1348
FRAC. 4	FL-1866	3.1	33.7	6.3	32.9	8.6	46.3	-1.7	0.2	1651
FRAC. 5	FL-1867	2.8	37.8	5.8	38.6	7.5	59.3	-1.6	0.2	1564
LALCGO	FL-1443	2.9	37.7	5.6	42.2	8.3	49.4	-1.9	0.2	1710
FRAC. 0	FL-1597	3.6	28.2	6.8	28.9	11.7	28.5	-2.0	0.1	1887
FRAC. 1	FL-1598	3.3	30.5	6.1	34.8	9.3	40.4	-1.6	0.2	1642
FRAC. 2	FL-1599	3.2	31.7	5.8	38.0	8.3	48.7	-1.4	0.2	1515
FRAC. 3	FL-1600	3.1	33.7	5.7	39.8	8.2	50.6	-1.5	0.2	1557
FRAC. 4	FL-1601	2.8	39.0	5.7	39.2	7.9	53.7	-1.8	0.2	1681
FRAC. 5	FL-1602	2.6	44.1	5.3	45.7	6.7	72.2	-1.7	0.2	1564
FRAC. 6	FL-1603	2.2	54.9	4.9	39.2	7.2	62.6	-2.4	0.1	1887
SRD	FL-1627	2.2	56.2	5.3	45.9	7.5	58.6	-2.6	0.1	1976
FRAC. 1	FL-1793	3.1	33.9	5.8	37.9	8.9	43.4	-1.8	0.2	1705
FRAC. 2	FL-1794	2.7	41.1	4.3	70.8	8.0	52.6	-2.0	0.1	1717
FRAC. 3	FL-1795	2.7	40.5	5.3	45.6	7.6	58.8	-1.8	0.2	1664

**Table 8. Ignition Delay Times, CVCA Cetane Numbers, and Arrhenius Coefficients
For Delay (ms) = $A_1 \exp(A_2/T)$
(continued)**

Sample Name	ID No.	@ 582°C (ms)	CN @ 582°C	@ 582°C (ms)	CN @ 482°C	@ 426°C (ms)	CN @ 426°C	Ln (A1)	A1	A2
FRAC. 4	FL-1796	2.6	42.5	5.3	44.6	7.8	54.6	-2.0	0.1	175
FRAC. 5	FL-1797	2.5	45.1	4.7	56.5	7.3	61.8	-2.0	0.1	169
FRAC. 6	FL-1798	2.1	64.2	4.5	62.0	6.8	70.0	-2.6	0.1	192
FRAC. 7	FL-1799	-	-	4.5	60.3	6.2	84.0	-	-	-
LASRD	FL-1873	2.1	61.3	5.0	51.6	7.0	66.2	-2.5	0.0	194
									7	
FRAC. 0	FL-1876	4.2	23.1	7.6	24.5	12.7	25.3	-1.6	0.2	174
FRAC. 1	FL-1877	3.2	31.7	6.0	36.4	9.4	40.2	-1.7	0.2	169
FRAC. 2	FL-1878	2.8	38.6	5.7	39.4	7.4	59.9	-1.6	0.2	157
FRAC. 3	FL-1879	2.6	44.3	5.5	41.9	8.0	51.9	-2.2	0.1	184
FRAC. 4	FL-1880	2.4	48.8	5.0	50.8	7.4	60.6	-2.2	0.1	180
FRAC. 5	FL-1881	2.1	64.2	4.6	60.1	7.2	62.6	-2.7	0.1	201
FRAC. 6	FL-1882	1.9	79.1	4.1	78.0	6.9	68.4	-3.0	0.1	209

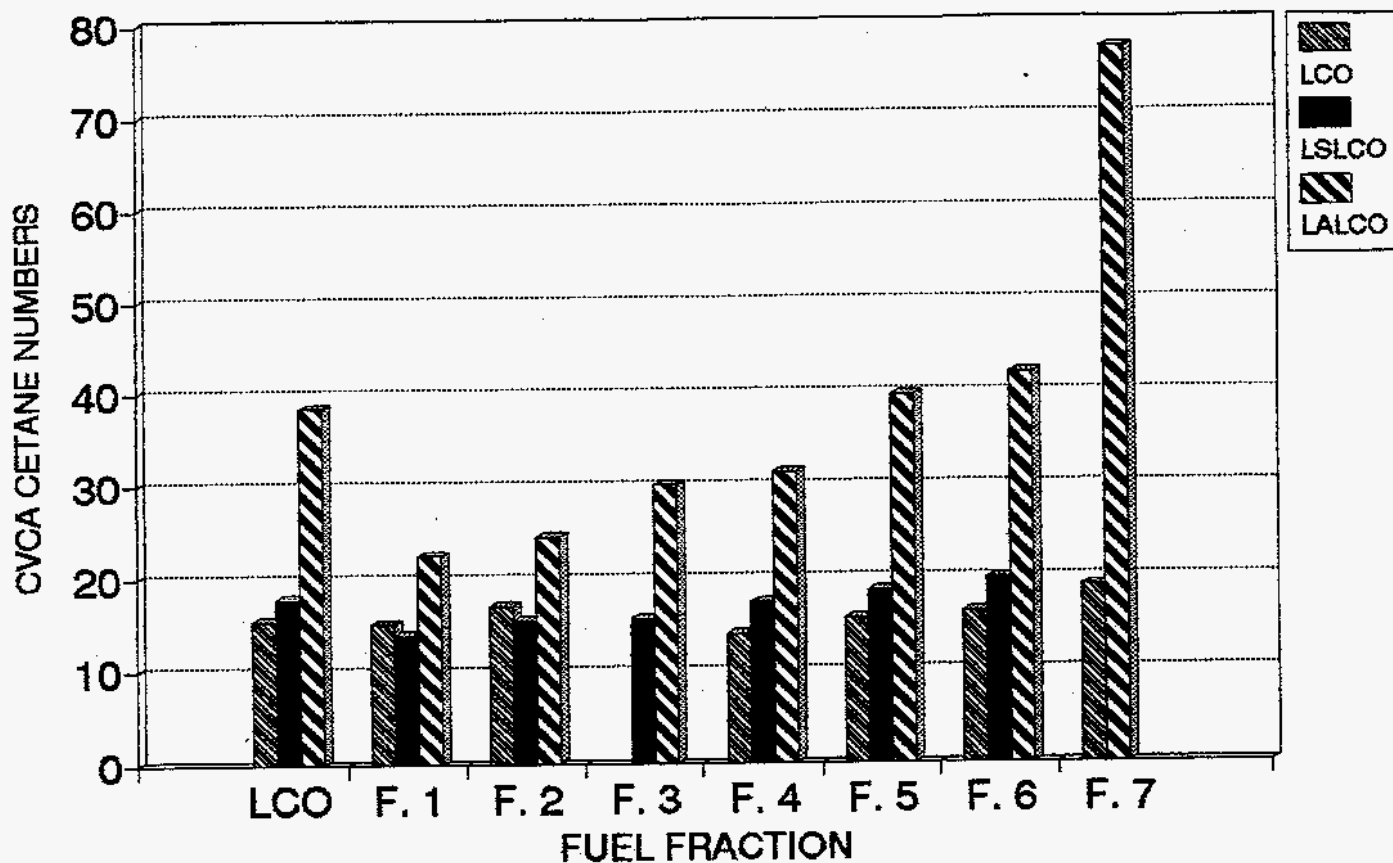


Figure 14. CVCA cetane numbers of LCOs at 582°C

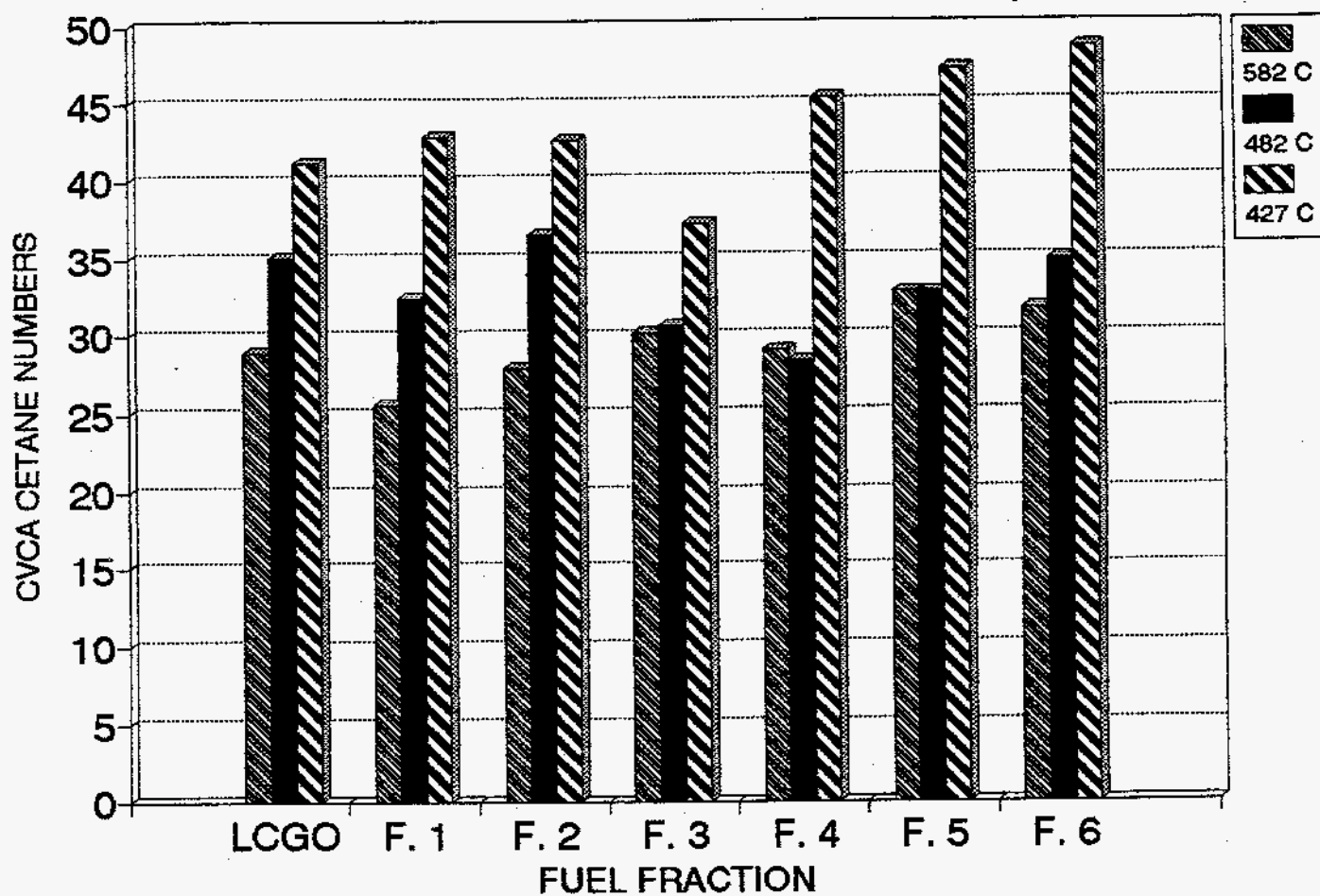


Figure 15. CVCA cetane number of LCGO at three test temperatures

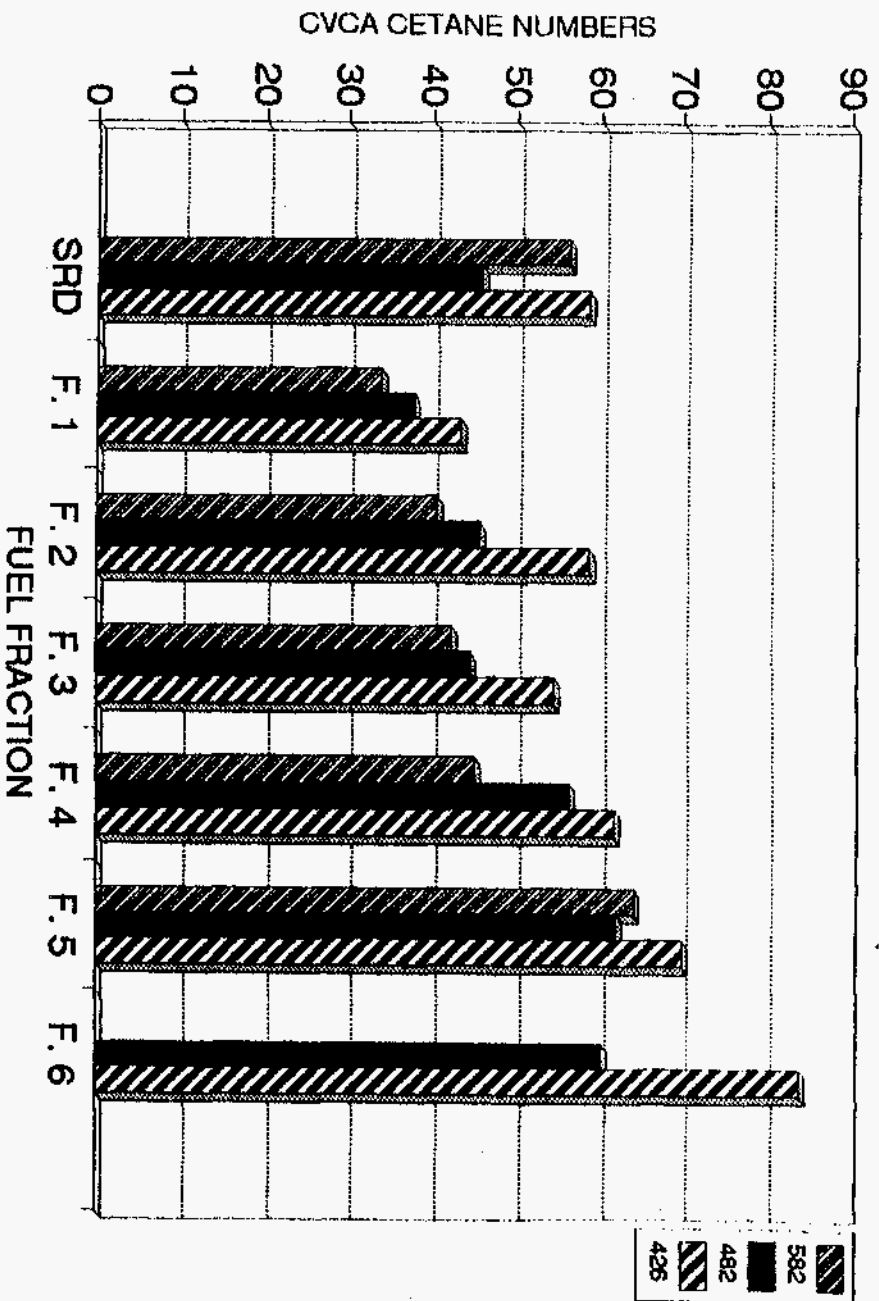


Figure 16. CVCA cetane number of SRD at three test temperatures

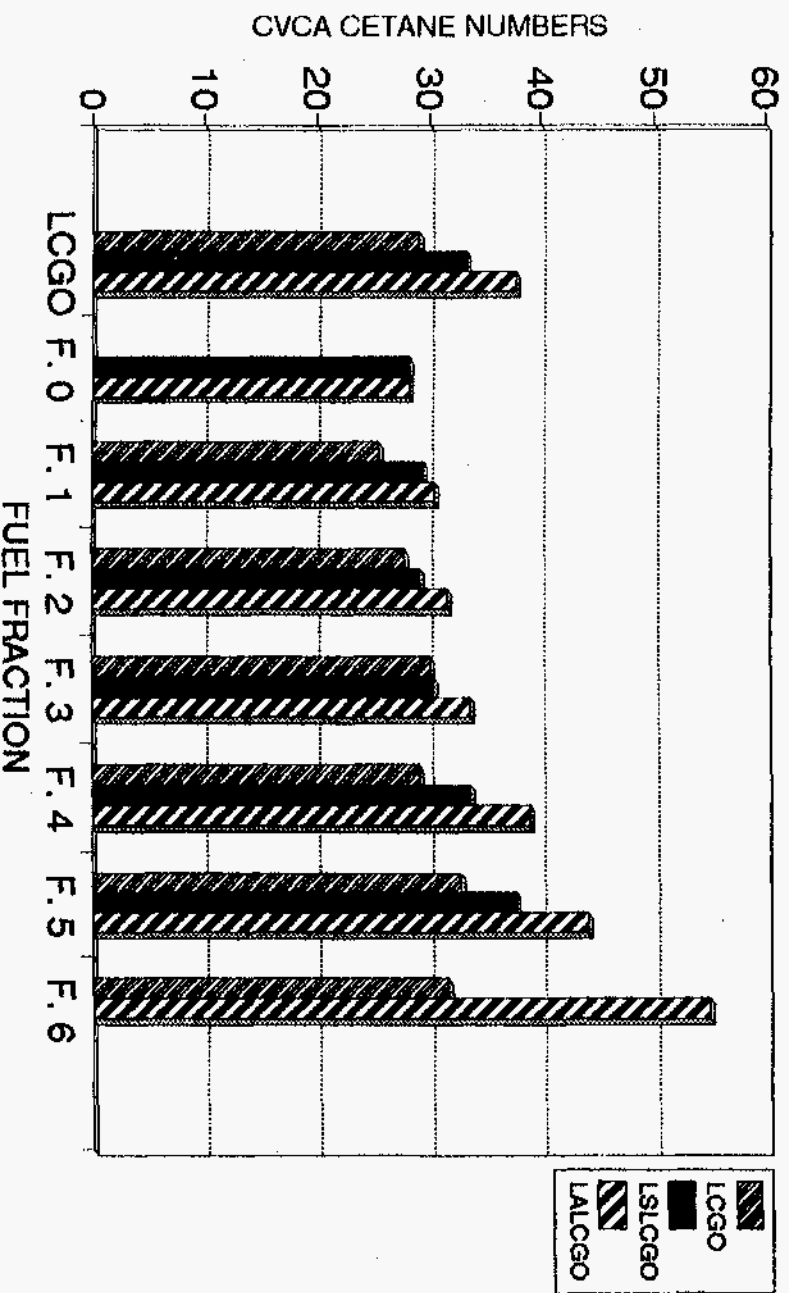


Figure 17. CVCA cetane numbers of LCGOs at 582°C

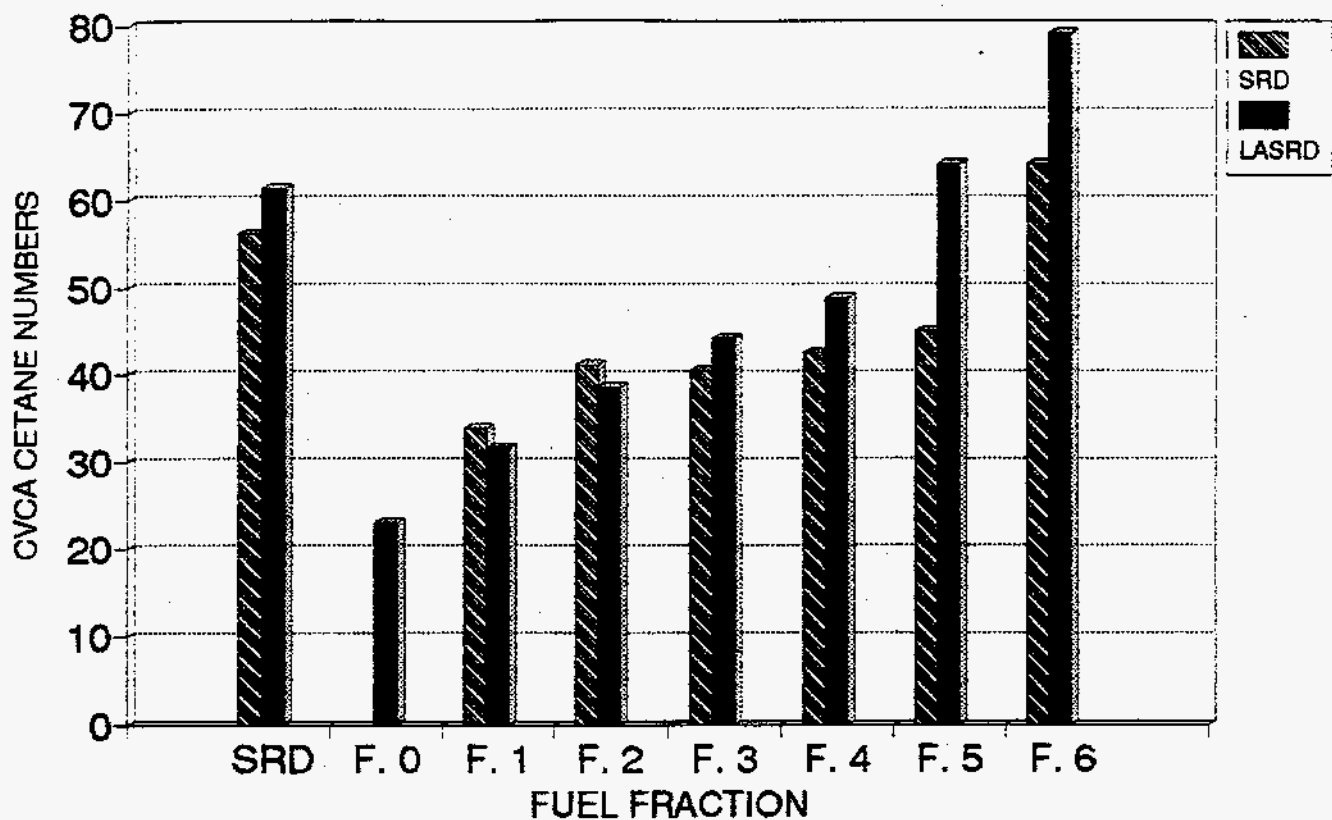


Figure 18. CVCA cetane numbers of SRDs at 582°C

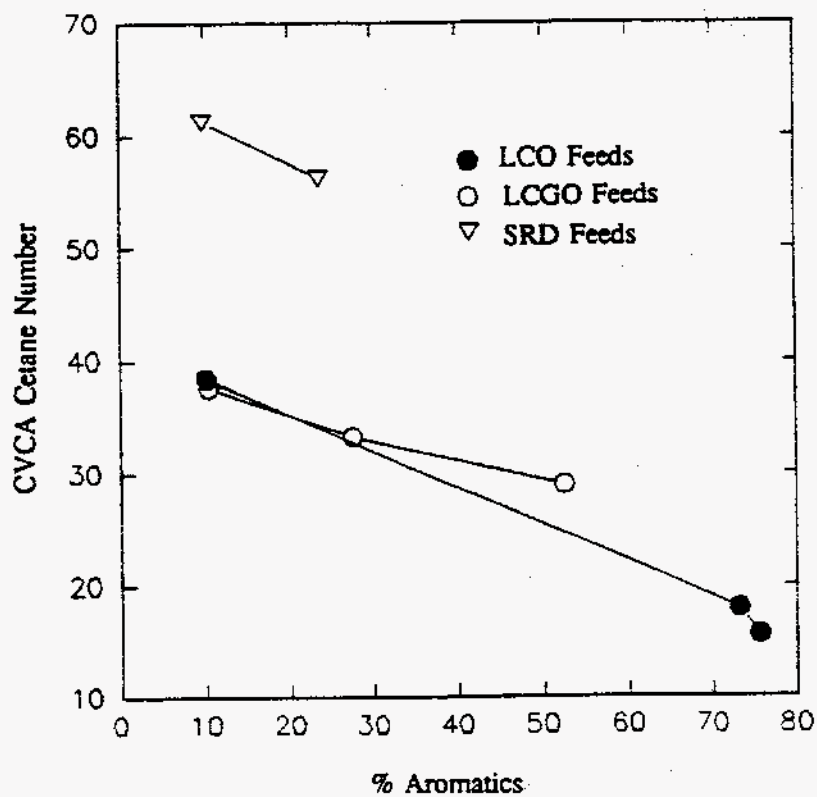


Figure 19. CVCA cetane number versus aromatics for the three feedstocks

and significantly different from the straight-run diesel fuel. However, the slopes of all the lines are similar, suggesting that the sensitivity of cetane number to aromatics is uniform for the test materials.

The correlation of CVCA cetane number to the cetane index are presented in Figure 20 for the light-cycle oils and the ASTM D 976 Cetane Index Method. The Index — an empirical correlation developed for fully formulated commercial diesel fuels — is a computed parameter based on the 50% D 86 temperature and the API gravity. As seen in Figure 20, the correlation between the CVCA cetane number and the cetane index is good at the higher cetane numbers, corresponding to the lower aromatic contents that are more typical of the commercial diesel fuels. In addition, the correlation is very good for the straight-run diesel fuels, as shown in Figure 21. These results indicate that it is probably not appropriate to use cetane index for materials that are either higher in aromatic content, or significantly different than the commercial diesel fuels used in the development of the Index.

Engine Ignition Quality

The engine tests were performed in the VCR described earlier in this report, in Appendix B, and by Ryan et al., 1993. The performance and emissions tests were performed at five different test conditions, where the speed and air-fuel ratio (load) were held constant for all of the fuels. The data from these tests were separated and treated in the preliminary analysis as independent experiments. This approach made it possible to examine the fuel effects independent of the normally dominant effects of speed and load.

The complete data set is presented in Appendix A. The results of the ignition quality rating experiments are plotted in Figure 22 as the cetane number determined in the VCR engine versus the cetane number obtained in the CVCA. The important points to note from the comparison presented in Figure 22 are:

1. The data are highly correlated, indicating that both techniques provide consistent indications of the ignition quality of the fuels.
2. The data scatter which increases significantly as the cetane number increases, is associated with defining the start of combustion in the engine at the low compression ratios needed for these fuels. The problem in the CVCA is because the ignition delay times are so short that the normal error represents a larger fraction of the total delay time.
3. The CVCA consistently rates the fuel lower than the engine test. This difference has been observed and reported previously (Ryan et al., 1988). The CVCA technique involves calibration using the primary reference fuels, which consists of two pure hydrocarbons. We believe that the difference between the engine and the CVCA is because the CVCA responds to the reference fuels differently than the engine techniques. This difference is manifested by the CVCA consistently displaying two-stage ignition (ignition and slow combustion, followed by an abrupt increase in the combustion rate) on the 15 CN reference fuel. The difference between the engine and the CVCA is consistent and can be accounted for by applying a constant correction factor to the calibration curve.

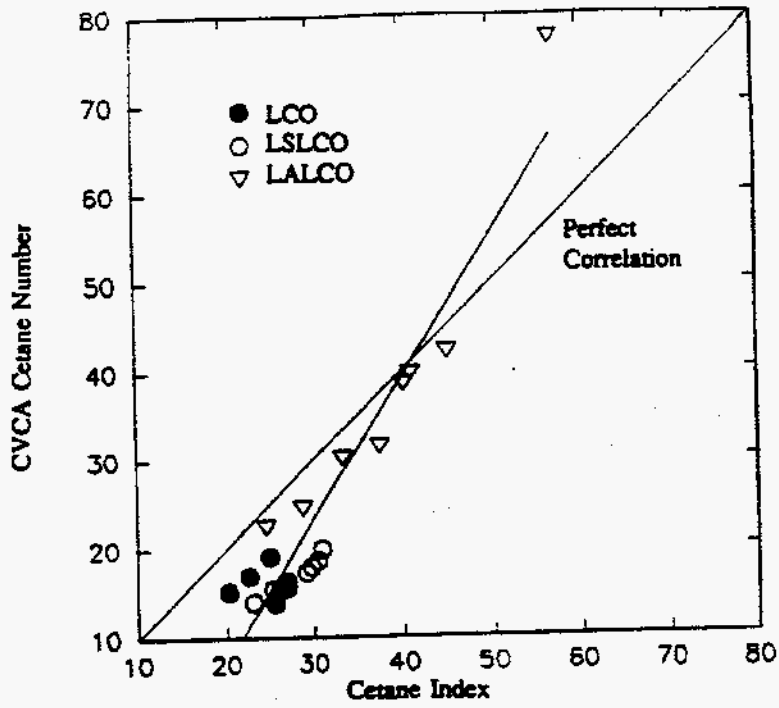


Figure 20. CVCA cetane number vs cetane index for the light cycle oils

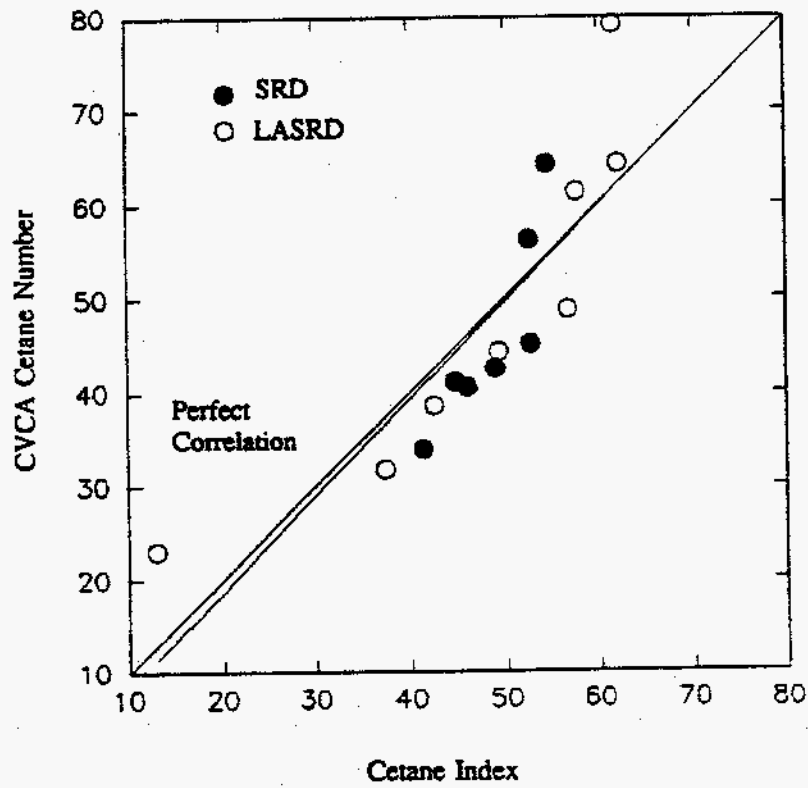


Figure 21. CVCA cetane number vs cetane index for the straight run diesel fuels

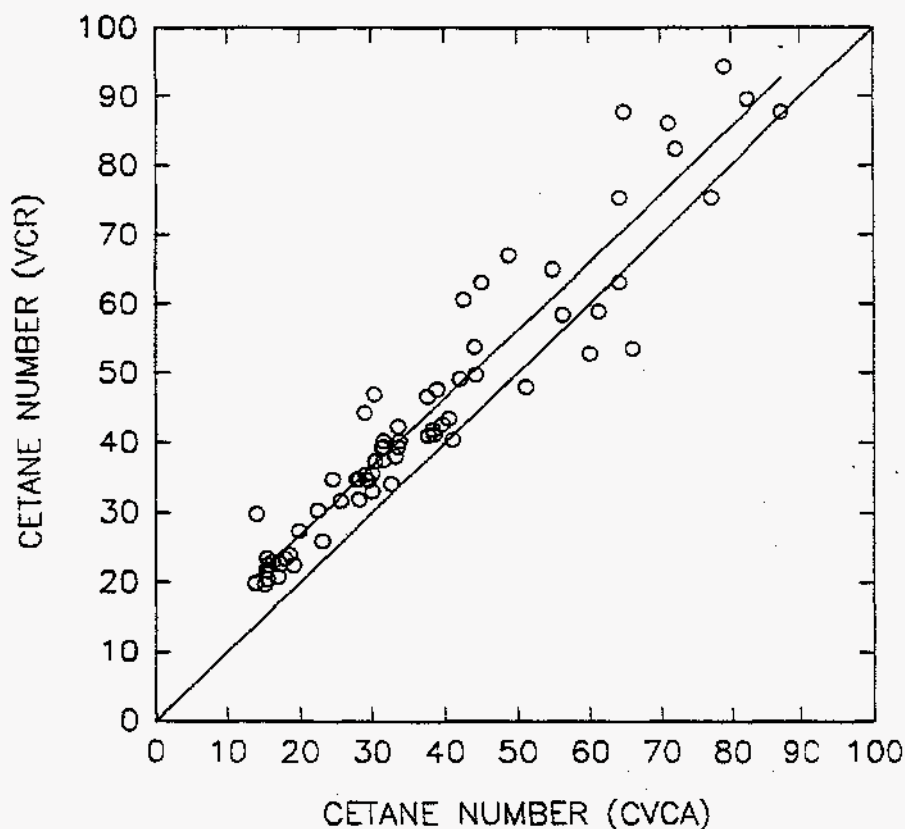


Figure 22. VCR cetane number versus CVCA cetane number

The trends of the VCR engine ratings of the various fuels and fuel fractions are the same as those reported for the CVCA data (Ryan et al., 1992). The results for all of the LCO-based fuels are presented in Figure 23. Cetane Number, or ignition quality, is uniformly distributed across the boiling range of the base material. Hydrotreating to the low-sulfur level had only minor impact on the cetane number, mainly in the higher boiling point fractions. Hydrotreating to the low-aromatic level, however, had a significant effect on the cetane number of all fractions; again, hydrotreating was most effective in increasing the cetane number of the higher boiling point fractions. Based on the corresponding data on aromatic content, it is clear that the sulfur reduction was accomplished with very little consumption of hydrogen. It also appears that the heavier fractions consume more hydrogen than the lighter fractions.

The light coker gas oil (LCGO) data are presented in Figure 24. The results are very similar to those of the LCOs, with a uniform distribution of cetane number across the boiling range for the base material. The one exception is that cetane numbers of all of the fractions are higher than those of the corresponding LCOs. The aromatic content of these materials are lower than the aromatic content of the LCOs, and hydrotreating apparently produces a more-uniform effect on reducing the aromatic content and increasing the cetane number across the boiling range. Hydrotreating does, however, have a more pronounced effect on increasing the cetane number of the heavier fractions. Similar results for cetane index were given in Figure 12.

The results for the straight-run diesel (SRD) fuel and the Fischer-Tropsch (F-T) distillate are presented in Figure 25. The cetane number of these materials are higher than the other components, and all three have a high proportion of the cetane number concentrated in the higher boiling-point fractions. Because the sulfur content of the SRD was already very low, hydrotreating was used only to reduce the aromatic content of the fuel. Similar to the other fuels, the processing was more effective in increasing the cetane number of the heavier fractions. The F-T distillate, already a highly processed material, had effectively no sulfur or aromatics and was not further processed in this project.

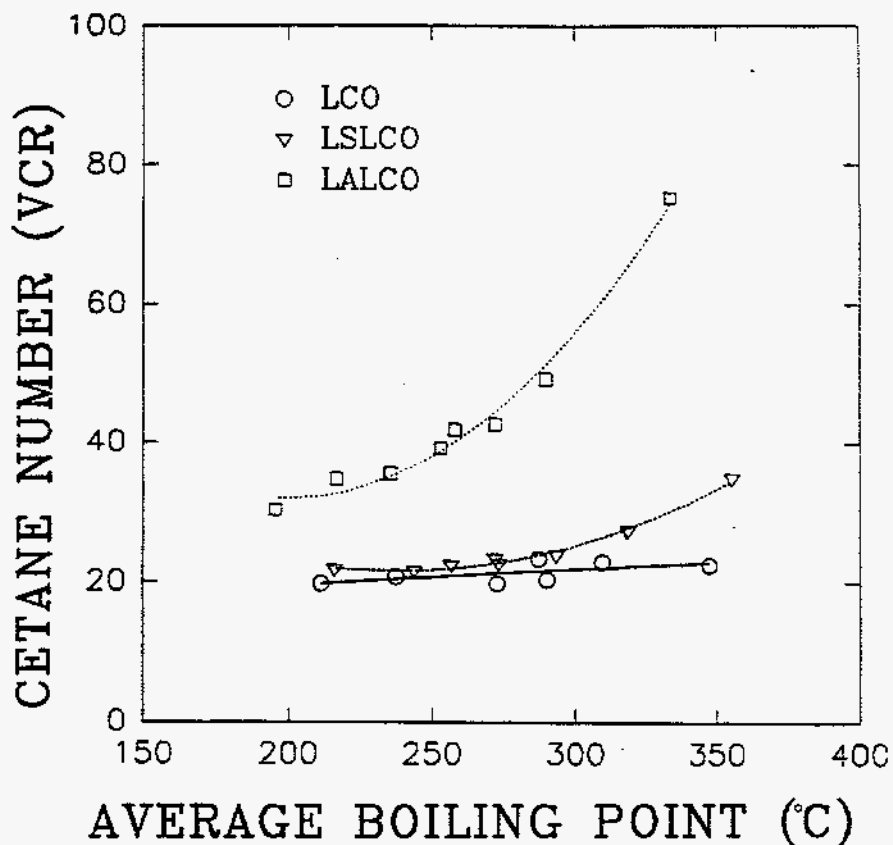


Figure 23. Cetane number (VCR) versus the average boiling point for the light-cycle oil

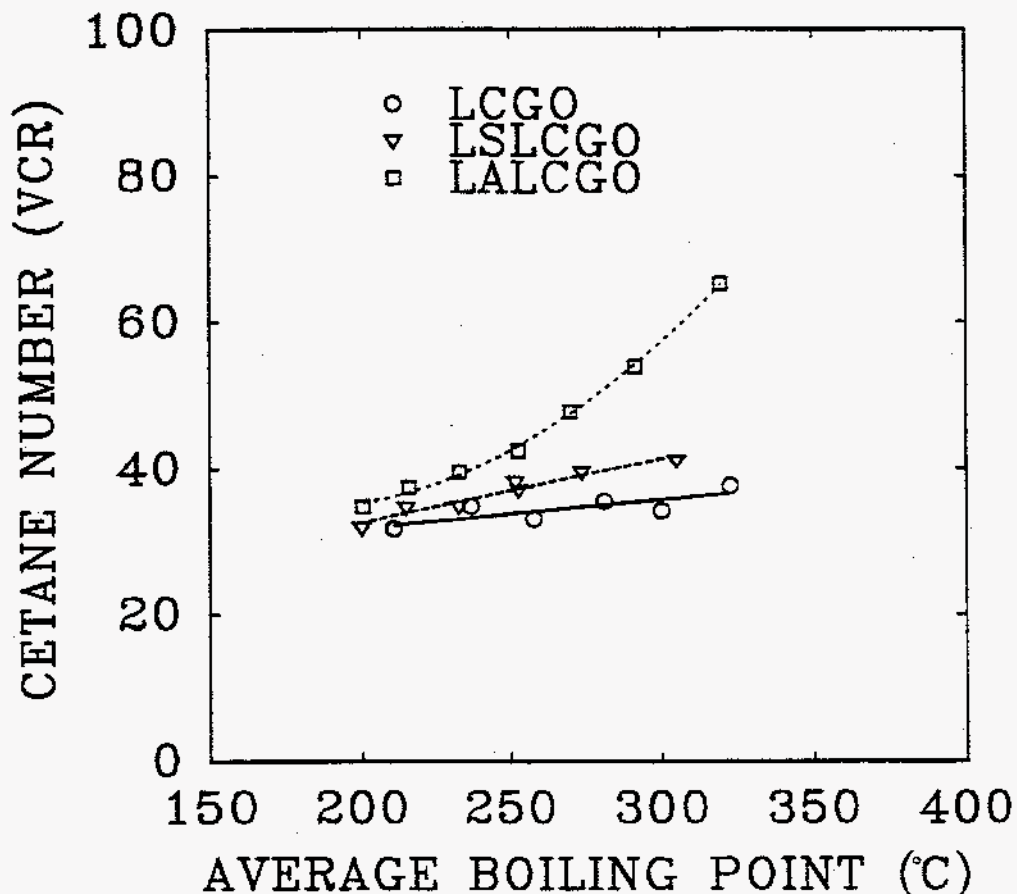


Figure 24. Cetane number (VCR) versus average boiling point for the light-coker gas oil

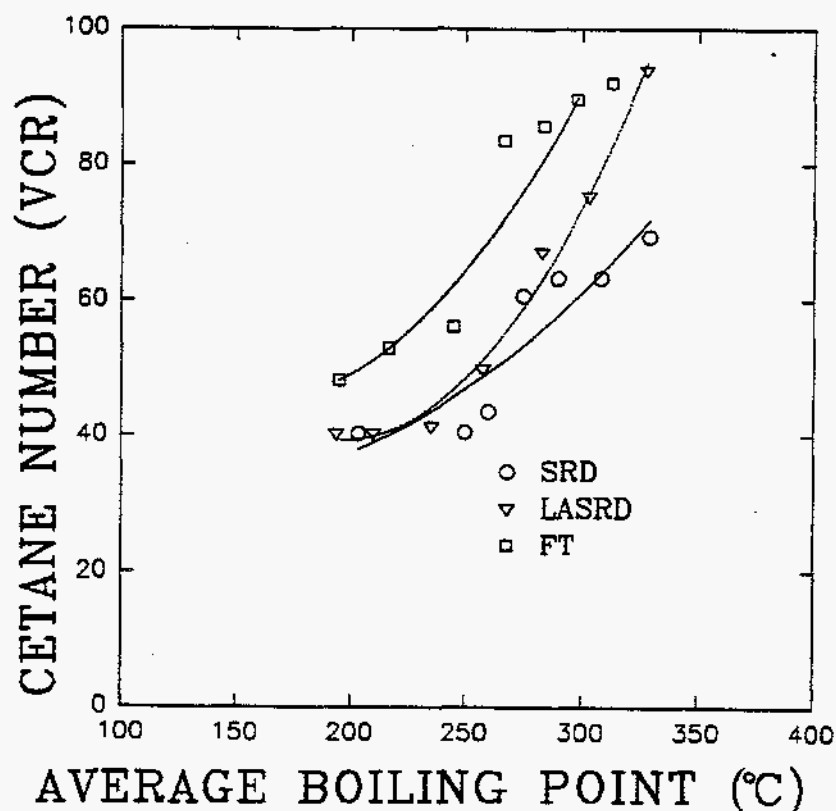


Figure 25. Cetane number versus the average boiling point for the straight-run diesel fuels and Fischer-Tropsch fuels

These results indicate that, while hydrotreating has a nearly uniform effect in reducing the aromatic content across the boiling range, it is more effective in increasing the cetane number of the heavier fractions. Consistent with the results of the CVCA measurements, hydroprocessing apparently not only reduces the aromatics content, but also produces materials in these heavier fractions that have much higher cetane number than the products appearing in the lighter fractions.

Preliminary stepwise regression analysis of the VCR results indicated that 89% of the variation in the cetane number in the test fuel matrix can be accounted for by using only the average boiling point and the specific gravity. The analysis also indicated that wt% carbon and concentration of alkyl groups associated with aromatic rings were directly related to the cetane number.(12) These relationships are reflected in the final regression equation:

$$\text{CN} = A_1 + A_2 \times (\text{Alkylbenzenes}) + A_3 \times (\text{T50\%}) \\ + A_4 \times (\text{Indenes}) + A_5 \times (\text{Paraffins}) \\ + A_6 \times (\text{Specific Gravity}) + A_7 \times (\text{Viscosity@40}^\circ\text{C})$$

where the concentrations are in wt%, specific gravity is in gM/mL, viscosity is in centistokes (cSt), and where:

$A_1 = 277.1$		$R^2 = 0.94$
$A_2 = 0.54$	$A_5 = -0.13$	
$A_3 = 0.31$	$A_6 = -437.3$	
$A_4 = -1.83$	$A_7 = -1.98$	

The direct relationship between the cetane number and the aromatic associated alkyl groups and boiling point information is consistent with the preliminary analysis. The inverse relationship with the viscosity is probably related to the effect on fuel atomization and evaporation, and the resulting influence on the physical aspects of the ignition delay time. The specific gravity effect is consistent with previous findings, as reflected in the correlations used to compute cetane index. The inverse relationship with the indenenes is consistent with the fact that indenenes have *relatively* high octane numbers, high autoignition temperature, and correspondingly low cetane number.

The inverse relationship with the paraffins, however, is somewhat surprising in that the autoignition temperatures of the paraffins are generally low, and the corresponding cetane numbers are high relative to the aromatic materials. This relationship is reflected in the numerically small coefficient of the paraffin term, $A_5 = 0.13$, in the cetane number equation. The inclusion of the paraffins may possibly account for the fact that hydroprocessing did not result in an increase in the paraffins in all cases; most noticeably, the light-cycle oil as multicyclics were converted to monocyclics and were still aromatic. Hydroprocessing did, however, always increase the cetane number of the products, due to the increases in higher-cetane-number compounds, including paraffins and cycloparaffins. The conversion process and the distribution of products is dependent on the composition of the feedstock.

The effect of boiling range for the straight-run diesel (SRD) fuel and the Fischer-Tropsch (F-T) distillate are presented in Figure 26. The cetane numbers of these materials are higher than the other components and all three have a high proportion of the cetane number concentrated in the higher boiling-point fractions. Because the sulfur content of the SRD was already very low, hydrotreating was used only to reduce the aromatic content of the fuel. Similar to the other fuels, the processing was more effective in increasing the cetane number of the heavier fractions.

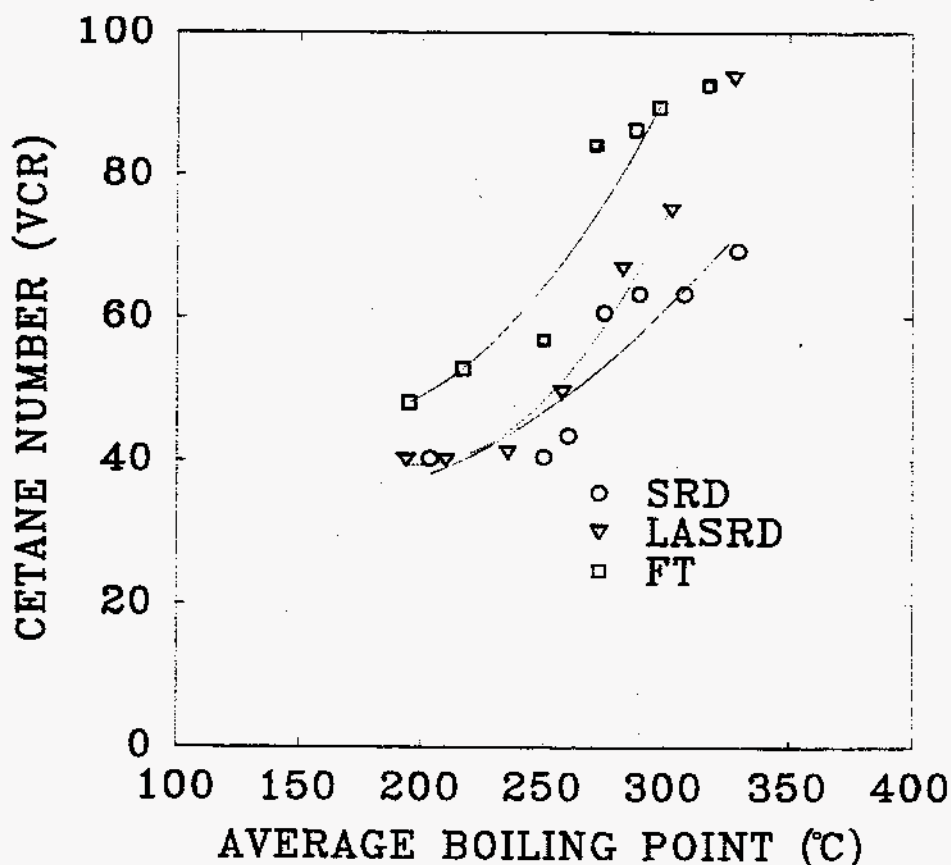


Figure 26. Effect of hydrogenation by boiling range

Of particular interest is the value of F-T distillate as a cetane blending stock. We did a blending study in which F-T fuel was blended in different concentrations with each of the three petroleum blendstocks.

The cetane number of these blends based on the CVCA technique is plotted in Figure 27 versus the concentration of the blendstocks in the F-T fuel. The cetane number of blends appears to be a linear function of the concentration for the three materials. While the relationships are essentially linear, the nonlinearity occurs for each material as cetane number decreases:

Sample	Cetane Number of Sample	Max. Deviation of Blend from Linear, %
D-2	32.1	2.1
LCGO	29.2	6.6
LCO	15.9	15.7

This progression tracks the increase in differences in hydrocarbon types between the F-T component and the other three samples. These deviations are small enough to permit an approximation of the cetane number of F-T blends as a linear combination of the volume-weighted values of cetane number for the blend components.

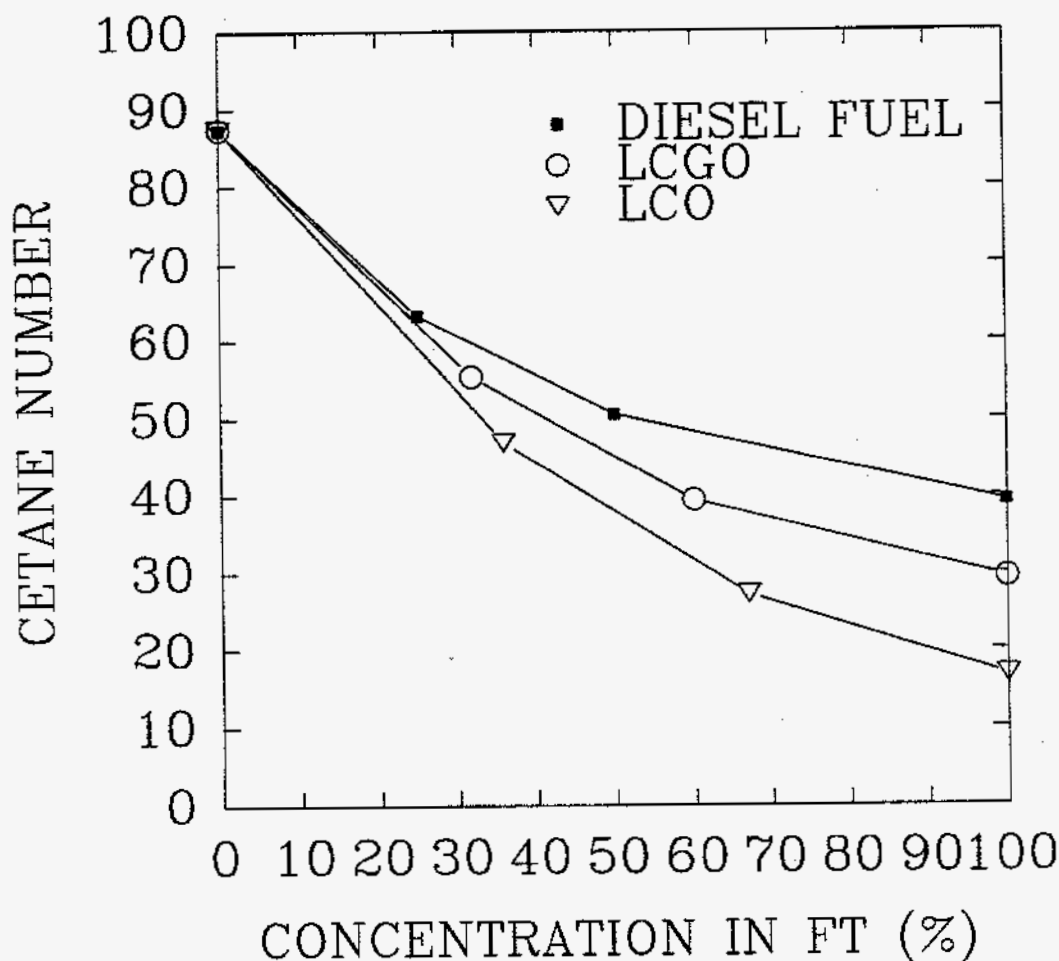


Figure 27. Cetane numbers of blends of F-T distillate with diesel components

Performance and Emissions

Each of the test fuels was run in the VCR engine at five different conditions, representative of rated torque, rated power, and part loads at the rated power speed. The basis for selection of these conditions was an extensive engine mapping done early in this project to define the rated torque point, rated power point, and the timing settings for both the best torque and for the equivalent of a 5-gM/hp-hr NO_x level. To review, the test conditions were defined as follows:

- Mode 1 Condition is representative of rated torque speed and overall equivalence ratio, using an injection timing (3° BTDC) for the controlled NO_x condition on a baseline diesel fuel.
- Mode 2 Includes the same speed and load conditions as Mode 1, but using the best torque injection timing for each test fuel.
- Modes 3-5 Rated power and part load conditions at the rate power speed, using a fixed timing of 3° BTDC.

The engine settings for the five modes were given in Table 6.

Normally, the results of engine studies of fuel effects on performance and emissions are dominated by variations in the engine test conditions — in particular, speed, load, and ignition timing. The data obtained in this study are separated into five data sets that can be treated independently, thereby eliminating the dominance of the engine conditions in the results.

Preliminary Examination – We initially developed scatter plots showing the relationships among the dependent variable and each of the independent variables. Statistical analysis of the data sets indicated that fuel properties do play a role in most of the engine performance and emissions characteristics measured. In some cases, the majority of the variation of these characteristics could be related to the fuel properties. In many other cases, however, only a portion of the variations were accounted for in the fuel properties, and the rest of the variations were due to the fact that the effects were small and experimental error becomes a more significant factor.

Power – Our analysis of the power in a given data set (Mode) indicated that the power was not a very strong function of the fuel properties. The scatter plots did indicate that the power within a Mode was directly related to the combustion efficiency of the fuel, as shown in Figure 28 for Mode 1. These results, indicated graphically and in linear regression analysis, showed that the variations in power within a given mode were not highly correlated with the fuel properties.

CO Results – The behavior of CO emissions was very similar to the power data, at least in the higher power modes, where the emissions levels were related more strongly to the combustion parameters than to the fuel properties, within the data sets for each Mode. The power in these experiments was fixed within some range of variation that depended on minor variations in the combustion process. The power settings were defined based on fixed overall air-fuel ratios held constant for all tests within the given Mode. It appears that of the fuels that would actually run in the engine, the properties of the fuel must be within a range of acceptability that produces similar results in the global performance parameters, such as the power and the CO emissions. At the lighter load conditions, the initial statistical analysis indicated that the fuel properties did play a role in the CO emissions, with the boiling-point distribution and the aromatic structure playing the most important roles.

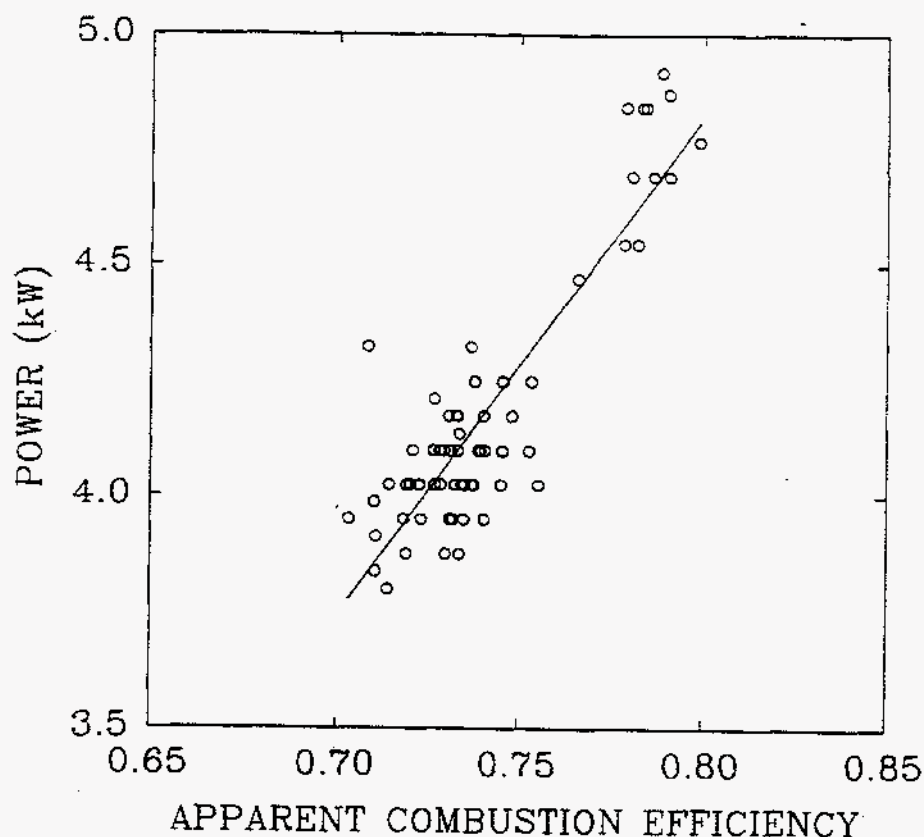


Figure 28. Power variations in Mode 1 versus apparent combustion efficiency

Hydrocarbons – Scatter plots of the hydrocarbon emissions indicated that the fuel physical properties dominated the results within each mode. Figure 29 shows the hydrocarbon emissions plotted versus the viscosity for the Mode 1 test condition. Similar results were obtained for the other test conditions. The preliminary statistical analysis indicated that the relationships between the hydrocarbon emissions and the fuel properties were, in fact, dominated by the boiling-point distribution and the viscosity for all test conditions.

Smoke – Statistical analysis of the smoke data indicated that fuel properties play a significant role in controlling these emissions. Fuel structure appears to dominate these relationships, with total aromatic content an important factor at all test conditions. Other important fuel properties are the sulfur content, the aromatic ring structure, and the boiling-point distribution. The order of importance of these properties varies somewhat as the engine load is reduced: the boiling-point distribution and viscosity become more important at the lighter loads, where the injection process might be more affected by these properties than at the higher load conditions.

NO_x Results – Scatter plots of the NO_x data indicated dominant effects of fuel composition and cetane number at all but the lightest load condition. These trends are demonstrated in the scatter plots of these fuel variables, presented in Figures 30 and 31 for the Mode 1 condition. The preliminary statistical analysis indicated that the aromatic content and structure, and the structure of the alkyl groups are important.

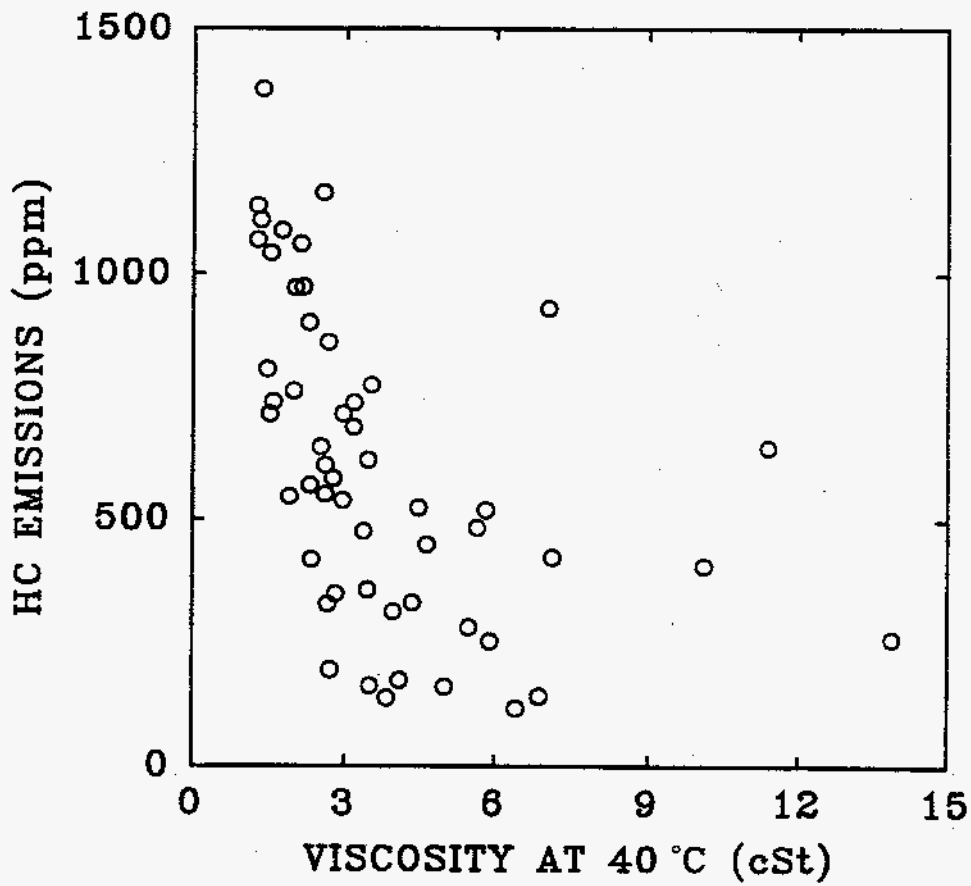


Figure 29. Hydrocarbon emissions versus viscosity for the Mode 1 test condition

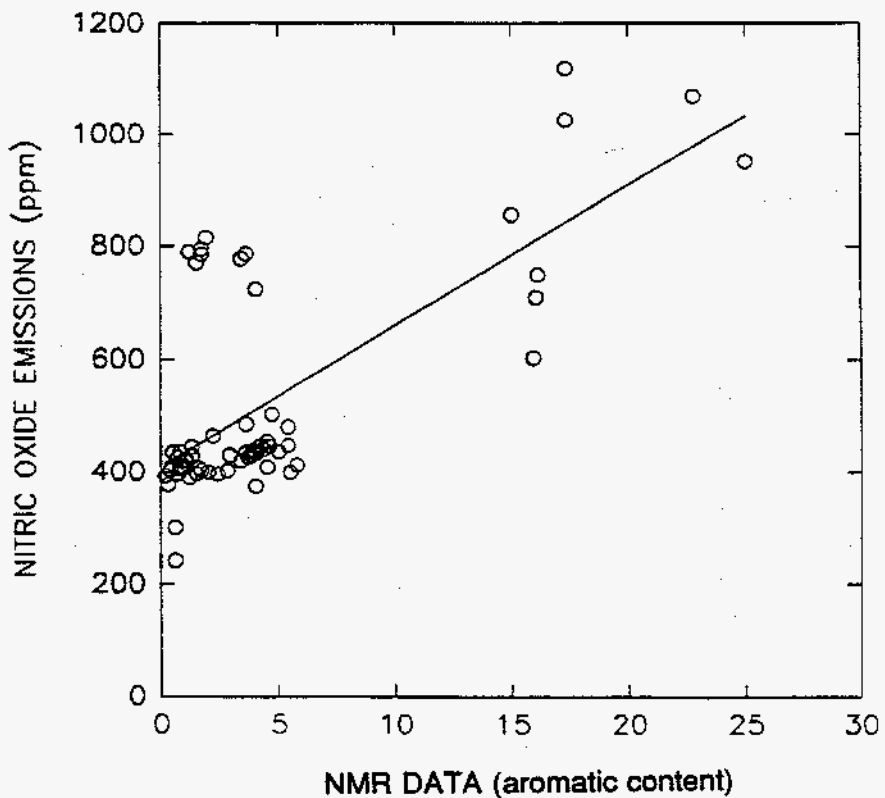


Figure 30. NOx emissions versus NMR aromatic content for Mode 1

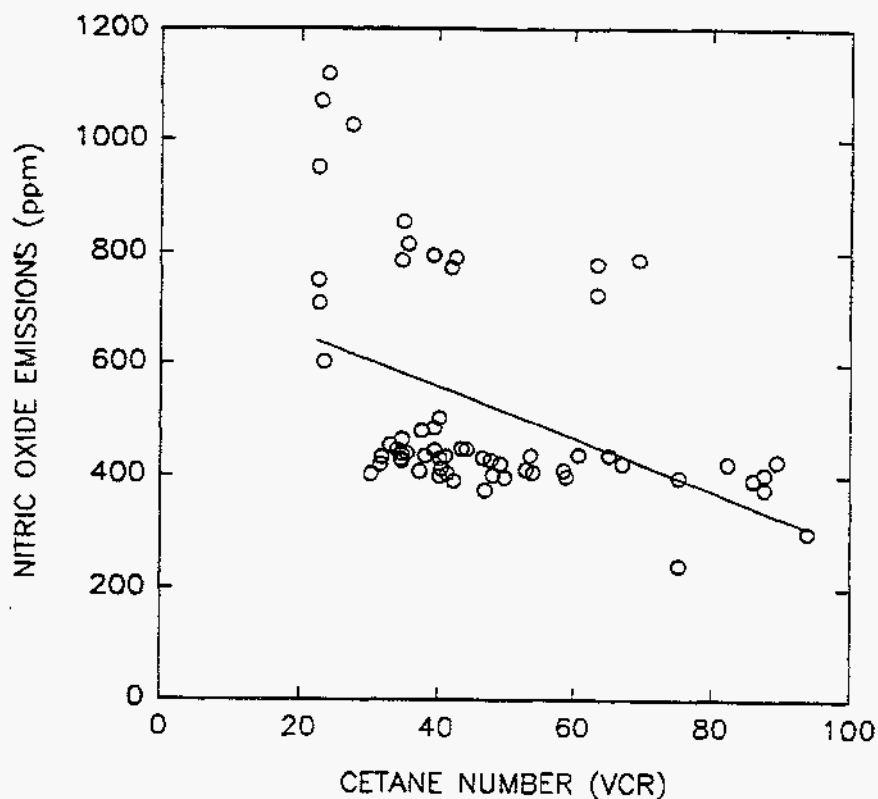


Figure 31. NO_x versus cetane number (VCR) for Mode 1

Statistical Analysis – The results of the statistical analysis verified that Mode 2 represented the best test condition for examining the fuel composition and property effects on the NO_x, smoke and HC emissions. The stepwise analysis was first performed using three subsets of the independent variables. The subsets were defined to include the combustion parameters, the physical properties, and the chemical properties. Although different properties could have been included in each subset, the goal was to determine where, or if, the physical properties or chemical properties, or combustion parameters dominated the emissions characteristics. For instance, one result was that power and CO emissions did not display significant fuel dependence at any combination of test conditions.

The *combustion* properties include the air-fuel ratio, peak combustion pressure, peak heat-release rate, the angles of occurrence of these peak values, beginning of injection, indicated and brake power, energy input, cumulative heat release, and the combustion efficiency. NO_x emissions were highly correlated with the combustion characteristics at the rated power and rated torque conditions, with R^2 in the range of 0.97. The R^2 value dropped dramatically at the part-load conditions. The other emissions were not highly correlated with the combustion parameters, based on R^2 values below 0.5.

The fuel *physical properties* include average boiling point, heating value, initial boiling point, T50, T95, specific gravity, viscosity, cetane number, vol% aromatics, olefins, and saturates, and wt% carbon, hydrogen, and sulfur. The NO_x emissions displayed dependence on T50, specific gravity, the heating value, and vol% aromatics at all but the lightest load condition. The smoke number correlated mainly with boiling point distribution and viscosity across the load range (R^2 in the range 0.5 – 0.75), indicating a dominance of the physical processes on the soot formation and oxidation.

The stepwise regression analysis included a very broad range of *chemical composition* variables. In stepwise regression, the computer method substitutes a succession of regression models into the data to determine the best fit each model can obtain, thereby exploring several functional forms for the

correlation. The initial analysis included both the NMR characterizations and the GC/MS hydrocarbon-type breakdowns. As expected, the NMR and GC/MS data were highly colinear. The NMR data provide a great deal of structural information regarding the location and environment of the hydrogen within the fuel molecules, and in that sense provide more information regarding the structure of the fuel. The statistical analysis indicated that both the NMR and GC/MS data provided nearly equivalent representations of the results. We believe that NMR analyses is less routine than GC/MS; therefore, the subsequent statistical analysis included only the component hydrocarbon composition data obtained by GC/MS. NO_x emissions displayed a strong dependence, (across the speed and load range of the engine) on the hydrocarbon-type data, with R² in the range 0.6 – 0.8. The ignition quality, in terms of the engine-based cetane number, was also highly correlated with the chemical composition.

Following the stepwise regression analysis, we calculated linear fits using all possible combinations of those fuel variables found to be important in one or more of the fits for each subset. We used these results as the basis for selecting the best linear models for each independent variable at each test condition. Although scatter plots of the residuals (degree of statistical fit of each dependent variable) were indicative of linear behavior, we tried to improve the linear models by using natural-log-transformed, curvilinear, and interactive terms. The R², or fit, of the model was not improved by the inclusion of these nonlinear terms.

We developed the final models for each of the emissions at each speed-load condition. The results of these analyses for the Mode 2 test condition appear to present the best indication of the effects of the fuel properties and composition on the cetane number and the emissions. We discussed the Mode 2 models in detail in the following paragraphs, and definitions of the terms are presented in Appendix B.

NO_x – The NO_x emissions were highly correlated with the combustion parameters, reflecting the kinetic nature of the NO_x formation mechanism. The Zeldovich kinetic model for NO_x relates the formation process to the concentrations of the nitrogen and oxygen species in the flame zone and the time and temperature of reaction (Zeldovich, 1946; Hanson & Salimian, 1984). The local adiabatic flame temperature is appropriate for use in the Zeldovich mechanism. The adiabatic flame temperature and the overall combustion rate are directly related to the chemical composition of the fuel. These dependencies are reflected in the regression equation that was developed for NO_x:

$$\text{NO}_x = A_1 + A_2 \times (\text{AlkylNaphthalenes}) \\ + A_3 \times (\text{Indenes}) + A_4 \times (\% \text{ Carbon}),$$

where concentrations are in wt% and the coefficients are:

$$A_1 = -96.34 \quad R^2 = 0.82 \\ A_2 = 0.22 \\ A_3 = 0.24 \\ A_4 = 1.17$$

The regression analysis included several variables describing the aromatic structure:

- Alkyl benzenes
- Indanes/Tetralin
- Indenes
- Naphthalene
- Alkyl naphthalene
- Acenaphthylenes
- Acenaphthenes
- Tricyclics

The results indicate that two-ring structures lead to higher NOx levels, while the level of unsaturation indicated by the indenenes tends to lower levels of NOx. The importance of the total aromatic nature of the fuel is reflected in the carbon content.

As indicated in the stepwise regressions discussed under "Statistical Analysis", the fuel physical properties provided a good indication of the NOx trends when they alone were used in the regression analysis. The final regression equation did not include fuel physical properties, however, because the stepwise analysis indicated that the physical properties added little to the prediction of the NOx emissions when the chemical composition parameters are included in the analysis. This finding is related to the fact that the physical properties and the chemical composition are colinear in many cases, that is, they tend to change in the same way if a fuel blend is varied, i.e., aromatic content increases with boiling point.

Smoke – The smoke number reflects the soot fraction of the particulate emission. Soot emissions depend on the difference between the soot formation and the soot oxidation rates in the engine. A great deal of soot is formed during combustion in diesel-engine cylinders, but most of this soot is oxidized prior to exhaust. The soot formation mechanism is dependent on fuel composition, the thermodynamic state in the combustion chamber, and the mode of combustion (premixed versus diffusion). The soot oxidation mechanism is dependent mostly on the thermodynamic state and the physical processes associated with mixing. Regression of the Bosch smoke data indicated that only a part of the variation could be accounted for in the fuel properties. This probably reflects the fact that the soot oxidation mechanism depends more on the physical processes than on the chemical composition of the fuel. That portion of the smoke emissions that can be accounted for in the final properties is best modeled using the following equation:

$$\begin{aligned} \text{Bosch Smoke} = & A_1 + A_2 \times (\text{Acenaphthylenes}) \\ & + A_3 \times (\text{Alkylbenzenes}) + A_4 \times (\text{Tricyclic aromatic}) \\ & + A_5 \times (\text{Total aromatics}) + A_6 \times (\text{vol\% aromatics}), \end{aligned}$$

where concentrations are in wt% except as indicated, and where:

$$\begin{aligned} A_1 &= 2.24 & R^2 &= 0.61 \\ A_2 &= -0.065 \\ A_3 &= -0.029 \\ A_4 &= 0.08 \\ A^5 &= 0.027 \\ A^6 &= -0.013 \end{aligned}$$

Most of the combustion event in the test engine occurred in diffusion burning of the fuel jets. Palmer and Curtis (1965) indicate that the tendency for soot formation in diffusion flames decreases in the order: naphthalenes > benzenes > diolefins > monolefins > paraffins, where the tendency to form soot decreases in each group with increasing molecular weight (except the paraffins) and increasing compactness.

The results of the regression analysis indicate a direct relationship with the total aromatic content and the concentration of three-ring aromatics. We expected this effect based on the conclusions of Palmer and Curtis. The inverse relationship with the acenaphthylenes and the alkyl benzenes may be related to the decreased stability of the tertiary carbon atoms in these structures, the increased molecular weight, or the compactness of these groups of compounds. Inclusion of the vol% aromatics provides a marginal improvement in the R^2 and may reflect an interaction with the density.

It should be noted that the Bosch smoke number is not an accurate measurement of the total mass of particulate emissions. The regression equations generated using these data reflect this limitation, and the resulting discussion should be considered in light of this limitation. Future experiments should consist of total mass measurements, with actual breakdown between the soot and the soluble fraction

HC – Surprisingly HC emissions decreased with increasing boiling point at all speed-load conditions. This relationship is demonstrated in Figure 32 for the Fischer-Tropsch fuels, where the HC emissions are plotted versus the fuel fraction or average boiling point. Figure 33 is a similar plot of the Mode 2 smoke data, showing that the smoke tends to increase with fraction number. The regression equation for the HC emissions reflected this inverse relation with the boiling-point distribution, as reflected in the T50 coefficient. As indicated above, the regression equations for smoke did not include boiling-point information. They did indicate, however, that boiling-point data could be used in lieu of some of the composition data to account for some variation of smoke. The regression equation for the HC emissions is:

$$\text{HC} = A_1 + A_2 \times (\text{Alkylbenzenes}) + A_3 \times (\text{T50}) \\ + A_4 \times (\text{Indenes}) + A_5 \times (\text{Monocycloparaffins}) \\ + A_6 \times (\% \text{ Carbon})$$

where concentrations are mass percentage, and where:

$$A_1 = 21.61 \quad R^2 = 0.83 \\ A_2 = 0.095 \\ A_3 = -0.004 \\ A_4 = -0.15 \\ A_5 = 0.029 \\ A_6 = -0.21$$

The unburned hydrocarbon emissions from diesel engines are dependent on both the physical processes that occur in the engine and the fuel properties that affect combustion efficiency. The physical processes include fuel atomization, vaporization, mixing and impingement, as well as quenching in the bulk gas due to over-rich or over-lean conditions and thermal quenching in the boundary layers; all these processes result in incomplete burning. If the HC emissions are in fact dominated by the physical processes that lead to incomplete combustion, the properties that lead to increased soot production will likely produce reduced HC emissions. One possibility is that the total mass of unreacted carbon is accounted for in either the HC or the smoke emission, with the distribution also dependent on the conditions in the engine and on the fuel properties.

The direct relationship between the HC and the alkylbenzenes and monocycloparaffins most probably reflects the stability of these structures relative to the other hydrocarbon groups. This hypothesis is supported by the inverse relationship with the less stable indenenes. The relationship to the wt% carbon probably reflects the propensity of the fuels to form soot rather than HC.

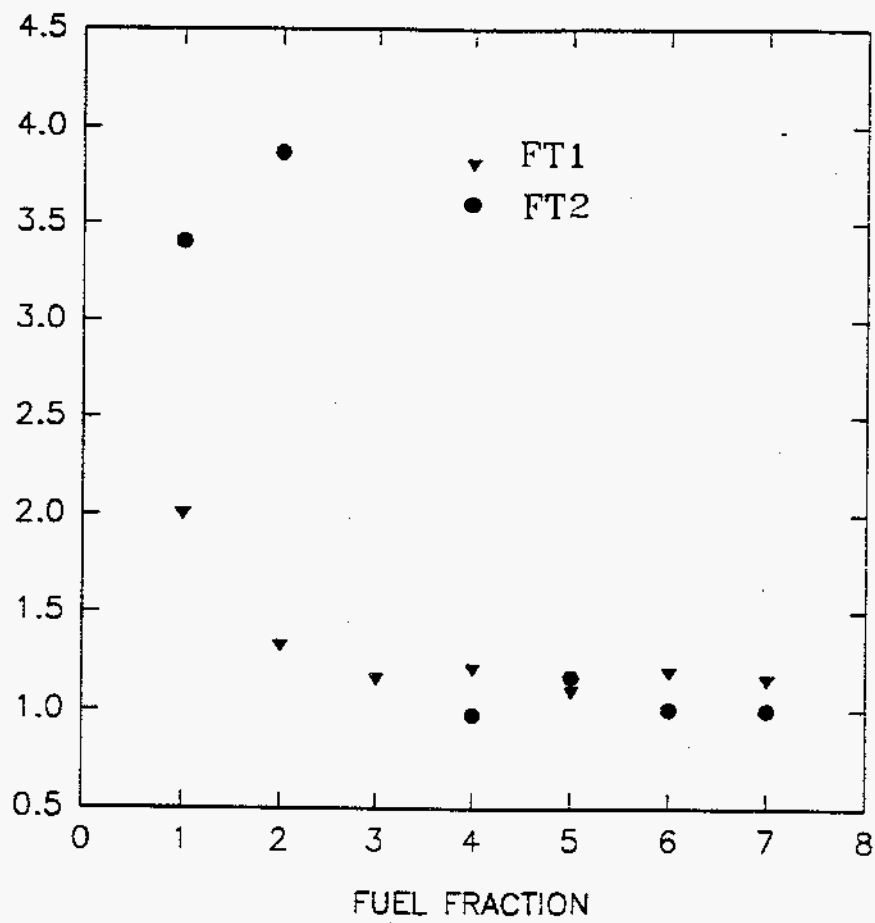


Figure 32. HC emissions versus fuel fraction for the F-T fuels at Mode 2

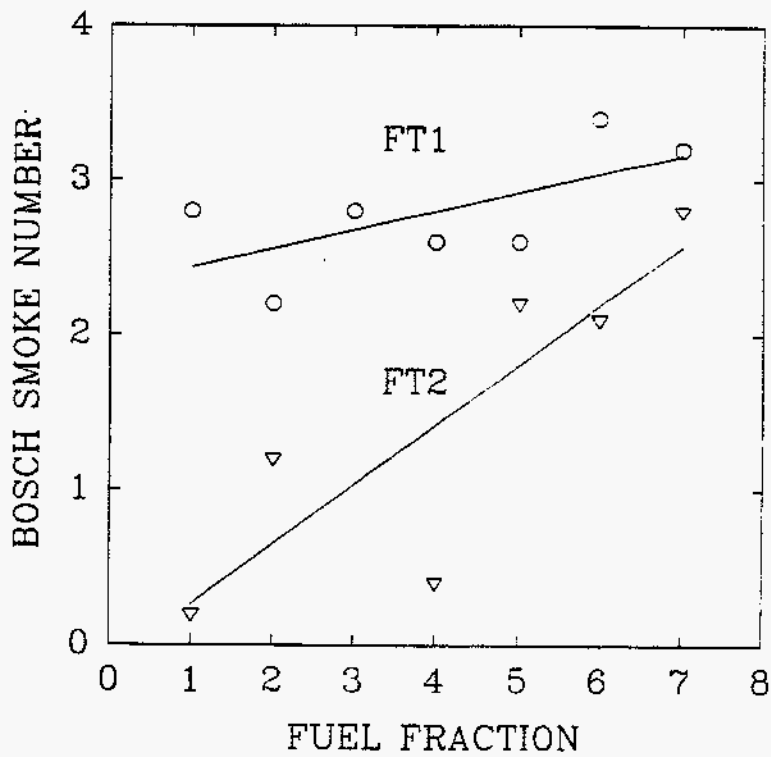


Figure 33. Bosch smoke number versus fuel fraction for the F-T fuels at Mode 2

TASK 3 CLEAN-FUEL STUDY

The goal of Task 3 was to study the results of the fuel fraction analyses and the emissions measurements to recommend methods to produce reduced-emissions diesel fuels. During the foregoing studies, the concepts of aromatics identity, aromatics concentration, and ignition quality (cetane number) emerged as the central variables for emissions control for a given boiling range. The comparisons with the F-T materials showed that the aromatics in the petroleum blendstocks are a crucial determining factor for emissions. With these observations in mind, we developed an approach to the Clean Fuel Study in which we would use the emissions measurements for the samples to select a formulation via linear programming for the lowest-emission test fuel meeting possible future diesel specifications — with and without F-T material. Continuing this approach, we used linear programming to formulate three fuels spanning the range of aromatics concentrations likely to be encountered at about 55 CN. The complementary set of three formulations spanning the likely cetane range at 15% aromatics were also developed by linear programming. These levels of aromatics content and cetane number are representative of those used in fuels certified as reformulated diesel fuels in California. (Nikanjam, 1993).

We processed enough of the selected materials to perform performance and emission tests similar to those in Table 6, which were obtained for the sample fractions. This testing was carried out on the same engine configuration and with the same standard diesel fuel as before. We then compared these results with the predicted values and the values of the correlations.

Determining Blend Compositions for Low-Emissions Fuels

The preliminary statistical analysis of the engine performance and emissions data indicated the dominant effects of the aromatic content, aromatic type, and cetane number, on the emissions. However, much more detailed analysis is required to develop relationships between the various fuel properties and the emissions. A simplified approach was therefore taken in the design and formulation of "low emissions" diesel fuels. The approach consisted of including the emissions data for each cut as properties that could be modeled using linear programming techniques.

Distillation of original components provided a large number of potential blend components. Collectively, they contained a wide range of properties, and in general, several different blend formulations could be determined with properties meeting any particular set of specifications. In general, our goals were to produce full-boiling-range fuels that would either provide the lowest possible emissions, or would indicate the independent effects of aromatic content and cetane number. The blend compositions of 10 different low-emissions fuel concepts were determined using the linear programming (LP) technique for selecting an optimal solution from many acceptable solutions. This process allowed us to rapidly select a blend formulation that was best for each particular concept.

We calculated a blend formulation for each low-emission fuel concept, which differed in the constraints placed on the problem or in the property that was optimized. Table 9 gives a description of each calculated blend. Of the four "minimum-emissions" test fuels, Fuel 1 was designed for the lowest possible emissions, using all of the available components. Fuel 2 had the added constraint of using the most of one of the least valued products — LALCO. Concentrations of LCO and LCGO, typical of actual refinery operation, were used to design the lowest possible emissions in Fuel 9. Fuel 10 had the same constraints as Fuel 1 except that the high-quality Fischer-Tropsch materials were not included in the blend.

Table 9. Low-Emissions Fuels Descriptions

Blend No.	Blend Concept Description
1	Minimum emissions
2	Minimum emissions with maximum use of light-cycle oil product (low-aromatics LCO)
3	Minimum aromatics concentration with CN 55 to 56
4	Maximum aromatics concentration with CN 55 to 56
5	Maximum cetane number with aromatics 15–16%
6	Minimum cetane number with aromatics 15–16%
7	50:50 mixture of blends 3 and 4*
8	50:50 mixture of blends 5 and 6*
9	Minimum emissions with LCO and LCGO products in typical abundance
10	Minimum emissions, F-T products excluded

* Not calculated directly by linear programming

Next, two sets of three test fuels each were devised to test two important trends. Fuels 3 and 4 were designed to examine the effects of aromatic content, at a constant cetane number of 55. Fuels 5 and 6 were designed to examine the effect of cetane number at constant aromatic content of 15%. Fuels 7 and 8 were designed to be the midpoints between Fuels 3 and 4 and Fuels 5 and 6, respectively.

Several preliminary actions facilitated the selection process. The Mode 2 data were selected as the most appropriate for the selection. Because the LP method optimizes on a single property, we defined an "emissions parameter" for each component by normalizing and adding the normalized emissions data in each concept. We normalized the emissions data by dividing the measured or predicted emissions data by the respective target value for each component. If the target emissions levels are achieved exactly for each emission, the emissions parameter (EP) equals 4. Values of EP below 4 indicate emissions levels better than the target, and values greater than 4 indicate that the target levels are not achieved. The EP provides a convenient parameter to compare different fuels, even if the target values are never achieved.

The targets, based on the rated torque condition, were:

- 4 g/hp-hr for CO,
- 2 g/hp-hr for HC,
- 5 g/hp-hr for NO_x,
- 2 for Bosch smoke number.

The LP problem was computerized using the optimization feature of Quattro Pro to include as many components as practical, and preliminary runs were made with the individual distillation cuts. The results showed that adjacent cuts were in general not selected in similar quantities, so more realistic, broad-range cut properties were calculated by linear combination of the individual cuts weighted by their yield. The goal was to select one, or at most two, cut points for a given stock. Accordingly, the LP was provided with artificial stocks comprising adjacent fractions, for example, fractions 1 through 4, or fractions 3 through 5, etc. The possible combinations of adjacent fractions provided the LP problem with about 215 different blendstocks, including the full-boiling-range products.

Two further actions helped reduce the scope to manageable proportions. The component properties were entered in a Quattro Pro spreadsheet library and set up so they could be input to the problem readily, allowing a large number of components to be tried rapidly by manual action. The other action reduced the number of artificial stocks requiring trials. In addition to the blend formulation, the LP solution

indicates the relative utility of unused components to the blend. Preliminary LP runs quickly established that similar cuts had similar utilities to the blends. For example, if a blend made of cuts 3 through 5 was not used in a blend and had low utility, a blend made of cuts 3 through 6 of the same product would also have low utility and would not be used. These actions allowed calculation of optimal blends from a set of fuels including the parent stocks, products, and all the practical distillation cuts.

In this way, linear programming computed the blend compositions based on the property and emissions data for each component. The properties of each of the blends were also computed based on the assumptions of linear blending. The results of these calculations for the aromatic content and the cetane number are summarized in Table 10. The measured cetane numbers, also listed in Table 10, are in some cases significantly different than the computed values, indicating the nonlinear nature of the cetane scale.

Table 10. Computed and Measured Properties of the Low-Emissions Fuels

Fuel Number	Aromatics (wt %)	Computed CN	VCR Measured CN
1	10	70	62
2	7.8	66	40
3	0.7	57	43
4	29	63	41
5	15	75	60
6	7.7	63	29
7	15	60	41
8	11.3	69	44
9	8.7	73	56
10	13.9	55	50

Clean-Fuel Experimental Results and Discussion

The Phase III test fuels included the 10 "low emissions" fuels described in the previous section, as well as repeats of the fractions of the Fischer-Tropsch wax material (FT1) and fractions of a straight-run material (FT2) from the Fischer-Tropsch processing of coal.

Linear programming was also used to compute the other properties and compositional data for each of the fuel blends. The statistical models for emissions are based mainly on the composition of the fuels and physical properties that are also linear functions of the composition. It is reasonable, therefore, to assume that the computed values of these properties are appropriate for use in the statistical models of the emissions. The results of the calculations of the properties and compositional data are presented in Table 11. These are linear combinations of component properties and variables such as viscosity which have blending indices were not transformed via a blending index.

Fischer-Tropsch Fuels

The Fischer-Tropsch fuels consisted of two different materials produced from the indirect liquefaction of coal. Each of these materials and seven fractions of both materials were subjected to both CVCA ignition experiments and VCR engine ignition and combustion and emissions testing. Both F-T liquids were added

to the project after its inception, but FT2 came at about the time Task 3 was started, so its evaluation was done as part of Task 3 and reported here.

The CVCA and VCR ignition quality ratings of the various materials were in excellent agreement with each other, both demonstrating that the full-boiling-range base materials had relatively high cetane numbers in the range of 65 to 85. The cetane numbers of the fractions of both materials demonstrated strong relationships to the boiling point, as shown in Figure 34 for the VCR cetane ratings. The lower-boiling fractions of each of these materials had relatively low cetane numbers. The cetane numbers increased dramatically in the higher-boiling-range fractions, to the point where it was not possible to provide accurate ratings of the highest-boiling-point fraction because the compression ratio of the VCR engine could not be lowered sufficiently to accomplish ignition at TDC.

Figure 34 shows that the cetane numbers of all fractions of the FT1 material were higher than the corresponding fractions of the FT2 material. These differences are clearly related to differences in the composition of the two materials. However, although the total aromatic contents of both materials were very low, the FT1 material had significantly higher levels of aromatics than the FT2 material.

All of the Fischer-Tropsch materials were tested at five different speed and load conditions in the VCR engine. As described previously, Mode 2 was the rated torque condition for the test engine. The injection timing was adjusted for each fuel to give the maximum torque output of the engine. Mode 2 represents a test condition at which the NO_x emissions are sensitive to the ignition quality of the fuel. The NO_x data for this condition are presented in Figure 35. Although data are missing for the FT2 materials, the NO_x emissions are clearly higher for the FT2 materials than for the FT1 materials. In addition, the differences are larger for the lower-boiling-point fractions, where the differences in the ignition quality are also larger. The corresponding data for the Mode 1 condition, a retarded timing and low-NO_x condition, indicated no systematic differences between the two fuels.

The smoke data at all test conditions indicated a systematic difference between the two materials, with the FT1 always higher than the corresponding FT2 fractions. This difference is probably related to the differences in aromatic content of the two materials where FT1 has effectively zero aromatic content and FT2 has only 2% vol aromatics. In addition, there was a trend at all test conditions for the smoke emissions to increase with boiling point, due most likely to the physical effect of the boiling point on the evaporation rates of the fuel in the engine. These trends are demonstrated in Figure 36 for the Mode 2 test condition.

The unburned hydrocarbon (HC) emissions displayed an interesting trend that was consistent at all test conditions. The trend consisted of a dramatic, systematic decrease in the HC emissions with increasing average boiling point. These results are demonstrated in Figures 37 and 38 for the Modes 1 and 2 test conditions, respectively. These results are not consistent with the intuitive impression that the higher-boiling fractions would produce high HC emissions. The results are probably because the higher-boiling fractions are higher molecular weight components that are emitted as particulate, or that agglomerate or condense in the exhaust system.

The value of the Fischer-Tropsch materials is indicated by the fact that the emissions parameters, or EPs, averaged over all of the fractions of both materials, were well below the averages for all of the test materials. The EP values for all of the test materials are presented in Figure 39 for the Mode 2 test condition. The dashed line in Figure 39 represents the average EP of approximately 4.3, indicating that on average, the emissions were above target values. The average EP for the FT1 fuel fractions was 3.8 and that for the FT2 fractions was 2.86, both well above average and both below the target value.

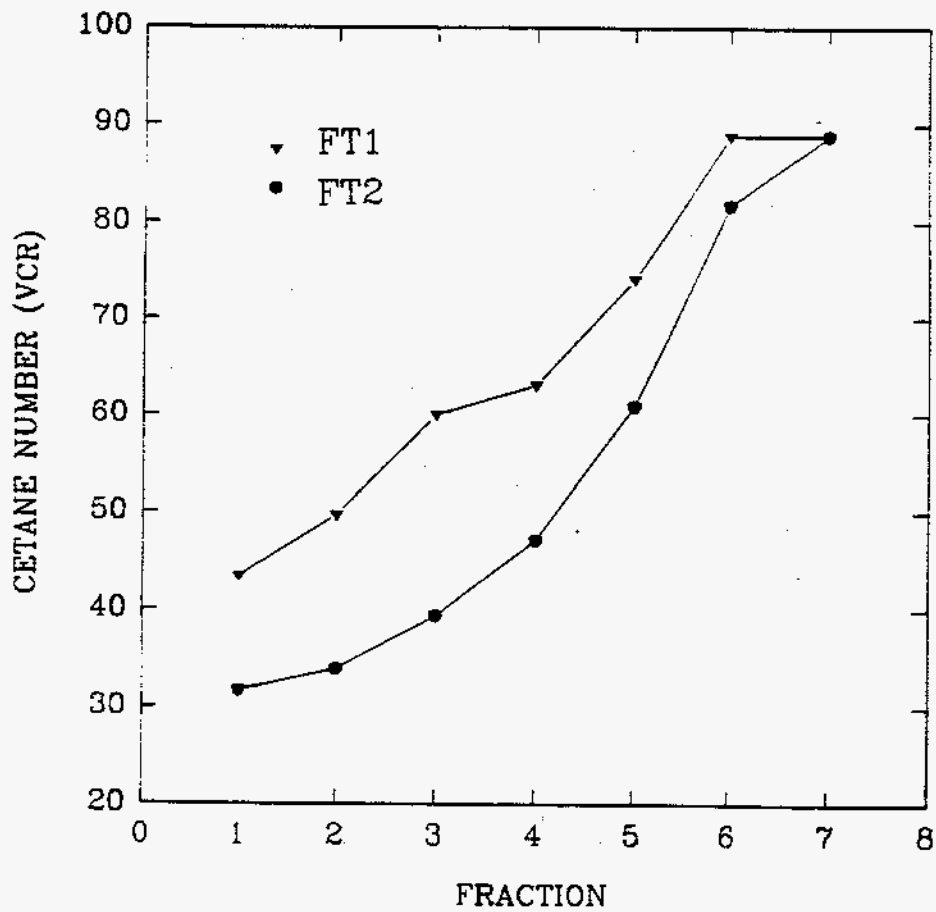


Figure 34. VCR cetane ratings of the Fischer Tropsch materials

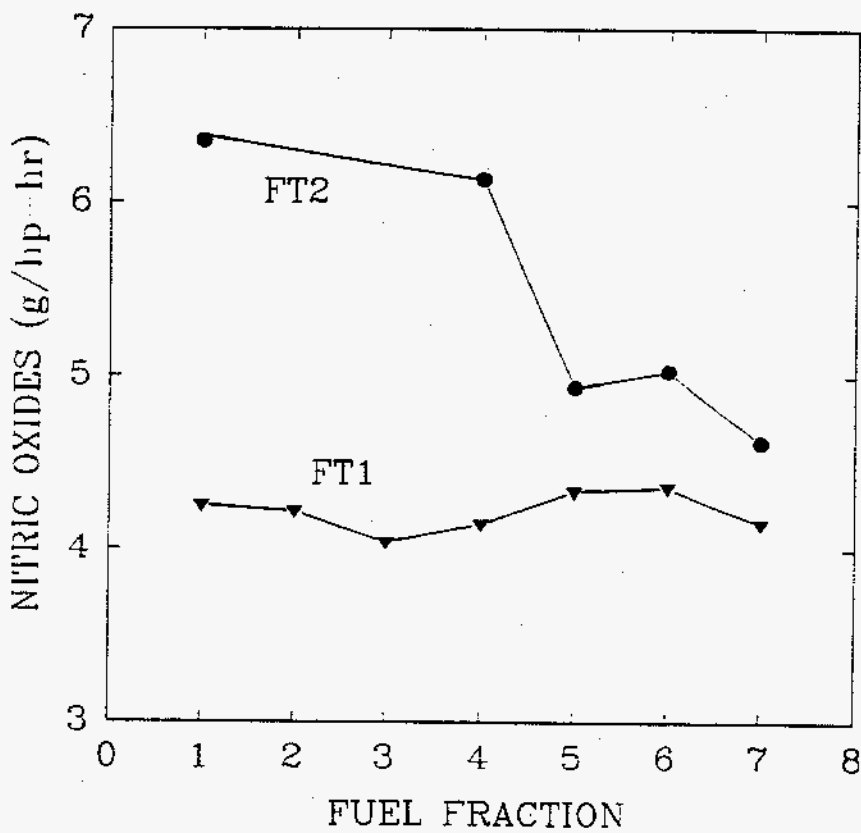


Figure 35. Nitric oxide emission data for the Mode 2 test condition

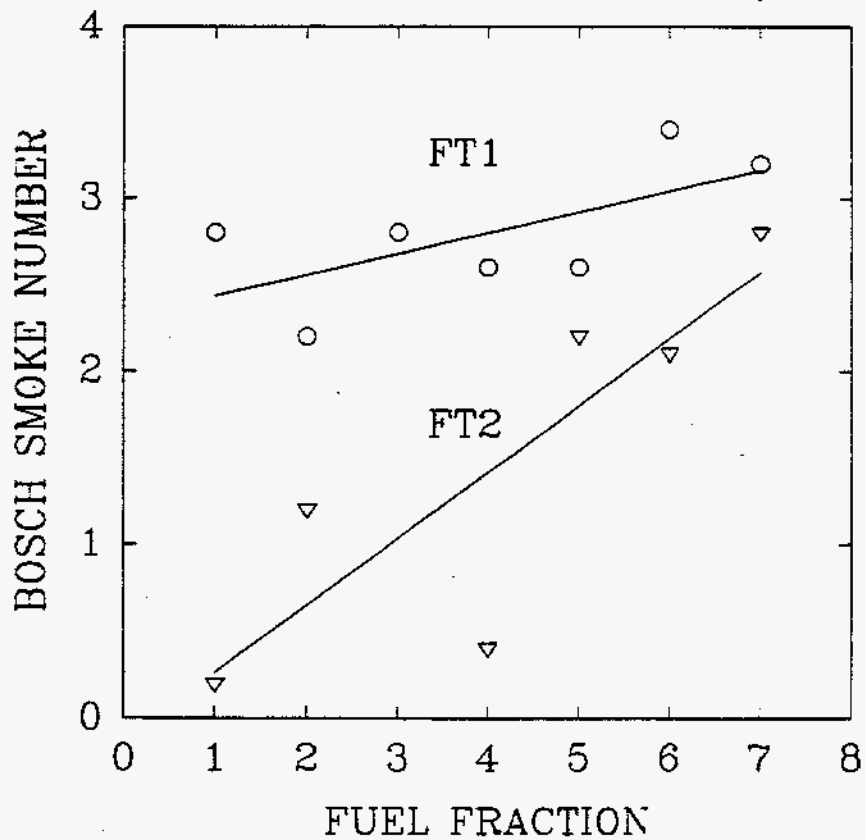


Figure 36. Bosch smoke numbers for the Mode 2 test conditions

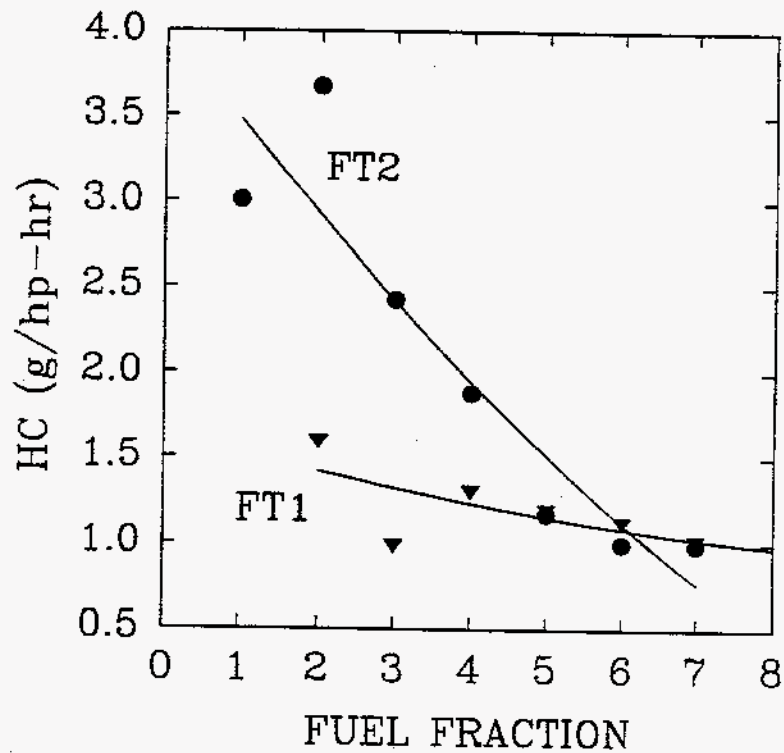


Figure 37. Hydrocarbon emissions for the Mode 1 test conditions

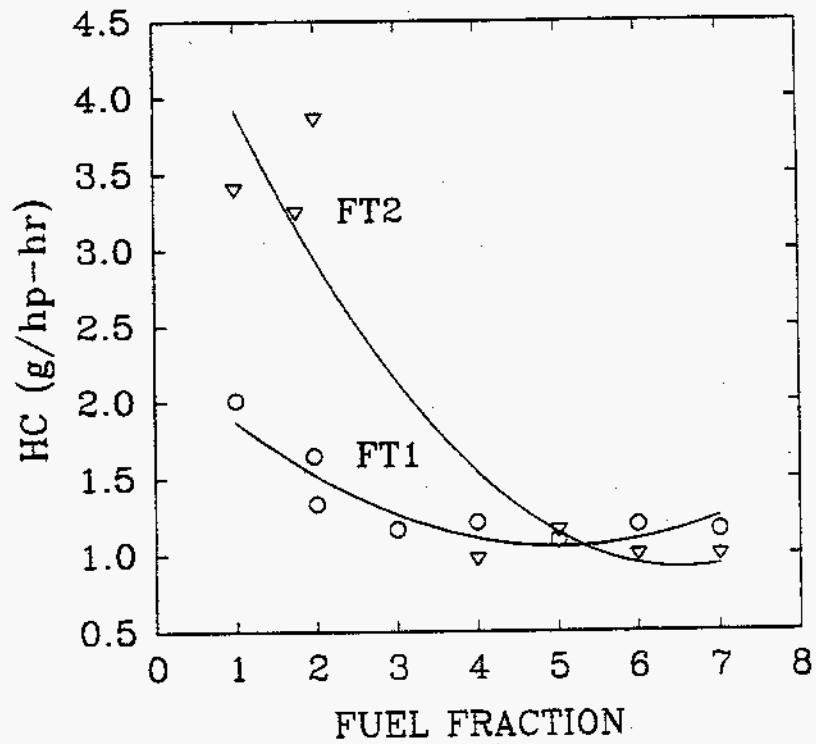


Figure 38. Hydrocarbon emissions for the Mode 2 test conditions

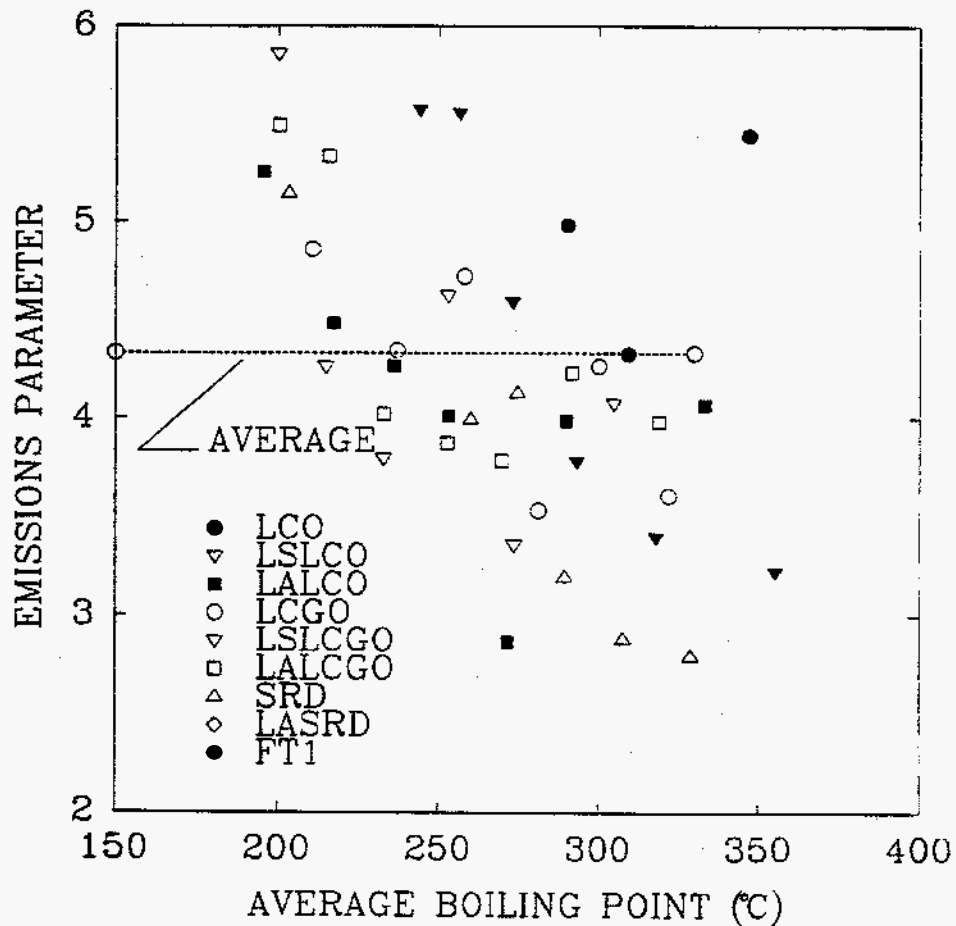


Figure 39. Emissions parameters for all test materials at the Mode 2 test conditions

Table 11. Task 3 Correlation Inputs

Name of Variables	FUEL IDENTIFICATION									
	Blend #1	Blend #2	Blend #3	Blend #4	Blend #5	Blend #6	Blend #7	Blend #8	Blend #9	Blend #10
Acnaphthe	0.268	0.335	0.055	4.723	2.396	1.359	2.389	1.878	1.064	0.299
Acnaphthy	0.171	0.205	0.039	2.789	1.469	1.034	1.414	1.252	0.767	0.120
Alkbenz	3.972	4.840	1.463	6.424	3.617	5.624	3.943	4.621	3.346	5.821
Alk_naph	0.545	0.503	0.050	4.129	2.094	0.719	2.090	1.407	2.101	0.627
Arotricy	0.027	0.039	0.006	0.401	0.203	0.597	0.203	0.400	0.287	0.023
Aro_tot	10.571	12.196	2.654	23.066	12.200	14.105	12.860	13.152	11.348	14.641
Indans	3.500	4.206	0.777	2.645	1.384	3.516	1.711	2.450	2.062	4.771
Indenes	2.076	2.053	0.259	1.801	0.959	1.187	1.030	1.073	1.604	2.954
Naphth	0.019	0.000	0.000	0.134	0.068	0.021	0.067	0.044	0.086	0.067
nmrAlp	3.344	3.983	0.866	10.875	5.688	5.335	5.870	5.512	2.611	4.534
nmrAro	1.625	1.783	1.240	6.657	3.654	2.911	3.948	3.283	2.012	1.878
nmrCh	8.373	16.487	6.966	6.134	4.619	24.352	6.550	14.486	9.062	13.969
nmrCh2	50.453	42.695	52.487	49.918	56.218	30.721	51.202	43.469	53.369	45.039
nmrCh3	31.243	35.024	38.451	26.404	29.804	36.700	32.427	33.252	32.320	33.252
Para	59.149	39.331	80.838	64.239	75.041	15.979	72.539	45.510	60.577	45.412
Para_di	6.116	14.319	3.963	1.899	1.626	22.946	2.931	12.286	6.892	10.548
Para_tri	2.083	7.464	2.314	0.077	0.039	9.738	1.196	4.888	3.007	4.409
Par_mono	17.073	26.668	10.245	10.648	11.007	37.250	10.447	24.128	17.472	23.657
Sat_tot	84.395	87.744	97.352	76.877	87.713	85.895	87.114	86.804	87.966	83.995
SpGr	0.774	0.842	0.781	0.843	0.816	0.872	0.812	0.844	0.816	0.824
Total UV	3.417	4.080	0.838	13.524	6.917	6.122	7.181	6.520	4.329	4.444
UVdi	0.686	0.730	0.075	6.722	3.409	1.568	3.399	2.489	1.790	0.765
UVmono	2.725	3.351	0.763	5.880	3.041	3.797	3.322	3.419	2.178	3.672
UVtri	0.000	0.000	0.000	0.938	0.476	0.761	0.469	0.619	0.360	0.000
Vis40	3.031	3.142	2.040	3.708	3.688	2.904	2.874	3.296	3.321	3.159
Vis100	1.169	1.220	0.894	1.336	1.352	1.147	1.115	1.250	1.278	1.220
VParom	14.721	14.440	10.264	35.700	23.434	15.996	22.982	19.715	15.239	13.782
VPolef	4.043	2.586	4.891	4.255	5.221	0.845	4.573	3.033	3.721	1.624
VPsat	76.268	82.940	84.886	60.054	71.349	83.127	72.470	77.238	80.226	83.229
WtPC	81.488	86.257	85.043	86.725	85.887	86.937	85.884	86.412	85.392	85.062
WtPH	13.663	13.670	14.951	13.475	14.254	12.924	14.213	13.589	14.033	13.711
WtPS	0.012	0.009	0.001	0.005	0.004	0.004	0.003	0.004	0.017	0.009

Low-Emissions Fuels

As discussed above, ten low-emissions fuels were formulated using linear programming techniques. The constraints on the properties and the compositions used in the calculations had to be relaxed in several cases to meet the emissions requirements. The aromatic content and the cetane number data, presented in Table 10, are plotted in Figures 40 and 41, respectively, for the ten low-emissions fuels. The target cetane number for fuels 3, 4, and 7 was 55 CN, while the aromatic content was to vary over a range from less than 10%–30%. The actual cetane numbers for these fuels were in the range 42 to 43 CN and the aromatics ranged from 1%–30%. The target aromatic content for fuels 5, 6 and 8 was 15%, with cetane number varying from 63 to 75 CN. The actual cetane numbers of these fuels ranged from 30 to 60 CN and the aromatic content varied from 8%–15%, with variation due to limits imposed by the available blending materials. It should be pointed out that several of the fuel components had to be recreated from the feedstocks for Task 3, making some variation of originally measured properties and the ones prevalent in Task 3. Further these materials were available in short supply making it impractical to perform the number of CN replicates necessary to reduce variability of results.

These results reiterate that the cetane number does not always blend linearly. The resulting fuels, although lower in cetane number than originally planned, do offer the opportunity to study the effects of variation in aromatic content at nearly constant cetane number (Fuels 3, 7 and 4 in order of aromatic content) and the effects of variation in cetane number at modest variation in aromatic content (Fuels 5, 8, and 6 in order of cetane number).

We believe that the Mode 2 test conditions provide a more-sensitive measurement of the fuel effects on the NO_x emissions than the other modes because the injection timing was adjusted for maximum torque on each fuel. The Mode 2 NO_x data for the 10 low-emissions fuels are presented in Figure 42. The corresponding data for HC, CO, and smoke emissions are presented in Figures 43 through 45, respectively. The results in Figure 42 indicate a trend towards increased NO_x emissions as the aromatic content is increased from 1%–30%. In addition, HC emissions appear to decrease and CO and smoke emissions increase with the increase in aromatic content.

Increasing the cetane number from 30 to 60, while holding aromatic content in the range from 8 to 15, results in a significant reduction in NO_x emissions. This variation in the cetane number results in a corresponding increase in HC, CO, and smoke emissions.

Fuel 1 was designed to be the lowest-emissions fuel that could be produced from the large number of potential blending materials that were available in this study. Although the NO_x emissions of this fuel were clearly the lowest, other fuels had lower levels of the other emissions. This demonstrates the utility of using the emissions parameter for the fuel-to-fuel comparisons.

The EPs computed from the linear programming model and the actual values based on the measured emissions are presented in Figure 46 for the Mode 2 test conditions, and several points can be made. First, the predicted EP values are all very close to the target level of 4. This is indicative of the results of the linear programming model, in which the EP was set as one of the constraints. The second point is that the actual EPs follow the same trends as the predicted, indicating that the basis of the modeling work is correct in a linear sense. The same conclusion was also arrived at in the detailed statistical analysis, where the relationships between the emissions and the fuel properties and composition are linear. The third observation is that the actual EP values are significantly below the predicted and the targets in 8 out of the 10 cases, with EPs in the range of 3.5.

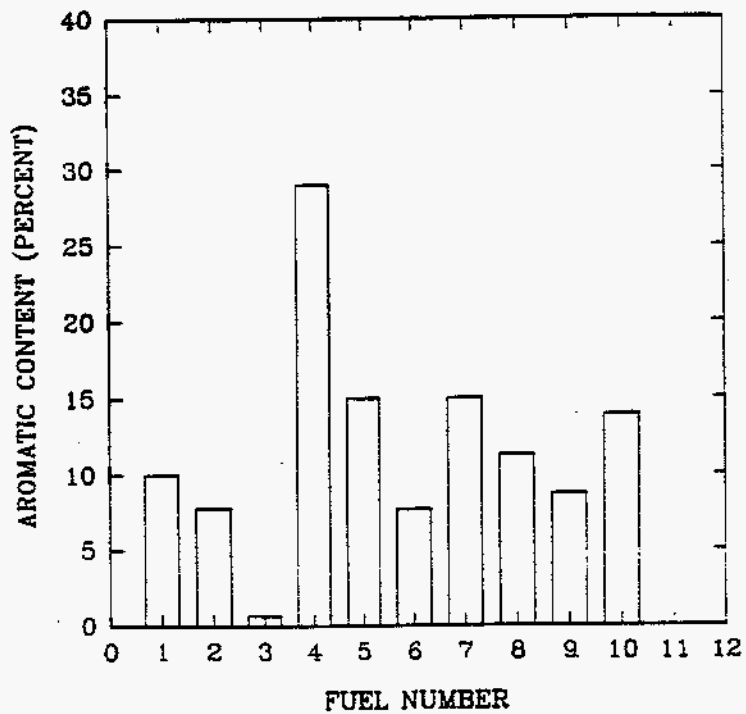


Figure 40. Aromatic content of the low-emissions fuels

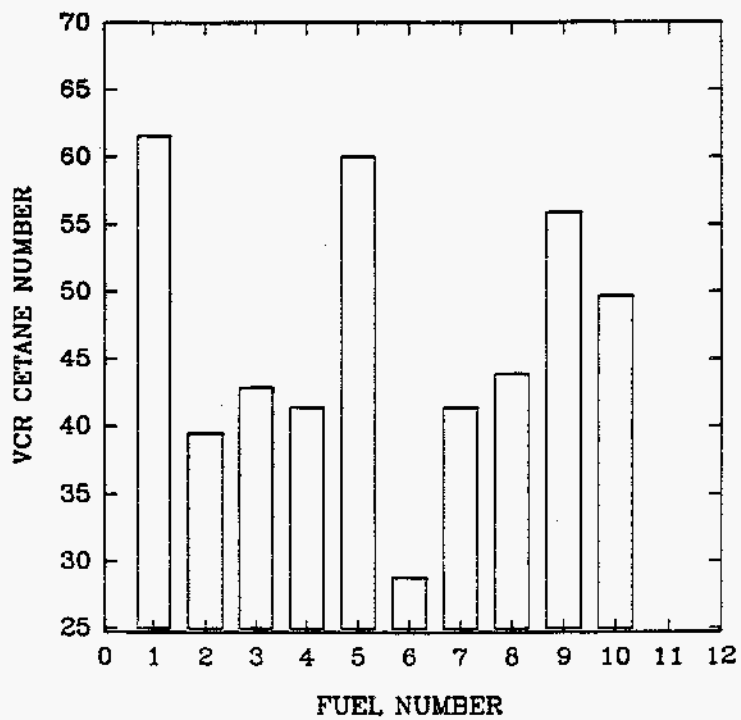


Figure 41. VCR cetane numbers of the low-emissions fuels

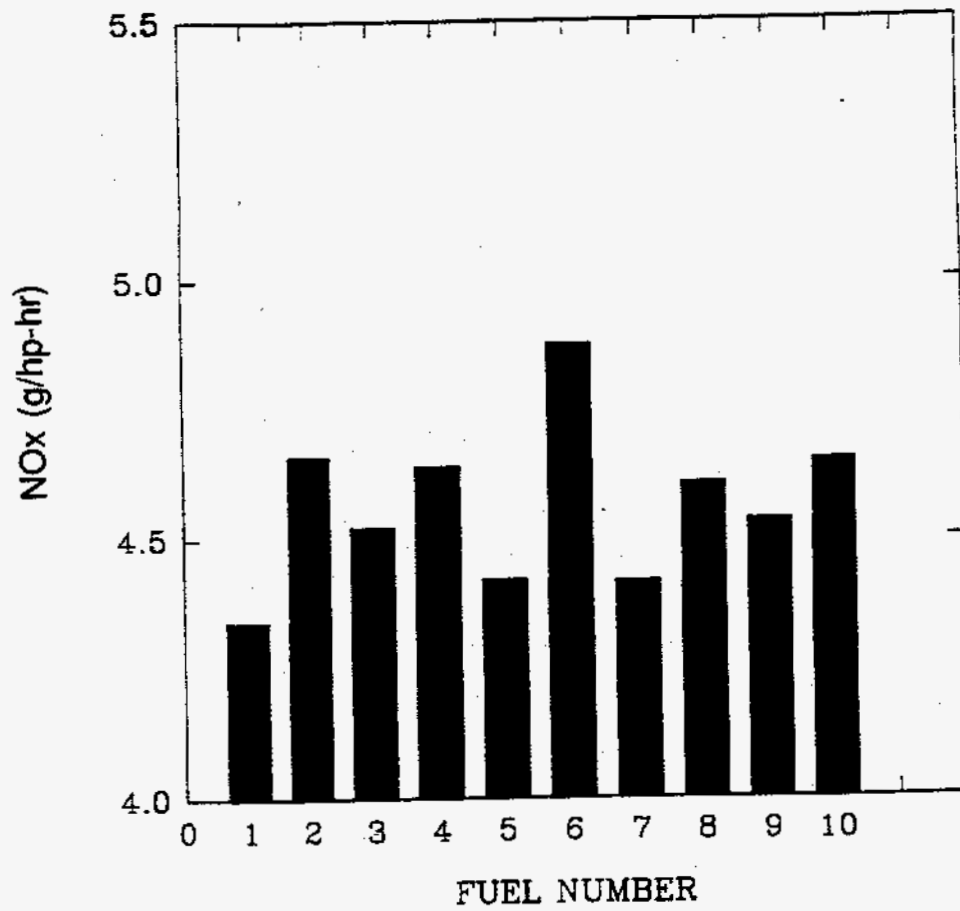


Figure 42. NOx emissions for the low-emissions fuel at Mode 2

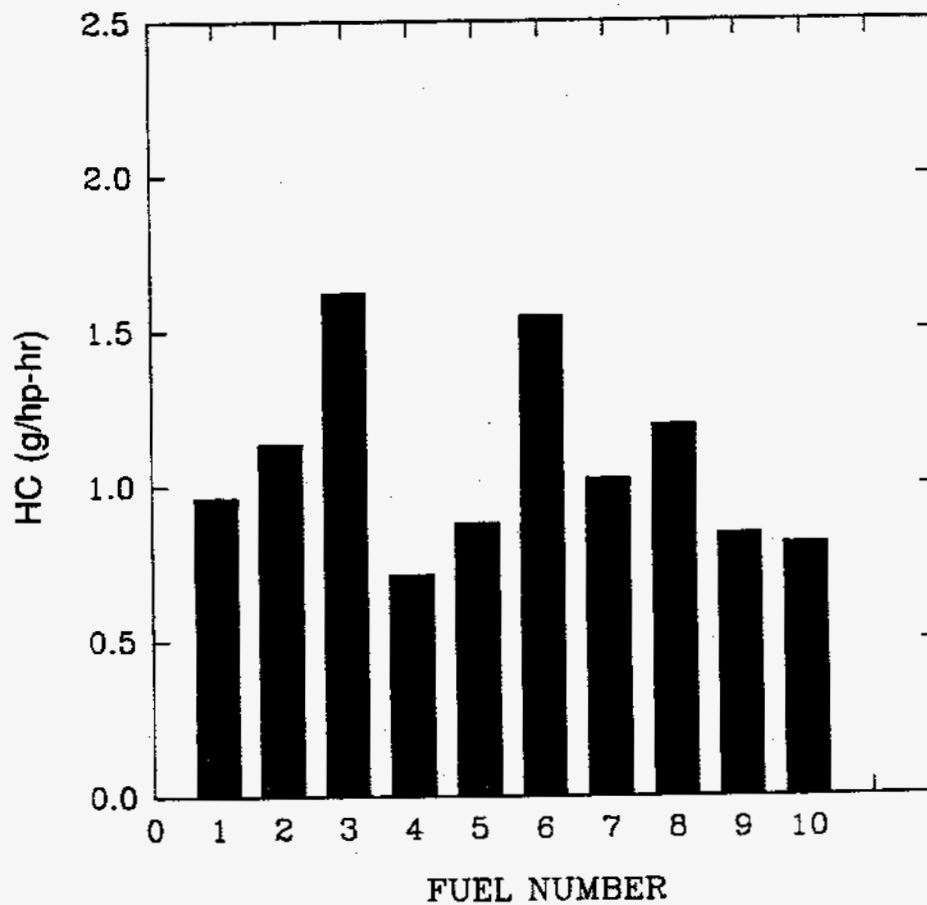


Figure 43. Hydrocarbon emissions for the low-emissions fuels at Mode 2

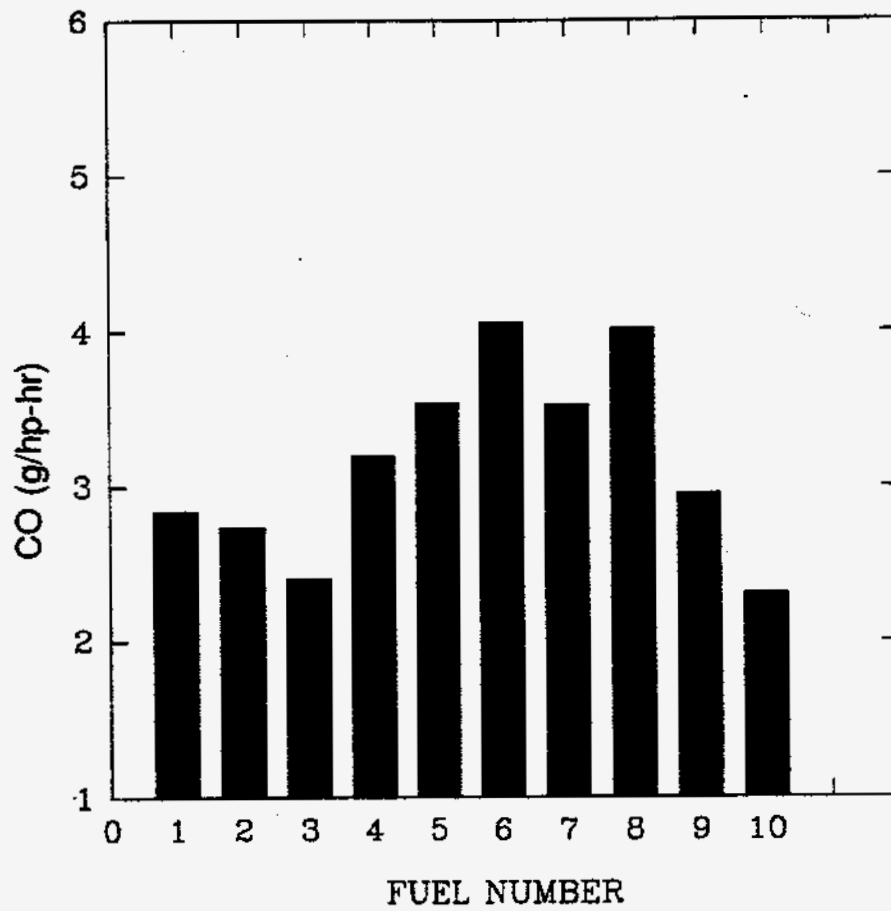


Figure 44. CO emissions for the low-emissions fuel at Mode 2

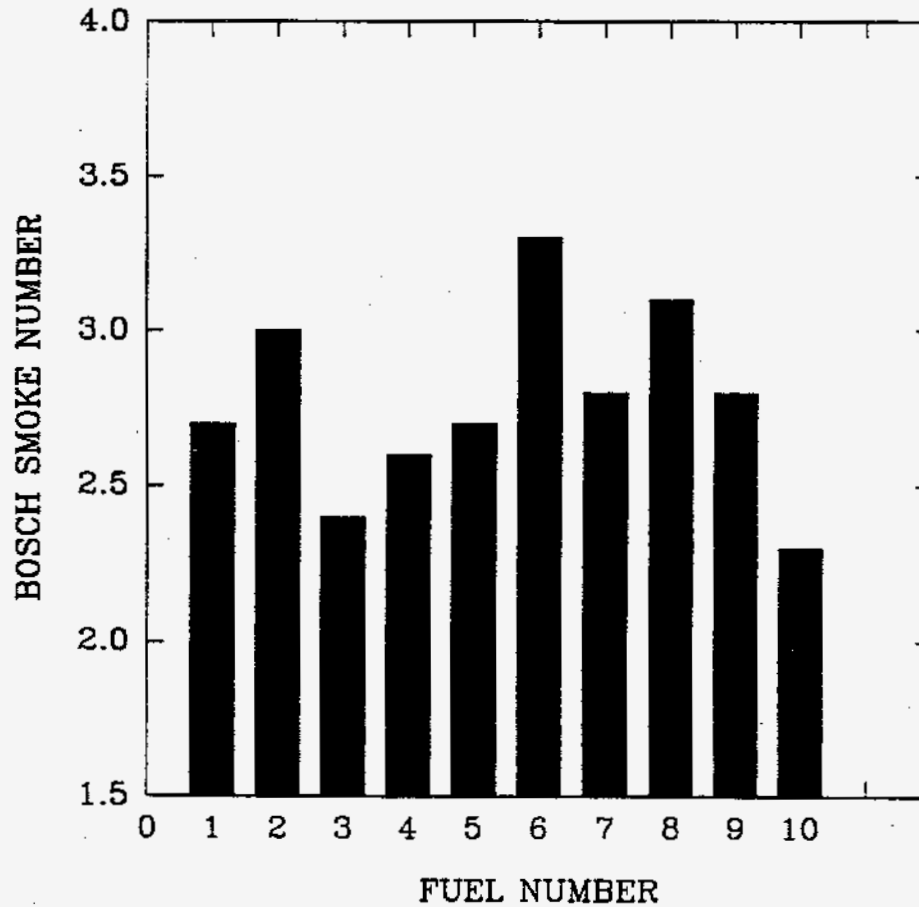


Figure 45. Bosch smoke number for the low-emissions fuels at Mode 2

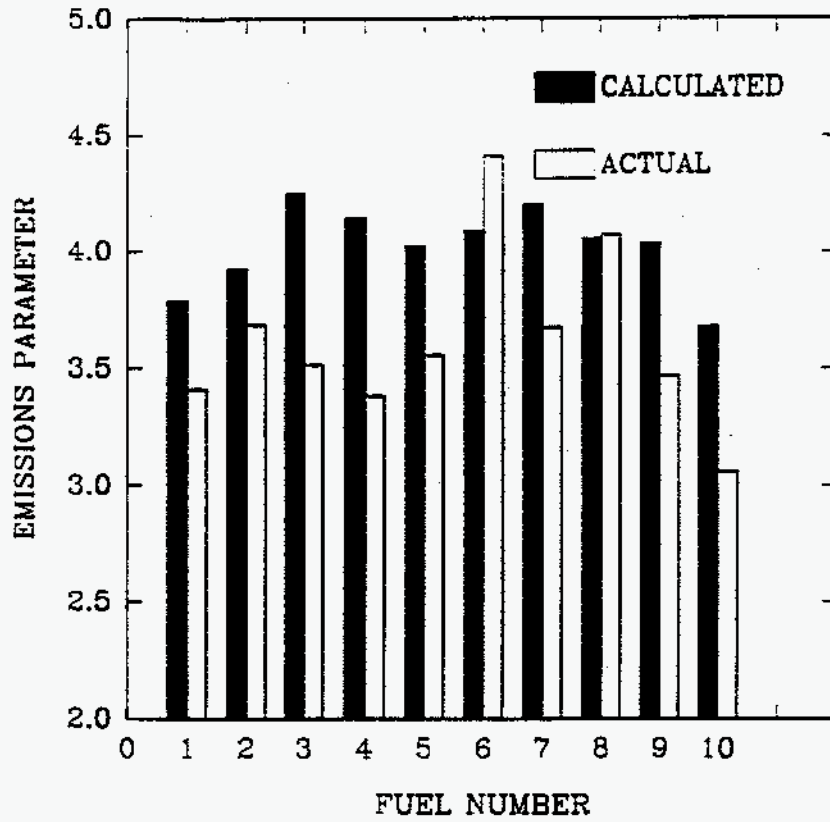


Figure 46. Emissions parameter, calculated and measured at Mode 2

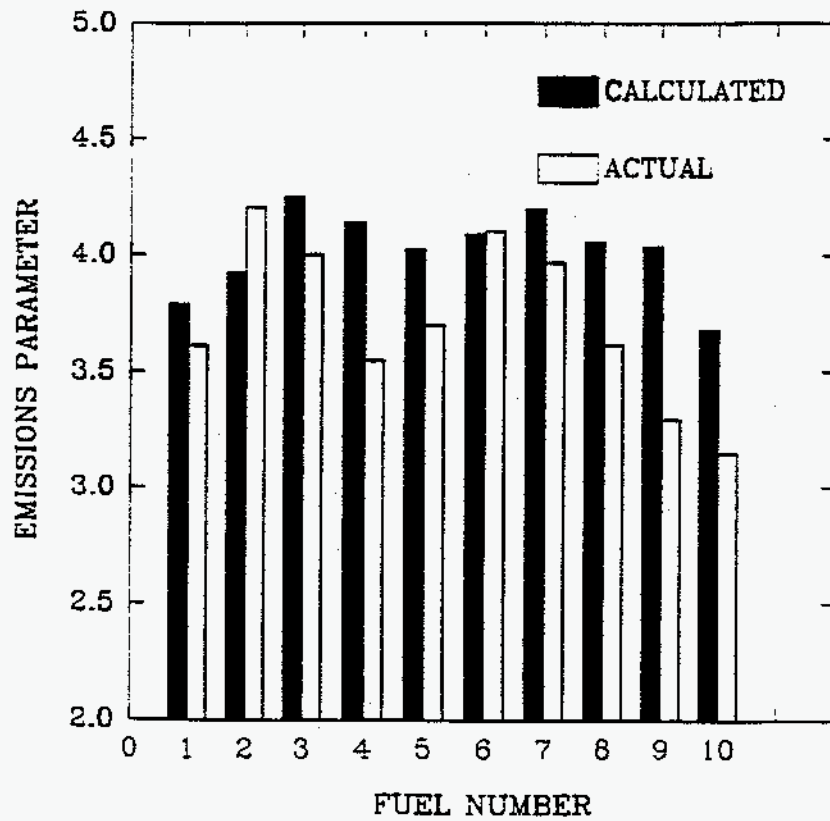


Figure 47. Emissions parameter, calculated and measured at Mode 1

As shown in Figure 39, the average EP for the 80 fuels examined in this project was 4.3 at the Mode 2 test condition. The reduction from 4.3 to 3.5 indicates that full-boiling-range low-emissions fuels can be designed and produced using actual blendstocks. Similar conclusions can be drawn from the data at the other test conditions, as can be verified by examining the Mode 1 EP values for the low-emissions fuels and all test materials, in Figures 47 and 48, respectively. The corresponding data for the other test conditions are presented in Appendix C.

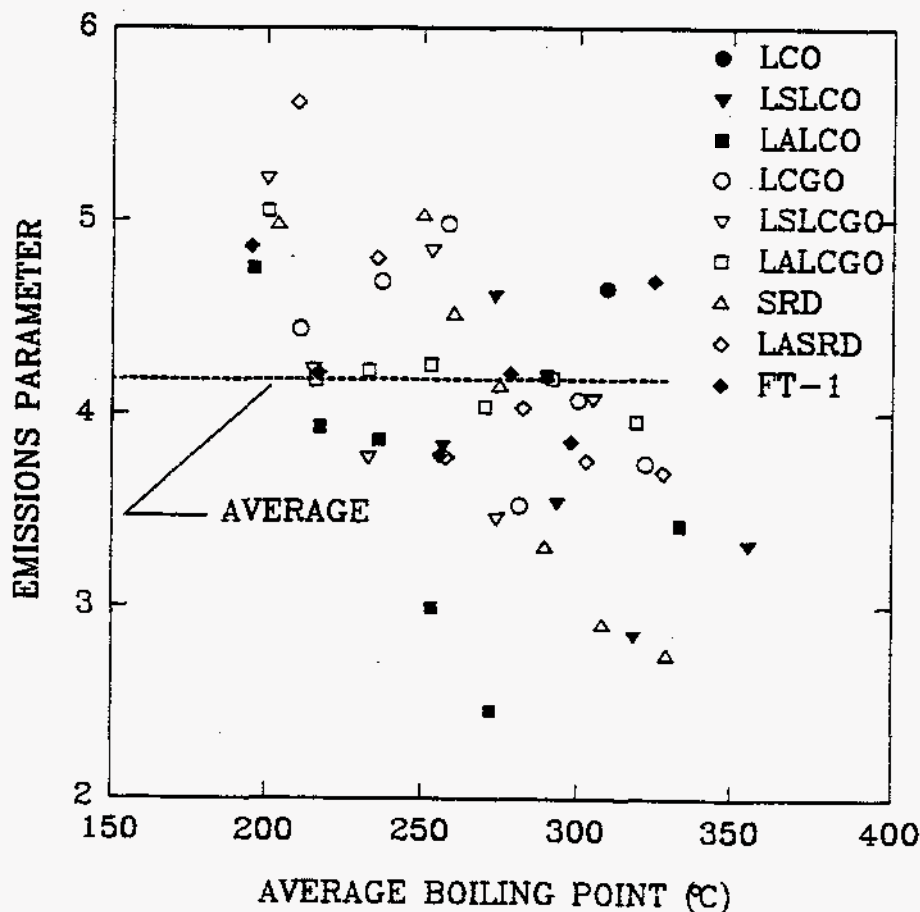


Figure 48. Emissions parameters for all test materials at the Mode 1 test conditions

Clean-Fuel Discussion

The results of the experiments indicated that aromatic content, aromatic type, cetane number, distillation, and density are all important in affecting the engine performance and emissions. These results agree with recent findings reported in the literature. The results, however, also indicate that the overall chemical structure is important in controlling the emissions and cetane number. It is simply not enough, for instance, to reduce the total aromatic content; the reduction of the tricyclic aromatic content also appears to be very important for NO_x and smoke control. This may be most efficiently accomplished by hydrotreating the heavier fractions of the diesel fuel. Also, the cetane number relationship to the emissions is simply a manifestation of chemical structure that inherently produces lower emissions. The data base from these experiments is extensive and could be the subject of much additional analysis. The following section is a brief summary of the most important conclusions drawn from analyses that have been completed to date.

Summary and Conclusions

Five different diesel-fuel feed and blendstocks were hydrotreated to at least two levels of sulfur and aromatic content. These materials were then distilled to seven or eight fractions by boiling point. The raw materials, as well as all of the fractions making 80 samples overall, were then subjected to a series of combustion-bomb and engine tests to determine the ignition, combustion, and emissions characteristics of each material. In addition, all materials were characterized extensively in terms of physical and chemical properties and chemical composition.

The resulting data base was statistically analyzed to develop preliminary relationships between the emissions characteristics and the fuel properties and composition. The results of these analyses indicated linear relationships. Linear programming techniques were then used to formulate 10 different low-emissions fuels based on blending to meet specific emissions targets designed to be indicative of future emissions standards. The predicted emissions performance and the actual emissions were trendwise similar over the speed/load range of the test engine. The actual emissions characteristics were, in fact, much better than targets and the corresponding baseline data for most of the fuels.

The following specific conclusions can be drawn from the results of this project:

1. Ignition quality and emissions characteristics are related to boiling point as indicated by the strong functional relationships between these parameters and the average boiling point of each fraction.
2. The proposed new specifications for reformulated diesel fuel limiting the end point and the aromatics content may not be compatible with each other and may lead to increased particulate emissions. Reducing the end point will reduce the cetane number in some feedstocks and can also reduce the effectiveness of hydrogenation in reducing the aromatics content. This overall cetane number reduction could have an adverse effect on NO_x also.
3. Ignition and emissions characteristics are directly related to aromatic content and type of fuel, where:

$$\begin{aligned} \text{CN} = & A_1 + A_2 \times (\text{Alkylbenzenes}) + A_3 \times (\text{T50\%}) \\ & + A_4 \times (\text{Indenes}) + A_5 \times (\text{Paraffins}) \\ & + A_6 \times (\text{Specific Gravity}) + A_7 \times (\text{Viscosity@40}^\circ\text{C}) \end{aligned}$$

where the concentrations are in wt%, specific gravity is in gM/mL, viscosity is in centistokes (cSt), and where:

$$A_1 = 277.1 \quad R^2 = 0.94$$

$$A_2 = 0.54$$

$$A_3 = 0.31$$

$$A_4 = -1.83$$

$$A_5 = -0.13$$

$$A_6 = -437.3$$

$$A_7 = -1.98$$

4. Because of the relationship between ignition quality and aromatics, the variation of the emissions characteristic is accounted for in the aromatic description of the fuel.
5. The aromatic content of the fuel is not always uniformly distributed across the boiling range of the fuel. In some cases, such as for the light-coker gas oil, the aromatics are concentrated in the heavier fractions.
6. Within the range of variation possible in the project, the relationships between emissions and fuel composition are linear, so that linear programming techniques can be used to design low-emissions diesel fuels.
7. Low-emissions diesel fuels can be formulated using raw materials that can, on the average, have relatively high-emissions characteristics. This is accomplished by processing and blending to achieve the emissions and cost goals.
8. The F-T diesels showed superior performance by two measures of cetane number determination. FT-1 blended linearly with petroleum stocks having a wide range of cetane numbers. The results did not show whether the contributions of aromatics dilution versus paraffin structure provide this good cetane number behavior.
9. The aromatics are distributed over the boiling range of the straight-run diesel fuel, similar to the light-cycle oils. Unlike the light-cycle oils, however, hydrotreatment appears to be much more effective in reducing the aromatics content of the heavier fractions of this fuel. In fact, cetane number was decreased by hydrogenation in mid boiling range.
10. The power output of the engine was not strongly affected by large variations in the fuel properties as long as the air-fuel ratio set point is held constant. Ignition depends on the cetane number, but the power is related mainly to the apparent combustion efficiency.
11. The emissions characteristics of the materials tested in this program are dominated by composition of the materials. The compositional data always provided more information in the regression models than the physical properties.
12. The nitric oxide emissions are modeled as:

$$\text{NOx} = A_1 + A_2 \times (\text{AlkylNaphthalenes}) + A_3 \times (\text{Indenes}) + A_4 \times (\% \text{ Carbon}),$$

where concentrations are in wt% and the coefficients are:

$$A_1 = -96.34 \quad R^2 = 0.82$$

$$A_2 = 0.22$$

$$A_3 = 0.24$$

$$A_4 = 1.17$$

where the aromatic structure dominates the relationship.

13. The smoke emissions are related to the fuel properties in the following relationship where:

$$\begin{aligned} \text{Bosch Smoke} = & A_1 + A_2 \times (\text{Acenaphthylenes}) \\ & + A_3 \times (\text{Alkylbenzenes}) + A_4 \times (\text{Tricyclic aromatic}) \\ & + A_5 \times (\text{Total aromatics}) + A_6 \times (\text{vol\% aromatics}), \end{aligned}$$

where concentrations are in wt% except as indicated, and where:

$$A_1 = 2.24 \quad R^2 = 0.61$$

$$A_2 = -0.065$$

$$A_3 = -0.029$$

$$A_4 = 0.08$$

$$A_5 = 0.027$$

$$A_6 = -0.013$$

And where a significant portion of the variation in smoke could not be accounted for in the fuel variables. Experimental error or physical processes may account for the remainder of the variations.

Acknowledgements

The authors send their appreciation to the U.S. Department of Energy and the National Renewable Energy Laboratory for their financial support of this project. This work was under the U.S. Department of Energy Office of Energy Efficiency and Renewable Energy Alternative Fuels - Utilization Program (AFUP), John A. Russell, manager, first through its operations at the Oak Ridge National Laboratory, Dr. R.L. Graves, project representative then at the National Renewable Energy Laboratory, Kenneth R. Stamper, program manager representative. Technical guidance was provided from NREL through Messrs. Brent K. Bailey and Christopher Colucci. We would also like to credit Norman R. Sefer, the first project manager of the AFUP Alternative Fuel Center at Southwest Research Institute, for the concept of the assay, Messrs. K.H. Childress, C.C. Cover, D.L. Hetrick, and G.R. Segura for round-the-clock pilot plant operations to process the test fuels, Messrs. C.S. Butcher, R.E. Powell, P.M. Rainwater, Mr. D.L. Present, and Ms R.C. Robledo for the laboratory analyses, Messrs. M.J. Maymar and S.D. Ott for the combustion experiments, Mr. J. W. Chessher for the emissions measurements, Mr. T.J. Callahan, Mr. W.M. Mason, and Dr. R.L. Mason for the statistical analysis of the data, and Ms. E.S. Martin and Ms. S.J. Hoover for their work in preparing the numerous typescripts.

References

- Bailey, B.K., Russell, J.A., Wimer, W.W., Buckingham, J.P., (October 1986) "Cetane Number Prediction from Proton-Type Distribution and Relative Hydrogen Population." Prepared for the SAE International Fuels and Lubricants Meeting, October 6-9, 1986. SAE Paper No. 861521. Philadelphia, PA,
- Bhatt, B.L., Schaub, E.S., and Heydom, E.C., (April 1993) "Recent Developments in Slurry Reactor Technology at LaPorte Alternative Fuels Development." Prepared for the 18th International Technical Conference on Coal Utilization and Fuel Systems, April 26, 1993.
- Bludis, J.A. and Christman, R.D., (February 1991) "Arge Wax Hydrocracking Study." DOE Project Report February 4, 1991. No. 125501.
- Burns, V.R., Ingham, M.C., and Doherty, H.M. (February 1992) *Auto/Oil Air Quality Improvement Research Program*, February 1992. SAE SP-920.
- Buzza, T.G. and Litzinger, T.A., (November 1987) "A Comparison of Three Coal-Derived, Middle Distillate, Synthetic Fuels in a Single Cylinder DI Diesel Engine." Prepared for the SAE International Fuels & Lubricants Meeting, November 2-5, 1987. SAE Paper No. 872036. Toronto, Ontario, Canada.
- Cookson, D.J., Lloyd, C.P., and Smith, B.E., (1988) "Investigation of the Chemical Basis of Diesel Fuel Properties," *Energy and Fuels*, volume 2, pp. 854-860, 1988.
- Cowley, L.T., Doyon, J., and Stadling, R.J., (October 1993) "The Influence of Composition and Properties of Diesel Fuel on Particulate Emissions from Heavy-Duty Engines." Prepared for the SAE 1993 International Fuels & Lubricants Meeting, October 18-21, 1993. SAE Paper No. 932732. Philadelphia, PA.
- Erwin, J., (August 1992) "Assay of Diesel Fuel Components, Properties, and Performance," Prepared for the ACS Symposium on Synthetic Fuels, August 23-28, 1992. Washington, DC.
- Federal Register, (August 1989) "Fuel Quality Regulations for Highway Diesel Fuel Sold in 1993 and Later Calendar Years." August 24, 1989." *Federal Register*, vol. 54, No. 163.
- Fortnagel, M., Gairing, M., Wagner, W., (1983) "Verbesserun des Diesel-Motors-Verschlechterung des Diesel-Kraftsoffs - ein Eiderspruch." *VDI Berichte* No. 466, 1983.
- Foster, D.E., Dimplefeld, P.M., Boggs, D.L., Bair, R.E., and Borman, G.L., (November 1987) "The Effects of Fuel Composition on Ignition Delay in Homogeneous Charge and Direct Injection Compression Ignition Engines." Prepared as Final Report, Contract DE-AC05-84OR21400, November 1987. U.S. Department of Energy, Alternative Fuels Utilization Program, Report No. ORNL/Sub/84-896771/1.
- Gairing, M., (1985) "Anforderungen and Diesel-Kraftsoffqualitat-heute und in Zukunft." *VDI Berichte* No. 559, *Emissionsminderung Automobilabgase - Dieselmotoren - VDI Verlag* 1985.
- Grant, J.G. and R.A. Pourciau, (September 1991)" RFG: Fractionate, Innovate, and Reformulate," *Fuel Reformulation*, Vol. 1, No. 1, September/October, 1991.

Hanson, Ronald, K., and Salimian, Siamak, (1984) "Survey of Rate Constants in the N/H/O System," *Combustion Chemistry*, p. 361, W.C. Gardiner, Jr. Ed., Springer-Verlag, NY.

Kohl, K.B., Bailey, B.K., Newman, F.M., and Mason, R.L., (June 1991) "Chemical Analysis of Aromatics in Diesel Fuels," report for California Air Resources Board, A932-125, June 20, 1991. Sacramento, CA.

McCarthy, C.I., (October 1992) "Diesel Fuel Property Effects on Exhaust Emissions from a Heavy Duty Diesel Engine that Meets the 1994 Emission Requirements," International Fuels & Lubricants Meeting and Exposition, October 19-22, 1992. San Francisco, CA.

Miyamoto, N., Ogawa, H., Shibuya, M., and Suda, T., (October 1992) "Description of Diesel Emissions by Individual Fuel Properties." Prepared for the International Fuels & Lubricants Meeting & Exposition, October 19-22, 1992. SAE Paper No. 922221. San Francisco, CA.

Nikanjam, M., (March 1993) "Development of the First CARB Certified California Alternative Diesel Fuel." Prepared for the SAE International Congress & Exposition, March 1-5, 1993. SAE Paper No. 930728. Detroit, MI.

Olson, D.R., Mechel, N.T., Quillian, R.D., (November 1960) "Combustion Characteristics of Compression Ignition Engine Fuel Components," Paper No. 263A, SAE National Fuels and Lubricants Meeting, November 2-4, 1960.

H.B. Palmer and C.F. Curtis, (1965) "The Formation of Carbon from Gases," *Chemistry and Physics of Carbon*, P.L. Walker, 1st. Ed. Mercel Dekker, Inc., N.Y., 1965.

Ryan T.W., III, (December 1986) "The Development of New Procedures for Rating the Ignition Quality of Fuels for Diesel Engines." Prepared for the U.S. Army Belvoir RD&E Center, BFLRF, December 1986. Interim Report 223. San Antonio, TX, Southwest Research Institute.

Ryan III, T.W. and Erwin, J., (October 1992) "Effects of Fuel Properties and Composition on the Temperature Dependent Autoignition of Diesel Fuel Fractions." Prepared for the International Fuel & Lubricants Meeting & Exposition, October 18-22, 1992. SAE Paper No. 922229. San Francisco, CA.

Ryan, III, T.W., (October 1985) "Correlation of Physical and Chemical Ignition Delay to Cetane Number." Prepared for the International Fuels & Lubricants Meeting & Exposition, October 1985. SAE Paper No. 852103. Tulsa, OK.

Ryan III, T.W. and Stapper, B., (February 1987) "Diesel Fuel Ignition Quality as Determined in a Constant volume Combustion Bomb." Prepared for the SAE International Congress & Exposition, February 23-27, 1987. SAE Paper No. 870586. Detroit, MI.

Ryan, III, T.W. and Callahan, T.J., (October 1988) "Engine and Constant volume Bomb Studies of Diesel Ignition and Combustion." Prepared for the International Fuels & Lubricants Meeting & Exposition, October 10-13, 1988. SAE Paper No. 881626. Portland, OR.

Ryan, T.W. III., and Erwin, J., (October 1993) "Diesel Fuel Composition Effects on Ignition and Emissions," SAE Technical Paper No. 932735, International Fuels & Lubricants Meeting Exposition, October 17-21, 1993, Philadelphia, PA.

Ryan III, Thomas W., Storum, J.O., Wright, B.R., and Waytulonis, R., (September 1981) "The Effects of Fuel Properties and Composition on Diesel Engine Exhaust Emissions—A Review." Prepared for the International Off-Highway Meeting & Exposition, September 14-17, 1981. SAE Paper No. 810953. Milwaukee, WI.

Ryan III, T.W., (November 1987) "Ignition Delay as Determined in a Variable-Compression Ratio Direct-Injection Diesel Engine." Prepared for the SAE International Fuels & Lubricants Meeting & Exposition, November 2-5, 1987. SAE Technical Paper No. 872036. Toronto, Ontario, Canada.

Siebers, D.L., (October 1985) "Ignition Delay Characteristics of Alternative Diesel Fuels: Implications on Cetane Number." Prepared for the Fuels & Lubricants Meeting & Exposition, October 21-24, 1985. SAE Paper No. 852102. Tulsa, OK.

Slodowske, W.J., Sienick, E.J., and Jass, R.E., (October 1992) "Diesel Fuel Property Effects on Exhaust Emissions from a Heavy-Duty Diesel Engine That Meets 1994 Emissions Requirements." Prepared for the International Fuels & Lubricants Meeting & Exposition, October 19-22, 1992. SAE Technical Paper No. 922267. San Francisco, CA.

Spadaccini, L.J. and TeVelde, J.A., (1983) "Autoignition Characteristics of Aircraft-Type Fuels," *Combustion and Flame*, Volume 46, pp. 283-300, 1983.

Tosaka, S. Fujiwara, Y., and Murayama, T., (March 1989) "The Effect of Fuel Properties on Diesel Engine Exhaust Particulate Formation." Prepared for the SAE International Congress & Exposition, March 1989. SAE Paper 890421, Detroit, MI.

Tosaka, S. Fujiwara, Y., and Murayama, T., (September 1989) "The Effect of Fuel Properties on Particulate Formation (The Effect of Molecular Structure and Carbon Number)." Prepared for the International Fuels & Lubricants Meeting Exposition, September 11-14, 1989. SAE Paper 891881. Milwaukee, WI.

Ullman, T., Mason, R.L., and Montalvo, D.A., (October 1990) "Effects of Fuel Aromatics, Cetane Number, and Cetane Improver on Emissions from a 1991 Prototype Heavy-Duty Diesel Engine." Prepared for the International Fuels & Lubricants Meeting & Exposition, October 22-25, 1990. SAE Paper 902171. Tulsa, OK.

Ullman, T.L., (March 1989) "Investigation of the Effects of Fuel Composition, and Injection and Combustion System Type on Heavy-Duty Diesel Exhaust Emissions." Prepared for the Final Report of the Coordinating Research Council, March 1989. CRC Contract CAPE-32-80, Project VE-1.

Ullman, T.L., (September 1989) "Investigation of the Effects of Fuel Composition, and Injection and Combustion System Type on Heavy-Duty Diesel Exhaust Emissions." Prepared for the International Fuels & Lubricants Meeting & Exposition, September 25-28, 1989. SAE Paper No. 892072. Baltimore, MD.

Weidmann, K., Menrad, H., Reder, K., and Hutchenson, R.C., (October 1988) "Diesel Fuel Quality Effects on Exhaust Emissions." Prepared for the SAE International Fuels & Lubricants Meeting and Exposition, October 10-13, 1988. SAE Paper No. 881649. Portland, OR.

Zeldovich, Ya. B., *Acta Physicochem. USSR* 21 577-628 (1946).

A. Dissolving and Head End

Irradiated slugs from the piles were charged to the dissolver with the aid of a special slug charger. The slugs used had, in general, an irradiation level of about 600 megawatt-days per ton (MWD/T) and were about 100 days from pile discharge when charged. A sufficient number of slugs were charged to provide a heel in the dissolver of 250 or 500 pounds of uranium after two 250-pound cuts had been dissolved.

The first step following charging was the removal of the aluminum alloy slug jackets. These were removed with a NaOH-NaNO₃ solution by a standard procedure which paralleled that used in the production plant. The chemistry of the process is discussed in the Redox Technical Manual (p. 303).⁽¹⁾ For a normal charging of 500 pounds of new slugs, 333 pounds of 26% NaNO₃ solution was added, the temperature was raised to about 95°C., and the air sparger was operated to give 2.5 SCFM. Eighty-seven pounds of 50% NaOH solution and 14 pounds of water were added and, after the reaction had subsided, the temperature was raised to 100 to 110°C. This amount of NaOH represents a NaOH/Al mol ratio of 1.8. The solution was maintained at the boiling point for three hours. It was then cooled, the sparger was turned off, and the solution was sent to the waste storage tank. The de-jacketed slugs were rinsed in hot water for an hour and were then ready for dissolution.

Two dissolution procedures were utilized. In the updraft procedure, which was followed in a majority of the runs, the E-1-1 reflux condenser was used. For a normal cut of 250 pounds of uranium, 600 pounds of 60% HNO₃ was added to the dissolver and the temperature was raised to the boiling point. The solution was maintained at the boiling point, generally without air sparging, until the specific gravity had reached about 1.79 at the temperature of the solution. The solution was jetted to the oxidizer and a second cut was made by the same procedure. The two cuts were combined in the oxidizer to provide the feed for a run.

component [12]

10. Experimental summary

Effective methods have been developed to search for the low rate of events from $t\bar{t}$ production in the presence of large backgrounds. These methods include the ability to identify b -jets, whose presence is a characteristic of $t\bar{t}$ events. Another important facet of the analysis is the way backgrounds in the counting experiments have been estimated directly from the data, essentially without reliance on Monte Carlo methods. The inclusion of the two W + jets + b -tagging searches together with the simpler dilepton search has increased the overall sensitivity for $t\bar{t}$ events by about a factor of five.

Because of the lack of dependence of the result of the counting experiments on Monte Carlo, too little has been said in this report about this important subject. The ISAJET program by Paige and Protopopescu [9], the HERWIG program by Marchiesini and Webber [10], and the VECBOS program by Berends, Giele, Kuijff and Tausk [11] in particular have been used extensively in all phases of the analysis to understand the data. All the estimates of acceptances, and therefore also the calculated $t\bar{t}$ production cross section, depend on Monte Carlo methods for event generation, parton evolution, jet fragmentation and detector simulation. The mass fitting techniques used to determine the most likely top mass also rely heavily on Monte Carlo event generators, both for the development of the fitting methods and for their validation (if an input top mass of M_{top} is used, what is the output? does it equal the input?).

Finally, to summarise the experimental results: The data obtained so far gives evidence for, but do not firmly establish the existence of top quark production in 1.8 TeV $\bar{p}p$ collisions. Under the assumption that the excess of events over background found by the three counting experiments is due to $t\bar{t}$ production, mass fitting of a subset of events yields a top quark mass, $M_{top} = 174 \pm 10^{+13}_{-12}$ GeV/c² and a $t\bar{t}$ production cross section of $13.9^{+6.1}_{-4.8}$ pb.

11. Prospects for top physics

Given the results summarised in this report, the immediate priority for the experiment is to collect more data to confirm the evidence obtained. The data collection process started again at the beginning of 1994, and has so far (July, 1994) resulted in an additional 10 pb^{-1} of integrated luminosity being recorded, containing one additional $e\mu$ event. The new data includes information from a radiation hard Silicon Vertex Detector (SVX') which has replaced the earlier, radiation-soft SVX. Work is now in progress to align the new detector, and to measure its tagging

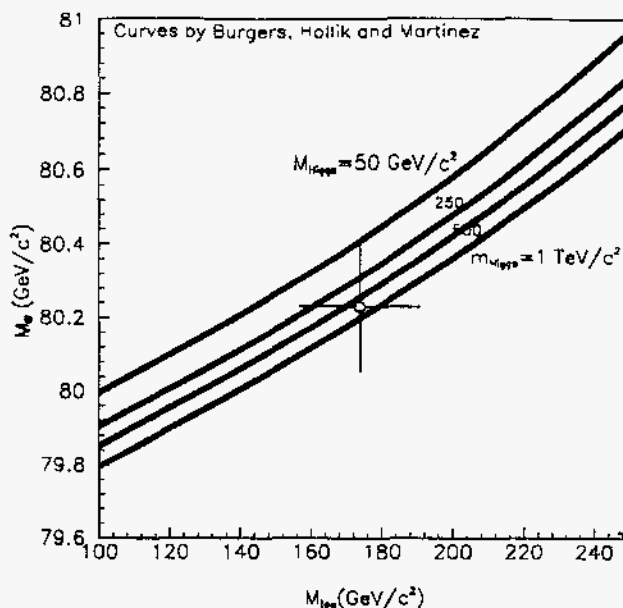


Figure 14. The calculated dependence of M_W on M_{top} in the standard model, using the LEP value of $M_Z = 91.1895 + 0.0044 \text{ GeV}/c^2$, is shown for Higgs masses of 50, 250, 500 and 1000 GeV/c^2 . The width of the band for each Higgs mass does not include the uncertainty on $\alpha(M_Z)$. The data point is at $M_{top} = 174 \pm 17 \text{ GeV}/c^2$, $M_W = 80.23 \pm 0.18 \text{ GeV}/c^2$, where the value for M_{top} is from the CDF mass fit, while the value for M_W is from direct M_W -measurements alone.

efficiency. News that the Tevatron Collider has reached a record luminosity of $1.4 \times 10^{31} \text{ cm}^{-2} \text{ sec}^{-1}$ arrived during the conference. This improvement means that a total integrated luminosity of 200 pb^{-1} could be reached within the next 2 years.

Longer term, the Main Injector, which is scheduled to turn on in 1998, should provide luminosities in the range $5 - 10 \times 10^{31} \text{ cm}^{-2} \text{ sec}^{-1}$ and therefore, after a few years of operation, data sets in excess of 1000 pb^{-1} .

Given the good prospects for significant increases in luminosity over what has been used for the analysis described in this report (19.3 pb^{-1}), let me now turn briefly to the physics of top quarks that may be addressed.

What makes the top quark interesting is that it is surprisingly heavy, much heavier than all other fermions. Said differently, it is strongly coupled to the Higgs boson, breaker of the electroweak symmetry. To see this, recall that the fermion-Higgs coupling in the standard model is given by the term

$$\mathcal{L}_{Yukawa} = -G_{fermion} (\bar{R}(\Phi^\dagger L) + (\bar{L}\Phi)R)$$

where $G_{fermion}$ is an arbitrary coupling constant, Φ is the Higgs field and R and L are the Right and Left fermion fields. This Yukawa coupling generates the fermion masses $M_{fermion} = G_{fermion} \times v/\sqrt{2}$, where $v = 246 \text{ GeV}$ is the vacuum expectation value parameter

TABLE A1. LABORATORY ANALYSES FOR DIESEL FROM FISCHER-TROPSCH ARGE WAX (FT1)

Test	ASTM Method	Feed FL-1840	Frac. 1 FL-1898	Frac. 2 FL-1899	Frac. 3 FL-1900	Frac. 4 FL-1901	Frac. 5 FL-1902	Frac. 6 FL-1903	Frac. 7 FL-1904
TBP Cut Pts. °F °C	-		≤400	400-440	440-480	480-520	520-560	560-600	600 +
			≤204	204-227	227-249	249-271	271-293	293-315	315+
Yield, Vol%			0-20	20-31.5	31.5-42.5	42.5-54	54-67	67-82.5	82.5-100
Vol% of Fraction	-		20	11.5	11.0	11.5	13.0	15.5	17.5
Density	D 1298								
Specific Gravity		0.7770	0.7539	0.7632	0.7711	0.7783	0.7852	0.7914	0.7990
°API		50.6	56.2	53.9	52.0	50.3	48.7	47.3	45.6
g/mL		0.7767	0.7536	0.7630	0.7708	0.7780	0.7849	0.7910	0.7986
Distillation, °C/°F,	D 86								
IBP		187/368	169/336	197/386	218/424	242/467	266/511	286/547	313/595
5%		202/396	178/352	202/395	224/436	247/477	271/519	290/555	318/605
10%		208/407	179/355	203/397	226/438	248/478	272/522	292/558	319/607
30%		232/449	183/362	207/404	229/444	252/485	274/526	294/562	322/611
50%		261/502	189/373	213/416	234/453	254/490	277/531	297/566	324/615
70%		287/550	198/388	221/429	238/461	258/496	279/535	299/571	326/619
90		311/592	216/420	233/452	246/475	264/507	285/545	304/579	331/628
95%		319/606	226/438	239/463	250/482	266/511	287/549	306/583	334/633
EP		327/620	236/456	246/474	253/488	272/521	292/557	309/589	337/638
Carbon, wt%	D 3178	84.92	84.53	84.68	84.78	85.0	84.95	85.18	84.93
Hydrogen, wt%		15.12	15.39	15.44	15.29	15.0	15.20	14.91	15.22
Sulfur, wt%	D 2622	0.003	0.001	0.003	0.002	0.003	0.001	0.002	0.003
Aromatics	Hydro-carbon type	1.1	1.3	-	-	0.9	-	-	1.4
Olefins		1.1	0.6	-	-	0.9	-	-	0.8
Saturates		Vol%	97.8	98.1	-	-	98.2	-	-
Vis. @ 40°C	D 445	2.42	1.16	1.48	1.85	2.37	3.11	4.01	5.71
@ 100°C		1.05	0.62	0.74	0.86	1.02	1.24	1.46	1.88
RI @ 20°C	D 1218	1.4342	1.4214	1.4266	1.4303	1.4344	1.4382	1.4411	1.4450
Cetane No.	CVCA	64.8	51.2	60.1	66.0	72.1	71.1	82.3	87.3
Cetane Index	D 976	75.4	62.7	67.9	71.0	73.2	74.9	75.1	74.6
	D 4737	81.4	67.2	73.3	78.9	84.2	90.4	95.4	102.2
UV	TOTAL	0.2	0.4	0.3	0.2	0.2	0.1	0.1	0.1
Aromatics	MONO	0.2	0.4	0.3	0.2	0.2	0.1	0.1	0.1
Analyses	DI	0.0	0.0	0.0	0.0	0.0	0.0	0.0	0.0
Wt% Total Carbon	TRI	0.0	0.0	0.0	0.0	0.0	0.0	0.0	0.0
Cloud Pt., °C/°F	D 2500	-20/-4	<-60/-76	-55/-67	-50/-58	-37/-35	-22/-8	-12/10	+1/34
Pour Pt., °C/°F	D 97	-20/-4	<-60/-76	-55/-67	-45/-49	-35/-31	-25/-13	-17/1	-4/25
Aniline Pt., °C/°F	D 611	92.8/199	80.6/178	84.0/183	88.6/192	92.0/198	96.3/205	99.7/212	104.7/221
Smoke Pt., mm	D 1322	+35	+50	+50	+50	+45	+35	+35	N/A

N/A = Not applicable

TABLE A2. LABORATORY ANALYSES FOR F-T STRAIGHT-RUN PRODUCT (FT2)

Test	ASTM Method	FL-2095	Frac. 1 FL-2115	Frac. 2 FL-2116	Frac. 3 FL-2117	Frac. 4 FL-2118	Frac. 5 FL-2119	Frac. 6 FL-2120	Frac. 7 FL-2121
TBP Cut Points, °F °C		-	300-400	400-440	440-480	480-520	520-580	580-600	600+
			149-204	204-227	227-249	249-271	271-304	304-315	315+
Vol% of Fraction		-	16.3	10.1	12.0	10.5	18.2	17.3	15.7
Density	D 1298								
Specific Gravity		0.8081	0.7783	0.7936	0.8058	0.8086	0.8104	0.8132	0.8146
°API		43.6	50.3	46.8	44.1	43.5	43.1	42.5	42.2
g/mL		0.8077	0.7780	0.7932	0.8054	0.8082	0.8100	0.8128	0.8142
Distillation, °C/°F	D 86								
IBP		184/363	102/216	158/316	181/358	200/392	228/442	250/482	276/529
5%		199/391	130/266	163/326	192/377	214/418	239/462	263/506	287/549
10		208/406	134/274	168/334	193/380	218/424	252/468	268/514	292/557
30		238/461	144/292	173/344	199/391	223/434	250/482	276/529	297/566
50		265/509	152/306	179/354	206/403	228/442	254/489	281/537	299/571
70		286/547	162/324	188/370	214/418	233/452	259/498	283/542	303/577
90		309/588	179/354	202/395	228/442	243/470	264/508	289/553	307/585
95		319/606	189/372	208/408	138/459	250/482	269/516	292/558	311/591
EP	331/627	200/392	220/428	281/537	272/522	274/526	296/565	317/603	
Carbon, Mass%	D 5291	82.62	79.18	77.78	80.71	82.17	82.03	82.72	84.21
Hydrogen, Mass%		13.76	13.11	13.27	13.54	13.88	13.39	13.49	13.96
Sulfur, Mass%	D 2628	0.031	0.001	<0.001	0.002	0.001	0.003	0.003	<0.001
Hydrocarbon Type	D 1319	Unreliable readings							
Aromatics									
Olefins									
Saturates									
Vis. @ 40°C		2.52 cSt	0.89	1.16	1.58	2.02	2.48	3.14	3.75
@ 100°C		1.08 cSt	0.49	0.61	0.76	0.90	1.07	1.27	1.49
RI @ 20°C		1.4414	1.4196	1.4274	1.4339	1.4381	1.4421	1.4451	1.4476
Cetane No.	CVCA	82.4	34.6	47.0	52.8	66.5	69.2	79.3	94.9
Cetane Index	D 976	62.2	28.9	37.3	44.7	51.6	58.6	63.2	65.5
	D 4737	64.6	35.3	40.5	46.2	53.8	63.2	72.3	80.1
Ring Carbon	UV								
Mono		1.6	2.0	2.1	2.0	1.5	1.7	2.1	0.8
Di		0.1	0.0	0.0	0.1	1.8	0.1	0.1	0.0
Tri		0.0	0.0	0.0	0.1	0.2	0.1	0.0	0.0
Cloud Point, °C	D 2500	-5	less than -60	-54	-36	-25	-12	1	9
Pour Point, °C	D 97	-7	less than -60	-57	-37	-26	-13	-1	7
Aniline Point, °C	D 611	43.2	16.2	20.1	21.7	27.2	37.4	50.1	66.1

TABLE A3. LABORATORY ANALYSES FOR STRAIGHT-RUN DIESEL

Test	ASTM Method	Feed FL-1627	Frac. 1 FL-1793	Frac. 2 FL-1794	Frac. 3 FL-1795	Frac. 4 FL-1796	Frac. 5 FL-1797	Frac. 6 FL-1798	Frac. 7 FL-1799	Frac. 8 FL-1800
TBP Cut Pts. °F			<400	400-440	440-480	480-520	520-560	560-600	600-640	640+
°C			≤204	204-227	227-249	249-271	271-293	293-315	315-338	338+
Cut Range, Vol%			0-11.5	11.5-20.5	20.5-28.5	28.5-45	45-61.5	61.5-75.5	75.5-86.5	86.5-100
Yield, Vol%			11.5	9.0	8.0	16.5	16.5	14.0	11.0	13.5
Sp. Gr. @ 60°F(°C)	D 1298	0.8458	0.8146	0.8445	0.8483	0.848	0.845	0.847	0.859	0.863
Gravity, °API		35.8	42.2	36.1	35.3	35.3	36.0	35.5	33.3	32.4
Density, g/mL		0.8453	0.8142	0.8440	0.8479	0.8476	0.8446	0.8466	0.8586	0.8625
Distillation, °C/°F, IBP	D 86	178/353	81/282	139/452	247/476	261/502	280/536	299/570	321/610	347/657
5%		220/428	104/324	162/464	251/484	265/509	283/542	302/576	324/616	351/663
10%		241/466	116/338	170/465	252/486	268/514	284/544	303/578	325/617	352/666
30%		273/523	134/377	192/473	256/492	270/518	286/546	305/581	327/620	354/669
50%		288/551	142/404	207/480	259/498	273/523	288/550	307/584	328/622	356/673
70%		305/581	152/425	218/488	263/506	275/527	291/555	309/589	330/626	358/677
90%		335/635	168/452	233/501	269/516	283/542	296/564	314/597	334/634	364/687
95%		347/657	175/462	239/506	272/521	288/550	298/568	317/602	337/638	366/691
EP		356/672	180/475	246/515	276/529	292/556	302/576	321/610	339/643	370/698
Carbon, wt%	D 3178	86.82	86.64	87.08	87.14	87.10	87.06	86.27	86.47	86.38
Hydrogen, wt%		13.31	12.82	12.49	12.44	12.56	12.69	13.59	13.41	13.89
Sulfur, wt%	D 2622	0.052	0.007	0.013	0.018	0.026	0.043	0.073	0.121	0.111
Aromatics	D 1319 Hydro-	23.6	23.4	24.5	25.0	25.4	23.3	22.9	23.7	too heavy
Olefins	carbon Type	1.0	1.1	1.0	1.5	1.6	1.6	1.1	1.2	too heavy
Saturates	Vol%	74.7	75.5	74.5	73.5	73.0	75.1	76.0	75.1	too heavy
Vis. cSt @ 40°C	D 445	3.52	1.26	2.28	2.60	3.18	3.85	5.00	6.86	10.41
cSt @ 100°C		1.34	0.58	0.99	1.10	1.25	1.42	1.70	2.08	2.79
RI @ 20°C	D 1218	1.4718	1.4550	1.4717	1.4742	1.4737	1.4713	1.4726	1.4787	1.4873
Cetane No.	CVCA	56.2	33.9	41.1	40.5	42.5	45.1	64.2		
Cetane Index	D 976	52.6	41.4	44.8	46.0	49.0	52.8	54.5	52.7	52.0
	D 4737	54.6	41.5	45.1	47.0	52.2	59.3	64.8	66.2	80.7
Aromatic, wt%	UV									
Total		11.4	12.3	13.5	13.3	12.5	10.9	8.7	9.3	17.2
Mono-aromatic		4.3	7.9	4.6	4.4	4.3	4.0	3.2	3.1	5.7
Di-aromatic		5.8	4.4	8.6	8.5	7.4	5.7	3.7	3.5	6.2
Tri-aromatic		1.3	0.1	0.4	0.4	0.8	1.2	1.8	2.7	5.2
Cloud Pt., °C/°F	D 2500	1/34	-44/-47	-28/-18	-21/-6	-14/7	-6/21	6/43	12/54	36/97
Pour Pt., °C/°F	D 97	-1/30	-45/-49	-25/-13	-18/0	-12/10	-3/27	6/43	15/59	39/102
Aniline Pt., °C/°F	D 611	73.0/163	54.4/130	62.4/144	64.4/148	68.6/155	75.0/167	80.1/176	82.1/180	88.4/191
Smoke Point, mm	D 1322	17.2	19.5	15.7	15.0	15.3	15.8	16.2	NA	NA

TABLE A4. LABORATORY ANALYSES FOR LOW-AROMATICS STRAIGHT-RUN DIESEL

Test	ASTM Method	Feed FL-1873	Frac. 1 FL-1876	Frac. 2 FL-1877	Frac. 3 FL-1878	Frac. 4 FL-1879	Frac. 5 FL-1880	Frac. 6 FL-1881	Frac. 7 FL-1882	Frac. 8 FL-1883
TBP Cut Pts. °F			IBP-400	400-440	440-480	480-520	520-560	560-600	600-640	640 +
°C			IBP-204	204-227	227-249	249-271	271-293	293-315	315-338	338+
Cut Range, Vol%			0-5	5-15	15-24.5	24.5-39.5	39.5-56	56-73.5	73.5-87	87-100
Yield, Vol%			5	10	9.5	15	16.5	17.5	13.5	13
Sp. Gr. @ 60°F	D 1298	0.8280	0.7892	0.8251	0.8373	0.8368	0.8304	0.8246	0.8314	0.8373
Gravity, °API		39.4	47.8	40.0	37.5	37.6	38.9	40.1	38.7	37.5
Density, g/mL		0.8276	0.7888	0.8247	0.8368	0.8364	0.8300	0.8242	0.8310	0.8368
Distillation, °C/°F, IBP	D 86	128/262	94/201	183/361	219/427	246/474	271/520	293/559	318/605	348/659
5%		193/380	100/212	194/381	226/438	249/480	276/528	297/567	323/613	354/670
10%		228/442	116/241	197/386	227/440	250/482	277/530	297/567	324/615	356/673
30%		264/507	126/258	202/396	229/445	254/489	279/534	301/573	326/618	358/677
50%		282/539	137/278	207/404	233/452	257/494	281/538	303/577	327/620	362/683
70%		300/572	147/297	214/418	238/461	260/500	284/544	304/580	329/624	364/688
90%		328/622	162/323	226/438	246/474	266/510	289/552	308/587	333/631	371/699
95%		340/644	168/334	231/447	249/480	268/515	292/557	311/591	335/635	373/705
EP		351/664	177/351	235/455	253/488	274/526	294/562	314/597	338/641	379/715
Carbon, wt%	D 3178	85.99	86.61	86.26	86.07	86.00	85.87	85.80	85.62	85.68
Hydrogen, wt%		14.86	13.62	14.03	13.91	14.01	14.37	14.50	14.67	14.53
Sulfur, wt%	D 2622	<0.001	<0.001	<0.001	<0.001	<0.001	<0.001	<0.001	<0.001	<0.001
Aromatics	D 1319 Hydro-	9.8	22.7	14.6	14.9	12.5	9.1	7.6	7.6	NA
Olefins	carbon Type	0.6	0.7	0.9	0.9	2.7	1.8	1.0	2.8	NA
Saturates	Vol%	89.6	76.9	84.5	84.2	84.8	89.1	91.4	89.6	NA
Vis. cSt @ 40°C	D 445	3.17	0.75	1.53	2.12	2.81	3.46	4.35	5.89	8.70
cSt @ 100°C		1.29	0.45	0.75	0.96	1.16	1.32	1.58	1.94	2.54
RI @ 20°C	D 1218	1.4580	1.4403	1.4557	1.4610	1.4608	1.4576	1.4565	1.4595	NA
Octane No.	CVCA	61.3	23.1	31.7	38.6	44.3	48.8	64.2	79.1	-
Octane Index	D 976	57.7	13.0	37.4	42.6	49.3	56.7	62.1	61.7	60.5
	D 4737	60.1	23.8	38.1	42.7	51.3	64.1	78.4	81.5	82.2
Aromatic, wt%	UV									
Total		3.3	7.7	5.8	5.0	3.6	2.6	1.5	1.1	0.8
Mono-aromatic		3.0	7.7	5.6	4.6	3.2	2.2	1.3	0.9	0.6
Di-aromatic		0.3	0.1	0.3	0.4	0.4	0.3	0.2	0.2	0.2
Tri-aromatic		0.0	0.0	0.0	0.0	0.0	0.0	0.0	0.0	0.0
Cloud Pt, °C/°F	D 2500	1/34	<-78/-108	-53/-63	-34/-29	-20/-4	-9/16	0/32	15/59	26/79
Pour Pt, °C/°F	D 97	-3/27	<-78/-108	-51/-60	-33/-27	-18/0	-7/19	3/37	16/61	28/82
Aniline Pt, °C/°F	D 611	80.8/177	35.4/96	47.0/117	64.0/147	72.7/163	81.0/178	88.6/191	93.2/200	101.7/215
Smoke Point, mm	D 1322	25.5	20.5	21.5	21.2	21.9	25.9	29.6	NA	NA

TABLE A5. LABORATORY ANALYSES FOR LIGHT-COKER GAS OIL

	ASTM Method	Feed FL-1440	Frac. 1 FL-1546	Frac. 2 FL-1547	Frac. 3 FL-1548	Frac. 4 FL-1549	Frac. 5 FL-1550	Frac. 6 FL-1551
TBP Cut Pts. °F	-	-	330-440	440-480	480-520	520-560	560-600	600-651
			°C	166-227	227-249	249-271	271-293	293-315
Cut Range, Vol%	-	-	0-25	25-42.7	42.7-59.7	59.7-75.8	75.8-88.8	88.8-100
Yield, Vol%	-	-	25.0	17.7	17.0	16.1	13.0	11.2
Sp. Gravity @ 60°F	D 1298	0.8676	0.8403	0.8565	0.8740	0.8871	0.8927	0.9094
Gravity, °API		31.6	36.9	39.7	30.4	28.0	27.0	24.1
Density, g/mL		0.8671	0.8398	0.8561	0.8735	0.8867	0.8922	0.9089
Distillation, °F, IBP	D 86	196/385	193/379	227/440	249/480	272/521	293/559	315/599
5%		216/420	199/391	229/445	252/485	276/529	296/564	316/601
10%		224/435	202/395	230/446	252/486	277/530	296/565	317/603
30%		239/462	206/403	233/451	255/491	278/533	298/569	319/606
50%		256/492	210/410	236/456	257/495	281/537	299/571	321/609
70%		276/528	214/417	239/462	260/500	283/541	301/574	323/614
90%		301/574	221/429	245/473	264/508	286/547	304/580	329/624
95%		310/590	224/436	248/478	267/512	288/551	306/583	335/635
EP		320/608	238/461	255/491	274/526	296/565	313/595	341/645
Carbon, wt%	D 3178	85.18	85.36	85.70	85.68	85.77	85.96	85.82
Hydrogen, wt%		12.58	13.16	12.46	12.35	12.09	12.27	11.97
Sulfur, wt%	D 2622	1.41	1.16	1.08	1.36	1.48	1.32	1.33
Aromatics	D 1319 Hydro-carbon Type	52.4	29.1	31.8	38.7	46.4	49.0	too heavy
Olefins		5.9	18.0	17.0	15.8	12.7	14.9	too heavy
Saturates		41.7	52.9	51.2	45.5	40.9	36.1	too heavy
Vis. cSt @ 40°C	D 445	2.56	1.46	2.01	2.77	3.97	5.64	10.08
cSt @ 100°C		1.10	0.73	0.90	1.11	1.40	1.69	2.40
RI @ 20°C	D 1218	1.4797	1.4629	1.4729	1.4831	1.4907	1.4942	Too dark
Cetane No.	CVGA	29.0	25.6	27.9	30.1	29.1	32.8	31.7
Cetane Index	D 976	39.3	33.3	37.0	37.9	39.2	40.6	38.8
	D 4737	38.7	32.0	31.9	35.6	37.5	41.2	41.2
Aromatic, wt%	UV							
Total		15.7	11.4	13.8	14.4	15.1	14.7	15.2
Mono-aromatic		8.4	9.1	8.6	7.1	6.7	6.2	5.6
Di-aromatic		5.9	1.6	4.4	6.3	7.2	6.8	6.1
Tri-aromatic		1.4	0.6	0.8	1.0	1.3	1.7	3.5
Cloud Point, °C/°F	D 2500	Too dark	-65/-85	-54/-65	-38/-36	-27/-17	-21/-36	Too dark
Pour Point, °C/°F	D 97	-30/-22	-65/-85	-55/-67	-38/-6	-27/-17	-21/-6	-5/23
Aniline Point, °C/°F	D 611	47.6/118	43.4/110	46.7/116	46.2/115	49.0/120	53.4/128	Too dark
Smoke Point, mm	D 1322	13.3	16.6	16.7	12.4	11.9	11.0	NA

TABLE A6. LABORATORY ANALYSES FOR LOW-SULFUR LIGHT-COKER GAS OIL

Test	ASTM Method	Feed FL-1442	Frac. 1 FL-1862	Frac. 2 FL-1863	Frac. 3 FL-1864	Frac. 4 FL-1865	Frac. 5 FL-1866	Frac. 6 FL-1867
TBP Cut Pts. °F			<400	400-440	440-480	480-520	520-560	560+
°C			<204	204-227	227-249	249-271	271-293	293+
Cut Range, Vol%			0-13.5	13.5-29.0	29.0-48.5	48.5-66.5	66.5-82.0	82-100
Yield, Vol%			13.5	15.5	19.5	18.0	15.5	18.0
Sp. Gr. @ 60°F	D 1298	0.8463	0.8184	0.8299	0.8403	0.8524	0.8628	0.8697
Gravity, °API		35.7	41.4	39.0	36.9	34.5	32.5	31.2
Density, g/mL			0.8180	0.8295	0.8398	0.8520	0.8623	0.8692
Distillation, °C/°F, IBP	D 86	193/380	169/337	193/379	216/421	239/462	260/500	292/558
5%		213/416	179/354	202/395	221/430	244/472	266/510	296/565
10%		219/427	182/360	204/399	222/432	245/473	267/512	297/567
30%		234/454	190/374	208/407	226/439	248/478	270/518	300/572
50%		247/476	198/389	213/415	231/447	251/484	273/523	303/577
70%		266/511	207/405	218/425	236/456	256/492	276/529	307/584
90%		289/552	219/427	228/442	245/473	262/504	282/539	314/598
95%		300/572	227/441	234/453	249/481	267/512	284/543	319/607
EP		315/599	236/457	242/467	256/492	274/526	288/550	329/624
Carbon, wt%	D 3178	86.85	86.48	86.43	86.59	86.99	86.74	86.72
Hydrogen, wt%		13.31	13.66	13.59	13.54	13.18	13.17	12.96
Sulfur, wt%	D 2622	0.04	0.007	0.009	0.014	0.024	0.041	0.052
Aromatics	D 1319 Hydro-	27.5	22.1	22.9	24.7	28.2	32.5	31.2
Olefins	carbon Type	2.1	1.9	1.8	1.9	1.9	1.6	1.3
Saturates	Vol%	70.4	76.0	75.3	73.4	69.9	65.9	67.5
Vis. cSt @ 40°C	D 445	2.31	1.26	1.52	1.90	2.52	3.45	5.81
cSt @ 100°C			0.58	0.76	0.87	1.06	1.30	1.58
RI @ 20°C	D 1218	1.4676	1.4537	1.4596	1.4646	1.4716	1.4771	1.4810
Cetane No.	CVCA	33.3	28.2	29.5	29.2	30.4	33.7	37.8
Cetane Index	D 976	43.5	36.4	38.0	40.7	42.7	44.5	47.2
	D 4737	43.5	37.4	38.2	40.5	42.7	45.5	52.6
Aromatic, wt%	UV							
Total		10.5	10.0	10.9	10.2	11.0	11.2	11.4
Mono-aromatic		8.2	9.4	9.8	8.4	8.2	7.7	7.2
Di-aromatic		2.3	0.6	1.1	1.8	2.8	3.4	3.5
Tri-aromatic		0.0	0	0	0	0	0.1	0.7
Cloud Pt., °C/°F	D 2500	-35	<-65/-85	-62/-80	-48/-54	-38/-36	-27/-17	-5/23
Pour Pt., °C/°F	D 97	-38/-36	<-65/-85	-6/-80	-45/-49	-35/-31	-27/-17	-2/28
Aniline Pt., °C/°F	D 611	58.6/137	51.7/125	53.5/128	56.2/133	58.2/137	61.2/142	69.6/157
Smoke Point, mm	D 1322	16.2	19.1	18.3	16.7	15.5	14.7	14.1

TABLE A7. LABORATORY ANALYSES FOR LOW-AROMATICS LIGHT-COKER GAS OIL

Test	ASTM Method	Feed FL-1443	Frac. 1 FL-1597	Frac. 2 FL-1598	Frac. 3 FL-1599	Frac. 4 FL-1600	Frac. 5 FL-1601	Frac. 6 FL-1602	Frac. 7 FL-1603
TBP Cut Pts. °F	-	-	326-400	400-440	440-480	480-520	520-560	560-600	600-746
°C	-	-	163-204	204-227	227-249	249-271	271-293	293-315	315-397
Cut Range, Vol%	-	-	0-8.5	8.5-24	24-42.3	42.3-58.4	58.4-73.4	73.4-85.9	85.9-100
Yield, Vol%	-	-	8.5	15.5	18.3	16.1	15.0	12.5	14.0
Sp. Gr. @ 60°F	D 1298	0.8393	0.8203	0.8265	0.8324	0.8418	0.8490	0.8498	0.8522
Gravity, °API	-	37.1	41.1	39.7	38.5	36.6	35.1	35.0	34.5
Density, g/mL	-	0.8388	0.8198	0.8261	0.8319	0.8413	0.8486	0.8494	0.8518
Distillation, °C/°F, IBP	D 86	211/412	181/358	201/394	221/429	241/466	259/498	281/537	307/585
5%	-	221/429	188/371	205/401	224/436	244/472	263/506	286/547	312/594
10%	-	224/436	190/374	207/404	225/437	246/474	264/508	287/548	313/595
30%	-	240/454	194/382	210/410	228/442	248/479	267/512	289/552	315/599
50%	-	255/491	199/390	214/417	231/448	251/483	269/516	291/556	317/602
70%	-	274/526	204/400	218/425	234/453	255/491	272/522	293/560	321/610
90%	-	302/576	212/414	227/440	242/468	262/503	277/530	297/566	328/622
95%	-	314/597	216/421	232/449	247/477	265/509	280/536	299/570	333/632
EP	-	322/612	221/430	241/466	252/485	271/520	286/546	301/574	340/644
Carbon, wt%	D 3178	86.29	86.22	86.40	86.53	86.53	86.66	86.42	86.73
Hydrogen, wt%	-	13.69	13.50	13.52	13.51	13.41	13.35	13.41	13.58
Sulfur, wt%	D 2622	<0.001	0.003	<0.001	<0.001	<0.001	<0.001	0.002	0.002
Aromatics	D 1319 Hydro-	10.4	10.5	9.1	8.7	10.2	11.9	13.0	14.3
Olefins	carbon Type	0.4	0.7	0.5	0.6	0.5	0.7	0.9	1.0
Saturates	Vol%	89.2	88.8	90.4	90.7	89.3	87.4	86.1	84.7
Vis. cSt @ 40°C	D 445	2.67	1.35	1.58	1.98	2.61	3.37	4.63	7.10
cSt @ 100°C	-	1.10	0.69	0.78	0.90	1.08	1.28	1.55	2.07
RI @ 20°C	D 1218	1.4608	1.4509	1.4539	1.4569	1.4616	1.4652	1.4662	1.4676
Cetane No.	CVCA	37.7	28.2	30.5	31.7	33.7	39.0	44.1	54.9
Cetane Index	D 976	48.0	36.1	39.7	43.6	46.2	47.9	51.7	53.8
	D 4737	49.2	36.6	39.9	44.0	47.2	50.6	57.7	65.9
Aromatic, wt%	UV								
Total		3.3	4.5	3.9	3.5	3.4	3.3	2.7	2.2
Mono-aromatic		3.0	4.3	3.7	3.3	3.1	2.9	2.3	1.8
Di-aromatic		0.3	0.2	0.2	0.3	0.4	0.4	0.4	0.4
Tri-aromatic	-	0	0	0	0	0	0	0	0
Cloud Pt., °C/°F	D 2500	-28/-18	<-48/-54	<-48/-54	<-48/-54	-41/-42	-31/-24	-21/-6	-4/25
Pour Pt., °C/°F	D 97	-33/-27	<-48/-54	<-48/-54	<-48/-54	-37/-35	-28/-18	-17/1	-4/25
Aniline Pt., °C/°F	D 611	71.2/160	57.4/135	62.9/145	66.0/151	69.5/157	73.0/163	79.7/175	88.6/191
Smoke Point, mm	D 1322	23.1	25.9	23.8	23.5	22.4	21.0	22.1	NA

TABLE A8. LABORATORY ANALYSES FOR LIGHT-CYCLE OIL

Test	ASTM Method	Feed FL-1538	Frac. 1 FL-1555	Frac. 2 FL-1556	Frac. 3 FL-1557	Frac. 4 FL-1558	Frac. 5 FL-1559	Frac. 6 FL-1560	Frac. 7 FL-1561
TBP Cut Pts. °F °C	-	-	367-440	440-480	480-520	520-560	560-600	600-640	640-689
			186-227	227-249	249-271	271-293	293-315	315-338	338-365
Cut Range, Vol%	-	-	0-8.9	8.9-18.1	18.1-38	38-53	53-67.3	67.3-79	79-100
Yield, Vol%	-	-	8.9	9.2	19.9	15.0	14.3	11.7	21.0
Sp. Gr. @ 60°F	D 1298	0.9490	0.8849	0.9147	0.9321	0.9440	0.9541	0.9685	0.9979
Gravity, °API		17.6	28.4	23.2	20.3	18.4	16.8	14.6	10.3
Density, g/mL		0.9485	0.8844	0.9142	0.9316	0.9434	0.9536	0.9679	0.9973
Distillation, °F, IBP	D 86	186/367	194/382	228/442	247/477	264/508	283/542	303/578	324/616
5%		236/457	196/384	229/444	249/481	268/514	286/546	306/582	336/636
10%		247/476	196/384	231/447	251/483	268/515	287/548	306/583	339/643
30%		265/509	203/397	235/455	252/486	270/518	288/550	308/586	341/645
50%		280/536	210/410	237/459	254/490	272/522	289/552	309/588	343/651
70%		301/573	218/424	240/464	256/492	274/525	291/556	311/591	348/658
90%		334/634	228/443	245/473	259/499	277/531	294/562	313/596	358/677
95%		347/656	232/449	248/479	262/503	279/534	297/566	316/601	376/709
EP		365/689	238/460	256/492	270/518	284/544	302/575	323/614	390/734
Carbon, wt%	D 3178	88.84	89.00	89.36	88.63	89.80	89.97	89.41	88.67
Hydrogen, wt%		9.84	10.74	10.08	9.69	9.65	9.70	9.41	9.18
Sulfur, wt%	D 2622	0.69	0.16	0.35	0.45	0.41	0.32	0.57	1.85
Aromatics	D 1319 Hydro-carbon Type	75.5	76.6	74.1	77.2	81.7	80.8	81.0	75.0
Olefins		3.6	2.7	5.4	5.1	4.5	3.0	3.0	1.8
Saturates		20.9	20.7	20.5	17.7	13.8	16.2	16.0	23.2
Vis. cSt @ 40°C	D 445	3.16	1.25	1.73	2.14	2.78	3.74	5.47	11.38
cSt @ 100°C		1.20	0.65	0.81	0.94	1.09	1.31	1.64	2.40
RI @ 20°C	D 1218	1.5537	1.5047	1.5279	1.5431	1.5532	1.5572	1.5641	1.5866
Cetane No.	CVCA	15.5	15.2	17.0	4.33	13.9	15.6	16.3	19.1
Cetane Index	D 976	26.1	20.2	22.6	23.8	25.5	26.7	26.9	24.9
	D 4737	23.8	19.3	17.5	17.0	18.1	19.5	19.7	17.6
Aromatic, wt%	UV								
Total		43.7	42.5	55.3	57.2	60.6	46.1	41.2	46.7
Mono-aromatic		6.3	26.7	14.5	6.8	5.1	3.3	4.9	6.4
Di-aromatic		28.3	15.0	39.8	49.6	53.9	37.2	25.2	11.8
Tri-aromatic		9.1	0.8	1.0	0.8	1.6	2.2	6.3	19.6
Cloud Pt., °C/°F	D 2500	-10/14	<-65/-85	-45/-49	-40/-40	-35/3-1	-22/-8	-8/18	9/48
Pour Pt., °C/°F	D 97	-12/10	<-65/-85	-45/-49	-40/-40	-35/-31	-22/-38	-9/16	9/48
Aniline Pt., °C/°F	D 611	9.8/50	35/23	0.5/33	1.3/34	2.0/36	6.5/44	17.3/63	34.0/93
Smoke Point, mm	D1322	6.2	7.2	6.0	6.2	6.0	5.1	5.4	4.1

TABLE A9. LABORATORY ANALYSES FOR LOW-SULFUR LIGHT-CYCLE OIL

Test	ASTM Method	Base FL-1615	Frac. 1 FL-1850	Frac. 2 FL-1851	Frac. 3 FL-1852	Frac. 4 FL-1853	Frac. 5 FL-1854	Frac. 6 FL-1855	Frac. 7 FL-1856
TBP Cut Pts. °F			400-440	440-480	480-520	520-560	560-600	600-640	640+
°C			204-227	227-249	249-271	271-293	293-315	315-338	338+
Cut Range, Vol%			0-12.3	12.3-28	28-48.5	48.5-65	65-79.1	79.1-89.1	89.1-100
Yield, Vol%			12.3	15.7	20.5	16.5	14.1	10.0	10.9
Sp. Gr. 60°F(°C)		0.9200	0.8849	0.9082	0.9153	0.9230	0.9352	0.9484	0.9497
Gravity, °API		22.3	28.4	24.3	23.1	21.8	19.8	17.7	17.5
Density, g/mL		0.9195	0.8844	0.9077	0.9147	0.9225	0.9347	0.9478	0.9491
Distillation, °C/°F, IBP	D 86	200/392	158/317	217/422	237/458	257/495	278/533	312/593	338/641
5%		224/436	180/356	227/440	243/469	261/502	283/541	312/593	341/645
10%		239/462	188/370	229/444	244/472	262/503	284/543	313/595	343/650
30%		255/491	206/403	236/456	248/478	266/510	287/549	315/599	346/655
50%		270/518	218/424	242/467	253/488	271/519	292/557	317/603	351/663
70%		290/554	229/444	248/479	259/498	276/529	296/565	321/609	356/673
90%		323/614	243/469	261/502	272/521	287/549	304/579	325/617	372/702
95%		339/642	249/481	269/516	278/533	293/559	307/585	328/622	386/727
EP		361/682	266/510	284/544	287/548	300/572	313/595	332/630	392/738
Carbon, wt%		D 3178	89.08	88.79	89.36	89.16	89.40	89.69	89.80
Hydrogen, wt%	10.65		11.03	11.10	11.07	11.04	10.78	10.50	10.86
Sulfur, wt%	D 2622	0.026	0.005	0.002	0.003	0.004	0.006	0.040	0.114
Aromatics	D 1319 Hydro	73.1	69.1	73.6	76.0	76.0	76.7	76.3	Too dark
Olefins	carbon Type	-	0.6	1.0	1.2	2.0	1.0	1.0	
Saturates	Vol%	26.9	30.3	25.4	22.8	22.0	22.3	22.7	
Vis. cSt @ 40°C	D 445	2.96	1.39	1.99	2.34	2.95	4.11	6.41	13.87
cSt @ 100°C		1.16	0.70	0.88	0.99	1.02	1.39	1.85	2.89
RI @ 20°C	D 1218	1.5249	1.4980	1.5125	1.5185	1.5264	1.5358	1.5466	1.5505
Cetane No.	CVCA	17.9	14.0	15.4	15.7	17.3	18.6	19.9	-
Cetane Index	D 976	29.8	23.1	25.3	26.9	29.2	30.4	30.9	32.1
	D 4737	28.6	21.6	22.1	23.4	25.1	26.0	27.7	35.5
Aromatic, wt%	UV								
Total		35.8	29.1	35.4	35.8	36.8	34.1	32.8	31.9
Mono-aromatic		16.6	23.3	22.9	20.4	16.7	11.8	6.8	2.4
Di-aromatic		15.0	5.8	12.5	15.1	19.0	19.6	17.5	9.5
Tri-aromatic	4.2	0	0	0.3	1.2	2.7	8.6	20.1	
Cloud Pt., °C/°F	D 2500	+12/-11	<-65/-85	-60/-76	-43/-45	-31/-24	-18/0	-3/27	too dark
Pour Pt., °C/°F	D 97	-25/-13	<-65/-85	-58/-72	-43/-45	-30/-22	-18/0	0/32	16/61
Aniline Pt., °C/°F	D 611	16.6/62	<8/46	8/46	8/46	14.0/57	17.0/63	29.2/85	552.2/126
Smoke Point	D 1322	7.1	8.7	7.1	7.1	7.3	7.1	5.4	NA

TABLE A10. LABORATORY ANALYSES FOR LOW-AROMATICS LIGHT-CYCLE OIL

Test	ASTM Method	Feed FL-1562	Frac. 1 FL-1566	Frac. 2 FL-1567	Frac. 3 FL-1568	Frac. 4 FL-1569	Frac. 5 FL-1570	Frac. 6 FL-1571	Frac. 7 FL-1572
TBP Cut Pts. °F	-		326-400	400-440	440-480	480-520	520-560	560-600	600-746
°C			163-204	204-227	227-249	249-271	271-293	293-315	315-397
Cut Range, Vol%			0-11.3	11.3-25.2	25.2-43	43-61.3	61.3-76.4	76.4-86.4	86.4-100
Yield, Vol%	-		11.3	13.9	17.8	18.3	15.1	10.0	13.6
Sp. Gr. @ 60°F	D 1298	0.8628	0.8483	0.8628	0.8681	0.8713	0.8740	0.8708	0.8453
Gravity, °API		32.5	35.3	32.5	31.5	30.9	30.4	31.0	35.9
Density, g/mL		0.8623	0.8479	0.8623	0.8676	0.8708	0.8735	0.8703	0.8448
Distillation. °C/°F, BP	D 86	199/390	171/340	206/402	226/439	244/472	266/511	284/543	315/599
5%		215/419	179/354	211/411	229/444	247/476	267/513	286/546	317/603
10%		223/433	183/362	211/412	230/446	247/477	268/514	286/547	319/606
30%		239/463	189/372	213/416	232/450	250/482	269/517	288/550	323/613
50%		253/488	196/384	217/422	234/454	252/486	271/520	289/552	327/620
70%		270/518	202/396	219/426	237/459	254/490	273/523	291/556	336/636
90%		305/581	208/406	223/434	243/470	259/499	277/530	294/561	354/669
95%		325/617	211/411	226/439	246/474	261/501	279/534	296/565	368/694
EP		347/657	215/419	234/453	253/488	268/514	284/544	301/574	379/715
Carbon, wt%	D 3178	86.49	86.67	86.78	86.73	86.73	86.68	86.55	86.07
Hydrogen, wt%		13.55	13.19	13.26	13.04	13.08	13.04	13.07	13.80
Sulfur, wt%	D 2622	0.003	<0.001	<0.001	<0.001	<0.001	<0.001	<0.001	<0.001
Aromatics	D 1319 Hydro-	10.10	12.6	9.1	11.7	11.6	9.9	10.3	8.1
Olefins	carbon Type	0.6	0.8	0.9	0.8	0.7	0.9	1.1	0.9
Saturates	Vol%	89.3	86.6	90.0	87.5	87.7	89.2	88.6	91.0
Vis. cSt @ 40°C	D 445	2.66	1.33	1.75	2.17	2.71	3.50	4.47	7.02
cSt @ 100°C		1.11	0.70	0.84	1.12	1.12	1.32	1.54	2.15
SI @ 20°C	D 1218	1.4708	1.4621	1.4681	1.4716	1.4736	1.4750	1.4741	1.4645
cetane No.	CVCA	38.4	22.4	24.5	30.1	31.4	39.6	42.1	77.2
cetane Index	D 976	40.1	24.6	28.8	33.3	37.4	40.9	45.0	56.9
	D 4737	39.8	24.6	26.7	31.2	35.5	40.5	47.3	72.6
Aromatic, wt%	UV								
Total		3.5	5.6	3.6	4.1	3.9	2.9	2.5	1.4
Mono-aromatic		3.1	5.4	3.4	3.7	3.4	2.5	2.0	1.0
Di-aromatic		0.4	0.2	0.2	0.4	0.5	0.4	0.5	0.4
Tri-aromatic		0	0	0	0	0	0	0	0
Cloud Pt., °C/°F	D 2500	-13/9	>-50/-58	>-50/-58	>-50/-58	>-50/-58	-40.5/-41	-25.5/-8	+12/54
pour Pt., °C/°F	D 97	-19/-2	>-50/-58	>-50/-58	>-50/-58	>-50/-58	-41/-42	-27.5/-18	+9/48
aniline Pt., °C/°F	D 611	63.6/146	43.0/109	49.3/121	53.7/129	58.5/137	66.3/151	73.6/164	93.3/200
smoke Point, mm	D 1322	20.4	19.5	19.8	19.3	18.1	18.5	19.3	NA

TABLE A11. COMPONENT HYDROCARBON COMPOSITION BY GC/MS

Hydrocarbon Type, Wt%/Vol%	SRD Feed 1627	SRD #1 1793	SRD #2/3/4 1794-96	SRD #5/6 1797/98	SRD #7 1799	SRD #8 1800	LCO Feed 1538	LCO #1/2 1555/56	LCO #3/4/5 1557-59	LCO #6 1560	LCO #7 1561
Paraffins	50.1/54.6	46.7/50.0	44.7/47.1	56.2/57.2	50.8/54.0	45.8/49.6	17.6/21.2	25.0/27.9	27.8/31.9	23.1/25.3	18.6/22.5
Monocycloparaffins	15.1/15.7	20.5/20.7	18.6/18.6	14.2/14.0	14.5/14.8	20.1/20.8	7.3/8.5	12.8/13.6	5.4/5.9	3.6/3.9	6.9/7.9
Dicycloparaffins	5.8/5.7	5.4/5.0	7.4/6.7	4.4/4.0	5.4/5.1	5.8/5.6	1.4/1.5	1.1/1.0	5.7/5.7	5.3/5.0	2.2/2.4
Tricycloparaffins	1.7/1.6	2.5/2.1	2.0/1.7	2.0/1.7	2.7/2.4	2.5/2.2	0/0	0/0	0.3/0.3	1.0/0.9	0.7/0.7
Alkylbenzenes	6.0/5.5	12.5/12.0	7.0/7.0	4.4/4.8	4.8/4.7	5.0/4.6	10.6/11.3	27.1/26.5	13.1/13.2	6.2/6.0	2.5/2.7
Indans/Tetralins	3.1/2.6	4.0/3.5	3.8/3.7	2.0/2.1	2.3/2.1	2.6/2.2	1.6/1.5	4.2/4.0	0/0	0/0	0.9/0.9
Indenes	3.7/3.0	0.6/0.5	4.5/4.2	3.5/3.4	3.1/2.6	2.9/2.3	1.8/1.6	2.5/2.3	1.9/1.7	0.3/0.3	0/0
Naphthalene	0.3/0.2	1.5/1.1	0.7/0.5	0.1/0.1	0/0	0/0	0.5/0.4	3.0/2.4	0.4/0.3	0.2/0.1	0/0
Naphthalenes, alkyl	7.1/5.6	5.5/4.5	8.0/7.4	5.7/5.5	4.4/3.8	4.0/3.2	31.2/28.0	22.1/20.1	28.0/24.9	11.2/10.5	14.0/12.7
Acenaphthenes	3.5/2.8	0.6/0.5	2.2/2.0	3.9/3.7	5.0/4.2	3.8/3.0	12.8/11.5	1.6/1.5	11.7/10.4	24.8/23.1	12.6/11.4
Acenaphthylenes	2.4/2.1	0.1/0.1	1.1/1.1	2.7/2.9	4.2/4.0	4.0/3.5	9.4/9.4	0.7/0.7	5.6/5.5	20.7/21.4	16.6/16.7
Tricyclic Aromatics	1.0/0.7	0/0	0/0	0.6/0.6	2.8/2.3	3.6/2.9	5.7/5.0	0/0	0/0	3.8/3.5	25.1/22.3
Total Saturates	72.8/77.5	75.1/77.8	72.7/74.2	76.8/77.0	73.4/76.4	74.2/78.2	26.4/31.2	38.9/42.5	39.3/43.9	33.0/35.2	28.3/33.4
Total Aromatics	27.2/22.5	24.9/22.2	27.3/25.8	23.2/23.0	26.6/23.6	25.8/21.8	73.6/68.8	61.1/57.5	60.7/56.1	67.0/64.8	71.7/66.6

TABLE A12. COMPONENT HYDROCARBON COMPOSITION BY GC/MS

Hydrocarbon Type, Wt%/Vol%	LoA SRD Feed 1873	LoA SRD #1 1876	LoA SRD #2 1877	LoA SRD #3 1878	LoA SRD #4 1879	LoA SRD #5 1880	LoA SRD #6 1881	LoA SRD #7 1882	LoA SRD #8 1883
Paraffins	57.2/60.2	23.3/25.0	37.7/40.2	40.7/44.0	49.3/53.2	59.4/62.6	64.6/67.6	62.6/65.5	60.9/63.9
Monocycloparaffins	16.9/16.8	38.8/39.1	32.1/32.2	20.4/20.9	18.6/18.8	16.4/16.4	21.0/20.5	21.2/20.8	23.7/23.2
Dicycloparaffins	11.3/10.3	0.8/0.8	14.8/13.6	16.8/15.7	12.4/11.7	8.8/8.1	4.7/4.5	6.6/6.0	7.2/6.5
Tricycloparaffins	6.2/5.2	0/0	2.2/1.8	5.5/4.8	4.9/4.3	5.1/4.3	3.1/2.7	3.7/3.1	3.3/2.8
Alkylbenzenes	4.5/4.1	37.1/35.1	7.6/7.3	7.3/6.7	6.6/5.7	4.8/4.4	3.2/2.5	2.9/2.4	2.3/1.9
Indans/Tetralins	2.3/2.0	0/0	5.3/4.7	7.7/6.5	5.5/4.2	2.2/1.8	1.1/0.7	0.8/0.5	0.7/0.5
Indenes	1.4/1.1	0/0	0.1/0.1	0.8/0.7	2.7/2.0	2.2/1.7	1.5/0.9	0.9/0.6	0.7/0.5
Naphthalene	0/0	0/0	0.1/0.1	0.2/0.2	0.0	0.2/0.1	0.1/0	0/0	0/0
Naphthalenes, alkyl	0.2/0.2	0/0	0.1/0.1	0.5/0.4	0.1/0	0.6/0.4	0.5/0.3	0.7/0.5	0.5/0.3
Acenaphthenes	0.1/0.1	0/0	0/0	0.1/0.1	0.1/0.1	0.2/0.2	0.2/0.1	0.4/0.3	0.4/0.3
Acenaphthylenes	0/0	0.0	0/0	0/0	0/0	0.1/0.1	0/0	0.1/0.1	0.1/0.1
Tricyclic Aromatics	0/0	0.0	0/0	0/0	0.0	0/0	0/0	0.0	0.1/0.1
Total Saturates	91.4/92.5	62.9/64.9	86.8/87.7	83.4/85.5	85.1/88.0	89.8/91.4	93.4/95.4	94.1/95.5	95.1/96.4
Total Aromatics	8.6/7.5	37.1/35.1	13.2/12.3	16.6/14.5	14.9/12.0	10.2/8.6	6.6/4.6	5.9/4.5	4.9/3.6

TABLE A13. COMPONENT HYDROCARBON COMPOSITION BY GC/MS

Hydrocarbon Type, Wt%/Vol%	LoS LCO Feed 1615	LoS LCO #1 1850	LoS LCO #2/3 1851/52	LoS LCO #4/5 1853/54	LoS LCO #6 1855	LoS LCO #7 1856	LoA LCO Feed 1562	LoA LCO #1/2 1566/67	LoA LCO #3/4 1568/69	LoA LCO #5/6 1570/71	LoA LCO #7 1572
Paraffins	27.8/31.5	22.5/24.9	28.0/31.0	28.7/30.5	29.1/33.5	29.3/32.6	23.0/25.2	4.1/4.2	13.5/14.9	30.9/34.1	55.1/57.8
Monocycloparaffins	11.1/11.9	17.7/18.2	10.9/11.5	9.3/9.4	8.5/9.3	7.5/8.0	30.3/31.6	54.6/57.3	42.3/43.8	16.2/16.8	20.2/20.0
Dicycloparaffins	3.0/2.9	5.2/4.9	4.1/3.9	2.2/2.0	2.5/2.5	3.5/3.5	22.6/21.6	31.9/31.0	24.4/23.3	16.0/15.3	8.6/7.8
Tricycloparaffins	0.0	0.1/0.1	0.4/0.3	0.1/0.1	0.1/0.1	1.5/1.4	14.1/12.3	0/0	8.9/7.9	26.6/23.6	8.0/6.8
Alkylbenzenes	18.5/18.4	31.5/30.4	22.7/21.9	13.7/13.0	6.6/6.6	2.4/2.4	4.7/4.6	7.0/5.6	5.2/5.1	3.8/3.9	2.4/2.3
Indans/Tetralins	7.5/6.9	15.4/14.7	13.4/12.7	4.5/4.6	0.2/0.2	2.6/2.6	3.7/3.3	2.3/1.7	4.7/4.2	3.2/3.1	1.1/1.1
Indenes	3.7/3.3	2.2/2.0	3.9/3.6	5.5/5.4	2.9/2.6	1.3/1.2	1.3/1.1	0/0	0.8/0.7	2.6/2.4	1.6/1.5
Naphthalene	0.8/0.6	0.1/0.1	0.1/0.1	0.6/0.5	0.1/0.1	0/0	0/0	0/0	0/0	0/0	0/0
Naphthalenes, alkyl	9.2/8.0	4.3/3.8	10.3/9.1	12.9/12.3	5.4/4.7	5.3/4.8	0.1/0.1	0/0	0/0	0.3/0.2	1.2/1.1
Acenaphthenes	9.4/8.1	0.9/0.8	4.8/4.3	14.5/13.9	21.3/18.6	12.5/11.3	0.1/0.1	0/0	0.1/0	0.4/0.3	0.9/0.8
Acenaphthylenes	6.4/6.2	0.1/0.1	1.2/1.2	7.7/8.1	17.5/16.9	14.9/15.0	0.1/0.1	0/0	0/0	0.2/0.2	0.7/0.7
Tricyclic Aromatics	2.5/2.1	0/0	0.2/0.2	0.1/0.1	5.7/4.9	19.3/17.2	0/0	0/0	0/0	0/0	0.2/0.2
Total Saturates	41.9/46.4	45.5/48.1	43.4/46.9	40.4/42.1	40.3/45.4	41.8/45.5	90.0/90.7	90.6/92.5	89.1/89.8	89.6/89.7	91.9/92.4
Total Aromatics	58.1/53.6	54.5/51.9	56.6/53.1	59.6/57.9	59.7/54.6	58.2/54.5	10.0/9.3	9.4/7.5	10.9/10.2	10.4/10.3	8.1/7.6

TABLE A14. COMPONENT HYDROCARBON COMPOSITION BY GC/MS

Hydrocarbon Type, Wt%/Vol%	LCGO Feed 1440	LCGO #1 1546	LCGO #2/3 1547/48	LCGO #4/5 1549/50	LCGO #6 1551	LoS LCGO Feed 1442	LoS LCGO #1/2 1862/63	LoS LCGO #3/4 1864/65	LoS LCGO #5 1866	LoS LCGO #6 1867
Paraffins	24.9/28.3	27.6/29.6	27.7/29.8	23.4/24.5	22.6/24.4	26.8/29.7	32.6/35.0	33.8/35.9	32.5/33.6	34.9/36.3
Monocycloparaffins	25.7/27.7	38.3/38.6	28.2/28.8	24.0/24.3	19.0/19.9	26.8/28.2	35.4/35.8	25.5/25.6	24.0/23.5	21.6/21.3
Dicycloparaffins	10.5/10.5	10.9/10.0	11.1/10.2	9.1/8.5	11.0/10.6	13.0/12.5	9.6/8.9	12.1/11.0	9.8/8.7	10.1/9.0
Tricycloparaffins	3.2/2.9	1.8/1.5	4.2/3.6	4.2/3.7	4.2/3.8	4.0/3.5	0.4/0.4	3.1/2.6	3.6/3.0	4.0/3.3
Alkylbenzenes	8.5/8.0	9.8/9.9	9.0/9.1	10.0/10.3	8.7/8.9	9.9/9.4	11.8/11.2	7.5/7.9	7.2/7.6	7.3/7.7
Indans/Tetralins	8.5/7.3	8.1/7.5	8.8/8.5	5.1/5.3	4.6/4.6	10.7/9.3	9.0/7.8	12.4/12.0	9.3/9.9	5.6/5.9
Indenes	6.4/5.2	1.2/1.1	6.1/5.6	8.8/8.6	4.8/4.5	6.0/5.0	0.3/0.2	4.0/3.7	8.4/8.5	7.0/7.0
Naphthalene	0.7/0.5	0.5/0.4	0.2/0.1	0.2/0.2	0/0	0/0	0.3/0.2	0/0	0.7/0.6	0.2/0.2
Naphthalenes, alkyl	5.1/4.1	0.8/0.7	3.4/3.1	6.9/6.6	7.4/6.8	1.6/1.3	0.5/0.4	1.2/1.1	2.6/2.6	3.3/3.2
Acenaphthenes	3.8/3.1	0.7/0.6	0.6/0.6	4.7/4.5	9.0/8.2	0.8/0.6	0/0	0.2/0.2	1.2/1.2	3.2/3.2
Acenaphthylenes	2.2/1.9	0.1/0.1	0.4/0.4	2.8/3.0	6.2/6.3	0.4/0.4	0/0	0/0	0.7/0.8	2.3/2.5
Tricyclic Aromatics	0.5/0.4	0/0	0.2/0.2	0.6/0.6	2.3/2.1	0.1/0.1	0/0	0.1/0	0/0	0.4/0.4
Total Saturates	64.3/69.5	78.7/79.7	71.2/72.4	60.7/61.0	56.9/58.6	70.5/74.0	78.1/80.1	74.5/75.0	69.9/68.8	70.6/69.9
Total Aromatics	35.7/30.5	21.3/20.3	28.8/27.6	39.3/39.0	43.1/41.4	29.5/26.0	21.9/19.9	25.5/25.0	30.1/31.2	29.4/30.1

TABLE A15. COMPONENT HYDROCARBON COMPOSITION BY GC/MS

Hydrocarbon Type, Wt%/Vol%	LoA LCGO Feed 1443	LoA LCGO #1/2 1597/98	LoA LCGO #3/4 1599/1600	LoA LCGO #5/6 1601/02	LoA LCGO #7 1603	FT Feed 1840	FT #1/2/3 1898-1900	FT #4/5/6 1901-03	FT #6 1903	FT #7 1904
Paraffins	32.5/35.0	26.6/28.6	31.9/34.3	36.9/39.6	43.7/46.4	89.5/90.7	94.8/95.2	83.3/84.2	89.3/90.4	88.1/89.5
Monocycloparaffins	35.3/36.5	49.6/50.4	40.0/40.7	29.2/29.6	29.0/28.3	7.3/6.9	4.3/4.1	14.0/13.4	8.5/8.0	9.7/9.0
Dicycloparaffins	13.9/13.4	13.3/12.4	14.0/13.2	15.0/13.9	14.6/13.6	0/0	0/0	1.9/1.7	1.0/0.8	0.3/0.2
Tricycloparaffins	3.1/2.8	0.7/0.6	3.1/2.7	8.4/7.2	6.3/5.4	0/0	0/0	0/0	0/0	0/0
Alkylbenzenes	8.8/7.7	6.5/5.5	5.1/4.5	3.9/3.8	2.6/2.3	2.7/2.1	0.7/0.6	0.5/0.5	0.7/0.5	1.6/1.1
Indans/Tetralins	4.1/2.9	3.0/2.2	4.4/3.5	3.2/2.9	0.9/0.7	0.1/0.0	0.2/0.1	0.1/0.1	0.1/0.1	0/0
Indenes	1.3/0.9	0.2/0.1	1.4/1.1	3.0/2.6	2.5/1.9	0.4/0.3	0/0	0/0	0.1/0	0.4/0.2
Naphthalene	0.1/0.1	0.1/0.1	0.1/0.1	0/0	0.5/0.3	0/0	0/0	0/0	0/0	0/0
Naphthalenes, alkyl	0.6/0.4	0/0	0/0	0.3/0.2	0/0	0/0	0/0	0/0	0/0	0/0
Acenaphthenes	0.1/0.1	0/0	0/0	0.2/0.2	0/0	0/0	0/0	0/0	0/0	0/0
Acenaphthylenes	0/0	0/0	0/0	0.1/0.1	0/0	0/0	0/0	0/0	0.3/0.2	0/0
Tricyclic Aromatics	0/0	0/0	0/0	0/0	0/0	0/0	0/0	0/0	0/0	0/0
Total Saturates	84.8/86.9	90.2/92.0	89.0/90.8	89.4/90.3	93.5/94.7	96.8/97.6	99.1/99.3	99.2/99.3	98.8/99.2	98.0/98.6
Total Aromatics	15.2/12.2	9.8/8.0	11.0/9.2	10.6/9.7	6.5/5.3	3.2/2.4	0.9/0.7	0.6/0.6	1.2/0.8	2.0/1.4


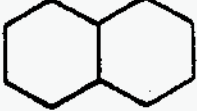
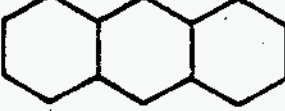

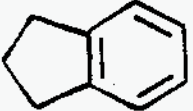
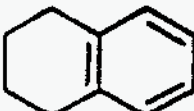
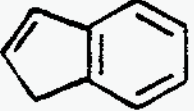
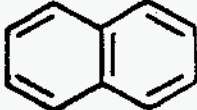
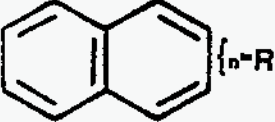
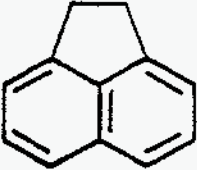
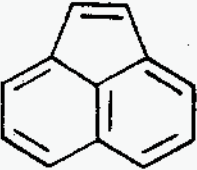
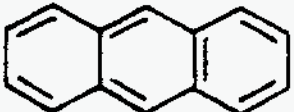
ASTM D2425 HYDROCARBON TYPE CLASSIFICATIONS	
HYDROCARBON TYPE	GENERAL STRUCTURES
Normal/Iso Paraffins	$\begin{array}{c} \\ -C- \\ \end{array} \{n-R$
Monocycloparaffins	 $\{n-R$
Dicycloparaffins	 $\{n-R$
Tricycloparaffins	 $\{n-R$
Alkyl Benzenes	 $\{n-R$
Indans/Tetralins	 $\{n-R$  $\{n-R$
Indenes	 $\{n-R$
Naphthalene	
Alkyl Naphthalenes	 $\{n-R$
Acenaphthenes	 $\{n-R$
Acenaphthylenes	 $\{n-R$
Tricyclic Aromatics	 $\{n-R$

TABLE A16. PROTON NMR CHEMICAL-SHIFT ASSIGNMENTS

Proton Type	Abbreviated Symbol	Description	Chemical Shift Region (ppm, Δ)
1. Alkane methyl	CH ₃	Terminal paraffin chain protons	0.5 - 1.05
2. Gamma methyl	CH ₃	Terminal alkyl chain protons at least three carbons from an aromatic ring	0.5 - 1.05
3. Alkane methylene	CH ₂	Mid-paraffin chain proton with no branching	1.05 - 1.4
4. Beta methyl	CH ₂	Terminal alkyl proton exactly two carbons from an aromatic ring	1.05 - 1.4
5. Gamma methylene	CH ₂	Mid-alkyl chain proton at least three carbons from an aromatic ring	1.05 - 1.4
6. Alkane methine	CH	Mid-chain proton with branching	1.4 - 2.0
7. Cycloalkane methylene	CH	Cycloalkane (naphthene) proton	1.4 - 2.0
8. Beta methylene	CH	Mid-alkyl chain proton exactly two carbons from an aromatic ring	1.4 - 2.0
9. Alpha methyl	ALP	Terminal alkyl chain on carbon adjacent to an aromatic ring	2.0 - 4.4
10. Alpha methylene	ALP	Alkyl chain proton on carbon adjacent to an aromatic ring	2.0 - 4.4
11. Alpha methine	ALP	Alkyl proton on carbon adjacent to an aromatic ring with branching	2.0 - 4.4
12. Aromatic	ARO (DI & MONO)	All aromatic ring protons on di- or mono-ring compounds	6.2 - 9.2

TABLE A17. PER CENT OF TOTAL PROTON RESONANCE INTENSITY FOR VARIOUS CHEMICAL-SHIFT RANGES

SAMPLE NO.	Chemical-Shift Ranges in ppm referred to TMS				
	0.5-1.05	1.05-1.4	1.4-2.0	2.0-4.4	6.2-9.2*
1440-F	30.5	33.3	17.1	14.9	4.2
1442-F	33.0	38.2	15.4	9.5	3.9
1546-F	33.6	30.8	17.3	14.9	3.4
1538-F	11.9	27.4	5.8	29.8	25.1
1538	13.0	27.3	5.5	29.3	24.9
1546-F	33.3	31.4	17.7	14.1	3.5
1547-F	33.5	31.5	16.4	14.7	3.9
1548-F	31.6	33.2	16.2	14.5	4.5
1549-F	30.1	35.2	15.8	14.6	4.3
1550-F	29.8	35.6	15.7	14.3	4.6
1551-F	27.5	36.9	15.6	14.6	5.4
1569-F	36.9	32.4	25.0	4.0	1.7
1570-F	36.8	35.5	23.4	3.1	1.2
1571-F	35.0	39.9	20.8	3.3	1.0
1572-F	27.1	56.5	13.2	2.5	0.6
1603-F	39.9	46.2	12.7	0.4	0.8
1615-F	16.6	29.1	11.4	27.0	15.9
1627-F	27.9	53.9	8.8	4.9	4.5
1793-F	32.1	44.9	10.9	6.5	5.5
1794-F	31.7	45.6	10.3	6.6	5.8
1795-F	30.2	46.6	10.5	7.3	5.4
1796-F	29.2	49.1	9.7	7.0	5.0
1797-F	28.6	53.3	9.0	6.1	4.0
1798-F	27.6	55.5	8.4	5.1	3.4
1799-F	24.7	57.1	9.1	5.5	3.6
1800-F	23.4	55.9	10.6	6.2	3.8

* This range contains the resonance from the residual protons in the solvent CDCl_3 corresponding to approximately 0.3%.

TABLE A17. PER CENT OF TOTAL PROTON RESONANCE INTENSITY FOR VARIOUS CHEMICAL-SHIFT RANGES (Continued)

	Chemical-Shift Ranges in ppm referred to TMS				
1840-F	37.2	59.3	2.8	0.3	0.4
1850-F	18.8	24.3	13.9	27.7	15.3
1851-F	16.4	25.2	13.4	29.2	15.8
1852-F	15.4	26.7	12.8	28.9	16.1
1853-F	17.1	28.2	11.1	27.6	16.0
1854-F	14.3	30.0	10.3	28.1	17.3
1855-F	14.7	33.6	8.6	25.8	17.3
1856-F	14.8	41.7	8.3	20.2	15.0
1862-F	37.2	36.3	14.3	8.2	4.0
1863-F	36.7	36.9	14.6	8.0	3.8
1864-F	36.0	37.2	14.6	8.5	3.7
1865-F	35.3	37.6	14.2	8.9	4.0
1866-F	32.5	39.3	14.8	9.8	3.6
1867-F	32.3	41.5	13.9	8.7	3.6
1898-F	41.4	53.3	3.2	0.1	2.0
1899-F	38.6	56.8	3.4	0.4	0.8
1900-F	37.4	58.4	3.2	0.5	0.5
1901-F	36.2	60.3	2.4	0.0	1.1
1902-F	32.2	62.8	4.2	0.6	0.2
1903-F	33.4	63.1	2.5	0.3	0.7
1904-F	31.7	64.7	2.9	0.4	0.3
1443-F	33.3	38.8	20.5	6.0	1.3
1555-F	16.5	24.4	7.5	31.9	19.6
1556-F	15.7	26.1	6.1	28.6	23.5
1557-F	13.1	25.7	5.6	30.1	25.4
1558-F	12.6	25.4	5.0	31.6	25.5
1559-F	11.6	27.1	5.5	31.9	24.0

* This range contains the resonance from the residual protons in the solvent CDCl_3 corresponding to approximately 0.3%.

**TABLE A17. PER CENT OF TOTAL PROTON RESONANCE INTENSITY FOR
VARIOUS CHEMICAL-SHIFT RANGES
(Continued)**

	Chemical-Shift Ranges in ppm referred to TMS				
1560-F	13.2	29.4	5.5	29.1	22.8
1561-F	12.5	33.7	4.7	24.2	25.0
1562-F	35.9	35.0	23.9	3.7	1.5
1566-F	39.6	24.9	27.9	4.8	2.8
1567-F	41.9	25.4	27.9	3.1	1.7
1568-F	39.5	28.7	26.3	3.7	1.9
1597-F	43.8	33.3	17.5	3.3	2.2
1598-F	40.9	35.0	18.5	4.0	1.6
1599-F	40.3	36.7	17.8	3.9	1.3
1600-F	38.7	38.3	17.8	4.0	1.2
1601-F	41.5	39.7	15.2	2.2	1.3
1602-F	37.1	42.7	16.1	3.3	0.9
1873-F	31.0	52.1	12.5	2.9	1.5
1876-F	34.3	37.9	13.9	9.1	4.7
1877-F	34.9	39.8	17.1	5.3	2.9
1878-F	34.4	46.7	13.7	3.5	1.7
1879-F	34.5	41.4	16.9	4.9	2.4
1880-F	31.4	52.3	12.4	2.9	1.1
1881-F	30.5	57.6	9.6	1.6	0.7
1882-F	27.4	61.3	9.4	1.4	0.6
1883-F	27.9	59.9	10.3	1.2	0.7

* This range contains the resonance from the residual protons in the solvent CDCl_3 corresponding to approximately 0.3%.

TABLE A18. COMBUSTION ANALYSES FOR FISCHER-TROPSCH DIESEL (FT1)

Properties	FT 1 FEED 1840	FT1 #1 1898	FT1 #2 1899	FT1 #3 1900	FT1 #4 1901	FT1 #5 1902	FT1 #6 1903	FT1 #7 1904
VCR Cetane No.	87.8	48.1	52.9	53.5	82.4	86.0	89.6	87.3
CVCA Cetane No.	64.8	51.2	60.1	66.0	72.1	71.1	82.3	87.3
M1 CO	6.29	6.15	5.67	4.68	4.97	5.87	4.32	5.83
M1 HC	2.45	3.40	2.12	1.92	1.83	2.06	1.98	2.44
M1 NO _x	3.54	3.34	3.37	3.59	3.43	3.30	3.58	3.20
M1 Smoke	2.00	1.83	2.05	1.80	1.85	2.00	2.10	2.60
M2 CO	5.43	6.24	5.91	4.65	4.56	6.35	4.94	5.66
M2 HC	2.03	2.94	1.91	1.36	1.06	1.41	1.78	1.24
M2 NO _x	3.53	3.49	3.35	3.51	3.57	3.18	3.32	3.27
M2 Smoke	2.00	2.30	2.00	1.85	1.90	2.00	2.30	2.00
M3 CO	5.50	7.25	6.42	6.60	5.26	6.55	4.82	6.17
M3 HC	1.55	2.27	1.74	1.71	1.35	1.33	1.43	1.87
M3 NO _x	3.33	2.91	3.50	3.57	3.34	3.21	3.43	3.34
M3 Smoke	1.90	1.75	1.75	2.00	4.25	1.70	2.00	2.05
M4 CO	3.95	4.44	4.04	3.94	4.08	3.93	3.48	-
M4 HC	3.71	5.49	3.63	2.79	2.06	1.55	2.07	-
M4 NO _x	2.97	4.35	3.77	3.75	3.61	3.97	3.36	-
M4 Smoke	0.90	0.80	1.00	1.00	0.90	1.20	1.25	-
M5 CO	4.95	4.60	4.15	4.54	4.35	4.89	4.56	-
M5 HC	7.21	6.92	5.72	3.28	1.45	1.52	2.30	-
M5 NO _x	3.62	5.00	4.25	4.30	4.20	4.48	3.64	-
M5 Smoke	0.60	0.60	0.60	0.80	0.70	0.95	1.00	-

TABLE A19. COMBUSTION ANALYSES FOR STRAIGHT-RUN DIESEL

Properties	SRD Feed 1627	SRD #1 1793	SRD #2 1794	SRD #3 1975	SRD #4 1796	SRD #5 1797	SRD #6 1798	SRD #7 1799	SRD #8 1800
VCR Cetane No.	58.5	40.3	40.5	43.5	60.7	63.3	63.3	69.4	-
CVCA Cetane No.	56.2	33.9	41.1	40.5	42.5	45.1	64.2	-	-
M1 CO	5.21	5.39	5.59	6.65	4.70	0.93	1.00	0.87	-
M1 HC	2.42	3.41	2.99	1.72	2.38	0.37	0.43	0.38	-
M1 NOx	3.48	3.49	3.78	3.87	3.90	5.29	5.62	5.67	-
M1 Smoke	2.30	2.50	2.80	2.50	2.03	3.70	2.65	2.40	-
M2 CO	5.01	6.27	-	5.50	5.20	0.89	1.01	0.82	-
M2 HC	2.01	3.11	-	1.31	1.65	0.47	0.59	0.34	-
M2 NOx	3.64	3.63	-	3.99	3.98	6.34	6.49	6.39	-
M2 Smoke	2.40	2.60	-	2.40	2.50	3.00	2.10	2.30	-
M3 CO	6.18	6.14	4.89	5.41	5.08	0.76	0.78	0.92	-
M3 HC	1.15	2.21	1.96	1.56	1.37	0.38	0.47	0.32	-
MC NOx	3.55	3.65	3.39	3.83	4.02	6.23	6.33	6.16	-
M3 Smoke	2.60	2.40	2.50	2.15	2.75	1.60	1.05	1.25	-
M4 CO	3.78	3.57	3.96	4.06	2.18	1.68	1.95	-	-
M4 HC	6.46	2.74	2.04	3.42	0.57	0.46	0.53	-	-
M4 NOx	4.45	3.62	4.91	4.23	6.14	5.30	5.26	-	-
M4 Smoke	1.30	1.60	1.00	1.50	1.60	1.25	1.25	-	-
M5 CO	5.19	5.73	5.35	5.34	5.36	3.77	4.15	-	-
M5 HC	7.01	6.27	3.45	3.80	2.71	0.85	0.95	-	-
M5 NOx	4.95	3.94	5.76	4.62	6.98	5.27	5.36	-	-
M5 Smoke	0.90	1.20	0.80	1.40	1.70	1.15	1.35	-	-

A-23

TABLE A20. COMBUSTION ANALYSES FOR LOW-AROMATICS STRAIGHT-RUN DIESEL

Properties	LoA SRD Feed 1873	LoA SRD #1 1876	LoA SRD #2 1877	LoA SRD #3 1878	LoA SRD #4 1879	LoA SRD #5 1880	LoA SRD #6 1881	LoA SRD #7 1882	LoA SRD #8 1883
VCR Cetane No.	58.9	40.3	40.3	41.3	49.8	67.1	75.3	93.0	-
CVCA Cetane No.	61.3	23.1	31.7	38.6	44.3	48.8	64.2	79.1	-
M1 CO	7.37	3.18	5.69	5.26	5.57	5.43	4.70	2.17	-
M1 HC	2.14	8.75	3.45	3.39	1.08	1.99	1.03	0.80	-
M1 NOx	3.31	4.51	3.86	3.47	3.31	3.60	3.39	2.48	-
M1 Smoke	2.55	1.70	2.65	2.15	2.35	1.90	2.40	1.10	-
M2 CO	5.48	3.24	5.68	5.65	5.01	5.69	6.25	6.96	-
M2 HC	1.86	7.20	2.87	2.38	1.28	1.31	1.24	1.37	-
M2 NOx	3.50	5.40	3.38	3.76	3.55	3.49	3.26	3.39	-
M2 Smoke	2.60	1.80	2.50	2.35	2.35	1.95	2.20	2.35	-
M3 CO	5.01	-	4.78	4.91	5.23	5.67	4.40	5.68	-
M3 HC	1.70	-	1.95	1.96	1.33	1.02	1.36	1.27	-
MC NOx	3.57	-	3.75	3.79	3.52	3.62	3.70	3.59	-
M3 Smoke	2.30	-	2.15	2.10	2.15	2.00	1.80	2.00	-
M4 CO	-	-	4.02	3.73	3.99	3.54	3.56	-	-
M4 HC	-	-	4.52	2.44	1.15	1.78	1.66	-	-
M4 NOx	-	-	4.42	4.45	4.17	4.20	4.05	-	-
M4 Smoke	-	0.95	1.20	1.00	0.90	1.10	1.00	-	-
M5 CO	-	-	4.77	4.86	4.74	4.59	4.47	-	-
M5 HC	-	-	5.31	1.33	1.50	1.70	1.79	-	-
M5 NOx	-	-	5.14	4.74	4.48	4.64	4.40	-	-
M5 Smoke	-	0.80	1.80	0.85	0.80	0.90	0.80	-	-

A-24

TABLE A21. COMBUSTION ANALYSES FOR LIGHT-COKER GAS OIL

Properties	LCGO Feed 1440	LCGO #1 1546	LCGO #2 1547	LCGO #3 1548	LCGO #4 1549	LCGO #5 1550	LCGO #6 1551
VCR Cetane No.	44.3	31.8	34.8	33.1	35.5	34.2	37.6
CVCA Cetane No.	29.0	25.6	27.9	30.1	29.1	32.8	31.7
M1 CO	7.97	5.43	4.55	6.11	4.89	5.60	5.80
M1 HC	3.63	2.60	3.18	1.88	0.98	1.52	1.23
M1 NOx	3.82	3.71	3.97	4.04	3.89	3.89	4.05
M1 Smoke	2.10	2.10	2.35	2.50	2.10	2.30	1.80
M2 CO	6.41	5.17	4.26	5.84	4.38	5.98	4.94
M2 HC	2.18	3.01	2.67	2.31	0.91	1.55	1.18
M2 NOx	4.78	4.12	4.35	4.40	4.18	4.10	4.36
M2 Smoke	2.20	2.50	2.20	2.50	2.35	2.40	1.90
M3 CO	5.80	7.32	5.65	4.63	4.87	4.50	5.17
M3 HC	1.07	2.36	2.09	1.71	1.02	1.50	1.17
MC NOx	3.91	3.76	4.11	3.95	3.83	3.82	3.98
M3 Smoke	1.80	2.40	2.45	2.20	2.20	2.20	2.80
M4 CO	3.30	4.73	4.00	3.83	3.51	3.74	-
M4 HC	2.86	7.30	5.95	3.27	1.85	1.22	-
M4 NOx	4.95	4.26	5.20	4.36	4.37	4.25	-
M4 Smoke	0.50	1.10	1.15	1.10	1.45	1.35	-
M5 CO	7.59	6.15	6.73	6.62	6.04	8.96	-
M5 HC	13.73	7.22	6.31	2.58	3.55	2.10	-
M5 NOx	6.22	6.09	5.30	5.59	5.29	5.46	-
M5 Smoke	0.80	0.40	0.90	1.00	1.40	1.60	-

TABLE A22. COMBUSTION ANALYSES FOR LOW-SULFUR LIGHT-COKER GAS OIL

Properties	LoS LCGO Feed 1442	LoS LCGO #1 1862	LoS LCGO #2 1863	LoS LCGO #3 1864	LoS LCGO #4 1865	LoS LCGO #5 1866	LoS LCGO #6 1867
VCR Cetane No.	38.1	31.9	34.6	34.8	47.0	39.5	41.1
CVCA Cetane No.	33.3	28.2	29.5	29.2	30.4	33.7	37.8
M1 CO	5.72	5.48	5.13	4.55	7.05	4.13	5.36
M1 HC	1.79	3.74	2.29	1.76	2.14	1.08	1.69
M1 NOx	3.74	3.86	3.76	3.73	3.38	4.00	3.90
M1 Smoke	2.15	2.40	2.10	2.05	2.70	2.20	2.40
M2 CO	4.95	6.28	5.12	4.47	6.70	4.60	6.02
M2 HC	1.31	4.71	2.13	1.72	1.50	0.72	1.58
M2 NOx	4.15	4.45	4.08	4.16	3.93	4.07	3.71
M2 Smoke	2.30	2.10	2.20	2.00	2.85	2.10	2.10
M3 CO	4.32	5.73	4.55	4.57	6.14	4.16	5.14
M3 HC	1.51	2.30	1.73	1.58	1.25	0.97	1.63
MC NOx	3.71	3.36	3.84	3.74	3.70	3.80	3.69
M3 Smoke	1.95	2.15	2.15	2.00	2.65	2.15	2.50
M4 CO	3.92	3.54	3.34	3.90	3.16	3.42	-
M4 HC	6.09	3.97	3.85	2.34	1.09	1.51	-
M4 NOx	3.79	4.66	4.44	4.39	4.54	3.72	-
M4 Smoke	1.40	1.20	1.25	1.30	1.10	1.60	-
M5 CO	5.66	5.47	4.95	5.27	4.68	5.68	-
M5 HC	7.37	6.94	4.98	4.73	1.18	3.07	-
M5 NOx	4.55	5.51	5.09	4.69	5.22	3.85	-
M5 Smoke	1.30	0.80	0.75	1.00	0.80	1.30	-

TABLE A23. COMBUSTION ANALYSES FOR LOW-AROMATICS LIGHT-COKER GAS OIL

Properties	LoA LCGO Feed 1443	LoA LCGo #1 1597	LoA LCGO #2 1598	LoA LCGO #3 1599	LoA LCGO #4 1600	LoA LCGO #5 1601	LoA LCGO #6 1602	LoA LCGO #7 1603
VCR Cetane No.	46.7	34.8	37.4	39.5	42.4	47.7	53.9	65.1
CVCA Cetane No.	37.7	28.2	30.5	31.7	33.7	39.0	44.1	54.9
M1 CO	4.59	4.49	4.52	4.79	5.95	5.67	5.75	5.27
M1 HC	2.78	4.38	2.33	2.44	1.94	1.49	1.40	1.32
M1 NOx	3.77	4.00	3.48	3.89	3.39	3.66	3.47	3.68
M1 Smoke	2.30	1.90	2.40	2.10	2.25	2.30	2.70	2.50
M2 CO	4.59	5.27	5.96	4.42	5.78	5.72	6.99	5.62
M2 HC	2.78	4.51	3.81	2.27	1.17	0.95	1.47	1.51
M2 NOx	3.77	4.43	3.89	3.78	3.58	3.83	3.54	3.63
M2 Smoke	2.30	2.10	2.40	2.10	2.25	2.25	2.10	2.20
M3 CO	5.54	6.10	6.29	5.77	4.59	4.49	5.08	5.04
M3 HC	1.81	2.36	1.68	2.50	1.46	0.92	1.31	1.09
MC NOx	3.78	3.76	3.36	4.79	3.51	3.57	3.31	3.53
M3 Smoke	2.30	2.25	2.90	2.00	2.10	2.10	3.10	2.40
M4 CO	3.80	3.84	3.86	3.21	3.44	3.58	3.70	-
M4 HC	6.89	4.88	5.17	1.76	1.86	1.91	1.33	-
M4 NOx	4.73	3.77	4.43	4.38	4.06	3.28	4.26	-
M4 Smoke	1.85	1.30	0.95	1.00	1.20	1.60	1.10	-
M5 CO	4.90	4.82	4.50	4.69	4.28	5.23	4.97	-
M5 HC	7.07	6.23	6.02	2.48	1.50	3.17	1.67	-
M5 NOx	5.14	4.36	4.79	4.95	4.46	3.48	4.52	-
M5 Smoke	2.55	1.00	0.75	0.70	0.80	1.05	1.10	-

TABLE A24. COMBUSTION ANALYSES FOR LIGHT-CYCLE OIL

Properties	LCO Feed 1538	LCO #1 1555	LCO #2 1556	LCO #3 1557	LCO #4 1558	LCO #5 1559	LCO #6 1560	LCO #7 1561
VCR Cetane No.	23.4	19.7	20.8	-	19.9	20.4	22.9	22.5
CVCA Cetane No.	15.5	15.2	17.0	-	13.9	15.6	16.3	19.1
M1 CO	-	-	-	-	-	-	6.38	9.56
M1 HC	-	-	-	-	-	-	0.87	1.92
M1 NOx	-	-	-	-	-	-	9.49	8.18
M1 Smoke	-	-	-	-	-	-	1.70	9.00
M2 CO	4.69	3.96	3.70	-	-	4.72	4.23	4.09
M2 HC	1.75	3.62	3.04	-	-	0.47	0.63	0.67
M2 NOx	13.43	13.72	14.08	-	-	14.16	11.23	11.08
M2 Smoke	2.95	1.80	2.10	-	-	1.80	1.70	4.00
M3 CO	-	-	-	-	-	-	1.89	-
M3 HC	-	-	-	-	-	-	0.55	-
MC NOx	-	-	-	-	-	-	8.89	-
M3 Smoke	-	-	-	-	-	-	0.85	-
M4 CO	-	-	-	-	-	-	-	-
M4 HC	-	-	-	-	-	-	-	-
M4 NOx	-	-	-	-	-	-	-	-
M4 Smoke	-	-	-	-	-	-	-	-
M5 CO	-	-	-	-	-	-	-	-
M5 HC	-	-	-	-	-	-	-	-
M5 NOx	-	-	-	-	-	-	-	-
M5 Smoke	-	-	-	-	-	-	-	-

TABLE A25. COMBUSTION ANALYSES LOW-SULFUR LIGHT-CYCLE OIL

Properties	LoS LCO Feed 1615	LoS LCO #1 1850	LoS LCO #2 1851	LoS LCO #3 1852	LoS LCO #4 1853	LoS LCO #5 1854	LoS LCO #6 1855	LoS LCO #7 1856
VCR Cetane No.	23.4	29.8	21.6	22.5	22.7	23.9	27.4	35.0
CVCA Cetane No.	17.9	14.0	15.4	15.7	17.3	18.6	19.9	-
M1 CO	7.73	-	-	4.47	5.74	2.84	1.81	1.79
M1 HC	2.30	-	-	1.31	1.71	0.47	0.32	0.71
M1 NOx	5.53	-	-	6.64	6.40	8.60	7.93	6.66
M1 Smoke	2.70	-	-	1.60	2.23	1.90	1.45	2.50
M2 CO	4.66	5.07	4.06	6.24	5.25	1.93	1.67	1.90
M2 HC	1.51	3.22	2.57	2.76	1.31	0.63	0.28	0.47
M2 NOx	6.83	12.52	12.60	7.90	8.05	10.83	9.62	8.15
M2 Smoke	1.85	2.20	1.70	2.20	2.20	1.80	2.00	1.90
M3 CO	5.81	-	-	4.92	4.85	1.39	1.39	1.13
M3 HC	1.57	-	-	1.12	2.13	0.29	0.29	0.33
MC NOx	4.45	-	-	4.67	4.92	7.68	7.72	7.49
M3 Smoke	2.64	-	-	2.60	2.40	1.15	1.25	0.85
M4 CO	12.29	-	-	21.47	14.00	8.78	5.09	3.82
M4 HC	5.50	-	-	6.31	4.27	1.05	0.77	0.92
M4 NOx	6.82	-	-	7.34	8.60	8.39	8.22	6.82
M4 Smoke	0.30	-	-	0.35	0.33	0.75	0.95	1.05
M5 CO	-	-	-	-	-	-	8.77	-
M5 HC	-	-	-	-	-	-	1.50	-
M5 NOx	-	-	-	-	-	-	6.91	-
M5 Smoke	-	-	-	-	-	0.95	0.85	-

TABLE A 26. COMBUSTION ANALYSIS FOR LOW-AROMATICS LIGHT-CYCLE OIL

Properties	LoA LCO Feed 1562	LoA LCO #1 1566	LoA LCO #2 1567	LoA LCO #3 1568	LoA LCO #4 1569	LoA LCO #5 1570	LoA LCO #6 1571	LoA LCO #7 1572
VCR Cetane No.	41.9	30.4	34.8	35.6	39.3	42.7	49.1	75.3
CVCA Cetane No.	38.4	22.4	24.5	30.1	31.4	39.6	42.1	77.2
M1 CO	1.16	4.40	1.42	1.14	1.21	0.95	5.30	2.48
M1 HC	0.87	3.65	2.97	2.65	0.53	0.44	1.66	2.93
M1 NOx	5.54	3.62	5.83	6.05	5.94	5.79	3.66	2.01
M1 Smoke	2.10	2.20	1.90	2.10	2.50	1.70	2.40	1.20
M2 CO	1.07	4.25	1.46	1.20	1.14	0.91	5.13	5.35
M2 HC	2.17	4.47	3.23	2.99	2.58	0.53	1.45	1.48
M2 NOx	6.86	4.28	7.41	7.15	7.05	6.64	3.97	3.45
M2 Smoke	1.90	2.20	2.10	2.10	2.10	2.10	2.40	2.50
M3 CO	0.97	6.21	1.05	0.88	0.90	0.83	5.05	6.27
M3 HC	0.81	2.28	1.85	1.62	0.39	0.62	1.34	1.16
MC NOx	5.76	3.56	6.36	6.41	6.13	6.27	3.30	3.29
M3 Smoke	1.45	6.00	1.05	0.85	0.95	1.25	2.20	4.50
M4 CO	2.10	4.03	2.28	2.22	2.17	2.51	4.06	3.16
M4 HC	2.33	6.59	4.58	4.20	2.52	0.96	2.82	1.10
M4 NOx	5.57	4.08	6.00	5.56	5.70	5.50	3.79	4.03
M4 Smoke	0.85	1.60	1.05	1.05	0.85	1.45	1.25	1.60
M5 CO	5.16	7.95	5.33	4.80	5.30	4.42	4.79	-
M5 HC	6.08	9.10	6.57	3.12	0.94	3.66	1.61	-
M5 NOx	4.20	8.17	6.23	5.76	5.96	3.40	4.51	-
M5 Smoke	1.20	0.85	0.85	0.85	0.85	1.10	1.40	-

**APPENDIX B
VCR ENGINE MODIFICATION**

VCR Engine Modifications

The design target for this phase of the project was to develop a swirl ratio of 2.66:1 for the Variable Compression Ratio (VCR) cylinder head. The following paragraphs give the chronological development process, beginning with background information.

The VCR cylinder head was flow-tested on the SwRI Flow Bench. A schematic of the Flow Bench is shown in Figure B-1. The cylinder head was tested for performance characteristics such as flow coefficient, swirl ratio, and pressure loss. We define these parameters in the ensuing discussion and describe below the SwRI Flow Bench and the methods of analyzing the data. The output from the data reduction program is shown in Appendix B. We used an impulse swirl meter. The impulse swirl meter to determine swirl ratio. The impulse swirl meter is preferred over a paddle, or vane meter because the latter tends to under predict the swirl level by as much as 30%. The pressure difference over all ports was maintained at 20 inches (508 mm) of water to ensure that the flow was fully turbulent, and hence, yield the equality between the steady-state flow bench and an actual operating engine.

Initially, a baseline test was performed of the un-modified head to provide a reference point for future development. Sensitivity of swirl ratio and pressure loss were evaluated for changes in compression ratio and engine speed. tests 1-4 consisted of a compression ratio of 16:1 and 22:1, each at an engine speed of 900 and 1800 rpm. A summary of these results is shown in Table B-1. Both swirl ratio and pressure loss proved to be insensitive to compression ratio. For the two engine speeds, the swirl ratio changed less than 2%. Pressure loss across the port changed with engine speed.

Table B-1. Compression Ratio and Engine Speed Sensitivity Results

Engine Speed, (rpm)	Compression Ratio Pressure Loss (kPa)	Swirl Ratio
900	16 +0.228	2.48
1800	16 +0.224	9.41
900	22 +0.228	2.49
1800	22 +0.241	9.48

The initial direction of development was to create a helical port out of the existing port because helical ports have the ability to generate high levels of swirl most efficiently. Tests 5-14 created the helical port by means of strategically placing modeling clay within the existing port to determine the correct port geometry. This procedure was an iterative process, relying on test results and intake port design experience.

After nine iterations in creating a helical port, we performed a so-called rotational test to determine the location of the directed swirl component and the percent helical/directed flow. A rotational test consists of moving the cylinder about the intake valve in 15 increments while maintaining the design distance between the centers. In this manner, the location of the largest value of non-dimensional swirl can be found. Non-dimensional swirl (N_s) is a measure of the level of swirl. The results of this test are shown in Figure B-2.

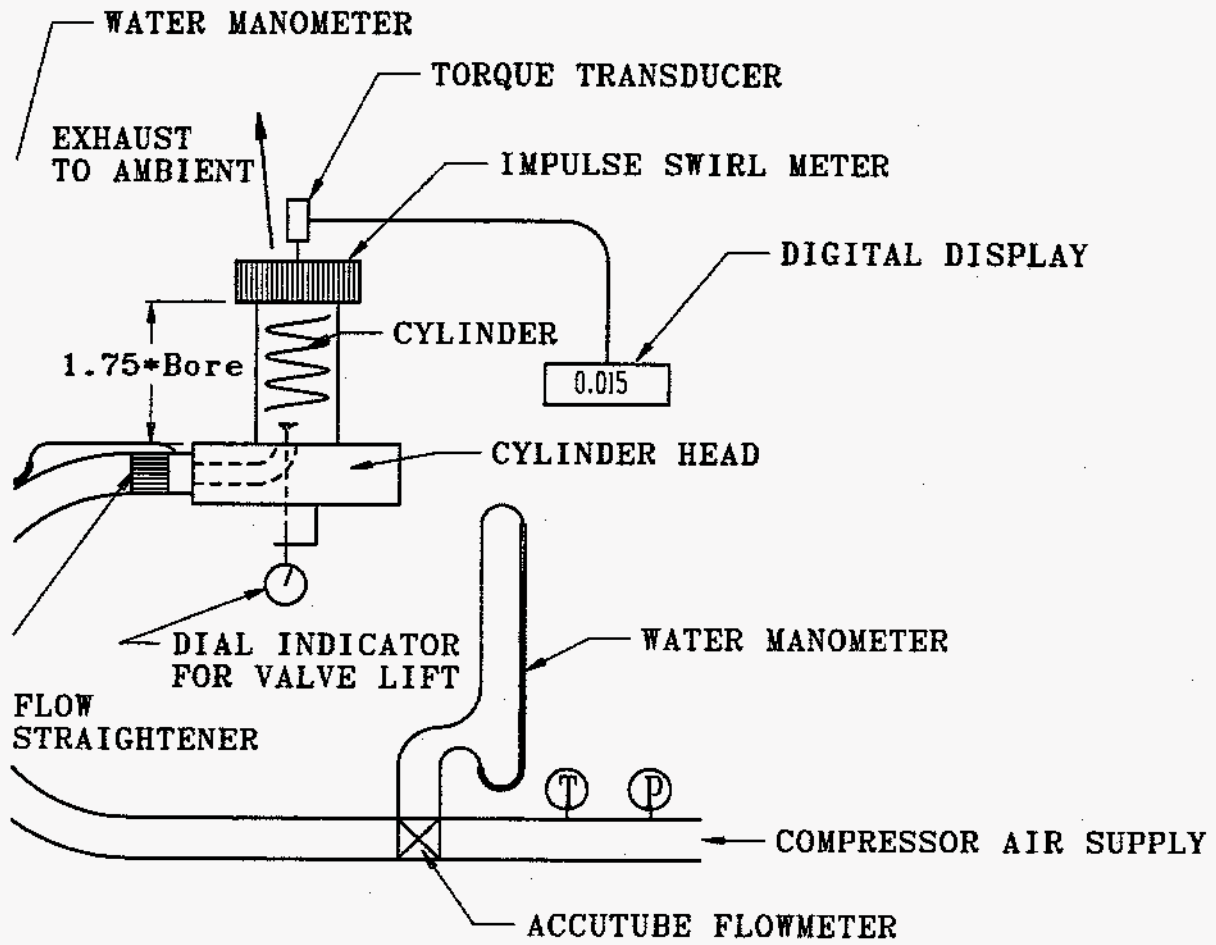


Figure B-1. SwRI flow bench schematic

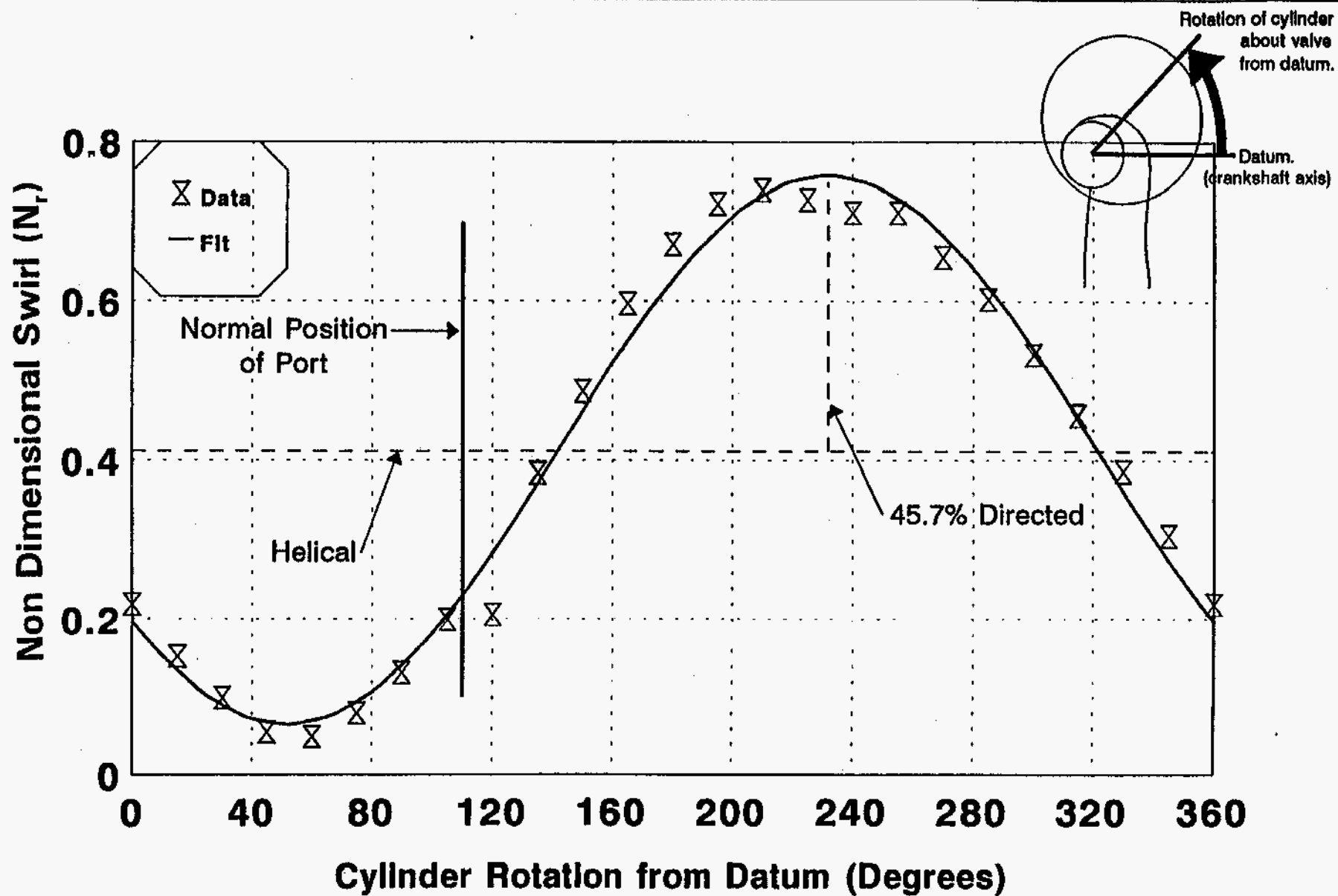


Figure B-2. SwRI rotational test - Labeco VCR - Mod.; #9 - Lift = 8.3 mm

The helical port of the swirl ratio is a horizontal line at $Nr = 0.41$. The directed component is the sinusoidal curve in which the maximum directed portion is given as $Nr = p.35$ at 225° cylinder rotation from datum. The normal position of the port is shown at 110° cylinder rotation from the datum. For the optimum design, the location of the maximum non-dimensional swirl (helical plus directed) should be coincident with the normal position of the port. In this case the location of the maximum non-dimensional swirl was 115° out-of-phase with the normal position of the port. The locations of the velocity vectors are illustrated in a top view of the cylinder in Figure B-3. The desired position of the velocity vector is shown tangential to the normal position of 110° counter-clock-wise from the datum. The actual velocity vector is shown pointing towards the center of the cylinder.

From the location of the velocity vector, the value of swirl ratio and the value of pressure drop across the port, we determined that the helical port solution to this problem is ineffective as tried. In Figure B-4, the velocity vector was oriented 115° from where it should be. Due to the spatial constraints of the VCR cylinder head, the necessary geometry cannot be created to allow the proper orientation of the velocity vector. Because swirl ratio is directly related to the velocity vector, the value of the swirl ratio cannot be dramatically increased without the re-orientation of the velocity vector. The maximum swirl ratio attained during clay modifications was 1.68:1 with a pressure drop of 6.85 (kPa). Table B-2 gives a summary of the baseline, target, and best clay modification. The pressure loss of the clay modification was 2.75 times higher than that of the baseline, and the swirl ration was 36% away from the target. We decided that the helical port solution to this problem was ineffective and that another approach should be taken.

Table B-2. Best Clay Modification

	Baseline	Target	Best Clay
Swirl Ratio	-0.23:1	2.66:1	1.69:1
Pressure Loss (kPa)	2.49	—	6.85

The second direction of development was to employ a shrouded valve. A shrouded valve directs a large portion of the air flow through an unrestricted section of the valve. Thus, the velocity vector can be forced in a desired direction. A masked valve was manufactured in which the unrestricted section measured 150° . To determine the proper orientation, we performed a standard test (test #16) in which the shrouded valve was rotated until the torque readout maximized at each valve lift position. From these results, we selected a valve position in which higher valve lifts were weighted more due to higher mass flow rates. The standard test was repeated (test #17) at a fixed valve position, and the results are shown in Table B-3. The pressure loss was 3.96 kPa and was only 1.6 times higher than the baseline pressure loss. The swirl ration was 16.5% away from the target swirl ratio. The orientation of the masked valve is shown in B-6.

Table B-2. Shrouded Valved Results

	Baseline	Target	Shrouded Valve
Swirl Ratio	-0.23:1	2.66:1	3.10:1
Pressure Loss (kPa)	2.49	—	3.96

We used two important non-dimensional parameters — non-dimensional swirl and non-dimensional flow coefficient — to compare the masked valve to the baseline. Non-dimensional swirl (Nr) is shown versus non-dimensional valve lift in Figure B-5. The nearly horizontal trend indicates that the baseline configuration does not produce swirl. The masked valve exhibits traits of a helical/directed combination.

TOP VIEW

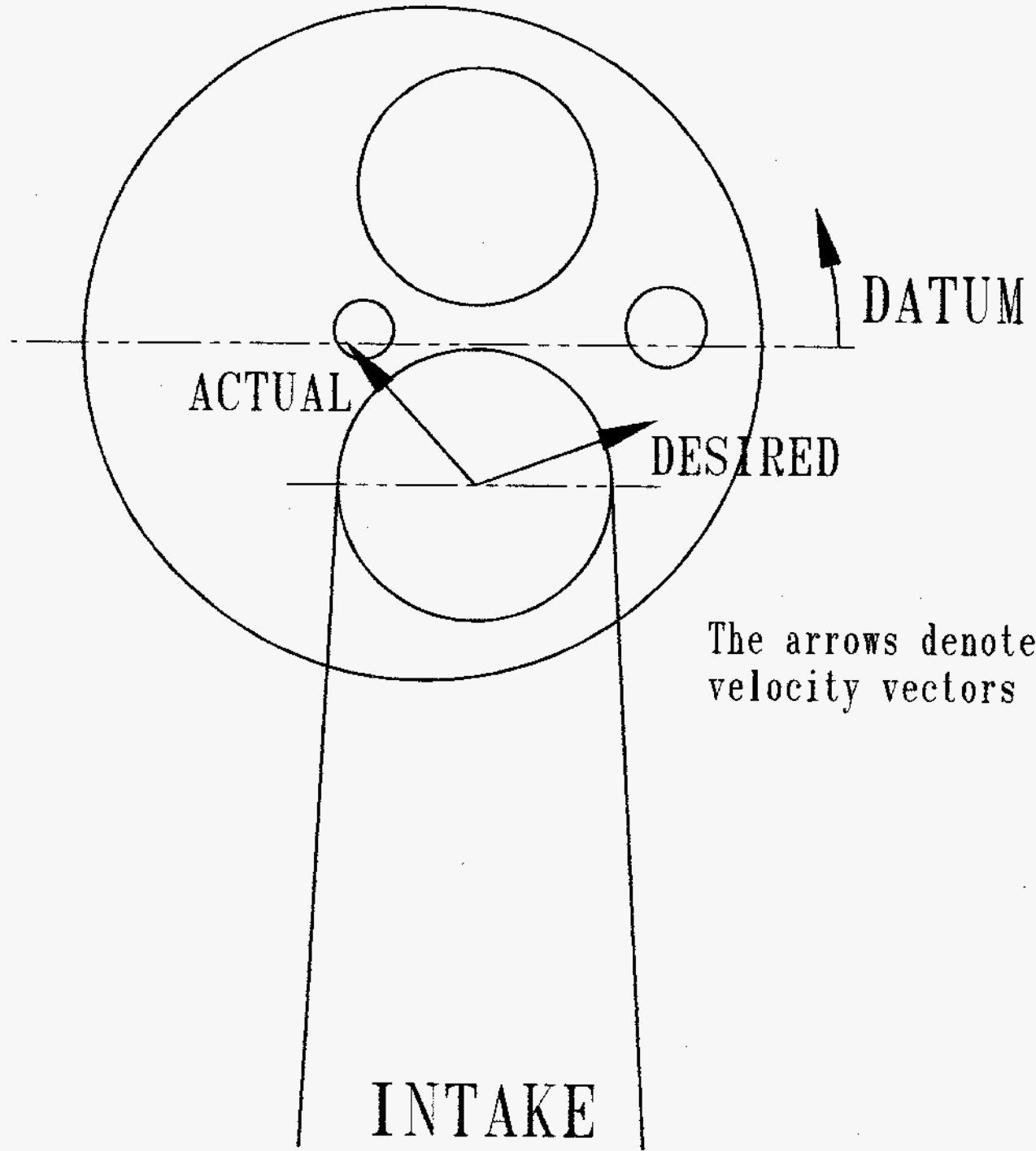


Figure B-3. Top view of cylinder - datum

TOP VIEW

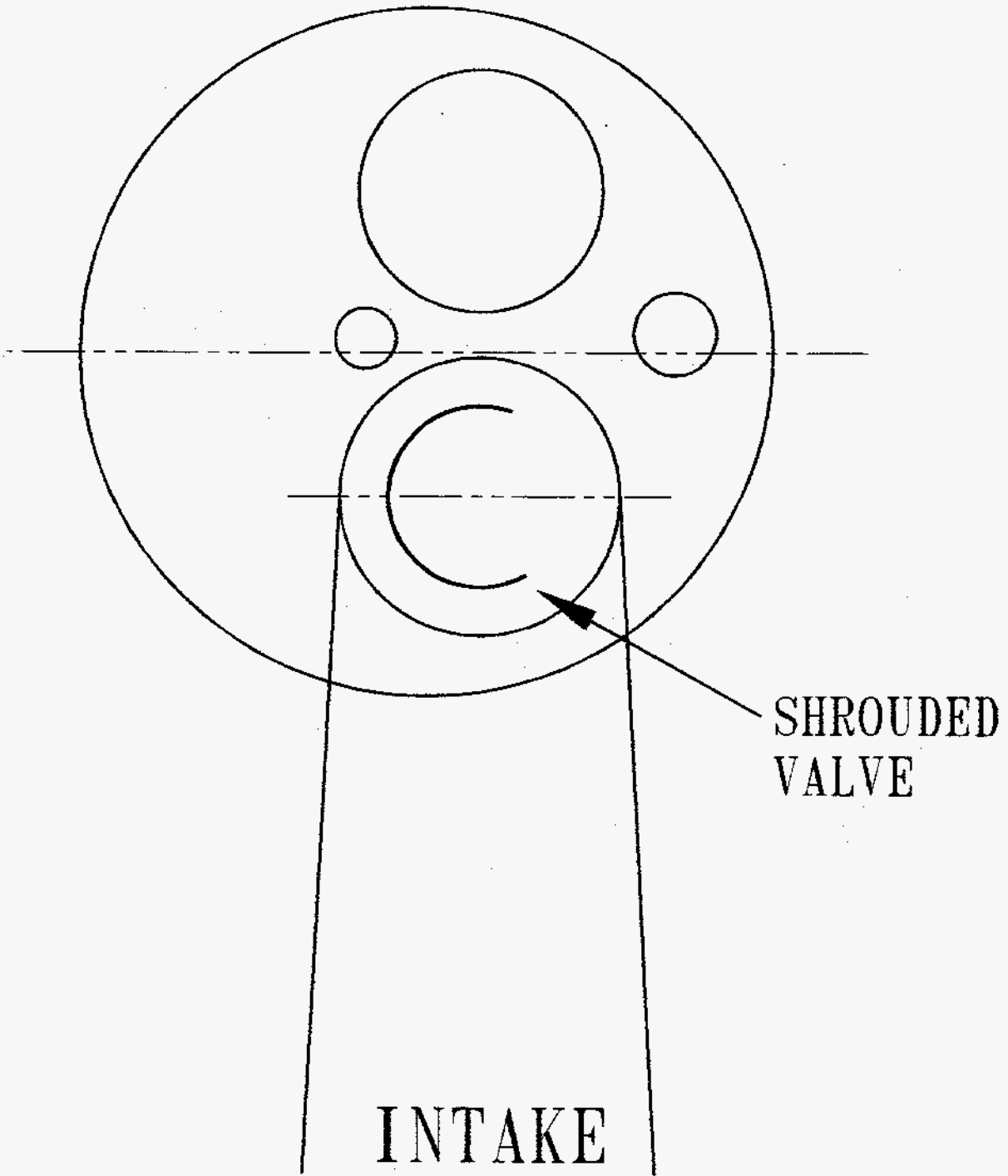


Figure B-4. Top view shrouded valve

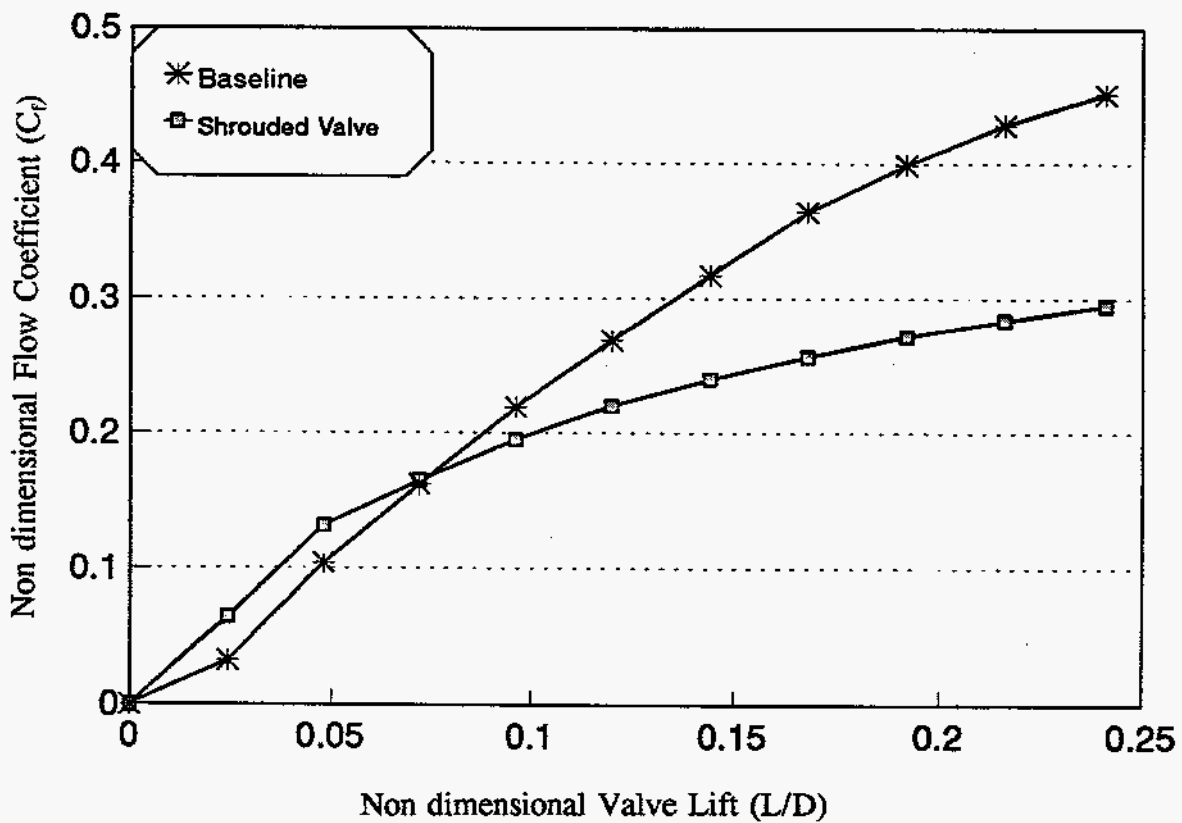
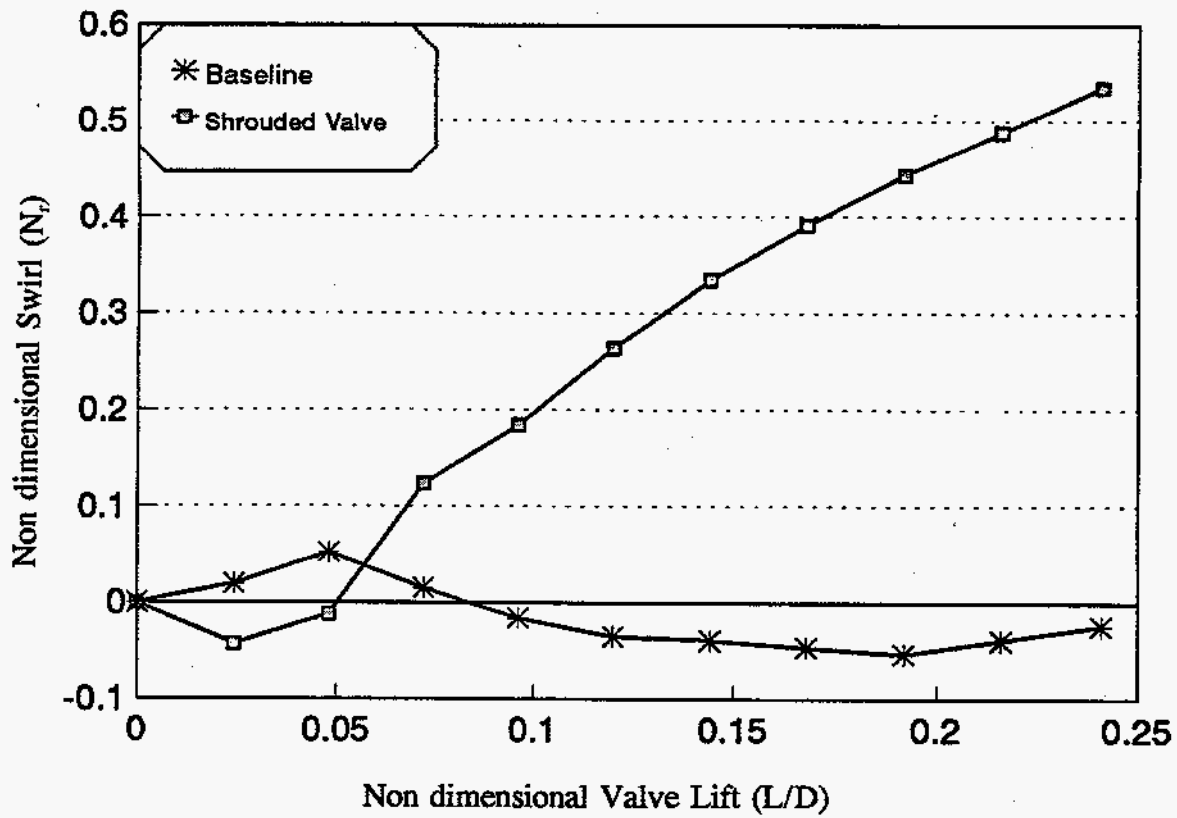


Figure B-5. SwRI flow bench standard test results Labeco VCR - 900 rpm - CR 16.10:1

Swirl is created at lower lifts and steadily increases. The non-dimensional flow coefficient (C_f) is defined as the actual flow divided by the ideal flow. Therefore, the larger C_f , the less restriction offered. The non-dimensional flow coefficient versus L/D is shown in Figure B-6. The baseline configuration is revealed to have a higher C_f than the masked valve. This was expected, because the masked valve obstructed the flow area and increased pressure loss.

It is often desirable to compare the swirl ratio and pressure loss of various cylinder heads. To do this, the cylinder heads must be evaluated on an equal basis. SwRI has accumulated a data base of swirl ratios and pressure losses and has determined the "state-of-the-art" for both 4-valve and 2-valve engines. For our particular engine, and 11.2 m/s piston speed equates to 3527 rpm. The baseline and masked valve configurations are shown in Figure B-6.

We selected the 210 masked valve to complete the design phase of the project. Even though the swirl ratio target was 2.66:1, we considered the masked swirl ratio of 3:10:1 satisfactory. Further, small increases of the swirl ratio from the one obtained would be costly and time consuming and were not pursued.

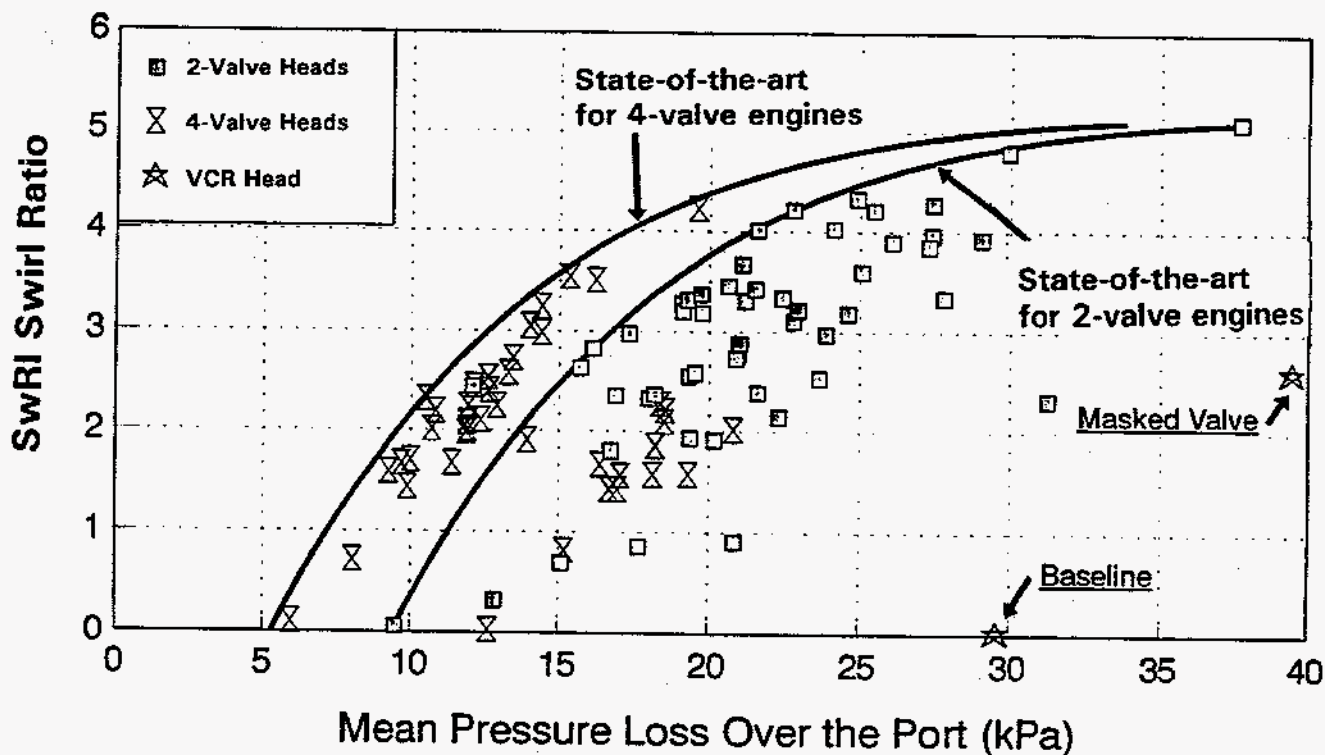


Figure B-6. SwRI swirl ratio comparison of different intake ports at the same mean piston speed of 11.2 m/s

FLOW BENCH and DATA REDUCTION TECHNIQUES

The flow bench is a time-tested steady-state air rig used to test the flow performance of the ports in a cylinder head. The techniques and analysis are appropriate for either spark-ignited (SI) or compression-ignited (CI) engines. A diagram of the SwRI Flow Bench is shown in Figure B-1.

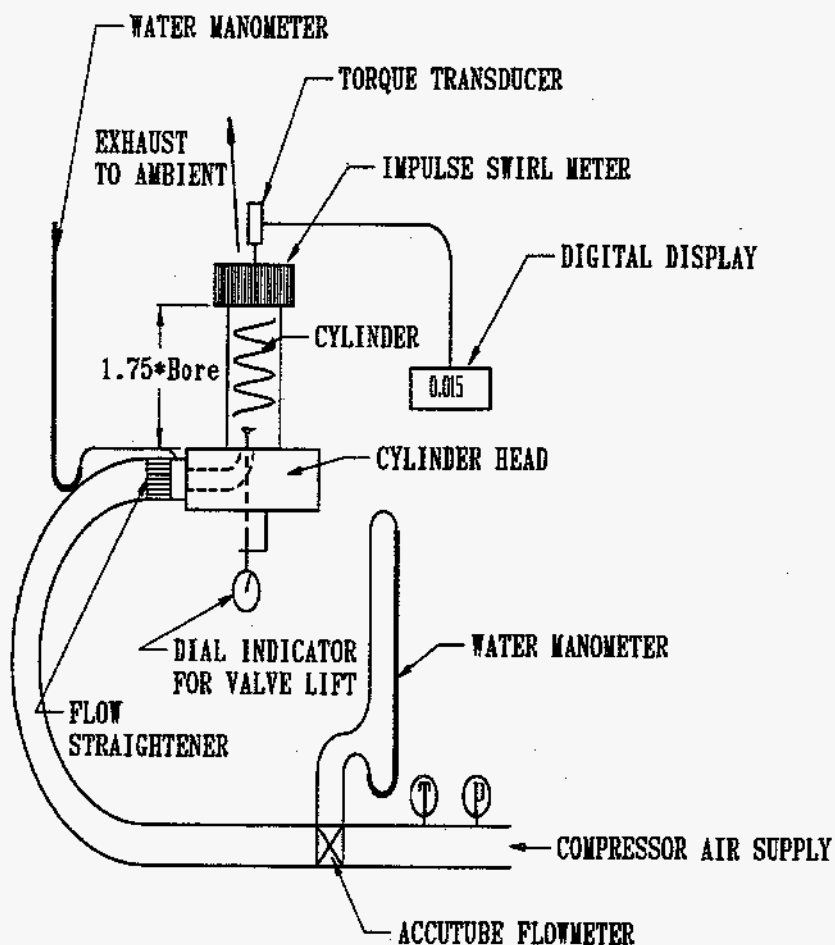


Figure B-1. SwRI Flow Bench Schematic

Flow benches have been used extensively in the past to determine flow capacity, usually in (CFM) cubic feet per minute. Since the 1970's, the ability to estimate in-cylinder air motion is the main strength of the flow bench. Swirl and tumble are the two components of the overall in-cylinder air motion that the flow bench can predict. The concepts of swirl and tumble are illustrated in Figures B-7 and B-8, respectively.

The generation of swirl and/or tumble is dependent upon many things, including port orientation, chamber masking, number of valves, and piston crown, among others. It is also beneficial to analyze the flow bench data in terms of non-dimensional parameters so as to allow comparisons independent of size. A discussion of non-dimensional parameters will be given below.

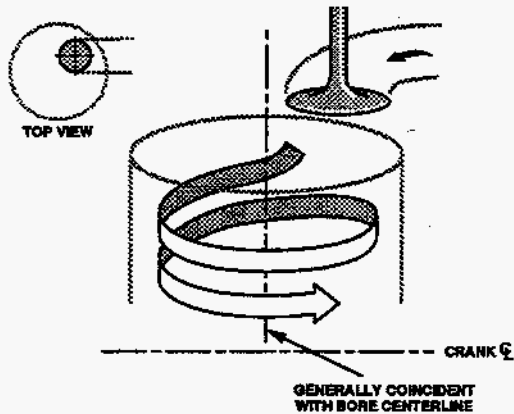


Figure B-7. Swirl Motion

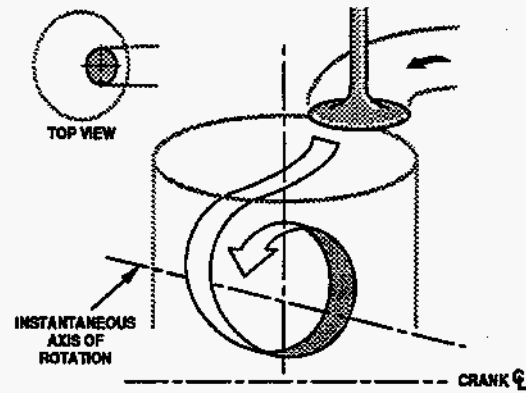


Figure B-8. Tumble Motion

The Purpose of Using Non-Dimensional Parameters

The non-dimensional parameters used to describe flow, swirl and tumble conditions at each valve lift are:

Flow Coefficient

$$C_F = \frac{Q}{n \cdot A \cdot V_o}$$

Non-Dimensional Swirl

$$N_R = \frac{8 \cdot G}{M \cdot B \cdot V_o}$$

Coefficient of Performance

$$C_P = \sqrt{\left[\frac{B \cdot N_R}{4 \cdot D \cdot n} \right]^2 + \left[\frac{D \cdot C_F}{4 \cdot L} \right]^2}$$

Angle of Outflow

$$\text{Theta} = \text{Tan}^{-1} \left[\frac{B \cdot L \cdot N_R}{n \cdot D^2 \cdot C_F} \right]$$

$$\text{Non-Dimensional Valve Lift} = L/D$$

- where: α is crank angle degrees
 A is valve seat area (m²)
 $A = \frac{\pi \cdot D^2}{4}$
 B is the bore (m)
 D is the inner valve seat diameter (m)
 G is the torque measured on the swirl meter (N.m)
 I is the moment of inertia (kg-m²)
 L is the valve lift (m)

M	is the total mass flow through the port (kg/sec)
n	is the number of valves open, usually one or two
Q	is the total volume flow (m ³ /sec)
r	is the pressure ratio over the port (p _{o2} /p _{o1})
R	is the gas constant for air (287.1 J/kg. °K)
S	is the stroke (m)
T	is the air temperature at the port (°K)
γ	is the ratio of specific heats for air (C _p /C _v)
V _o	is the velocity head upstream of the port (m/sec)

$$V_o = \sqrt{\frac{2 \cdot \gamma R \cdot T}{\gamma - 1} \left[1 - \frac{(1)^{\frac{\gamma-1}{\gamma}}}{(r)} \right]}$$

The port properties are described in non-dimensional terms as these do not vary with Reynolds number; that is, the non-dimensional terms are unchanged when the pressure drop over the port varies. This is because the flow is in the fully turbulent regime, so it exhibits Reynolds number similarity. This feature is important as it means that the port has the same flow properties in the engine as on the flow bench. This permits an emptying and filling engine model to predict terminal swirl from the non-dimensional flow properties on the flow bench.

The independence of the non-dimensional port properties to pressure drop also means that it does not really matter at what pressure differential the port is tested provided the flow is in the fully turbulent region. For engines under 150 mm bore diameter, this is usually above 350 mm water pressure differential.

The independence of non-dimensional parameters with pressure differential over the port also allows the emptying and filling model to predict conditions in an engine from the measurements made on the flow bench even though the flow bench measurements were made at a different pressure differential. The accurate extrapolation of flow bench measurements to running engine conditions allows the meaningful prediction of swirl in the engine.

The significance of the non-dimensional parameters that have already been defined will now be discussed:

Flow Coefficient

$$C_F = \frac{Q}{n \cdot A \cdot V_o} = \frac{\text{Actual Flow}}{\text{Ideal Flow}}$$

This is analogous to a flow coefficient based in the valve seat area. For two intake valves (n=2) then C_F represents the average flow coefficient for both ports.

Non-Dimensional Swirl or Tumble

$$N_R = \frac{8 \cdot G}{M \cdot B \cdot V_o}$$

$$N_R = \frac{\omega \cdot B}{V_o} = \frac{2 \times \text{Swirl Velocity at Cylinder Wall}}{V_o}$$

This is a measure of the level of swirl (or tumble), where ω is the equivalent swirl velocity in radians/sec. The non-dimensional swirl is independent of the number of intake valves, as it is calculated from global measurements, which by themselves, are not a function of the number of intake valves open.

Coefficient of Performance

$$C_p = \sqrt{\left[\frac{B \cdot N_R}{4 \cdot D \cdot n} \right]^2 + \left[\frac{D \cdot C_f}{4 \cdot L} \right]^2}$$

$$C_p = \sqrt{\frac{V_T^2 + V_R^2}{V_o^2}}$$

$$\text{Coefficient of Performance} = V/V_o$$

Coefficient of Performance is the relative velocity vector at the valve seat in a plane perpendicular to the valve stem axis divided by the maximum possible velocity upstream of the port. It is the weighted sum of the radial (or flow) component (V_R) and the tangential (or swirl) component (V_T). Coefficient of Performance is a useful parameter as it indicates the efficiency of the port in its ability to generate flow and swirl.

Angle of Outflow

$$\text{Theta} = \text{Tan}^{-1} \left[\frac{B \cdot L \cdot N_R}{n \cdot D^2 \cdot C_f} \right]$$

$$\text{Theta} = \text{Tan}^{-1} \left(\frac{V_T}{V_R} \right)$$

Theta is the angle subtended by these two components, V_T and V_R and indicates the proportion of velocity given to swirl or the flow. Theta increases with higher swirl.

Discussion of the Various Swirl Models

All of the swirl models predict swirl ratio. This is defined as:

$$\text{Swirl Ratio } (R_s) = \frac{\text{Swirl Speed at the End of Induction}}{\text{Engine Speed}}$$

As the flows in the engine are fully turbulent, swirl ratio does not change very much with engine speed.

The swirl models predict the solid-body terminal swirl by integrating the angular momentum flux at each crank position during induction. Dividing this value by the induced charge mass then gives terminal swirl speed.

SwRI Method

This method used the same equations as used by other, more sophisticated emptying and filling programs. It integrates between TDC and inlet valve closing and assumes an initial pressure in the port and in the cylinder of 1 bar, and assumes there is no heat transfer. Although this method requires compression ratio as input, it calculates volumetric efficiency, while the other methods stipulate 100 percent volumetric efficiency. This method also accounts for compressible flow.

$$\text{Terminal Swirl } (\omega) = \frac{1}{I_{\text{final}}} \int_{\text{tdc}}^{\text{ivc}} \bar{I} \cdot \omega \cdot dt$$

where: $\bar{I} \cdot \omega$ is the angular momentum flux ($\text{kg} \cdot \text{m}^2 / \text{sec}^2$)

I_{final} is the moment of inertia of the induced charge at intake valve closing ($\text{kg} \cdot \text{m}^2$)

Ricardo Method

This method assumes a constant pressure drop over the port during induction. This pressure drop is calculated from the mean flow coefficient during intake valve opening. The momentum flux at any crank angle is then determined from this pressure drop and the valve lift at that crank angle. This method assumed 100 percent volumetric efficiency and incompressible flow.

$$\text{Swirl Ratio} = \frac{B \cdot S \cdot \int_{\text{ivc}}^{\text{ivo}} C_F \cdot N_R \cdot d\alpha}{n \cdot D^2 \left[\int_{\text{ivc}}^{\text{ivo}} C_F \cdot d\alpha \right]^2}$$

AVL Method

This method assumes that the flow rate equals the rate of piston displacement. It therefore integrates only between top and bottom dead centers (TDC to BDC), and assumes 100% volumetric efficiency.

SwRI Impulse Swirl Meter

The swirl meter is shown in Figure B-9 below. This is the impulse type that has the advantage over vane or paddle wheel swirl meters in that it measures the torque reaction from the arrested swirl. This equals momentum flux that is used directly by the swirl prediction model. A paddle wheel meter has the disadvantage in that flow profiles in the flow bench cylinder must be assumed, and that these assumptions can cause significant errors in the swirl predictions.

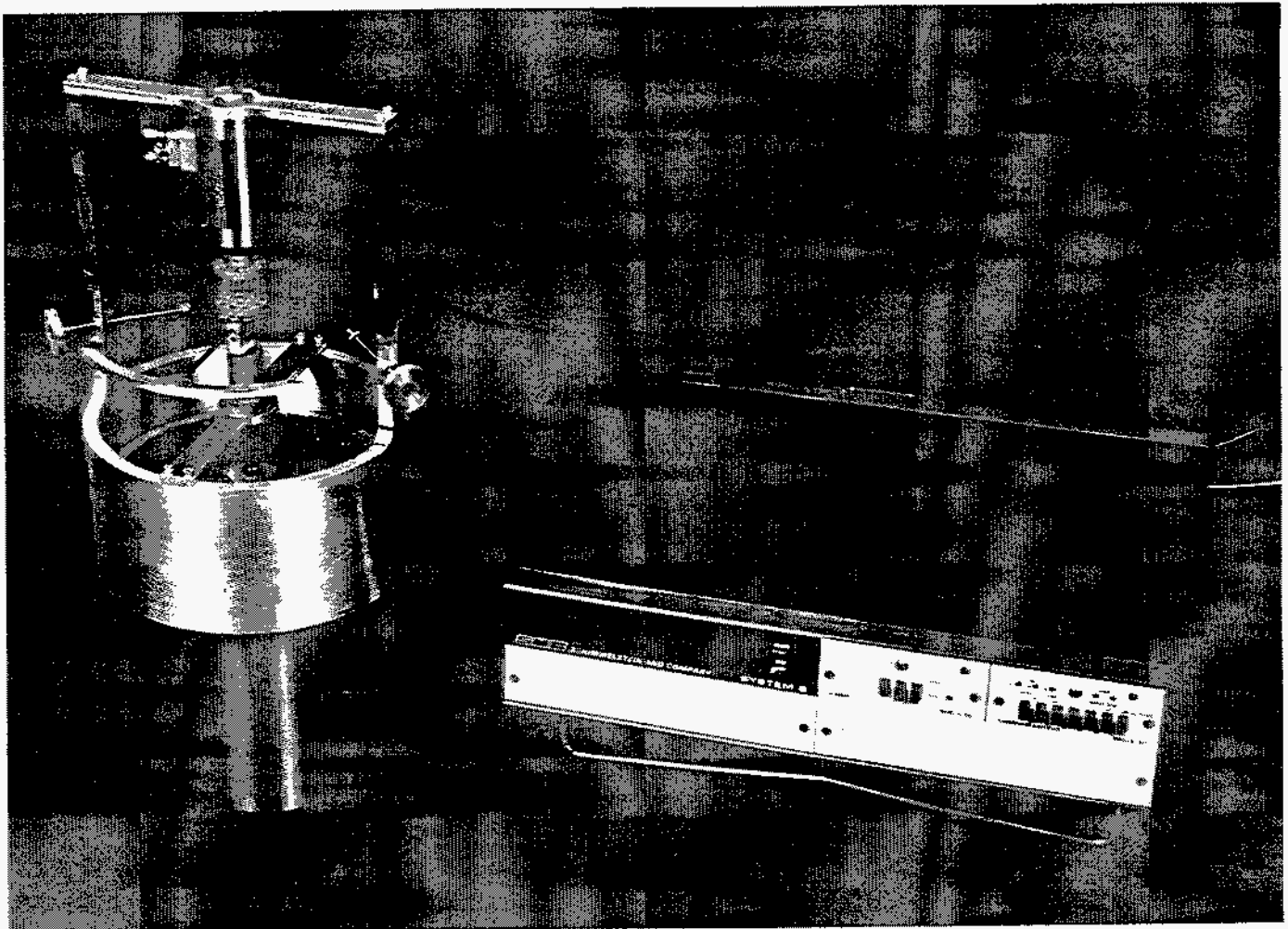


Figure B-9. Impulse type swirl meter on SwRI flow bench

It can be seen that for swirl, the cylinder head is tested in the upside down position on the SwRI flow bench. This allows simple repositioning of the flow bench cylinder. The swirl meter is positioned 1.75 bore lengths downstream of the head for swirl measurements. The flow bench is calibrated monthly with a standard calibration cylinder head, and the impulse swirl meter is calibrated monthly with a static deadweight procedure.

SwRI Rotational Test

A more detailed characterization of the swirl motion can be gained with the use of the SwRI Rotational Test. The measured swirl is comprised of a *directed* (or radial) and a *helical* (or tangential) component. These two components add vectorially to produce the measured swirl. This test determines the percentage of the directed and helical components of the swirl and also the orientation of the maximum directed component. This test allows the designer to ensure that the directed component is effectively utilized.

The Rotational Test consists of rotating the center of the cylinder about the center of the intake valve maintaining the normally design separation distance between the two centers. This test is conducted at a fixed valve lift; normally at maximum intake valve lift. Figure B-10 shows the principle of the Rotational Test. This test can be conducted on individual ports for a four-valve head and also on heads with an integral combustion chamber.

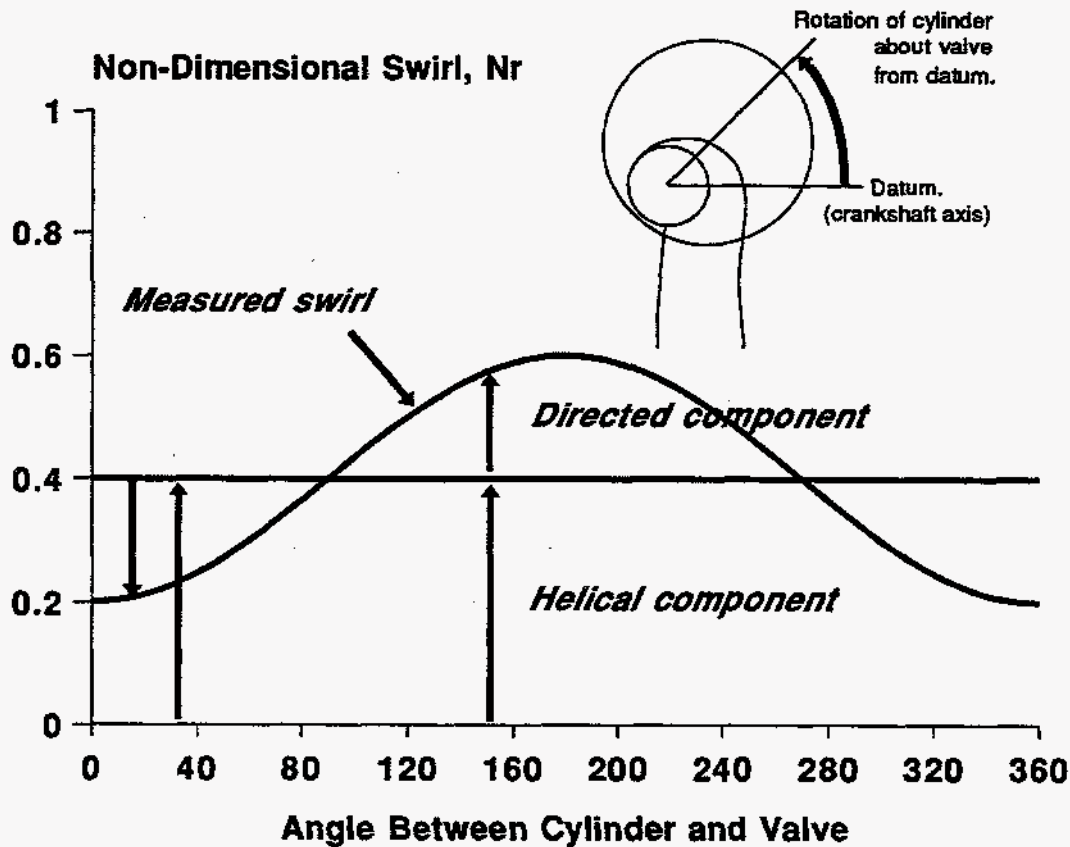


Figure B-10. Description of rotational test result

Effect of Manifold on Flow and Swirl

Tests are also conducted with and without the intake manifold to assess the contribution of the manifold to the overall calculated mean pressure loss, and to assess its effect on cylinder-to-cylinder air distribution.

Cylinder-to-Cylinder Variability Tests

In addition to the variability of the air quantity supplied to each cylinder due to the manifolding the individual cylinders or heads are tested to quantify the amount of swirl, tumble, and flow variation from cylinder-to-cylinder due to casting and/or machining defects. Flow bench results quantify the effect of any core shifts or machining errors and molds of the ports help visualize the direction and extent of any anomaly. SwRI has port design techniques that make the performance of the port insensitive to any of these defects.

Tumble Testing

As shown in Figure B-8, tumble motion is defined as rotation about an axis perpendicular to the cylinder centerline. Tumble is also thought of as an end-over-end cascading motion or a that of a vortex. Tumble motion has been shown to break down into small scale turbulence near TDC helping flame propagation rates in SI engines.

The SwRI approach to measuring tumble on the flow bench is illustrated in Figure B-11. The SwRI convention for measuring tumble is shown in Figure B-12.

Combined Swirl Ratio

Rarely is in-cylinder air motion just comprised of swirl or just tumble through the entire intake and compression strokes. The effect of squish motion, which plays an important role near TDC, has not been considered either. However, in an attempt to better predict total in-cylinder swirl SwRI vectorially summarizes the individual angular momentums of the swirl and tumble orthogonal components and calls this Combined Swirl. Figure B-13 illustrates the concept of combined swirl. The combined swirl ratio has resulted in better engine/flow bench correlations than traditional swirl alone.

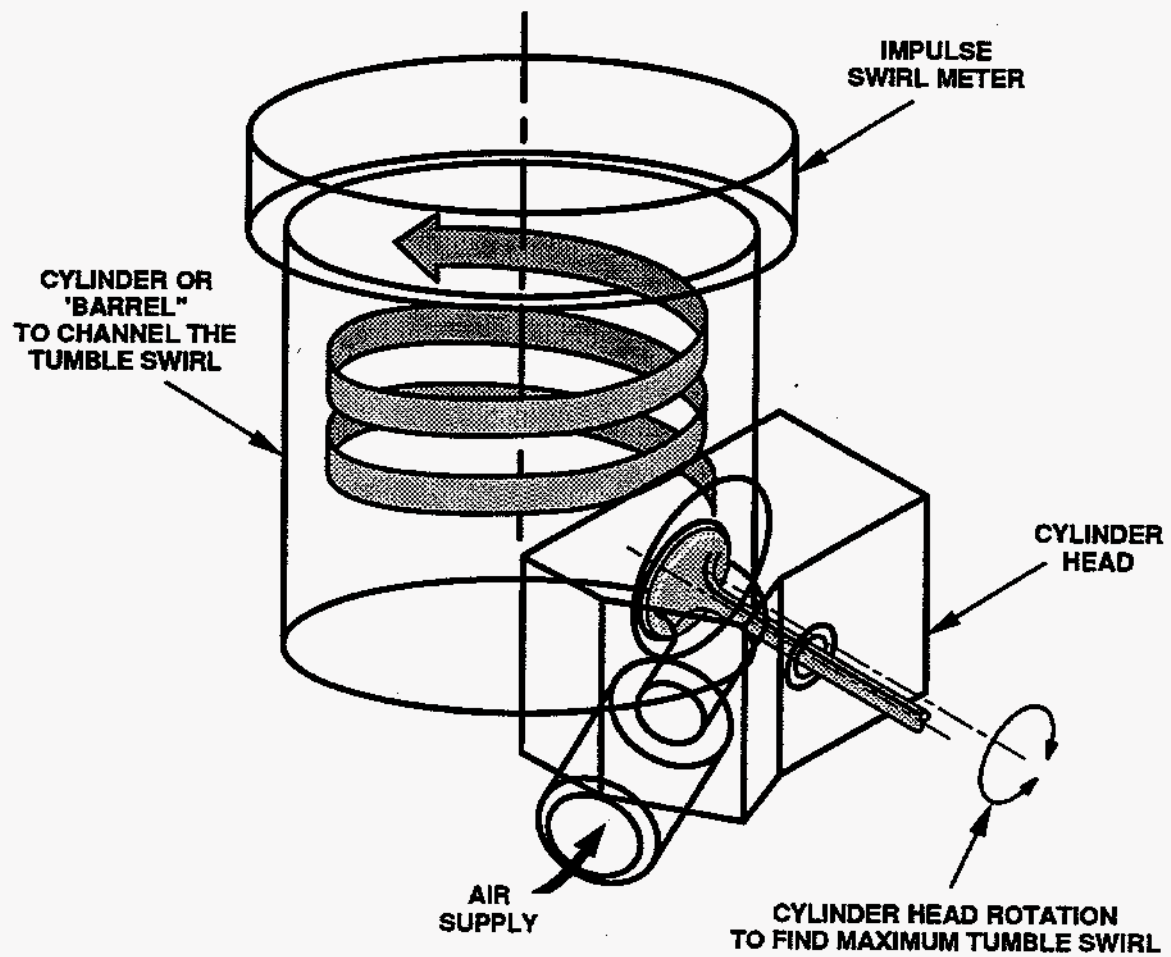


Figure B-11. Measurement of Tumble

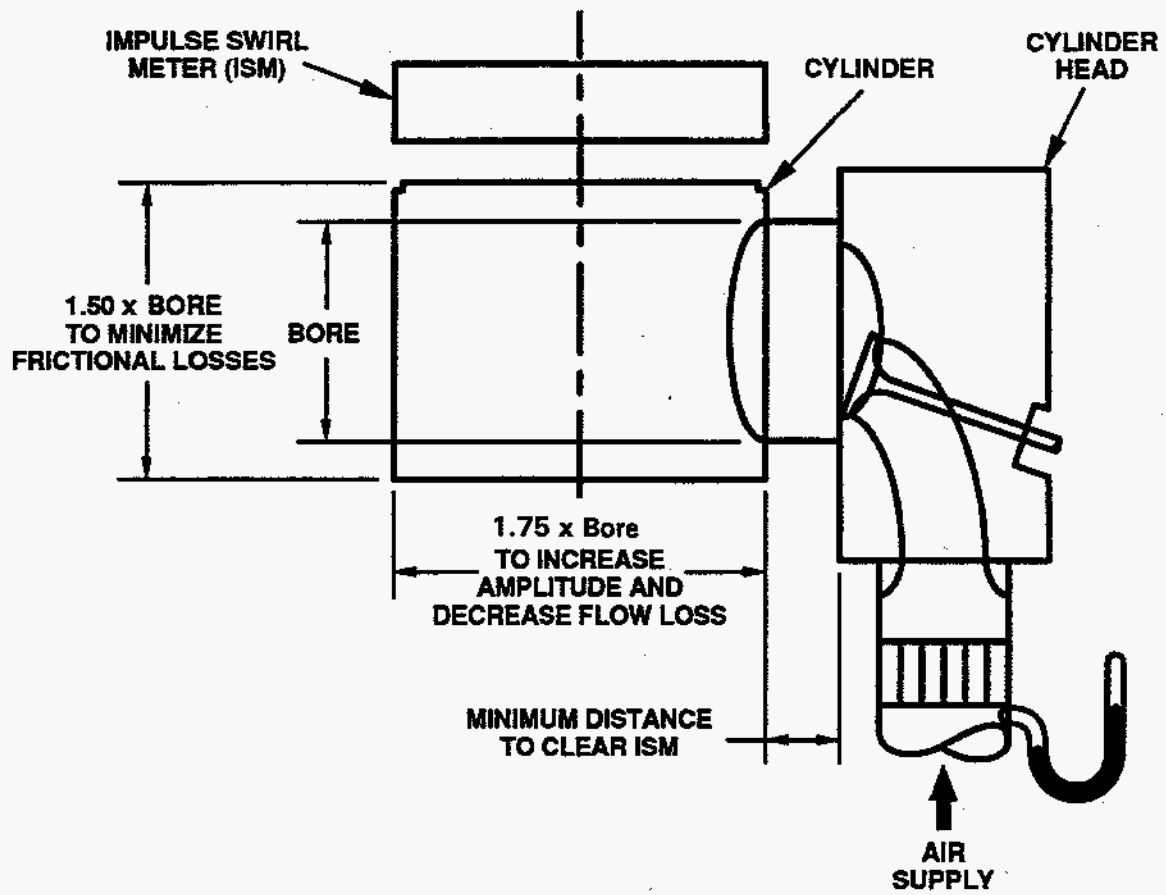


Figure B-12. Tumble Convention

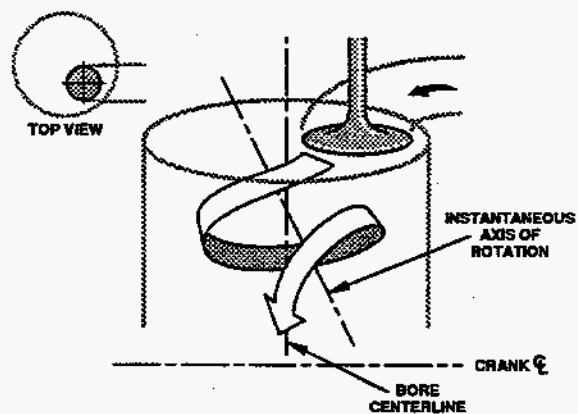


Figure B-13. Concept of Combined Swirl

ANALYSIS OF SWRI FLOW BENCH RESULTS

Test Number 1 Date: 16 FEB 92

VCR Head: SwRI Project 03-4764-280. Standard Test.

Bore	96.52 (mm)	Inner Valve Seat	41.58 (mm)	Valve Opens	-30.00 deg	Compression Ratio	16.00:1
Stroke	95.25 (mm)	Maximum Valve Lift	8.38 (mm)	Valve Closes	230.00 deg	Engine Speed with	
Connecting Rod	166.62 (mm)	Number Of Valves	1	Engine Speed	900. rpm	11.2 m/sec Mean	
						Piston Speed	3527 rpm

SwRI Method = Simulating Gas Exchange Based on Mass and Energy Conservation
 Ricardo Method = Flow Dependent Upon Valve Lift
 AVL Method = Flow Equals Rate of Piston Displacement

	SwRI		Ricardo		AVL	
RPM	900	3527	900	3527	900	3527
Swirl Ratio	-.228	-.249	-.208	-.208	-.226	-.226
Mean Flow Coefficient			.199	.199	.214	.214
Gulp Factor	.182	.621	.226	.885	.209	.820
Mean Pressure Loss (kPa)	2.48	29.56	1.71	26.28	3.06	47.07
Port Effectiveness (%)			25.49	25.49	23.13	23.13
Volumetric Efficiency (%)	1.028	.866				
Maximum Mach Number	.621	.865				

Max Flow Coeff = .411

Valve Lift (mm)	Valve Lift Seat Diameter	Differential Pressure (mm water)	Volume Flow (m**3/s)	Mass Flow (kg/s)	Flow Coeff (Cf)	Torque (N.mm)	N-D Swirl (Nr)	Coeff of Performance (Cp)	Theta (deg)	Momentum Ratio (Vr)	AVL Swirl Number (nd/n)
1.00	.024	508.00	.0040	.0049	.032	.10	.019	.334	1.9	.997	.984
2.00	.048	508.00	.0129	.0157	.104	.90	.052	.542	3.2	.854	.843
3.00	.072	508.00	.0202	.0245	.162	.40	.015	.562	.9	.156	.154
4.00	.096	508.00	.0273	.0330	.219	-.60	-.016	.569	-1.0	-.128	-.127
5.00	.120	508.00	.0337	.0406	.269	-1.60	-.035	.560	-2.1	-.226	-.223
6.00	.144	508.00	.0397	.0479	.317	-2.10	-.039	.550	-2.4	-.213	-.210
7.00	.168	508.00	.0456	.0550	.364	-2.80	-.046	.540	-2.8	-.216	-.213
8.00	.192	508.00	.0501	.0603	.399	-3.60	-.053	.519	-3.4	-.230	-.227
9.00	.216	508.00	.0540	.0650	.429	-2.80	-.039	.496	-2.6	-.154	-.152
10.00	.241	508.00	.0569	.0684	.452	-1.80	-.024	.470	-1.7	-.089	-.088

ANALYSIS OF SWRI FLOW BENCH RESULTS

Test Number 2 Date: 16 FEB 92

VCR Head: SwRI Project 03-4764-280. Standard Test.

Bore	96.52 (mm)	Inner Valve Seat	41.58 (mm)	Valve Opens	-30.00 deg	Compression Ratio	16.00:1
Stroke	95.25 (mm)	Maximum Valve Lift	8.38 (mm)	Valve Closes	230.00 deg	Engine Speed with	
Connecting Rod	166.62 (mm)	Number Of Valves	1	Engine Speed	1800. rpm	11.2 m/sec Mean	
						Piston Speed	3527 rpm

SwRI Method = Simulating Gas Exchange Based on Mass and Energy Conservation
 Ricardo Method = Flow Dependent Upon Valve Lift
 AVL Method = Flow Equals Rate of Piston Displacement

	SwRI		Ricardo		AVL	
RPM	1800	3527	1800	3527	1800	3527
Swirl Ratio	-.244	-.249	-.208	-.208	-.226	-.226
Mean Flow Coefficient			.199	.199	.214	.214
Gulp Factor	.348	.621	.452	.885	.419	.820
Mean Pressure Loss (kPa)	9.41	29.56	6.84	26.28	12.26	47.07
Port Effectiveness (%)			25.49	25.49	23.13	23.13
Volumetric Efficiency (%)	.989	.866				
Maximum Mach Number	.591	.865				

Max Flow Coeff = .411

Valve Lift (mm)	Valve Lift Seat Diameter	Differential Pressure (mm water)	Volume Flow (m**3/s)	Mass Flow (kg/s)	Flow Coeff (Cf)	Torque (N.mm)	N-D Swirl (Nr)	Coeff of Performance (Cp)	Theta (deg)	Momentum Ratio (Vr)	AVL Swirl Number (nd/n)
1.00	.024	508.00	.0040	.0049	.032	.10	.019	.334	1.9	.997	.984
2.00	.048	508.00	.0129	.0157	.104	.90	.052	.542	3.2	.854	.843
3.00	.072	508.00	.0202	.0245	.162	.40	.015	.562	.9	.156	.154
4.00	.096	508.00	.0273	.0330	.219	-.60	-.016	.569	-1.0	-.128	-.127
5.00	.120	508.00	.0337	.0406	.269	-1.60	-.035	.560	-2.1	-.226	-.223
6.00	.144	508.00	.0397	.0479	.317	-2.10	-.039	.550	-2.4	-.213	-.210
7.00	.168	508.00	.0456	.0550	.364	-2.80	-.046	.540	-2.8	-.216	-.213
8.00	.192	508.00	.0501	.0603	.399	-3.60	-.053	.519	-3.4	-.230	-.227
9.00	.216	508.00	.0540	.0650	.429	-2.80	-.039	.496	-2.6	-.154	-.152
10.00	.241	508.00	.0569	.0684	.452	-1.80	-.024	.470	-1.7	-.089	-.088

ANALYSIS OF SwRI FLOW BENCH RESULTS

Test Number 3 Date: 16 FEB 92

VCR Head: SwRI Project 03-4764-280. Standard Test.

Bore	96.52 (mm)	Inner Valve Seat	41.58 (mm)	Valve Opens	-30.00 deg	Compression Ratio	22.00:1
Stroke	95.25 (mm)	Maximum Valve Lift	8.38 (mm)	Valve Closes	230.00 deg	Engine Speed with	11.2 m/sec Mean
Connecting Rod	166.62 (mm)	Number Of Valves	1	Engine Speed	900. rpm	Piston Speed	3527 rpm

SwRI Method - Simulating Gas Exchange Based on Mass and Energy Conservation
 Ricardo Method - Flow Dependent Upon Valve Lift
 AVL Method - Flow Equals Rate of Piston Displacement

	SwRI		Ricardo		AVL	
RPM	900	3527	900	3527	900	3527
Swirl Ratio	-.228	-.248	-.208	-.208	-.226	-.226
Mean Flow Coefficient			.199	.199	.214	.214
Gulp Factor	.183	.631	.226	.885	.209	.820
Mean Pressure Loss (kPa)	2.49	30.14	1.71	26.28	3.06	47.07
Port Effectiveness (%)			25.49	25.49	23.13	23.13
Volumetric Efficiency (%)	1.029	.867				
Maximum Mach Number	.627	.884				

Max Flow Coeff = .411

Valve Lift (mm)	Valve Lift Seat Diameter	Differential Pressure (mm water)	Volume Flow (m**3/s)	Mass Flow (kg/s)	Flow Coeff (Cf)	Torque (N.mm)	N-D Swirl Performance (Nr)	Coeff of Performance (Cp)	Theta (deg)	Momentum Ratio (Vr)	AVL Swirl Number (nd/n)
1.00	.024	508.00	.0040	.0049	.032	.10	.019	.334	1.9	.997	.984
2.00	.048	508.00	.0129	.0157	.104	.90	.052	.542	3.2	.854	.843
3.00	.072	508.00	.0202	.0245	.162	.40	.015	.562	.9	.156	.154
4.00	.096	508.00	.0273	.0330	.219	-.60	-.016	.569	-1.0	-.128	-.127
5.00	.120	508.00	.0337	.0406	.269	-1.60	-.035	.560	-2.1	-.226	-.223
6.00	.144	508.00	.0397	.0479	.317	-2.10	-.039	.550	-2.4	-.213	-.210
7.00	.168	508.00	.0456	.0550	.364	-2.80	-.046	.540	-2.8	-.216	-.213
8.00	.192	508.00	.0501	.0603	.399	-3.60	-.053	.519	-3.4	-.230	-.227
9.00	.216	508.00	.0540	.0650	.429	-2.80	-.039	.496	-2.6	-.154	-.152
10.00	.241	508.00	.0569	.0684	.452	-1.80	-.024	.470	-1.7	-.089	-.088

ANALYSIS OF SwRI FLOW BENCH RESULTS

Test Number 4 Date: 16 FEB 92

VCR Head: SwRI Project 03-4764-280. Standard Test.

Bore	96.52 (mm)	Inner Valve Seat	41.58 (mm)	Valve Opens	-30.00 deg	Compression Ratio	22.00:1
Stroke	95.25 (mm)	Maximum Valve Lift	8.38 (mm)	Valve Closes	230.00 deg	Engine Speed with	11.2 m/sec Mean
Connecting Rod	166.62 (mm)	Number Of Valves	1	Engine Speed	1800. rpm	Piston Speed	3527 rpm

SwRI Method - Simulating Gas Exchange Based on Mass and Energy Conservation
 Ricardo Method - Flow Dependent Upon Valve Lift
 AVL Method - Flow Equals Rate of Piston Displacement

	SwRI		Ricardo		AVL	
RPM	1800	3527	1800	3527	1800	3527
Swirl Ratio	-.241	-.248	-.208	-.208	-.226	-.226
Mean Flow Coefficient			.199	.199	.214	.214
Gulp Factor	.354	.631	.452	.885	.419	.820
Mean Pressure Loss (kPa)	9.48	30.14	6.84	26.28	12.26	47.07
Port Effectiveness (%)			25.49	25.49	23.13	23.13
Volumetric Efficiency (%)	.989	.867				
Maximum Mach Number	.596	.884				

Max Flow Coeff = .411

Valve Lift (mm)	Valve Lift Seat Diameter	Differential Pressure (mm water)	Volume Flow (m**3/s)	Mass Flow (kg/s)	Flow Coeff (Cf)	Torque (N.mm)	N-D Swirl Performance (Nr)	Coeff of Performance (Cp)	Theta (deg)	Momentum Ratio (Vr)	AVL Swirl Number (nd/n)
1.00	.024	508.00	.0040	.0049	.032	.10	.019	.334	1.9	.997	.984
2.00	.048	508.00	.0129	.0157	.104	.90	.052	.542	3.2	.854	.843
3.00	.072	508.00	.0202	.0245	.162	.40	.015	.562	.9	.156	.154
4.00	.096	508.00	.0273	.0330	.219	-.60	-.016	.569	-1.0	-.128	-.127
5.00	.120	508.00	.0337	.0406	.269	-1.60	-.035	.560	-2.1	-.226	-.223
6.00	.144	508.00	.0397	.0479	.317	-2.10	-.039	.550	-2.4	-.213	-.210
7.00	.168	508.00	.0456	.0550	.364	-2.80	-.046	.540	-2.8	-.216	-.213
8.00	.192	508.00	.0501	.0603	.399	-3.60	-.053	.519	-3.4	-.230	-.227
9.00	.216	508.00	.0540	.0650	.429	-2.80	-.039	.496	-2.6	-.154	-.152
10.00	.241	508.00	.0569	.0684	.452	-1.80	-.024	.470	-1.7	-.089	-.088

ANALYSIS OF SWRI FLOW BENCH RESULTS

Test Number 5 Date: 16 FEB 92

VCR Head: SWRI Project 03-4764-280. Standard Test.

Bore	96.52(mm)	Inner Valve Seat	41.58(mm)	Valve Opens	-30.00 deg	Compression Ratio	16.00:1
Stroke	95.25(mm)	Maximum Valve Lift	8.38(mm)	Valve Closes	230.00 deg	Engine Speed with	11.2 m/sec Mean
Connecting Rod	166.62(mm)	Number Of Valves	1	Engine Speed	900. rpm	Piston Speed	3527 rpm

SWRI Method = Simulating Gas Exchange Based on Mass and Energy Conservation
 Ricardo Method = Flow Dependent Upon Valve Lift
 AVL Method = Flow Equals Rate of Piston Displacement

RPM	SWRI		Ricardo		AVL	
	900	3527	900	3527	900	3527
Swirl Ratio	-.255	-.272	-.267	-.267	-.250	-.250
Mean Flow Coefficient			.193	.193	.031	.031
Gulp Factor	.188	.624	.233	.913	1.438	5.637
Mean Pressure Loss (kPa)	2.58	29.88	1.82	27.92	144.74	*****
Port Effectiveness (%)			23.99	23.99	.49	.49
Volumetric Efficiency (%)	1.056	.865				
Maximum Mach Number	.662	.873				

Max Flow Coeff = .410

Valve Lift (mm)	Valve Lift Seat Diameter	Differential Pressure (mm water)	Volume Flow (m ³ /s)	Mass Flow (kg/s)	Flow Coeff (Cf)	Torque (N.mm)	N-D Swirl (Nr)	Coeff of Performance (Cp)	Theta (deg)	Momentum Ratio (Vr)	AVL Swirl Number (nd/n)
1.00	.024	508.00	.0028	.0034	.023	-10	.026	.237	3.7	1.994	1.968
2.00	.048	508.00	.0127	.0153	.102	-50	.030	.528	1.9	.498	.492
3.00	.072	508.00	.0200	.0242	.161	-20	.007	.556	.4	.080	.079
4.00	.096	508.00	.0272	.0328	.218	-80	-.022	.566	-1.3	-.173	-.171
5.00	.120	508.00	.0337	.0406	.269	-1.80	-.040	.560	-2.4	-.254	-.251
6.00	.144	508.00	.0399	.0480	.318	-2.50	-.047	.551	-2.8	-.252	-.249
7.00	.168	508.00	.0454	.0546	.361	-3.00	-.049	.537	-3.0	-.234	-.231
8.00	.192	508.00	.0501	.0602	.398	-3.60	-.054	.518	-3.4	-.231	-.228
9.00	.216	508.00	.0539	.0648	.428	-2.80	-.039	.495	-2.6	-.155	-.153
10.00	.241	508.00	.0569	.0684	.452	-1.70	-.022	.470	-1.6	-.084	-.083

ANALYSIS OF SWRI FLOW BENCH RESULTS

Test Number 6 Date: 19 MAR 92

VCR Head: Mod 1 - Clayed Intake Port.

Bore	96.52(mm)	Inner Valve Seat	41.58(mm)	Valve Opens	-30.00 deg	Compression Ratio	16.00:1
Stroke	95.25(mm)	Maximum Valve Lift	8.38(mm)	Valve Closes	230.00 deg	Engine Speed with	11.2 m/sec Mean
Connecting Rod	166.62(mm)	Number Of Valves	1	Engine Speed	900. rpm	Piston Speed	3527 rpm

SWRI Method = Simulating Gas Exchange Based on Mass and Energy Conservation
 Ricardo Method = Flow Dependent Upon Valve Lift
 AVL Method = Flow Equals Rate of Piston Displacement

RPM	SWRI		Ricardo		AVL	
	900	3527	900	3527	900	3527
Swirl Ratio	-.248	-.199	-.193	-.193	-.259	-.259
Mean Flow Coefficient			.195	.195	.235	.235
Gulp Factor	.180	.632	.230	.900	.191	.749
Mean Pressure Loss (kPa)	2.53	30.37	1.77	27.16	2.55	39.22
Port Effectiveness (%)			24.66	24.66	27.76	27.76
Volumetric Efficiency (%)	1.012	.854				
Maximum Mach Number	.595	.846				

Max Flow Coeff = .383

Valve Lift (mm)	Valve Lift Seat Diameter	Differential Pressure (mm water)	Volume Flow (m ³ /s)	Mass Flow (kg/s)	Flow Coeff (Cf)	Torque (N.mm)	N-D Swirl (Nr)	Coeff of Performance (Cp)	Theta (deg)	Momentum Ratio (Vr)	AVL Swirl Number (nd/n)
1.00	.024	508.00	.0056	.0069	.045	-94	-.125	.478	-8.7	-4.705	-4.643
2.00	.048	508.00	.0147	.0178	.118	-1.82	-.092	.616	-5.0	-1.342	-1.325
3.00	.072	508.00	.0218	.0262	.174	-2.50	-.086	.606	-4.7	-.844	-.832
4.00	.096	508.00	.0280	.0336	.223	-4.15	-.111	.584	-6.3	-.852	-.841
5.00	.120	508.00	.0337	.0403	.268	-5.22	-.116	.562	-6.9	-.742	-.732
6.00	.144	508.00	.0386	.0462	.307	-3.86	-.075	.534	-4.7	-.417	-.412
7.00	.168	508.00	.0430	.0515	.342	-.65	-.011	.508	-.7	-.057	-.056
8.00	.192	508.00	.0469	.0560	.372	.86	.014	.483	.9	.063	.062
9.00	.216	508.00	.0503	.0601	.399	1.05	.016	.461	1.1	.067	.066
10.00	.241	508.00	.0529	.0632	.419	1.54	.022	.436	1.7	.089	.088

ANALYSIS OF SwRI FLOW BENCH RESULTS
Test Number 7 Date: 19 MAR 92

VCR Head: Mod 2 - 180 deg Masking (Clayed IP)

Bore	96.52(mm)	Inner Valve Seat	41.58(mm)	Valve Opens	-30.00 deg	Compression Ratio	16.00:1
Stroke	95.25(mm)	Maximum Valve Lift	8.38(mm)	Valve Closes	230.00 deg	Engine Speed with	11.2 m/sec Mean
Connecting Rod	166.62(mm)	Number Of Valves	1	Engine Speed	900. rpm	Piston Speed	3527 rpm

SwRI Method = Simulating Gas Exchange Based on Mass and Energy Conservation
Ricardo Method = Flow Dependent Upon Valve Lift
AVL Method = Flow Equals Rate of Piston Displacement

	SwRI		Ricardo		AVL	
RPM	900	3527	900	3527	900	3527
Swirl Ratio	.639	.634	.583	.583	.626	.626
Mean Flow Coefficient			.194	.194	.232	.232
Gulp Factor	.181	.639	.231	.905	.193	.757
Mean Pressure Loss (kPa)	2.59	30.91	1.79	27.44	2.61	40.09
Port Effectiveness (%)			24.41	24.41	27.18	27.18
Volumetric Efficiency (%)	1.002	.847				
Maximum Mach Number	.579	.849				

Max Flow Coeff = .370

Valve Lift (mm)	Valve Lift (mm)	Differential Pressure (mm water)	Volume Flow (m ³ /s)	Mass Flow (kg/s)	Flow Coeff (Cf)	Torque (N.mm)	N-D Swirl (Nr)	Coeff of Performance (Cp)	Theta (deg)	Momentum Ratio (Vr)	AVL Swirl Number (nd/n)
1.00	.024	508.00	.0063	.0077	.051	-85	-.100	.531	-6.3	-3.377	-3.332
2.00	.048	508.00	.0150	.0181	.120	-46	-.023	.625	-1.2	-.326	-.322
3.00	.072	508.00	.0216	.0260	.173	-56	-.019	.599	-1.1	-.191	-.188
4.00	.096	508.00	.0277	.0332	.221	-17	-.005	.575	-3	-.035	-.035
5.00	.120	508.00	.0335	.0400	.266	1.93	.043	.554	2.6	.278	.275
6.00	.144	508.00	.0383	.0456	.304	5.24	.103	.530	6.5	.579	.571
7.00	.168	508.00	.0425	.0505	.337	8.06	.142	.507	9.4	.726	.716
8.00	.192	508.00	.0458	.0543	.362	7.67	.126	.476	8.8	.596	.588
9.00	.216	508.00	.0484	.0574	.383	11.38	.176	.454	13.0	.790	.780
10.00	.241	508.00	.0507	.0602	.401	14.30	.211	.434	16.4	.904	.892

ANALYSIS OF SwRI FLOW BENCH RESULTS
Test Number 8 Date: 19 MAR 92

VCR Head: Mod 3 - 230 deg Masking (Clayed IP)

Bore	96.52(mm)	Inner Valve Seat	41.58(mm)	Valve Opens	-30.00 deg	Compression Ratio	16.00:1
Stroke	95.25(mm)	Maximum Valve Lift	8.38(mm)	Valve Closes	230.00 deg	Engine Speed with	11.2 m/sec Mean
Connecting Rod	166.62(mm)	Number Of Valves	1	Engine Speed	900. rpm	Piston Speed	3527 rpm

SwRI Method = Simulating Gas Exchange Based on Mass and Energy Conservation
Ricardo Method = Flow Dependent Upon Valve Lift
AVL Method = Flow Equals Rate of Piston Displacement

	SwRI		Ricardo		AVL	
RPM	900	3527	900	3527	900	3527
Swirl Ratio	.012	.034	.039	.039	-.004	-.004
Mean Flow Coefficient			.182	.182	.218	.218
Gulp Factor	.194	.669	.247	.968	.206	.806
Mean Pressure Loss (kPa)	2.92	33.27	2.05	31.45	2.96	45.46
Port Effectiveness (%)			21.30	21.30	23.95	23.95
Volumetric Efficiency (%)	1.009	.818				
Maximum Mach Number	.593	.872				

Max Flow Coeff = .338

Valve Lift (mm)	Valve Lift (mm)	Differential Pressure (mm water)	Volume Flow (m ³ /s)	Mass Flow (kg/s)	Flow Coeff (Cf)	Torque (N.mm)	N-D Swirl (Nr)	Coeff of Performance (Cp)	Theta (deg)	Momentum Ratio (Vr)	AVL Swirl Number (nd/n)
1.00	.024	508.00	.0049	.0060	.039	-85	-.129	.416	-10.4	-5.628	-5.554
2.00	.048	508.00	.0136	.0164	.109	-1.43	-.079	.568	-4.6	-1.239	-1.223
3.00	.072	508.00	.0212	.0256	.170	-2.50	-.088	.591	-5.0	-.889	-.877
4.00	.096	508.00	.0273	.0327	.218	-2.30	-.063	.567	-3.7	-.499	-.492
5.00	.120	508.00	.0321	.0384	.256	-1.72	-.040	.532	-2.5	-.270	-.266
6.00	.144	508.00	.0365	.0436	.290	-.56	-.011	.503	-.8	-.067	-.066
7.00	.168	508.00	.0401	.0477	.318	.56	.011	.472	.7	.057	.056
8.00	.192	508.00	.0427	.0507	.338	2.51	.044	.440	3.3	.224	.221
9.00	.216	508.00	.0431	.0512	.341	7.28	.127	.401	10.6	.638	.630
10.00	.241	508.00	.0448	.0531	.354	8.94	.150	.378	13.3	.725	.716

ANALYSIS OF SWRI FLOW BENCH RESULTS
Test Number 9 Date: 19 MAR 92

VCR Head: Mod 4 - Helical Port Attempt 1 (Clayed IP)

Bore	96.52 (mm)	Inner Valve Seat	41.58 (mm)	Valve Opens	-30.00 deg	Compression Ratio	16.00:1
Stroke	95.25 (mm)	Maximum Valve Lift	8.38 (mm)	Valve Closes	230.00 deg	Engine Speed with	11.2 m/sec Mean
Connecting Rod	166.62 (mm)	Number Of Valves	1	Engine Speed	900. rpm	Piston Speed	3527 rpm

SWRI Method = Simulating Gas Exchange Based on Mass and Energy Conservation
Ricardo Method = Flow Dependent Upon Valve Lift
AVL Method = Flow Equals Rate of Piston Displacement

	SwRI		Ricardo		AVL	
RPM	900	3527	900	3527	900	3527
Swirl Ratio	.513	.460	.426	.426	.510	.510
Mean Flow Coefficient			.173	.173	.206	.206
Gulp Factor	.201	.698	.259	1.016	.217	.852
Mean Pressure Loss (kPa)	3.27	35.55	2.25	34.61	3.30	50.77
Port Effectiveness (%)			19.35	19.35	21.45	21.45
Volumetric Efficiency (%)	.996	.787				
Maximum Mach Number	.571	.899				

Max Flow Coeff = .304

Valve Lift (mm)	Valve Lift Seat Diameter	Differential Pressure (mm water)	Volume Flow (m ³ /s)	Mass Flow (kg/s)	Flow Coeff (Cf)	Torque (N.mm)	N-D Swirl (Nr)	Coeff of Performance (Cp)	Theta (deg)	Momentum Ratio (Vr)	AVL Swirl Number (nd/n)
1.00	.024	508.00	.0062	.0078	.051	.08	.009	.528	.6	.311	.307
2.00	.048	508.00	.0145	.0180	.118	.39	.020	.614	1.1	.287	.283
3.00	.072	508.00	.0211	.0262	.171	1.05	.037	.594	2.1	.368	.363
4.00	.096	508.00	.0267	.0330	.216	1.44	.040	.563	2.4	.315	.311
5.00	.120	508.00	.0306	.0377	.247	2.61	.063	.516	4.1	.437	.431
6.00	.144	508.00	.0341	.0421	.276	3.00	.065	.479	4.5	.403	.398
7.00	.168	508.00	.0359	.0443	.290	3.00	.062	.433	4.7	.364	.359
8.00	.192	508.00	.0376	.0462	.303	3.97	.078	.397	6.6	.442	.436
9.00	.216	508.00	.0379	.0466	.306	5.82	.113	.359	10.6	.637	.628
10.00	.241	508.00	.0381	.0469	.307	6.51	.126	.328	12.9	.703	.694

ANALYSIS OF SWRI FLOW BENCH RESULTS
Test Number 10 Date: 19 MAR 92

VCR Head: Mod 5 - Helical Port Attempt 2 (Clayed IP).

SWRI Project 03-4764-280. Labeco Variable Compression Ratio Engine.

Bore	96.52 (mm)	Inner Valve Seat	41.58 (mm)	Valve Opens	-30.00 deg	Compression Ratio	16.00:1
Stroke	95.25 (mm)	Maximum Valve Lift	8.38 (mm)	Valve Closes	230.00 deg	Engine Speed with	11.2 m/sec Mean
Connecting Rod	166.62 (mm)	Number Of Valves	1	Engine Speed	900. rpm	Piston Speed	3527 rpm

SWRI Method = Simulating Gas Exchange Based on Mass and Energy Conservation
Ricardo Method = Flow Dependent Upon Valve Lift
AVL Method = Flow Equals Rate of Piston Displacement

	SwRI		Ricardo		AVL	
RPM	900	3527	900	3527	900	3527
Swirl Ratio	.410	.357	.353	.353	.407	.407
Mean Flow Coefficient			.159	.159	.190	.190
Gulp Factor	.217	.747	.282	1.104	.236	.924
Mean Pressure Loss (kPa)	3.84	38.74	2.66	40.91	3.89	59.79
Port Effectiveness (%)			16.37	16.37	18.21	18.21
Volumetric Efficiency (%)	.998	.741				
Maximum Mach Number	.578	.949				

Max Flow Coeff = .274

Valve Lift (mm)	Valve Lift Seat Diameter	Differential Pressure (mm water)	Volume Flow (m ³ /s)	Mass Flow (kg/s)	Flow Coeff (Cf)	Torque (N.mm)	N-D Swirl (Nr)	Coeff of Performance (Cp)	Theta (deg)	Momentum Ratio (Vr)	AVL Swirl Number (nd/n)
1.00	.024	508.00	.0063	.0077	.051	-.26	-.031	.528	-2.0	-1.053	-1.039
2.00	.048	508.00	.0146	.0180	.118	.20	.010	.613	.5	.147	.145
3.00	.072	508.00	.0206	.0254	.167	.86	.031	.578	1.8	.316	.312
4.00	.096	508.00	.0253	.0311	.204	1.05	.031	.531	1.9	.259	.255
5.00	.120	508.00	.0288	.0353	.232	1.73	.045	.484	3.1	.329	.324
6.00	.144	508.00	.0317	.0388	.256	2.32	.054	.444	4.1	.363	.359
7.00	.168	508.00	.0333	.0408	.268	2.03	.045	.399	3.8	.288	.284
8.00	.192	508.00	.0337	.0412	.271	2.61	.057	.354	5.4	.363	.358
9.00	.216	508.00	.0345	.0421	.278	2.51	.054	.322	5.6	.333	.329
10.00	.241	508.00	.0350	.0427	.281	2.42	.051	.294	5.8	.312	.308

ANALYSIS OF SwRI FLOW BENCH RESULTS
Test Number 11 Date: 23 MAR 92

VCR Head: Mod 6 - Helical attempt 3:sharp wall edges, more ramp.

SwRI Project 03-4764-280. Labeco Variable Compression Ratio Engine

Bore	96.52(mm)	Inner Valve Seat	41.58(mm)	Valve Opens	-30.00 deg	Compression Ratio	16.00:1
Stroke	95.25(mm)	Maximum Valve Lift	8.38(mm)	Valve Closes	230.00 deg	Engine Speed with	11.2 m/sec Mean
Connecting Rod	166.62(mm)	Number Of Valves	1	Engine Speed	900. rpm	Piston Speed	3527 rpm

SwRI Method = Simulating Gas Exchange Based on Mass and Energy Conservation
Ricardo Method = Flow Dependent Upon Valve Lift
AVL Method = Flow Equals Rate of Piston Displacement

	SwRI		Ricardo		AVL	
RPM	900	3527	900	3527	900	3527
Swirl Ratio	1.596	1.208	1.280	1.280	1.606	1.606
Mean Flow Coefficient			.129	.129	.152	.152
Gulp Factor	.266	.864	.348	1.363	.294	1.154
Mean Pressure Loss (kPa)	5.91	46.66	4.06	62.31	6.06	93.13
Port Effectiveness (%)			10.75	10.75	11.72	11.72
Volumetric Efficiency (%)	.997	.618				
Maximum Mach Number	.585	1.000				

Max Flow Coeff = .209

Valve Lift (mm)	Valve Lift Seat Diameter	Differential Pressure (mm water)	Volume Flow (m**3/s)	Mass Flow (kg/s)	Flow Coeff (Cf)	Torque (N.mm)	N-D Swirl Performance (Nr)	Coeff of Performance (Cp)	Theta (deg)	Momentum Ratio (Vr)	AVL Swirl Number (nd/n)
1.00	.024	508.00	.0063	.0077	.051	.76	.090	.531	5.6	3.031	2.991
2.00	.048	508.00	.0143	.0176	.116	1.34	.070	.603	3.8	1.031	1.017
3.00	.072	508.00	.0192	.0237	.156	2.80	.108	.543	6.6	1.189	1.174
4.00	.096	508.00	.0223	.0274	.180	4.07	.135	.475	9.5	1.288	1.271
5.00	.120	508.00	.0247	.0302	.199	5.14	.154	.424	12.2	1.330	1.313
6.00	.144	508.00	.0253	.0310	.204	5.34	.156	.365	14.4	1.312	1.295
7.00	.168	508.00	.0257	.0314	.207	5.34	.154	.320	16.3	1.281	1.264
8.00	.192	508.00	.0258	.0315	.208	5.43	.156	.285	18.5	1.289	1.272
9.00	.216	508.00	.0261	.0319	.210	5.53	.157	.260	20.6	1.281	1.264
10.00	.241	508.00	.0261	.0319	.210	5.53	.157	.237	22.6	1.281	1.264

ANALYSIS OF SwRI FLOW BENCH RESULTS
Test Number 12 Date: 23 MAR 92

Mod 7 - Helical attempt 4:filled in around valve stem, higher & steeper.

SwRI Project 03-4764-280. Labeco Variable Compression Ratio Engine.

Bore	96.52(mm)	Inner Valve Seat	41.58(mm)	Valve Opens	-30.00 deg	Compression Ratio	16.00:1
Stroke	95.25(mm)	Maximum Valve Lift	8.38(mm)	Valve Closes	230.00 deg	Engine Speed with	11.2 m/sec Mean
Connecting Rod	166.62(mm)	Number Of Valves	1	Engine Speed	900. rpm	Piston Speed	3527 rpm

SwRI Method = Simulating Gas Exchange Based on Mass and Energy Conservation
Ricardo Method = Flow Dependent Upon Valve Lift
AVL Method = Flow Equals Rate of Piston Displacement

	SwRI		Ricardo		AVL	
RPM	900	3527	900	3527	900	3527
Swirl Ratio	1.587	1.154	1.264	1.264	1.693	1.693
Mean Flow Coefficient			.123	.123	.141	.141
Gulp Factor	.287	.889	.363	1.425	.318	1.246
Mean Pressure Loss (kPa)	6.85	49.38	4.43	68.06	7.07	108.60
Port Effectiveness (%)			9.84	9.84	10.05	10.05
Volumetric Efficiency (%)	.974	.563				
Maximum Mach Number	.551	1.000				

Max Flow Coeff = .192

Valve Lift (mm)	Valve Lift Seat Diameter	Differential Pressure (mm water)	Volume Flow (m**3/s)	Mass Flow (kg/s)	Flow Coeff (Cf)	Torque (N.mm)	N-D Swirl Performance (Nr)	Coeff of Performance (Cp)	Theta (deg)	Momentum Ratio (Vr)	AVL Swirl Number (nd/n)
1.00	.024	508.00	.0063	.0077	.051	.08	.009	.528	.6	.311	.307
2.00	.048	508.00	.0132	.0161	.107	.66	.037	.554	2.2	.600	.592
3.00	.072	508.00	.0185	.0225	.149	2.03	.082	.518	5.2	.939	.926
4.00	.096	508.00	.0213	.0259	.171	3.19	.112	.450	8.3	1.116	1.102
5.00	.120	508.00	.0228	.0276	.183	3.97	.130	.388	11.2	1.218	1.202
6.00	.144	508.00	.0238	.0289	.191	4.46	.140	.341	13.7	1.252	1.235
7.00	.168	508.00	.0239	.0288	.191	5.14	.161	.299	18.2	1.443	1.424
8.00	.192	508.00	.0239	.0288	.191	5.24	.164	.266	20.9	1.470	1.451
9.00	.216	508.00	.0240	.0290	.193	5.34	.166	.242	23.4	1.477	1.457
10.00	.241	508.00	.0240	.0290	.193	5.34	.166	.222	25.7	1.477	1.457

ANALYSIS OF SWRI FLOW BENCH RESULTS
Test Number 13 Date: 23 MAR 92

Mod 8 - Helical attempt 5; lowered ramp's roof.

SWRI Project 03-4764-280. Labeco Variable Compression Ratio Engine.

Bore	96.52 (mm)	Inner Valve Seat	41.58 (mm)	Valve Opens	-30.00 deg	Compression Ratio	16.00:1
Stroke	95.25 (mm)	Maximum Valve Lift	8.38 (mm)	Valve Closes	230.00 deg	Engine Speed with	11.2 m/sec Mean
Connecting Rod	166.62 (mm)	Number Of Valves	1	Engine Speed	900. rpm	Piston Speed	3527 rpm

SWRI Method - Simulating Gas Exchange Based on Mass and Energy Conservation
Ricardo Method - Flow Dependent Upon Valve Lift
AVL Method - Flow Equals Rate of Piston Displacement

	SWRI		Ricardo		AVL	
RPM	900	3527	900	3527	900	3527
Swirl Ratio	1.431	.863	.833	.833	1.431	1.431
Mean Flow Coefficient			.116	.116	.142	.142
Gulp Factor	.289	.892	.387	1.516	.316	1.239
Mean Pressure Loss (kPa)	6.77	49.34	5.02	77.09	6.99	107.43
Port Effectiveness (%)			8.69	8.69	10.15	10.15
Volumetric Efficiency (%)	1.015	.569				
Maximum Mach Number	.619	1.000				

Max Flow Coeff = .195

Valve Lift (mm)	Valve Lift Seat Diameter	Differential Pressure (mm water)	Volume Flow (m ³ /s)	Mass Flow (kg/s)	Flow Coeff (Cf)	Torque (N.mm)	N-D Swirl (Nr)	Coeff of Performance (Cp)	Theta (deg)	Momentum Ratio (Vr)	AVL Swirl Number (nd/n)
1.00	.024	508.00	.0049	.0060	.039	.66	.101	.413	8.2	4.403	4.345
2.00	.048	508.00	.0132	.0161	.107	-1.65	-.037	.554	-2.2	-1.591	-1.583
3.00	.072	508.00	.0181	.0220	.145	-5.56	-.023	.504	-1.5	-2.270	-2.266
4.00	.096	508.00	.0215	.0261	.173	-1.18	.006	.449	1.4	.060	.059
5.00	.120	508.00	.0230	.0278	.184	2.61	.085	.387	7.3	.788	.777
6.00	.144	508.00	.0237	.0286	.190	4.17	.131	.338	13.0	1.186	1.171
7.00	.168	508.00	.0242	.0292	.194	4.75	.147	.300	16.5	1.297	1.280
8.00	.192	508.00	.0242	.0292	.194	5.14	.159	.268	20.1	1.403	1.385
9.00	.216	508.00	.0244	.0294	.195	5.73	.175	.247	24.3	1.542	1.521
10.00	.241	508.00	.0244	.0294	.195	6.12	.187	.230	28.2	1.647	1.625

ANALYSIS OF SWRI FLOW BENCH RESULTS
Test Number 14 Date: 24 MAR 92

Mod 9 - Helical attempt 6

SWRI Project 03-4764-280. Labeco Variable Compression Ratio Engine.

Bore	96.52 (mm)	Inner Valve Seat	41.58 (mm)	Valve Opens	-30.00 deg	Compression Ratio	16.00:1
Stroke	95.25 (mm)	Maximum Valve Lift	8.38 (mm)	Valve Closes	230.00 deg	Engine Speed with	11.2 m/sec Mean
Connecting Rod	166.62 (mm)	Number Of Valves	1	Engine Speed	900. rpm	Piston Speed	3527 rpm

SWRI Method - Simulating Gas Exchange Based on Mass and Energy Conservation
Ricardo Method - Flow Dependent Upon Valve Lift
AVL Method - Flow Equals Rate of Piston Displacement

	SWRI		Ricardo		AVL	
RPM	900	3527	900	3527	900	3527
Swirl Ratio	1.456	.984	1.013	1.013	1.464	1.464
Mean Flow Coefficient			.121	.121	.145	.145
Gulp Factor	.280	.881	.372	1.458	.309	1.212
Mean Pressure Loss (kPa)	6.49	48.25	4.64	71.32	6.69	102.71
Port Effectiveness (%)			9.39	9.39	10.62	10.62
Volumetric Efficiency (%)	1.009	.587				
Maximum Mach Number	.609	1.000				

Max Flow Coeff = .197

Valve Lift (mm)	Valve Lift Seat Diameter	Differential Pressure (mm water)	Volume Flow (m ³ /s)	Mass Flow (kg/s)	Flow Coeff (Cf)	Torque (N.mm)	N-D Swirl (Nr)	Coeff of Performance (Cp)	Theta (deg)	Momentum Ratio (Vr)	AVL Swirl Number (nd/n)
1.00	.024	508.00	.0056	.0069	.045	.86	.113	.477	7.9	4.273	4.217
2.00	.048	508.00	.0141	.0171	.114	.47	.025	.590	1.4	.373	.368
3.00	.072	508.00	.0190	.0229	.152	1.44	.057	.529	3.6	.638	.630
4.00	.096	508.00	.0222	.0266	.177	2.12	.072	.463	5.2	.693	.684
5.00	.120	508.00	.0238	.0285	.190	3.49	.110	.400	9.2	.992	.979
6.00	.144	508.00	.0246	.0295	.197	4.17	.127	.348	12.2	1.107	1.092
7.00	.168	508.00	.0247	.0295	.197	4.75	.145	.304	16.0	1.262	1.246
8.00	.192	508.00	.0247	.0295	.197	4.85	.148	.269	18.5	1.288	1.271
9.00	.216	508.00	.0248	.0296	.198	5.34	.161	.247	22.3	1.399	1.380
10.00	.241	508.00	.0249	.0296	.198	5.53	.167	.227	25.3	1.450	1.431

SWRI Flow Bench Data Output from FLOWDATA.EXE
 ROTATIONAL TEST RESULTS
 TEST NO. 15

Output File: vcr12.out
 Mod 9 - Rotational Test

Run Date: 3/25/1992

l/D	kg/sec	Cf	Nr	Vt	Vr	Cp	Theta
.1996	.0293	.1939	.2187	.1269	.2428	.2740	27.59
.1996	.0294	.1952	.1515	.0879	.2445	.2598	19.79
.1996	.0292	.1939	.0985	.0572	.2428	.2495	13.25
.1996	.0290	.1925	.0538	.0312	.2411	.2432	7.38
.1996	.0290	.1925	.0478	.0277	.2411	.2427	6.56
.1996	.0287	.1912	.0786	.0456	.2395	.2438	10.78
.1996	.0287	.1912	.1304	.0757	.2395	.2511	17.53
.1996	.0289	.1925	.1990	.1155	.2411	.2674	25.59
.1996	.0289	.1925	.2051	.1190	.2411	.2689	26.27
.1996	.0291	.1939	.3839	.2228	.2428	.3295	42.53
.1996	.0290	.1939	.4860	.2820	.2428	.3722	49.27
.1996	.0290	.1939	.5971	.3465	.2428	.4231	54.98
.1996	.0290	.1939	.6722	.3901	.2428	.4595	58.10
.1996	.0290	.1939	.7233	.4197	.2428	.4849	59.95
.1996	.0288	.1925	.7404	.4297	.2411	.4927	60.70
.1996	.0288	.1925	.7283	.4227	.2411	.4866	60.29
.1996	.0286	.1912	.7121	.4133	.2395	.4776	59.91
.1996	.0286	.1912	.7121	.4133	.2395	.4776	59.91
.1996	.0288	.1925	.6557	.3805	.2411	.4505	57.64
.1996	.0286	.1912	.6025	.3496	.2395	.4238	55.59
.1996	.0288	.1925	.5317	.3086	.2411	.3916	51.99
.1996	.0286	.1912	.4563	.2648	.2395	.3570	47.87
.1996	.0286	.1912	.3862	.2241	.2395	.3280	43.10
.1996	.0290	.1939	.3058	.1774	.2428	.3007	36.16
.1996	.0290	.1939	.2187	.1269	.2428	.2740	27.59

ANALYSIS OF SWRI FLOW BENCH RESULTS
 Test Number 16 Date: 16 FEB 92

VCR Head: SWRI 03-4764-280. Standard Test using valve w/shroud.

SWRI Project 03-4764-280. Labeco Variable Compression Ratio Engine.

Bore	96.52 (mm)	Inner Valve Seat	41.58 (mm)	Valve Opens	-30.00 deg	Compression Ratio	16.00:1
Stroke	95.25 (mm)	Maximum Valve Lift	8.38 (mm)	Valve Closes	230.00 deg	Engine Speed with	11.2 m/sec Mean
Connecting Rod	166.62 (mm)	Number Of Valves	1	Engine Speed	900. rpm	Piston Speed	3527 rpm

SWRI Method = Simulating Gas Exchange Based on Mass and Energy Conservation
 Ricardo Method = Flow Dependent Upon Valve Lift
 AVL Method = Flow Equals Rate of Piston Displacement

	SWRI		Ricardo		AVL	
	900	3527	900	3527	900	3527
RPM	900	3527	900	3527	900	3527
Swirl Ratio	3.090	2.608	2.383	2.383	3.065	3.065
Mean Flow Coefficient			.159	.159	.188	.188
Gulp Factor	.216	.753	.282	1.106	.239	.936
Mean Pressure Loss (kPa)	3.94	35.37	2.67	41.01	3.99	61.35
Port Effectiveness (%)			16.35	16.35	18.00	18.00
Volumetric Efficiency (%)	.993	.737				
Maximum Mach Number	.570	.965				

Max Flow Coeff = .277

Valve Lift (mm)	Valve Lift Seat Diameter	Differential Pressure (mm water)	Volume Flow (m ³ /s)	Mass Flow (kg/s)	Flow Coeff (Cf)	Torque (N.mm)	N-D Swirl (Nr)	Coeff of Swirl Performance (Cp)	Theta (deg)	Momentum Ratio (Vr)	AVL Swirl Number (nd/n)
1.00	.024	508.00	.0086	.0101	.068	.37	.033	.709	1.5	.820	.809
2.00	.048	508.00	.0170	.0199	.134	1.05	.047	.699	2.2	.599	.591
3.00	.072	508.00	.0205	.0241	.162	4.27	.158	.569	9.2	1.667	1.645
4.00	.096	508.00	.0244	.0286	.193	6.41	.199	.514	13.0	1.773	1.750
5.00	.120	508.00	.0278	.0325	.219	8.94	.244	.476	17.3	1.915	1.889
6.00	.144	508.00	.0306	.0358	.241	12.64	.313	.456	23.5	2.228	2.198
7.00	.168	508.00	.0332	.0388	.261	15.66	.357	.440	28.1	2.344	2.313
8.00	.192	508.00	.0346	.0404	.272	20.82	.456	.442	36.8	2.878	2.840
9.00	.216	508.00	.0363	.0423	.285	23.55	.493	.436	41.0	2.966	2.927
10.00	.241	508.00	.0377	.0440	.296	27.15	.546	.442	45.8	3.159	3.118

ANALYSIS OF SwRI FLOW BENCH RESULTS
Test Number 17 Date: 10 APR 92

03-4764-280. Standard Test using valve w/shroud @ #3 pos.

SwRI Project 03-4764-280. Labeco Variable Compression Ratio Engine.

Bore	96.52 (mm)	Inner Valve Seat	41.58 (mm)	Valve Opens	-30.00 deg	Compression Ratio	16.00:1
Stroke	95.25 (mm)	Maximum Valve Lift	8.38 (mm)	Valve Closes	230.00 deg	Engine Speed with	11.2 m/sec Mean
Connecting Rod	166.62 (mm)	Number Of Valves	1	Engine Speed	900. rpm	Piston Speed	3527 rpm

SwRI Method = Simulating Gas Exchange Based on Mass and Energy Conservation
Ricardo Method = Flow Dependent Upon Valve Lift
AVL Method = Flow Equals Rate of Piston Displacement

	SwRI		Ricardo		AVL	
	900	3527	900	3527	900	3527
Swirl Ratio	3.097	2.612	2.403	2.403	3.071	3.071
Mean Flow Coefficient			.158	.158	.187	.187
Gulp Factor	.217	.755	.285	1.116	.240	.939
Mean Pressure Loss (kPa)	3.96	39.45	2.72	41.74	4.02	61.69
Port Effectiveness (%)			16.06	16.06	17.91	17.91
Volumetric Efficiency (%)	.997	.734				
Maximum Mach Number	.576	.968				

Max Flow Coeff = .277

Valve Lift (mm)	Valve Lift Seat Diameter	Differential Pressure (mm water)	Volume Flow (m**3/s)	Mass Flow (kg/s)	Flow Coeff (Cf)	Torque (N.m)	N-D Swirl (Nr)	Coeff of Performance (Cp)	Theta (deg)	Momentum Ratio (Vr)	AVL Swirl Number (nd/n)
1.00	.024	508.00	.0080	.0097	.064	-.46	-.043	.668	-2.1	-1.142	-1.127
2.00	.048	508.00	.0165	.0199	.132	-.26	-.012	.688	-.6	-.155	-.153
3.00	.072	508.00	.0207	.0248	.165	3.39	.123	.577	7.1	1.274	1.257
4.00	.096	508.00	.0245	.0293	.195	6.02	.184	.519	11.9	1.620	1.599
5.00	.120	508.00	.0276	.0330	.220	9.72	.264	.482	18.5	2.059	2.032
6.00	.144	508.00	.0301	.0360	.240	13.42	.334	.459	25.0	2.386	2.354
7.00	.168	508.00	.0323	.0385	.257	16.83	.391	.444	30.8	2.617	2.583
8.00	.192	508.00	.0342	.0408	.272	20.24	.444	.437	36.1	2.797	2.760
9.00	.216	508.00	.0358	.0426	.284	23.26	.488	.433	40.8	2.947	2.909
10.00	.241	508.00	.0372	.0443	.295	26.47	.534	.436	45.2	3.097	3.057

Appendix C
Task 3 "Clean Fuel" Results

MODE 1 RESULTS

FUEL NAME	RUN	PHI	A/Fs	O ₂ %	CO ₂ %	CO PPM	NO _x PPM	HC PPM	BSCO	BSNO _x	BSNO _x CORR	BSHC	BHP	SMOKE	DURATION	P _{MAX}	Q _{TOT}
Base	760	0.513	14.503	10.730	7.610	506.000	754.000	636.000	2.683	6.566	5.855	1.778	5.900	2.000	34.200	882.000	1.047
FT2 Feed	765	0.522	14.787	10.590	7.550	459.400	830.900	513.000	2.363	7.020	6.271	1.421	6.200	0.500	33.000	942.000	1.061
FT2 Frac 1	770	0.526	14.773	10.570	7.560	358.700	783.100	1100.000	1.825	6.543	5.858	3.008	6.300	0.400	34.800	890.400	1.079
FT2 Frac 2	776	0.533	14.857	10.460	7.580	353.600	557.000	1237.000	1.941	5.023	4.510	3.674	5.900	1.600	46.200	940.300	1.070
FT2 Frac 3	777	0.525	14.801	10.560	7.530	392.800	704.600	901.000	1.960	5.776	5.174	2.422	6.500	0.800	36.000	916.800	1.132
FT2 Frac 4	780	0.520	14.829	10.660	7.500	280.000	846.300	678.000	1.439	7.142	6.369	1.880	6.300	0.000	34.800	947.000	1.069
FT2 Frac 5	785	0.515	14.731	10.660	7.450	510.300	695.300	408.000	2.741	6.133	5.479	1.174	6.000	2.400	37.800	953.000	1.045
FT2 Frac 6	790	0.514	14.731	10.670	7.430	530.000	703.000	354.000	2.800	6.101	5.431	1.002	6.100	2.600	39.000	963.000	1.041
FT2 Frac 7	795	0.515	14.773	10.630	7.380	773.000	629.800	333.000	4.308	5.765	5.114	0.997	5.800	3.000	40.200	945.000	1.027
FT1 Frac 1	815	0.533	15.036	10.320	7.390	628.000	702.900	672.000	3.485	6.407	5.738	2.043	5.800	2.800	41.400	1048.000	1.055
FT1 Frac 2	820	0.539	15.050	10.170	7.510	540.000	733.200	537.000	2.931	6.537	5.862	1.601	5.900	2.700	41.400	1057.000	1.055
FT1 Frac 3	825	0.534	15.009	10.250	7.480	711.000	654.300	337.000	3.831	5.792	5.189	0.994	6.000	2.700	42.600	1028.000	1.064
FT1 Frac 4	830	0.528	14.954	10.330	7.370	802.000	696.100	364.000	5.308	7.568	6.754	1.312	4.900	2.800	42.600	1046.000	1.028
FT1 Frac 5	835	0.524	14.995	10.540	7.390	579.000	582.100	381.000	3.342	5.519	4.914	1.202	5.600	2.300	39.600	939.000	1.013
FT1 Frac 6	840	0.526	14.926	10.530	7.470	785.000	576.000	379.000	4.317	5.203	4.642	1.134	5.800	3.000	63.600	943.000	4.700
FT1 Frac 7	845	0.530	14.995	10.400	7.430	855.000	548.000	347.000	4.629	4.874	4.345	1.027	5.900	3.200	42.000	947.000	1.043
CF10	860	0.516	14.703	10.640	7.520	440.600	601.000	308.000	2.386	5.354	4.777	0.893	5.900	2.300	0.000	930.000	0.000
CF1	865	0.522	14.815	10.520	7.490	537.700	590.800	395.000	2.940	5.306	4.739	1.165	5.900	2.700	42.000	934.000	1.032
CF2	870	0.518	14.703	10.580	7.480	668.800	566.700	465.000	3.811	5.304	4.727	1.417	5.700	3.200	42.600	905.000	1.005
CF3	875	0.525	14.968	10.480	7.380	639.000	623.000	493.000	3.487	5.585	4.980	1.467	5.900	2.800	0.000	950.800	0.000
CF9	880	0.514	14.773	10.700	7.450	486.000	506.000	312.000	2.885	4.934	4.367	0.996	5.400	2.400	45.600	858.900	1.035
CF7	885	0.518	14.773	10.620	7.460	562.000	533.000	416.000	3.185	4.962	4.429	1.267	5.700	3.300	42.600	925.000	1.030
CF4	890	0.522	14.603	10.450	7.660	615.000	532.000	257.000	3.494	4.964	4.428	0.776	5.700	2.800	43.800	899.000	1.040
CF5	895	0.526	14.787	10.410	7.550	680.000	543.000	320.000	3.769	4.944	4.402	0.955	5.800	2.800	40.800	914.000	1.053
CF6	900	0.511	14.575	10.720	7.460	726.000	513.000	579.000	4.197	4.871	4.330	1.772	5.600	2.600	44.400	889.000	1.011
CF8	905	0.515	14.674	10.660	7.470	614.000	525.000	440.000	3.485	4.895	4.379	1.332	5.700	2.400	44.400	879.000	1.016

MODE 2 RESULTS

FUEL NAME	RUN	PHI	A/Fa	O ₂ %	CO ₂ %	CO PPM	NO _x PPM	HC PPM	BSCO	BSNO _x	BSNO _x CORR	BSHC	BHP	SMOKE	DURATION	P _{MAX}	Q _{TOY}
Base	761	0.504	14.503	10.860	7.520	371.900	856.100	355.000	1.981	7.490	6.665	0.996	6.027	0.800	33.600	963.468	1.038
FT2 Feed	766	0.520	14.787	10.600	7.540	428.000	833.300	388.000	2.220	7.098	6.339	1.083	6.151	0.600	33.600	942.497	1.059
FT2 Frac 1	771	0.511	14.773	10.850	7.290	300.800	793.200	1161.000	1.646	7.128	6.353	3.406	5.879	0.200	34.800	856.998	0.942
FT2 Frac 2	775	0.527	14.857	10.590	7.480	345.700	424.700	1269.000	1.948	3.931	3.525	3.865	5.800	1.200	46.200	821.300	1.066
FT2 Frac 4	781	0.524	14.829	10.510	7.600	271.100	820.000	354.000	1.382	6.867	6.130	0.975	6.334	0.400	35.400	911.962	1.090
FT2 Frac 5	786	0.515	14.731	10.650	7.450	483.000	621.000	401.000	2.618	5.529	4.934	1.164	5.938	2.200	38.400	918.539	1.043
FT2 Frac 6	791	0.515	14.731	10.640	7.450	570.400	650.600	354.000	3.017	5.653	5.028	1.003	6.091	2.100	37.200	931.396	1.046
FT2 Frac 7	796	0.517	14.773	10.590	7.400	798.300	571.800	337.000	4.410	5.189	4.816	1.000	5.854	2.800	42.600	908.588	1.025
Base	801	0.511	14.503	10.630	7.510	596.500	653.900	385.000	3.298	5.939	5.304	1.122	5.950	2.600	37.800	954.523	1.028
FT1 Feed	811	0.521	14.575	10.510	7.670	346.200	616.700	569.000	2.012	5.887	5.273	1.754	5.584	2.800	39.600	934.680	1.041
FT1 Frac 1	816	0.528	15.036	10.430	7.340	535.400	514.600	652.000	3.013	4.757	4.252	2.009	5.714	2.800	41.400	881.568	1.054
FT1 Frac 2	821	0.530	15.050	10.350	7.390	385.700	519.000	439.000	2.134	4.718	4.218	1.333	5.808	2.200	41.400	884.964	1.054
FT1 Frac 3	826	0.543	15.009	10.070	7.590	684.100	511.000	396.000	3.689	4.502	4.038	1.164	6.016	2.800	44.400	886.872	1.085
FT1 Frac 4	831	0.523	14.954	10.430	7.330	549.800	504.800	397.000	3.082	4.648	4.143	1.211	5.792	2.600	40.600	905.401	4.932
FT1 Frac 5	836	0.524	14.995	10.550	7.400	612.600	625.000	356.000	3.456	4.865	4.332	1.097	5.721	2.600	41.400	911.750	1.043
FT1 Frac 6	841	0.531	14.926	10.420	7.530	900.100	527.400	390.000	5.064	4.874	4.353	1.194	5.676	3.400	43.200	904.623	1.047
FT1 Frac 7	846	0.527	14.995	10.440	7.360	873.400	509.200	381.000	4.861	4.655	4.148	1.158	5.762	3.200	88.800	922.433	0.725
DF-2	851	0.515	14.646	10.600	7.500	429.600	588.800	371.000	2.357	5.306	4.743	1.084	5.913	2.300	37.800	937.944	1.037
DF-2	856	0.512	14.603	10.760	7.500	533.200	645.700	599.000	2.982	5.931	5.306	1.778	5.778	2.600	38.400	972.825	1.010
CF10	861	0.515	14.703	10.650	7.510	422.900	583.100	279.000	2.301	5.210	4.651	0.812	5.904	2.300	75.600	931.776	7.178
CF1	866	0.521	14.815	10.510	7.470	518.700	540.300	326.000	2.842	4.863	4.343	0.963	5.899	2.700	4.800	900.304	-3.065
CF2	871	0.523	14.703	10.470	7.580	501.700	582.700	389.000	2.737	5.222	4.659	1.136	5.922	3.000	41.400	934.399	1.031
CF3	876	0.526	14.968	10.460	7.410	438.400	584.200	544.000	2.398	5.070	4.522	1.622	5.886	2.400	84.000	210.704	0.000
CF9	881	0.519	14.773	10.620	7.520	516.000	540.600	274.000	2.954	5.084	4.534	0.844	5.584	2.800	42.000	902.331	1.026
CF7	886	0.524	14.773	10.480	7.550	640.400	547.700	346.000	3.519	4.944	4.419	1.023	5.874	2.800	0.000	907.195	-0.075
CF4	891	0.520	14.603	10.500	7.650	570.900	566.000	239.000	3.195	5.204	4.640	0.711	5.767	2.600	89.400	938.101	0.578
CF5	896	0.526	14.787	10.380	7.550	635.100	543.700	293.000	3.531	4.966	4.422	0.877	5.781	2.700	84.000	128.816	0.000
CF6	901	0.512	14.575	10.700	7.490	716.400	589.800	517.000	4.050	5.477	4.875	1.548	5.717	3.300	40.800	984.253	0.998
CF8	906	0.515	14.674	10.650	7.460	698.400	545.100	390.000	4.015	5.147	4.605	1.198	5.639	3.100	39.600	939.770	1.021

3-2

MODE 3 RESULTS

FUEL NAME	RUN	PHI	A/Fa	O ₂ %	CO ₂ %	CO PPM	NO _x PPM	HC PPM	BSCO	BSNO _x	BSNO _x CORR	BSHC	BHP	SMOKE	DURATION	P _{MAX}	Q _{TOT}
Base	762	0.507	14.503	10.840	7.540	337.800	880.800	587.000	1.771	7.584	6.752	1.566	8.830	0.500	34.200	1029.189	1.241
FT2 Feed	767	0.514	14.787	10.720	7.460	272.700	967.700	482.000	1.352	7.878	7.003	1.285	9.250	0.200	33.000	1076.011	1.262
FT2 Frac 1	772	0.517	14.773	10.700	7.410	314.600	621.400	954.000	1.683	5.461	4.863	2.740	8.750	0.400	42.600	957.290	1.226
FT2 Frac 3	777	0.525	14.801	10.560	7.530	392.800	704.800	901.000	1.970	5.803	5.198	2.434	6.470	0.800	36.000	916.841	1.132
FT2 Frac 4	782	0.527	14.829	10.500	7.600	437.700	781.400	502.000	2.194	6.270	5.594	1.360	9.060	1.800	39.600	1061.803	1.262
FT2 Frac 5	787	0.514	14.731	10.680	7.440	446.700	704.400	478.000	2.332	6.041	5.384	1.337	8.900	1.900	39.000	1049.678	1.241
FT2 Frac 6	792	0.511	14.731	10.710	7.400	457.700	688.600	357.000	2.436	6.020	5.338	1.018	8.700	2.200	42.000	1039.316	1.232
FT2 Frac 7	797	0.514	14.773	10.640	7.390	457.400	666.900	305.000	2.484	5.949	5.276	0.890	8.560	2.000	42.600	1048.752	1.242
Base	802	0.512	14.603	10.650	7.540	509.000	688.900	479.000	2.795	6.034	5.367	1.366	8.540	2.200	42.000	1039.855	1.224
FT2 Frac 2	805	0.530	14.857	10.470	7.590	404.300	655.000	774.000	2.078	5.529	4.930	2.153	8.940	3.000	41.400	1045.741	1.307
FT1 Feed	812	0.510	14.575	10.760	7.500	372.700	650.100	597.000	2.271	6.507	5.808	1.927	7.600	2.300	40.800	1037.341	1.227
FT1 Frac 1	817	0.538	15.036	10.190	7.530	343.600	659.000	549.000	1.950	6.142	5.485	1.709	8.090	2.000	42.600	1044.228	1.296
FT1 Frac 2	822	0.534	15.050	10.250	7.450	304.900	609.700	471.000	1.741	5.718	5.100	1.476	8.160	2.000	43.200	1027.330	1.304
FT1 Frac 3	827	0.540	15.009	10.120	7.580	417.000	634.200	379.000	2.318	5.792	5.175	1.154	8.330	2.200	43.200	1043.307	1.297
FT1 Frac 4	832	0.530	14.954	10.270	7.450	405.300	596.300	340.000	2.259	5.460	4.859	1.033	8.370	2.000	42.600	1037.657	1.271
FT1 Frac 5	837	0.521	14.995	10.600	7.390	394.400	581.200	343.000	2.229	5.395	4.811	1.059	8.130	2.200	43.800	1026.419	1.245
FT1 Frac 6	842	0.529	14.928	10.430	7.550	526.400	581.000	311.000	2.972	5.388	4.815	0.956	8.140	2.400	43.800	1032.494	1.281
FT1 Frac 7	847	0.521	14.995	10.540	7.360	466.700	592.000	278.000	2.622	5.464	4.878	0.853	8.230	2.000	42.600	1055.064	1.271
DF-2	852	0.521	14.646	10.490	7.590	327.700	598.600	466.000	1.864	5.592	5.010	1.412	8.220	2.200	4.800	1000.706	-4.091
DF-2	857	0.519	14.603	10.600	7.660	273.100	732.900	516.000	1.505	6.634	5.950	1.511	8.340	1.500	39.000	1064.515	1.236
CF10	862	0.514	14.703	10.680	7.510	294.100	640.800	307.000	1.673	5.989	5.350	0.934	8.140	1.700	40.800	1031.748	1.225
CF1	867	0.518	14.815	10.590	7.450	340.600	615.500	347.000	1.913	5.680	5.074	1.051	8.220	2.000	42.600	1023.005	1.224
CF2	872	0.517	14.703	10.590	7.500	362.500	594.500	408.000	2.113	5.691	5.076	1.272	8.010	2.000	42.000	1025.084	1.209
CF3	877	0.524	14.968	10.480	7.400	359.200	593.300	421.000	2.001	5.430	4.851	1.279	8.300	1.700	84.000	134.085	0.000
CF9	882	0.513	14.773	10.740	7.460	304.800	563.800	305.000	1.838	6.685	4.986	0.989	7.640	1.600	45.000	979.285	1.222
CF7	887	0.517	14.773	10.620	7.470	448.600	553.200	335.000	2.522	5.109	4.565	1.012	8.280	2.100	0.000	964.441	-7.541
CF4	892	0.519	14.603	10.510	7.650	341.100	620.000	260.000	1.930	5.762	5.142	0.782	8.230	2.000	45.000	1018.340	1.243
CF5	897	0.519	14.787	10.540	7.470	405.000	540.100	267.000	2.306	5.051	4.499	0.818	8.140	2.400	0.600	973.420	-3.935
CF6	902	0.512	14.675	10.680	7.540	340.100	561.900	398.000	1.981	5.323	4.752	1.216	8.060	2.100	48.000	987.534	2.276

MODE 4 RESULTS

FUEL NUMBER	RUN	PHI	A/Fa	O ₂ %	CO ₂ %	CO PPM	NO _x PPM	HC PPM	BSCO	BSNO _x	BSNO _x CORR	BSHC	BHP	SMOKE	DURATION	P _{MAX}	Q _{TOT}
Base	763	0.357	14.503	13.920	5.260	214.600	477.500	351.000	1.763	6.445	5.542	1.491	5.760	0.000	33.000	953.774	0.898
FT2 Feed	768	0.368	14.787	13.740	5.240	215.300	490.800	435.000	1.815	6.798	5.848	1.932	5.060	0.100	31.200	880.864	0.820
FT2 Frac 1	773	0.365	14.773	13.850	5.120	237.000	344.900	1046.000	2.110	5.044	4.329	4.893	4.850	0.100	87.600	580.802	4.312
FT2 Frac 3	778	0.517	14.801	10.710	7.380	582.600	638.400	893.000	3.002	5.695	4.981	2.563	8.770	0.800	38.400	976.051	1.242
FT2 Frac 4	783	0.368	14.829	13.770	5.230	232.900	469.600	488.000	1.973	6.533	5.610	2.094	5.050	0.600	35.400	930.208	0.822
FT2 Frac 5	788	0.367	14.731	13.730	5.250	228.800	434.800	371.000	1.931	6.028	5.188	1.644	5.070	0.800	35.400	905.965	0.815
FT2 Frac 6	793	0.360	14.731	13.790	5.170	198.100	446.400	172.000	3.515	13.010	11.157	1.601	2.420	0.900	36.000	902.273	0.806
FT2 Frac 7	798	0.370	14.773	13.540	5.280	200.300	446.900	149.000	1.598	5.855	5.021	0.626	5.380	0.800	36.000	910.132	0.827
Base	803	0.362	14.503	13.760	5.280	217.700	438.900	481.000	1.886	6.246	5.366	2.154	4.990	1.000	36.000	913.172	0.818
FT2 Frac 2	806	0.371	14.857	13.790	5.180	196.900	428.800	1072.000	1.643	5.879	5.040	4.731	5.170	0.200	55.800	843.377	3.226
FT1 Feed	813	0.363	14.575	13.790	5.270	253.400	391.000	486.000	2.270	5.754	4.952	2.261	4.810	1.300	36.000	907.612	0.797
FT1 Frac 1	818	0.375	15.036	13.560	5.160	185.800	437.700	660.000	1.539	5.957	5.118	2.928	5.180	0.700	34.800	923.218	0.838
FT1 Frac 2	823	0.375	15.050	13.510	5.160	190.500	393.600	418.000	1.558	5.281	4.545	1.830	5.300	0.600	35.400	910.339	0.845
FT1 Frac 3	828	0.377	15.009	13.450	5.240	175.300	439.400	211.000	1.381	5.687	4.889	0.890	5.450	1.900	35.400	915.674	0.850
FT1 Frac 4	833	0.371	14.954	13.530	5.170	193.500	404.300	163.000	1.586	5.444	4.664	0.712	5.290	1.800	35.400	906.126	0.830
FT1 Frac 5	838	0.524	14.995	10.540	7.390	578.600	582.100	381.000	4.853	7.689	6.854	1.674	5.250	0.900	36.000	902.089	0.841
FT1 Frac 6	843	0.369	14.926	13.750	5.220	209.000	390.000	180.000	1.734	5.314	4.581	0.794	5.150	1.000	36.600	901.002	0.838
FT1 Frac 7	848	0.369	14.995	13.650	5.150	193.800	378.700	161.000	1.612	5.174	4.468	0.715	5.180	0.900	34.800	907.020	0.830
DF-2	853	0.365	14.646	13.710	5.260	199.600	384.600	345.000	1.699	5.376	4.646	1.532	5.070	0.800	34.200	891.008	0.813
DF-2	858	0.363	14.603	13.810	5.270	248.200	448.000	438.000	2.146	6.362	5.509	1.871	4.960	1.000	33.600	944.336	0.801
CF10	863	0.361	14.703	13.830	5.200	210.400	406.700	246.000	1.824	5.792	5.000	1.117	4.970	0.800	4.200	898.388	-2.797
CF1	868	0.366	14.815	13.700	5.190	208.100	401.400	259.000	1.794	5.684	4.899	1.178	4.990	0.800	68.400	895.281	0.330
CF2	873	0.367	14.703	13.680	5.260	219.600	418.000	328.000	1.888	5.903	5.071	1.477	4.990	1.000	90.600	912.291	5.785
CF3	878	0.376	14.988	13.530	5.240	197.400	423.900	419.000	1.621	5.719	4.946	1.836	5.230	0.600	0.000	814.281	-2.326
CF9	883	0.368	14.773	13.740	5.290	189.200	373.800	154.000	1.623	5.268	4.543	0.896	4.990	0.800	46.200	859.577	0.672
CF7	888	0.370	14.773	13.630	5.280	203.000	373.500	243.000	1.744	5.270	4.547	1.099	5.010	1.100	39.000	881.399	0.822
CF4	893	0.357	14.603	13.820	5.200	202.100	382.700	132.000	1.795	5.730	4.914	0.610	4.870	1.000	45.000	887.989	1.516
CF5	898	0.367	14.787	13.650	5.240	212.300	368.800	157.000	1.828	5.216	4.479	0.712	5.000	1.400	39.600	872.355	0.820
CF6	903	0.383	14.575	13.760	5.260	267.300	361.600	428.000	2.420	5.377	4.647	2.012	4.770	1.200	40.200	881.906	0.800

of the Higgs field. This means that, while for instance for the bottom quark, the second heaviest fermion, G_{bottom} is only ~ 0.03 , G_{top} is large. For the particular value $M_{top} = 174 \text{ GeV}/c^2$, $G_{top} \approx 1.00!$ Is this telling us something?

Hill and Parke [13], and Eichten and Lane [14] have used the fact that the top quark is so massive to point out that it may turn out to be a powerful probe of electroweak symmetry breaking physics. This was reported by K. Lane in a mini-review at this conference [15]. They suggest in particular that new states may exist, strongly coupled to the top, and that non-standard model, resonant $t\bar{t}$ production via such states, if they exist, could be observed with rather modest statistics. The $t\bar{t}$ invariant mass distribution could be particularly revealing. Any such observation of physics beyond the standard model would be highly interesting!

The measurement of the top quark mass to good precision is also important, both in its own right, and because of the light it may shed, together with a precision M_W measurement, on the Higgs mass. It can be seen from Figure 14 that there is as yet no constraint on the Higgs mass from the current knowledge of (M_{top}, M_W) . Expected improvements in the measurement of both these quantities during the remainder of this decade, to perhaps $\pm 5 \text{ GeV}/c^2$ for M_{top} and $\pm 50 \text{ MeV}/c^2$ for M_W , could put the standard model to the test, however.

With more statistics, the full subject of top physics will begin to unfold. It may turn out to be even more interesting than that of its sister particle, the b quark!

12. Acknowledgements

I am grateful to Ed Blucher, Milciades Contreras, Lina Galtieri, Richard Hughes, Gordon Watts, William Wester and Brian Winer for making figures for this report.

References

- [1] F. Abe *et al.*, Phys. Rev. Lett. **73** (1994) 220; J. Alitti *et al.* Phys. Lett. **B277** (1992) 194.
- [2] F. Abe *et al.*, Phys. Rev. Lett. **68** (1992) 447; and Phys. Rev. **D45** (1992) 3921.
- [3] S. Abachi *et al.*, Phys. Rev. Lett. **72** (1994) 2138.
- [4] F. Abe *et al.*, Phys. Rev. **D50** (1994) 2966.
- [5] F. Abe *et al.*, Phys. Rev. Lett. **73** (1994) 225.
- [6] D. Schaile, *Precision Tests of the Electroweak Interaction*, Session Pl-2 of these Proceedings.
- [7] E. Laenen, J. Smith and W.L. van Neerven, Phys. Lett. **B321** (1994) 254.
- [8] F. Abe *et al.*, Nucl. Instr. Meth. Phys. Res. **A271** (1988) 387.
- [9] F. Paige and S.D. Protopopescu, BNL Report No. 38034, 1986 (unpublished).

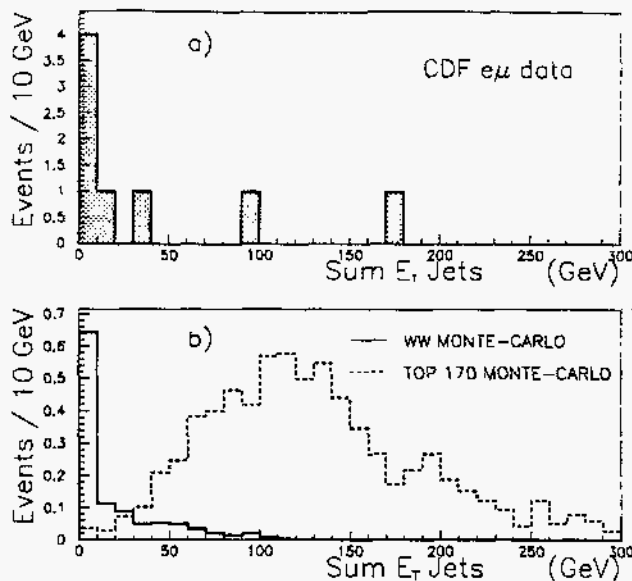


Figure 15. a) The Sum of $E_T(\text{jet})$, $\Sigma E_T(\text{jet})$, for the 8 $e\mu$ events passing the $P_T > 20 \text{ GeV}/c$ requirement on each lepton. Only jets with $E_T > 10 \text{ GeV}$ and $|\eta| < 2.4$ are included in the sum. The two events in the signal region of the dilepton analysis are the two events with the highest $\Sigma E_T(\text{jet})$. The six events at low $\Sigma E_T(\text{jet})$ fail both the two-jet cut and the \cancel{E}_T cut. b) Monte Carlo $\Sigma E_T(\text{jet})$ distribution for $t\bar{t}$ production ($M_{top} = 170 \text{ GeV}/c^2$), and for electroweak WW production, one of the backgrounds to the top search. The histogram for WW production is normalized to 19.3 pb^{-1} , the same as the data, while the $t\bar{t}$ histogram has an exaggerated normalization of 150 pb^{-1} to show more clearly the shape of the distribution. Note that the six events at low sum E_T in a) are unlikely to be mostly WW since they have low \cancel{E}_T .

- [10] G. Marchiesini and B.R. Webber, Nucl. Phys. **B310** (1988) 461; G. Marchiesini *et al.*, Computer Phys. Comm. **67** (1992) 465.
- [11] F.A. Berends, W.T. Giele, H. Kuijff and B. Tausk, Nucl. Phys. **B357** (1991) 32.
- [12] CDF Collaboration: H.H. Williams, *Top Quark Kinematics and Mass Determination*, Session Pa-18 of these Proceedings.
- [13] C.T. Hill and S.J. Parke, Phys. Rev. **D49** (1994) 4454.
- [14] E. Eichten and K. Lane, Phys. Lett. **B327** (1994) 129.
- [15] K. Lane, *Top Quark Production and Flavor Physics*, Session Pa-18 of these Proceedings.
- [16] G. Burgers, W. Hollik and M. Martinez, Proceedings of the Workshop on Z physics at LEP, CERN Report 89-08.

K. Hidaka, Tokyo Gakugei University:
What is the definition of the top mass?

H. Jensen:

The top mass is determined for each event by a fit to the final state lepton and jet energies, using the hypothesis $p\bar{p} \rightarrow t\bar{t} \rightarrow WbW\bar{b}$.

K. Hidaka, Tokyo Gakugei University:

Do you have any information on the width of the top

Files

Table 6.2 CSASIN sample problem files

<u>File name</u>	
SAMPLE2.ARR	} Sample Problem 2
SAMPLE2.BIA	
SAMPLE2.BND	
SAMPLE2.GEO	
SAMPLE2.IN	
SAMPLE2.LAT	
SAMPLE2.MIP	
SAMPLE2.PAR	
SAMPLE2.SEA	
SAMPLE2.STD	
SAMPLE3.ARR	} Sample Problem 3
SAMPLE3.BIA	
SAMPLE3.GEO	
SAMPLE3.IN	
SAMPLE3.LAT	
SAMPLE3.MIP	
SAMPLE3.PAR	
SAMPLE3.SEA	
SAMPLE3.STD	
